Correlations between vegetation, soil and geology in the semi-arid Bushmanland region of South Africa

C Faul

orcid.org 0000-0002-7304-275X

Dissertation submitted in fulfilment of the requirements for the degree *Master of Science in Environmental Sciences* at the North-West University

Supervisor: Mr PW van Deventer

Graduation May 2018

22869794

DISCLAIMER

The study was conducted under the supervision of Pieter Willem van Deventer. Appropriate acknowledgement has been made in the text where the use of work conducted by other researches has been included.

Although all care was taken to ensure the accuracy of this report, neither the sender and/or the North-West University can be held responsible for any errors or omissions that might have occurred. Although all possible care has been taken in the production of the reports and plans, North-West University and/or the sender cannot take any liability for perceived inaccuracy or misinterpretation of the information shown in this dissertation.

ACKNOWLEDGMENTS

I wish to attribute my work and accomplishments to the Lord Jesus Christ.

Proverbs 3: 5-6 ~ “Trust in the LORD with all your heart and lean not on your own understanding; in all your ways submit to him, and he will make your paths straight.”

I would like to extend my sincere gratitude to PW van Deventer for all his guidance, support and insight as my supervisor and mentor.

I would also like to thank Stefan Denysschen for the construction of all ArcGIS Maps, assistance with fieldwork and for all his moral support. I would also like to acknowledge Jana Geeringh, Claudia Schimmer, Ruan Ainslie, Elrica Myburgh, Reginald Scholtz and André de Beer for their help and assistance during field work and/or laboratory assistance.

I would like to thank Charné Malan, Sascha Roopa, Helga van Coller, Willem Kruger and Bea Hurter for their assistance and reviews.

Last but not least I would like to extend my most sincere gratitude to my family, for their moral and financial support, love and assistance.

ABSTRACT

Since the early 1900's scientists have investigated the different factors that play a part in biodiversity and species richness with respect to vegetation composition. Plant species have different needs for nutrients, moisture as well as the amount of radiation that it receives. Therefore, the species composition for each environment will differ according to the chemical-, physical- and anthropogenic properties of that environment which include geological properties, soil properties, climate, topography as well as anthropogenic influences

Limited knowledge is available with respect to the geology-soil relationships as well as relationships between vegetation and soils in the semi-arid regions of southern Africa. Existing information just refers to brief descriptions of the vegetation-soil interactions. The main aim of this study is to determine if there are relationships between vegetation, soil and geology in the semi-arid Bushmanland region of South-Africa.

The study was conducted on an area approximately 60 km south south-west of Kakamas in the Northern Cape of South Africa. This site was chosen based on the homogenous climate and topography, minimal anthropogenic influences, as well as its plant diversity and richness in soil- and geological differences. In order to fulfil the main aim of this study, vegetation, soil and geological assessments and surveys were conducted. Soil forms the intermediate medium between geology and vegetation and has an extensive influence on plant ecology and diversity. Therefore, soil forms, pedochemical properties and physical characteristics were examined in detail. A vegetation assessment was done primarily to assess the role of parent material and soil medium in the development of plant communities and for the identification of vegetation habitats. This information was finally used to identify two-tier and three their relationships.

Method 1 was used to identify four interrelationships between plant communities and either soil forms or geological formations and lithology. With the help of Method 2, a total of 19 three-tier combinations were identified. It was established that a three-tier relationship between grassland vegetation, calcic soils and surficial calcrete deposits is typical for the semi-arid Bushmanland region. Drainage systems in this part of South Africa are associated with shrubs and grasses (in particular *Rhigozum trichotomum* which dominates these areas) as well as cumulic soils.

***Keywords*: Correlations; semi-arid; Bushmanland; pattern recognition; intermediate medium; diversity; interrelationship.**

OPSOMMING

Navorsing is alreeds vanaf die vroeë 1900's gedoen, rakende die faktore wat 'n rol speel in biodiversiteit and spesie rykheid te opsigte van plantegroei. Verskillende plantspesies het verskillende behoeftes aan voedingstowwe, vog asook die hoeveelheid straling wat dit ontvang. Dus verskil die spesie samestelling vir elke omgewing volgens die chemiese-, fisiese- en antropogeniese eienskappe van daardie omgewing. Dit sluit ook geologiese eienskappe, grondseienskappe, klimaat, topografie en antropogene invloede in.

Inligting ten opsigte van die geologie-grondverwantskappe sowel as verhoudings tussen plantegroei en gronde in die semi-ariede Boesmanland streek van Suid-Afrika is beperk. Bestaande inligting verwys slegs na kort beskrywings van die plant-grond-interaksies. Die hoofdoel van hierdie studie is om vas te stel of daar verhoudings tussen plantegroei, grond en geologie in die semi-ariede Boesmanland streek van Suid-Afrika bestaan.

Die studie area is ongeveer 60 km suid suidwes van Kakamas geleë, in die Noord-Kaap Provinsie van Suid-Afrika. Hierdie area was gekies weens die homogene klimaat en topografie, minimale antropogeniese invloede, asook plantdiversiteit en verskille in grondvorms en geologiese formasies. Ten einde die doel van hierdie studie te bereik, is plant-, grond- en geologiese opnames gedoen. Grond vorm die intermediêre medium tussen geologie en plantegroei en het 'n groot invloed op plantekologie en diversiteit. Daarom is grondvorms, pedochemiese eienskappe asook fisiese eienskappe in meer besonderhede ondersoek. 'n Plant opname is hoofsaaklik gedoen om die rol van moedermateriaal en grondmedium in die ontwikkeling van plantgemeenskappe te bepaal en om plant habitatte te identifiseer. Hierdie inligting is uiteindelik gebruik om tweeledige en drieledige verhoudings te identifiseer.

Metode 1 is gebruik om vier verwantskappe tussen plantgemeenskappe en grondvorms of geologiese formasies en litologie te identifiseer. Met behulp van metode 2 is 'n totaal van 19 drie-vlak kombinasies geïdentifiseer. Daar is vasgestel dat 'n drieledige verhouding tussen gras vlaktes, kalkgrond en oppervlakkige kalkreet afsettings tipies is vir die semi-ariede Boesmanland streek. Dreineringstelsels in hierdie deel van Suid-Afrika word geassosieer met struike en grasse (veral *Rhigozum trichotomum* wat hierdie gebiede oorheers).

***Sleutelwoorde*: Korrelasies; semi-aried; Boesmanland; patroon identifikasie; intermediêre medium; diversiteit; verwantskappe.**

TABLE OF CONTENTS

LIST OF TABLES

LIST OF FIGURES

LIST OF ACRONYMS

a	Anthropogenic factor in equation defying soil erosion
ADP	Adenosine diphosphate
Ag3	Land type consisting of freely drained, shallow (<300 mm deep), red, eutrophic, apedal soils that comprise >40% of the land type (yellow-brown soils comprise <10%).
Al^{3+}	Aluminium ion
am	Ante meridiem
ATP	Adenosine triphosphate
C	Average topsoil clay percentage of Land Type
Ca^{2+}	Calcium ion
CEC	Cation Exchange Capacity
cl	Climate in equation defying soil erosion
Cl^{-}	Chloride ion
cm^3	Cubic centimetre
cmol(+)/kg	Expression of exchangeable cations
Cu^{2+}	Copper ion
D	Dominant depth class of land type
dE	Degree of freedom
dm^3	Cubic decimetre
DNA	Deoxyribonucleic acid
EC	Electrical Conductivity
E_J	The ratio of evaporation during the warmest month
f	Function in equation defying soil erosion
F	Whether variability between mapping units is significantly different
Fe^{2+}/Fe^{3+}	Iron ion
g	Gram
H^{+}	Hydrogen ion
ha	Hectare
H_2O	Water
H_2S	Hydrogen sulphide
K^{+}	Potassium ion
KCl	Potassium chloride
kg	kilogram
km^2	Square kilometre
m	metre

Ma	Million years
Mg^{2+}	Magnesium ion
mm	millimetre
mol/dm^3	Concentration of aqueous solution defined as the amount of solutes (moles) dissolved in 1 dm^3 of solution
MS	Mean square
mS/m	MilliSiemens per meter
mu	Mapping Unit
n	Number of plant species
N^{3-}	Nitrogen ion
NaCl	Sodium chloride
Na_2SO_4	Sodium sulphate
NH_2	Amide
NMDS	Non-metric multidimensional scaling
Ni^{2+}	Nickel ion
NO_3^-	Nitrate
o	Organism (fauna and flora) in equation defying soil erosion
OH^-	Hydroxide
pm (Chapter 2)	Parent material in equation defying soil erosion
p (Chapter 4)	*p*-values below a certain threshold ($p < 0.05$) indicates significant differences between mapping units
P^{3-}	Phosphorus ion
P_a	Annual precipitation
PAST	Paleontological Statistics Software
PPL	Plane Polarised Light
PSD	Particle Size Distribution
r	Relief (topography) in equation defying soil erosion
Rb-Sr	Rubidium-Strontium
S	Soil category classes
s.e.	Standard error
SIMPER	Similarity Percentage Analysis
SO_4^-	Sulphate
SS	Sum of squared differences
t	Time in equation defying soil erosion
XPL	Crossed Polarised Light
Zn^{2+}	Zinc ion

GLOSSARY

TERMS	DEFINITION
Abiotic	Environmental non-living factors (chemical and physical).
Anthropogenic	Man-made
Areal interpolation	The re-aggregation of data into new geographic zones through the application of spatial algorithms. This technique rests on the perception that the estimated quantity at the intersecting zone is proportional to that proportion of the source zone.
Arid	Insufficient rainfall to support agriculture. Too dry or barren to support vegetation.
Aridity index	Numerical indicator for the degree of dryness for a given locality. Used to divide South Africa into arid, semi-arid, dry sub-humid, moist humid and humid zones.
Biodiversity	Diversity with respect to ecosystems, species and genetics. Variety of life.
Biome	Geographical and climatic defines area, with similarities in plant communities, animal communities and soil organisms.
Biotic	In connection or as a result of living organisms.
Drought	A critical water shortage with respect to supply, demand and availability.
Ecology	The scientific study of living organisms, processes controlling their distribution and abundance, their relationship with the environment as well as one another.
Edaphic	Influenced by factors inherent in soil (substrate), rather than climatic factors.
Ephemeral	Perennial plants with a short growth and reproduction phase, emerging in spring after rainfall.
Extractant	A liquid that are used to remove a solute from a solution.
Geostationary	A satellite moving in a geosynchronous orbit in the plant of the equator, appearing stationary above a fixed point.
Grazing capacity	The true number of animals supported by the vegetation of a specific area for a defined time.
Lithostratigraphy	Geological science associated with the study of rock layers, with geochronology, comparative geology and petrology as the main focus areas.
Saline soils	A non-sodic soil with sufficient soluble salt to affect the growth of vegetation. Defined by an Electrical Conductivity higher than 400 mS/m and an exchangeable sodium percentage lower than 15%.
Semi-arid	Partially arid or semi-dry area characterised by the growth of short grasses and shrubs.
Spatial autocorrelation	The measurement of sample similarity for a specific variable as a function of spatial distance. A generalization exists, stating that the values of samples taken in close proximity are generally more uniform than those taken further apart.
Strata	Layers of sedimentary rock or soil with internal characteristics separating it from other layers.
Terrane	A fragment of crustal material associated with a tectonic plate.
Thrust	A type of fault where the lower stratigraphic units are pushed up and over higher strata.

CHAPTER 1

CONCEPTUALISATION

1.1 Background

According to the staff from the Center for Brains, Minds and Machines (2017), one of the aspects which have been impossible to replicate in artificial intelligence systems is the ability of human kind to perform pattern recognition tasks by applying limited amounts of information with limited training. In nature, patterns can be recognised with respect to vegetation composition in accordance with various determining factors. The question however remains as to how these vegetation differences have developed.

Since the early 1900's scientists have investigated the different factors that play a part in biodiversity and species richness with respect to vegetation composition (Tansley & Rankin, 1911). According to Cottle (2004) and Lundqvist (1968) the most important factors influencing vegetation composition, richness and diversity include geology, soil, climate, topography as well as anthropogenic influences. The existence of an integrated relationship between these factors, governing any changes that occur within this system is definite. Based on current knowledge a diagram (Figure 1-1) was constructed to illustrate the integrated relationship between vegetation differences, soil properties, geology, topography and climate.

Geology has an influence on soil type, surface stability and functionality, topography, sediment transportation as well as vegetation units (Figure 1-1) (McDonald *et al.*, 1996; Shen *et al.*, 2000; Wentworth, 1981). Soil type affects the surface stability and functionality, sediment transportation as well as vegetation composition (Austin, 2002; Bezuidenhout, 2009; Pausas *et al.*, 2003; Tilman, 1982). Soil characteristics including particle size distribution (PSD), porosity, water retention, water holding capacity and nutrient status have an impact on vegetation composition, whereas surface stability and functionality contributes to solely vegetation composition (Billings, 1950; Dengler *et al.*, 2012; Reitalu *et al.*, 2014; Tansley & Adamson, 1925). Climate contributes to both vegetation composition and sediment transportation (weathering rates) (Cottle, 2004; Knight *et al.*, 1982; O'Brien, 1993; Richerson & Lum, 1980), whilst sediment transportation exerts a direct effect on surface stability and functionality, and an indirect effect on topography and vegetation composition. Topography directly affects vegetation, soil type, surface stability and surface functionality, and indirectly affects sediment transportation (Bennie *et al.*, 2008; McCune & Kean, 2002; Shen *et al.*, 2000). Vegetation has a direct influence on sediment transportation as well as surface stability and functionality.

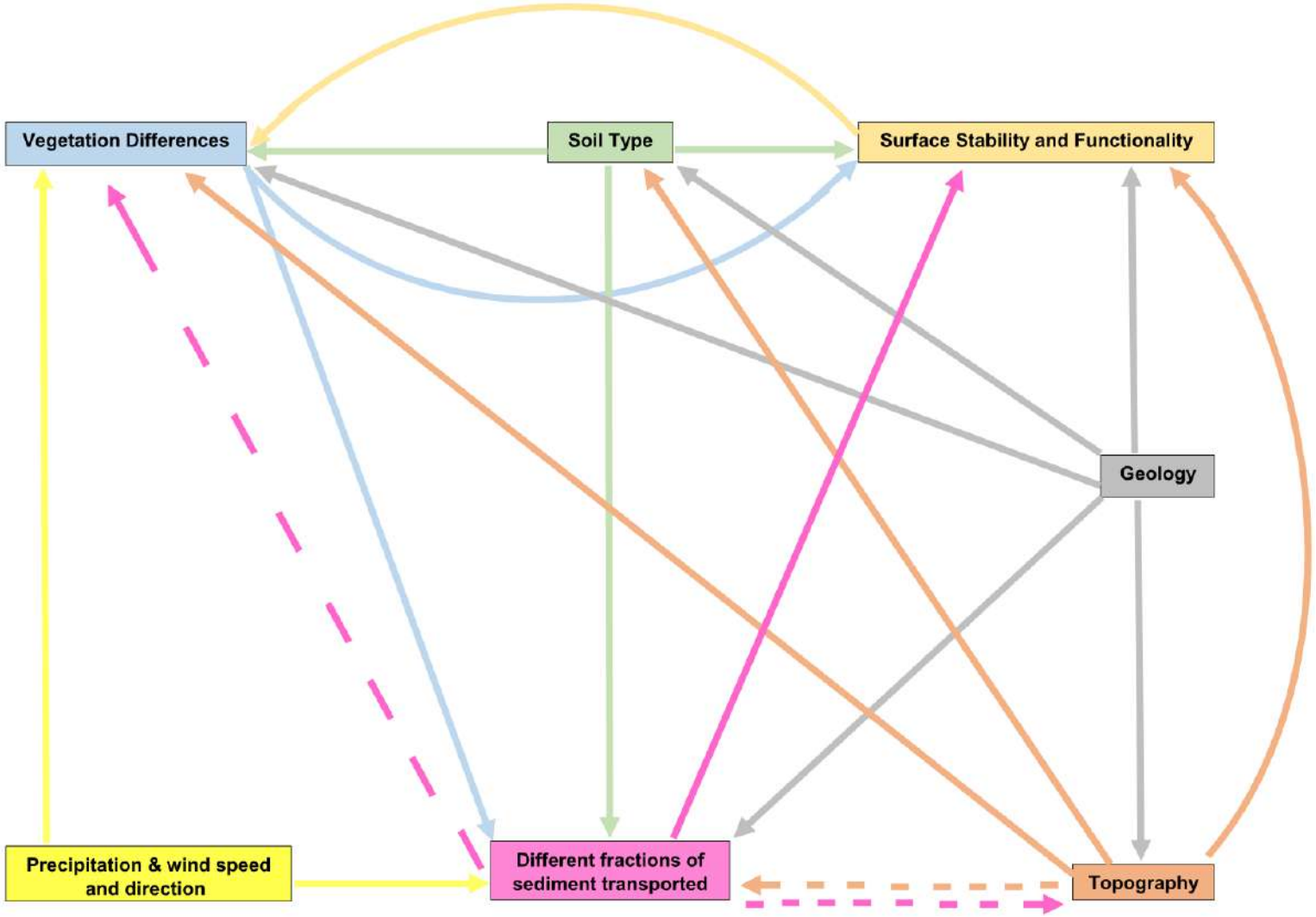

Figure 1-1: Integrated relationship between factors governing changes in vegetation.

1.2 Research Value and Purpose

When the vegetation type, substrata as well as lithological patterns for a specific area is well understood, new relationships between these variables can be identified. This identification method is considered as economically important due to the amount of information obtained by a basic surficial reconnaissance survey. The purpose of this research is to contribute to a data base, with respect to vegetation, soil and geology interrelationships, used for future studies in the semi-arid Bushmanland region of South Africa.

1.3 Research Aims and Objectives

1.3.1 General Aim

The aim of this study is to determine whether there are correlations between vegetation, soil and geology in the semi-arid Bushmanland region of South Africa. Variations in vegetation are governed by differences in geology, soil properties, climate, topography as well as anthropogenic influences. This study area was chosen due to its homogenous climate, topography and anthropogenic influences as well as its plant diversity and variations in soil and geology.

1.3.2 Objectives

In order to fulfil the aim of this project, the following objectives were formulated:

- Identify variations in species composition with vegetation mapping.
- Identify differences in local soil forms by means of soil identification, classification and mapping.
- Investigate the soil properties that govern differences between different soil forms.
- Identify geological differences by means of geological descriptions and mapping.
- Integrate the results obtained from the above four objectives to establish the relationship between geology, soil and vegetation.

1.4 Basic Hypothesis

Previous research has shown that relationships in nature between different environmental factors do exist. For example, Cottle (2004) wrote an entire book on the relationships between geological variations and vegetation differences in the English Highlands. In the semi-arid Bushmanland region of South Africa, *Rhigozum trichotomum* is typically associated with small drainage systems, while grasslands are found on calcareous soils. This lead to the assumption that three-tier relationships between the vegetation, soil and geology exist in the Bushmanland region.

1.5 Study Area

1.5.1 Site Locality

The study was conducted on an area of approximately 1032 ha located roughly 60 km south south-west of Kakamas in the Northern Cape of South Africa (Figure 1-2).

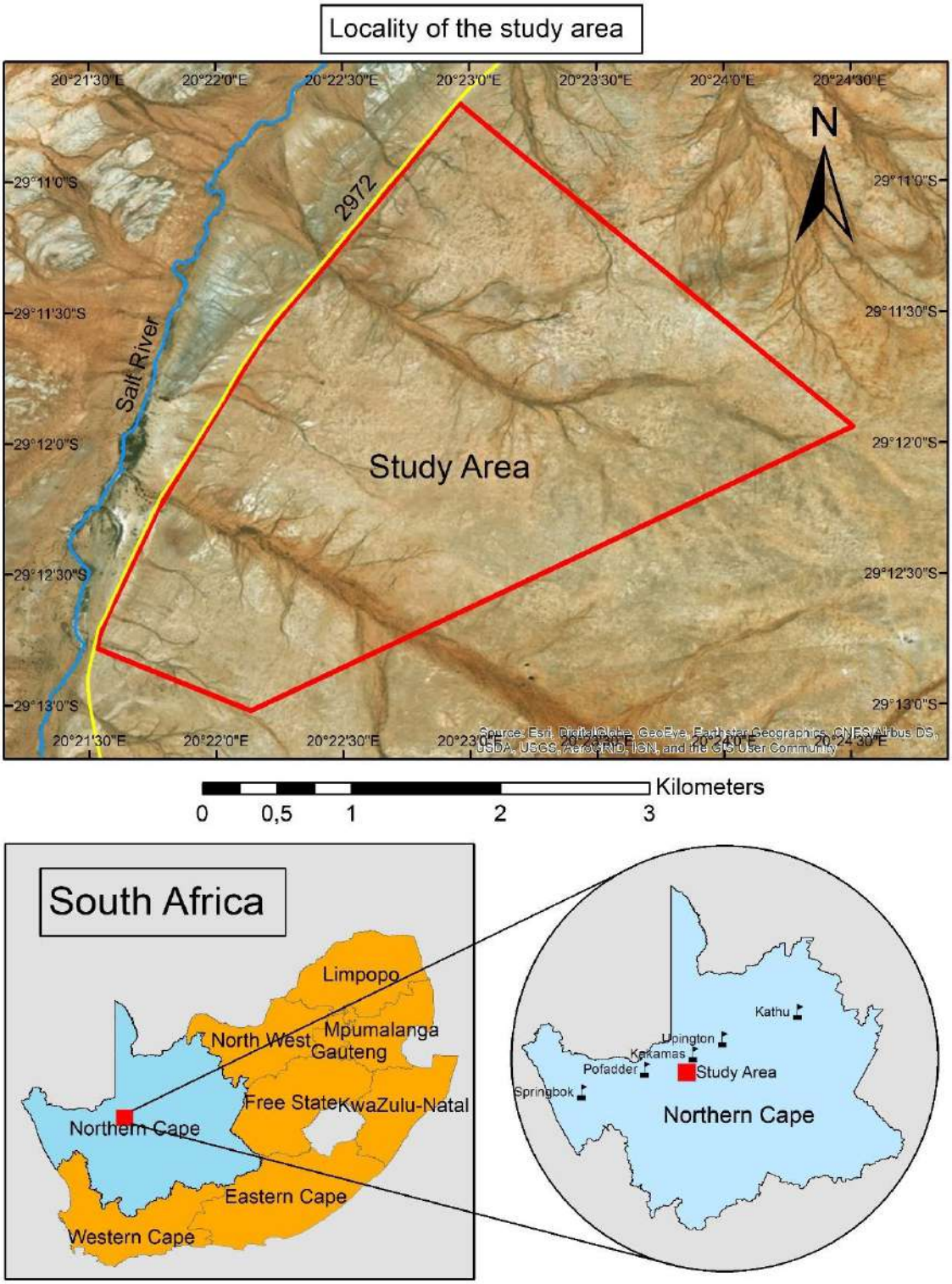

Figure 1-2: Locality map of the study area (Red line: The boundaries of the study area) (Google Earth, 2016).

This area lies south-east of the Kakamas-Loeriesfontein dirt road which is parallel to the Salt River. This site was chosen based on the homogenous climate and topography, minimal anthropogenic influences, as well as its plant diversity and richness in soil- and geological differences. As mentioned, these are some of the most influential factors affecting vegetation composition. Due to the prevailing homogenous climatic conditions as well as homogenous topography it can be assumed that the changes in vegetation composition and species richness on this site are due to the variation in geology and soil properties. This investigation will not focus on the geochemical-, physical-, pedophysical- or mineralogical properties of geology and soil, but rather concentrate on the variation in geological lithostratigraphy, soil forms and soil groups within this area.

1.5.2 Geology

Geology plays an important role in the integrated relationship between environmental factors through its contribution to soil formation and topography. The local geology of this area will be discussed based on the descriptions given by Cornell *et al.* (2006), Moore *et al.* (1990), South African Committee for Stratigraphy (SACS, 1980) as well as Thomas *et al.* (1994).

The study area falls within the geological province known as the Bushmanland Terrane, which forms part of the Namaqua Sector within the Namaqua-Natal Metamorphic Province. The Namaqua-Natal Metamorphic Province is a large area of contiguous structural fabric formed during a tectonic metamorphic event. The Bushmanland Terrane covers approximately 60 600 km^2 and is known as the largest crustal block in the Namaqua Sector. It is comprised of granitic gneisses (~2000 Ma), supracrustal rocks of amphibolite to granulite grade (1600 – 1200 Ma) and granitoids (1200 – 1000 Ma). The Groothoek Thrust and Wortel Belt form the northern boundary of the Bushmanland Terrane, and the Hartbees River Thrust the eastern boundary (Cornell *et al.*, 2006).

A description of the regional geology is provided in Chapter 2 and the local geology is discussed in Chapter 6.

1.5.3 Soil

Soil forms the intermediate medium between geology and vegetation and has a great influence on plant ecology and diversity. According to McDonald *et al.* (1996) and Shen *et al.* (2000) soil properties in return are highly dependent on environmental factors like geology, climate and topography.

Land type data entails the division of land into land types, typical terrain cross sections and dominant soil types for each terrain unit (consult Annexure C Figure C-1 for more information).

One land type (Ag3) dominates the entire study area. According to the Land Type Survey Staff (2003), 40% of land type Ag3 consists of freely drained, shallow (< 300 mm deep), red, eutrophic, apedal soils, with yellow-brown soils comprising less than 10% of this land type. The average depth of all soils is 280.5 mm. Approximately 77% of land type Ag3 consist of soils with a depth of ≤ 300 mm (depth class D1), whereas 12.5% consist of soil with a depth of 901 mm to 1200 mm (depth class D4). The average topsoil clay percentage of land type Ag3 is 10.7%. Around 88.5% of land type Ag3 consist of loamy sand soils (clay class C2), with an average clay percentage of 6.1% to 15% in the topsoil, whilst 1% consist of sandy loam soils (clay class C3) with an average clay percentage of 15.1% to 25% in the topsoil (Land Type Survey Staff, 2003).

A detailed discussion of the soil descriptions and classification for this study area is provided in Chapter 5.

1.5.4 Vegetation

According to Cowling and Roux (1987) variations in vegetation are governed by environmental factors including geology, soil properties, topography, climate as well as anthropogenic influences. The area under investigation (semi-arid Bushmanland region) forms part of the Nama Karoo Biome (Bezuidenhout, 2009). Based on the classification of Mucina and Rutherford (2006), the study area comprises mainly the Bushmanland Arid Grassland, the Bushmanland Sandy Grassland and the Bushmanland Basin Shrubland. The Bushmanland Arid Grassland is characterised by irregular plains dominated by *Stipagrostis* species. In some regions the vegetation structure is altered by low shrubs of *Salsola.* The Bushmanland Sandy Grassland is characterised by sandy grassland plains dominated by *Stipagrostis* and *Schmidtia* species. There is also a common occurrence of drought-resistant shrubs and after rainfall the display of ephemeral spring flora including *Grielum humifusum* and *Gazania lichtensteinii.* The Bushmanland Basin Shrubland is characterised by irregular plains dominated by shrubs including *Rhigozum, Salsola, Pentzia* and *Eriocephalus* as well as different *Stipagrostis* grass species. After rainfall *Gazania* and *Leysera* species may also be present (Mucina & Rutherford, 2006).

A detailed description of the vegetation as well as habitat and community classification is provided in Chapter 4.

1.5.5 Climate

Climate is considered one of the main attributing environmental factors determining vegetation composition and species richness. It also contributes to soil formation as well as soil moisture content and soil temperature regimes. For the purpose of climate descriptions, data from three weather stations were obtained (Weather Bureau, 2016). The localities of these weather stations are indicated in Figure 1-3.

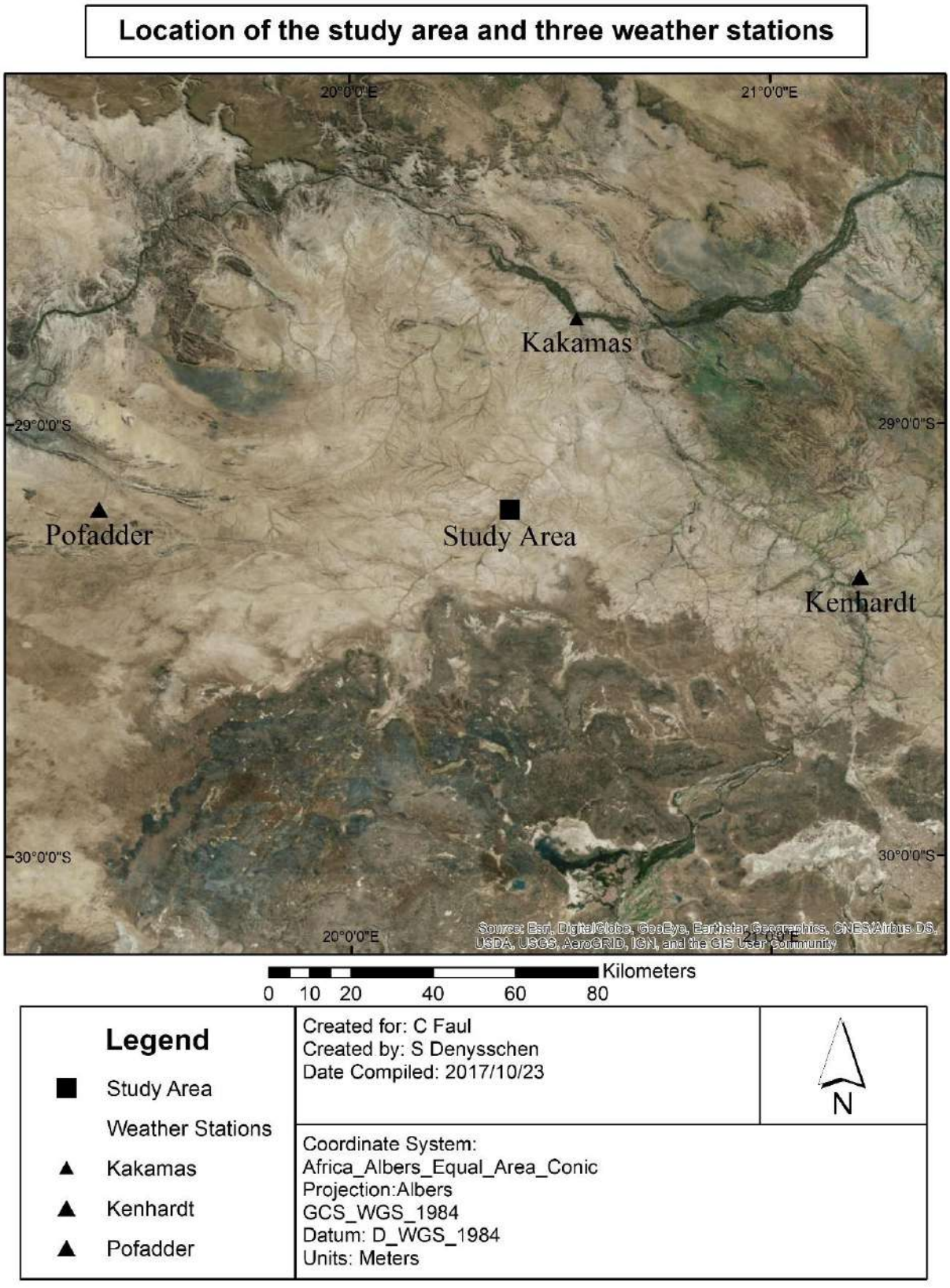

Figure 1-3: Map indicating the location of the study area, as well as the location of the weather stations where meteorological data were obtained (Google Earth, 2016).

The study area forms part of the semi-arid Bushmanland region and falls within the very late summer rainfall region (Schulze, 1997) with an annual rainfall (1992 – 2015) of 140 mm to 250 mm per annum (Weather Bureau, 2016) (Figure 1-4 and Figure 1-5).

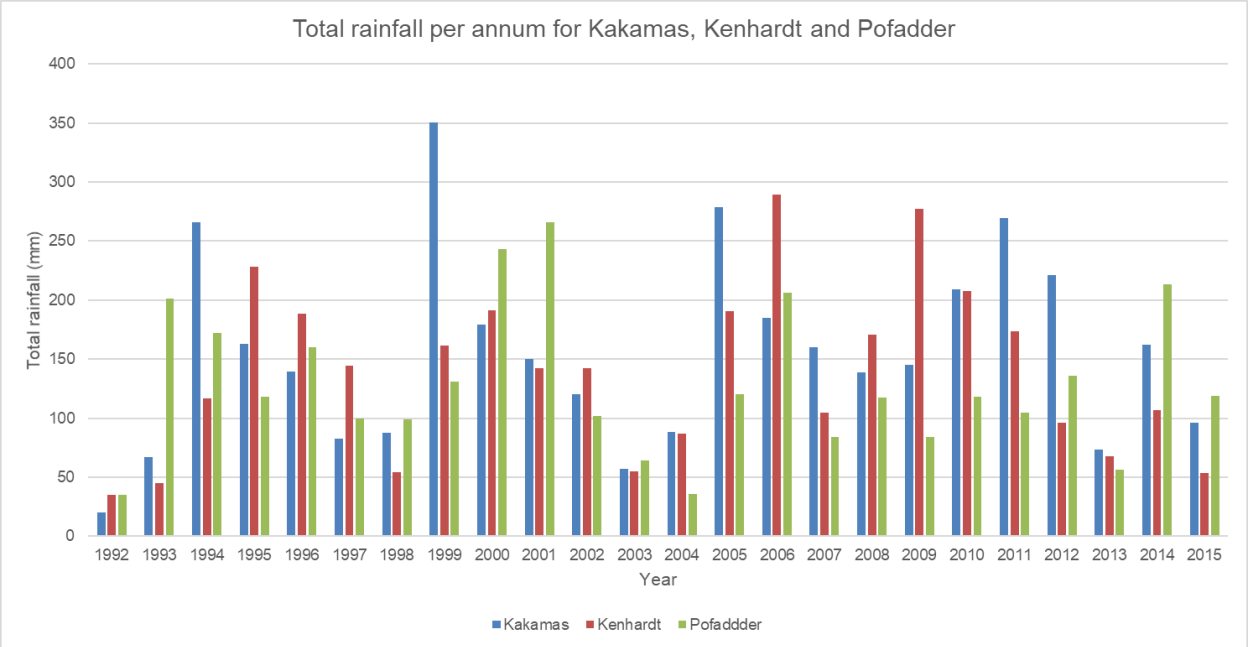

Figure 1-4: Total rainfall per annum for Kakamas, Kenhardt and Pofadder respectively (Weather Bureau, 2016).

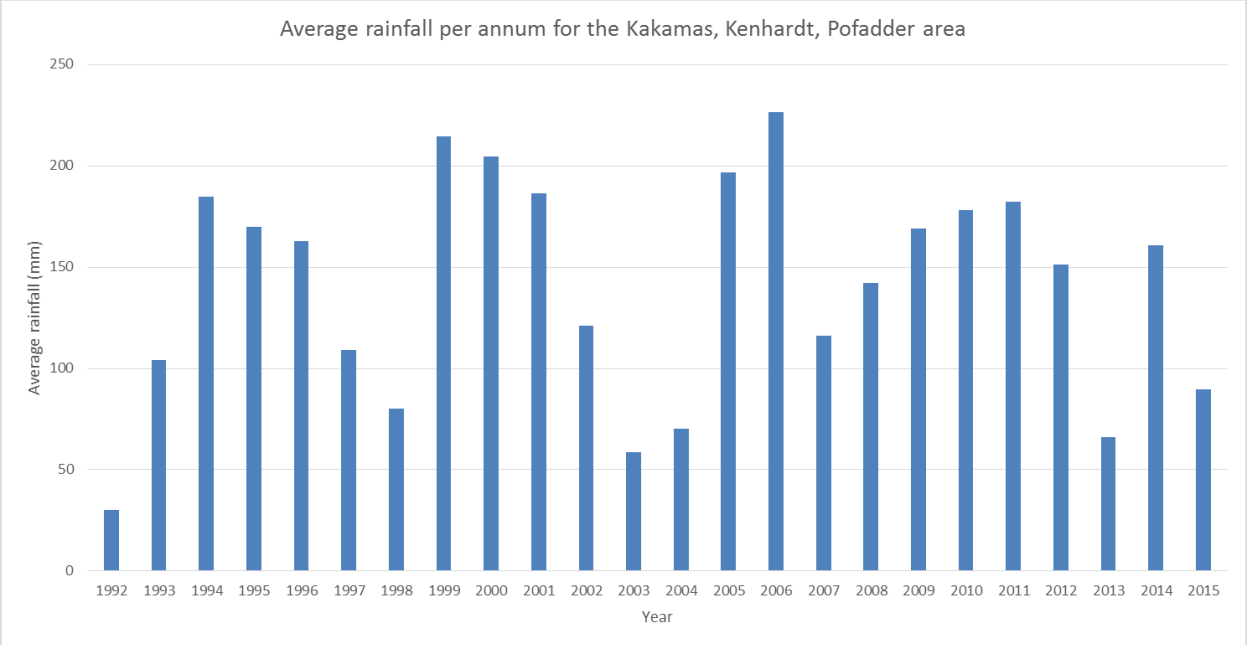

Figure 1-5: Average rainfall per annum for the Kakamas, Kenhardt and Pofadder area (Weather Bureau, 2016).

Figure 1-4 and Figure 1-5 revealed that severe drought conditions were experienced during 1992, 2003, 2004 and 2013. The variation in average temperatures within this area is extreme with maximum temperatures during the summer reaching up to 40.8 °C and minimum temperatures as low as -3 °C (Pillay & Swanepoel, 2013). Figure 1-6 illustrates the mean daily maximum temperatures (°C) for the Pofadder area while the mean daily minimum temperatures (°C) (measured at 8 am in the morning) for the same area are illustrated in Figure 1-7.

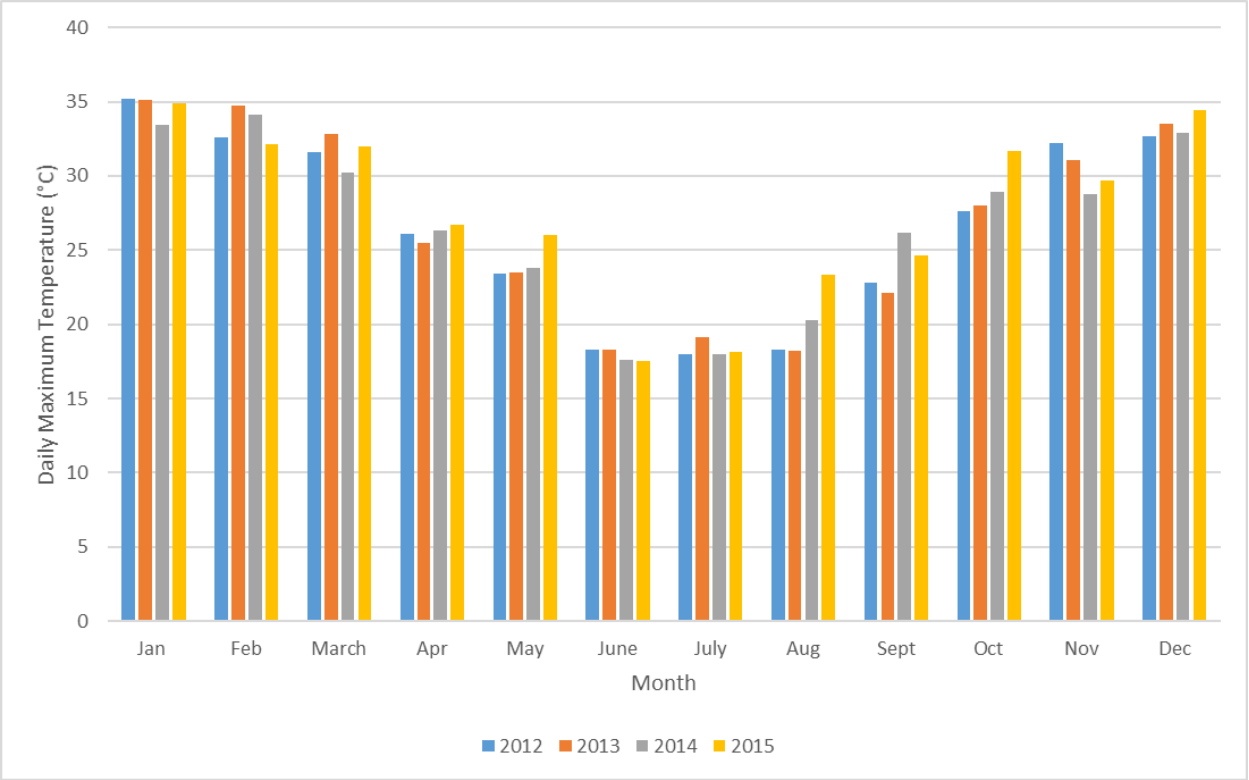

Figure 1-6: Mean daily maximum temperatures (°C) for the Pofadder area (Weather Bureau, 2016).

Mean daily maximum temperatures (Figure 1-6) range from 35 °C (January) to 17 °C (June) with daily minimum temperatures (Figure 1-7) ranging from 19 °C (February) to 4 °C (July). According to Mucina and Rutherford (2006) this site forms part of an area with a mean annual evaporation potential of 2771 mm per annum, experiencing between 21 and 30 mean frost days per annum.

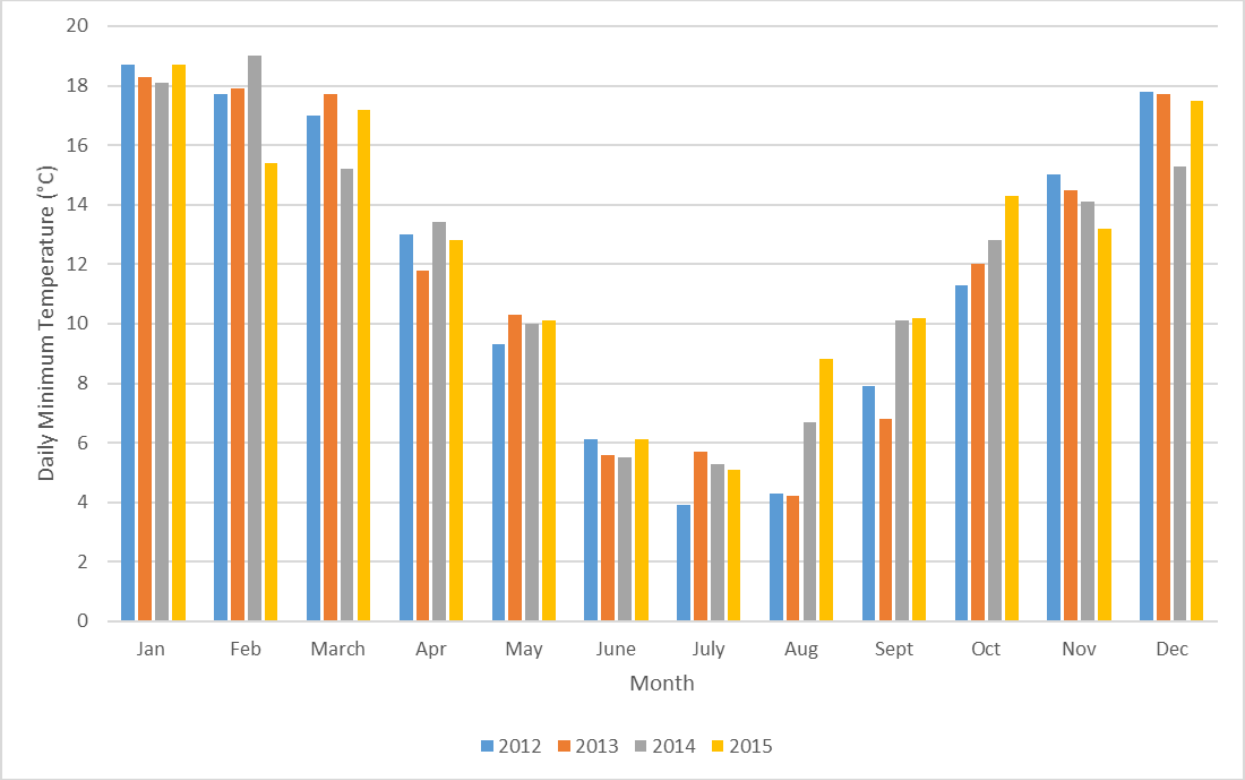

Figure 1-7: Mean daily minimum temperatures (°C) for the Pofadder area (Weather Bureau, 2016).

Due to the low precipitation and high evapotranspiration, moisture is considered one of the limiting factors for vegetation growth in this region and is relatively homogenous within the study area.

1.5.6 Topography

The overall topography of the site is relatively homogenous and ranges from 857 m to 880 m above mean sea level with the highest part of the landscape to the south-east and the lowest part to the north-west.

The area with the lowest elevation (north-west) lies south-east of the Salt River which is situated north-west of the study area. The Salt River flows to the north-east into the Hartbees River which eventually connects to the Gariep River.

1.5.7 Anthropogenic Influences

Anthropogenic influences are considered important attributes for habitat diversity and soil erosion. Most regions of southern Africa are susceptible to soil erosion and changes in natural habitats due to anthropogenic influences.

Natural vegetation has been subjected to various anthropogenic influences including livestock grazing, cultivation, burning, field or woodland management as well as the development of

infrastructure. Due to low agricultural potential of the semi-arid regions of southern Africa these areas are used for grazing (sheep) purposes. The grazing capacity of the proposed study area is low with approximately 40 ha per large stock unit (AGIS, 2007).

1.6 Dissertation structure and content

This dissertation attempts to prove the existence of three-tier relationships between the vegetation, soil and geology in the semi-arid Bushmanland region of South-Africa.

The dissertation is structured as follows:

Chapter 1 introduces the study by discussing the background as well as the aims and objectives.

Chapter 2 contains a literature review relating to previous research about correlations in nature as well as the attributing factors that governs variations in vegetation structure, vegetation distribution and species composition.

Chapter 3 explains the sampling techniques used to obtain data as well as the materials and methods that were used to process this data and information.

Chapter 4 provides results obtained from vegetation identification as well as habitat and plant community classification.

Chapter 5 provides detailed soil descriptions as well as soil identification, soil classification and physical and chemical data.

Chapter 6 provides a detailed geological report describing the local geology by means of field identification as well as petrographic descriptions and geological mapping.

Chapter 7 assesses the results obtained from Chapter 4, Chapter 5 and Chapter 6 by means of maps and diagrams, identifying and quantifying correlations.

Chapter 8 discusses the outcomes in relation to the aims and objectives of this study and provides a conclusion as well as recommendations for future research.

CHAPTER 2

LITERATURE REVIEW

This chapter focuses on providing background information with respect to the regional geology, soil and vegetation in order to create a framework for further interpretations and predictions. It also addresses the results of previous research regarding the correlations between vegetation differences in accordance with the associated controlling factors.

2.1 Correlations between vegetation differences and environmental factors

As described in Chapter 1 the main aim of this study is to establish if there are relationships between the vegetation, soil and geology in the semi-arid Bushmanland region of South Africa. The investigation of factors governing plant biodiversity and species richness has been a pronounced field of research since the early 1900's (Tansley & Rankin, 1911). Cottle (2004) also stated that clear broad relationships between the chemical and physical geological attributes and vegetation exist. Hence floral descriptions and definitions can be used to determine the geology of an area.

Plant species have different needs for nutrients, moisture as well as the amount of radiation that it receives. Therefore, the species composition for each environment will differ according to the chemical-, physical- and anthropogenic properties of that environment which include geological properties, soil properties, climate, topography as well as anthropogenic influences. According to Sagar *et al.* (2003) as well as Lavers and Field (2006) [cited by Toure *et al.*, 2015] differences in plant communities and biodiversity is controlled by abiotic and biotic factors.

In South Africa various studies have been conducted confirming correlations between vegetation patterns and environmental factors. Siebert *et al.* (2003) conducted a study in the Potlaka Nature Reserve and the surrounding areas in Sekhukhuneland, South Africa. From this study it was concluded that the species composition of plant communities correlates with certain environmental factors with the emphases being on soil depth, soil structure, rock cover and moisture availability. Bezuidenhout (2009) conducted a study in the Northern Cape Province where it was found that the identified soil type-cum-habitats correlated with the plant communities. Table 2-1 illustrates examples of international studies that found correlations between vegetation and environmental factors.

Table 2-1: Research that proved the existence of correlations between vegetation and environmental factors.

Reference	Supporting results
Tansley and Adamson, 1925	Tansley and Adamson (1925) found that the variety of herbaceous species increases with increasing soil depth, humus and water content.
Billings, 1950	According to Billings (1950), variations in physical soil properties will result in compositional differences and differences in patterns of climax plant species.
Mooney, 1966	Mooney (1966) found an edaphic difference for two *Erigeron* species, with *Erigeron clokeyi* occurring only on sandstone and *Erigeron pygmaeus* occurring only on dolomite.
Jarvis and Pigott, 1973	According to Jarvis and Pigott (1973), rock type and the chemistry thereof primarily control lichens.
Jarvis, 1974	Jarvis (1974) found that topographical factors and associated soil properties extensively control the development of plant communities.
Huston, 1980	Huston (1980) established correlations between tree species richness and variations in soil nutrients.
Wentworth, 1981	According to Wentworth (1981), differences in elevation, geology and soil at the Mule Mountains in Arizon resulted in differences in plant communities.
Tilman, 1982	According to Tilman (1982), soil properties play a significant role in flora structure and composition.
Boyle *et al.*, 1987	Boyle *et al.* (1987) found that lichen flora communities are good indicators of the chemical properties of substrate.
Kruckeberg, 2002	Kruckeberg (2002) found that species dominance (desert, Sierre Navada, California) differed according to geological differences, with *Artemisia tridentate* dominating on sandstone and *Pinus longaeva* dominating on dolomite.
Raina and Gupta, 2009	Raina and Gupta (2009) found correlations in the Mussoorie Forest of Uttarakhand between geology and soil and also between soil and vegetation. *Quercusleuco trichophora* and *Pinus roxburghii* only occurred on mollisols while *Dalbergia sissoo* was only found on ultisols.

Research dating back to 1925 suggests an integrated relationship between vegetation and sub-strata.

2.2 Geology

Geology is one of the most important attributes contributing to the maintenance of all living things by providing nutrients for vegetation growth by means of soil formation. In return vegetation is key for sustaining life on earth. Therefore, geology forms part of an integration between various factors

crucial for the survival of both animal and human. This section presents a background of the regional geology of the applicable area.

2.2.1 Kaapvaal Craton

The Kaapvaal Craton is dated at approximately 3000 Ma and is considered responsible for the deformation of the Namaqua-Natal Metamorphic Province (Shunqukela, 2014) currently situated to its west, southwest and south (Thomas *et al.*, 1994).

2.2.2 Namaqua-Natal Province

The name “Namaqualand Metamorphic Complex” was approved by the South African Committee of Stratigraphy (SACS) in 1980 for the lithostratigraphic units of this area (Visser, 1998). However, in 1984 the name “Namaqua-Natal Province” was proposed by Stowe *et al.* (1984) [cited by Visser, 1998].

The Namaqua-Natal Province is divided into two sectors known as the Namaqua Sector (area of ~ 100 000 km^2) and the Natal Sector (area of ~ 20 000 km^2). In the eastern part of the Namaqua Sector the metamorphic grade varies from upper amphibolite facies to granulite facies to greenschist facies. The syn-tectonic and post-tectonic Koras Group is overlain to the northwest by the sediments of the Nama Group (Pan African age) which are in turn covered by Glaciogenic sediments from the Permo-Carboniferous Dwyka Group. This area is overlain by extensive calcrete deposits which are covered by sediments of mixed origin from the Kalahari Group (Moen, 2007).

Moen (2007) subdivided the Namaqua Sector into four subprovinces recognised as the Richterveld Subprovince, Bushmanland Subprovince, Gordonia Subprovince and Kheis Subprovince (Figure 2-1); whilst Cornell *et al.* (2006) identified five subprovinces known as the Richtersveld Subprovince, Bushmanland Terrane, Kakamas Terrane, Areachap Terrane and Kaaien Terrane (Figure 2-2).

The study area falls within the Bushmanland Subprovince (Moen, 2007) or the Bushmanland Terrane (Cornell *et al.*, 2006). According to Joubert (1986) and Geringer *et al.* (1986), this subprovince is recognised as the crustal block that collided with the Gordonia cratonic block during the Namaqua Orogeny. In Table 2-2 the regional geology as well as the structural geology and metamorphism of the Bushmanland Subprovince and Bushmanland Terrane are discussed.

Table 2-2: Description of the regional geology, structural geology and metamorphism.

	Bushmanland Subprovince **(**Boelema, 1994; Eglington, 2006; Hartnady *et al.*, 1985; Joubert, 1974, 1981, 1986; Moen, 2007; Stowe, 1986; Tankard *et al.*, 1982; Thomas *et al.*, 1994; Visser, 1998**)**	**Bushmanland Terrane** **(**Cornell *et al.*, 2006; Moore *et al.*, 1990; SACS, 1980; Thomas *et al.*, 1994**)**
Geology	The Bushmanland Subprovince is separated from the Gordonia Subprovince by the Hartbees River Thrust, with the Kameel Puts Formation covering the centre Rietput Formation. The Kameel Puts Formation in return is overlain by the Droëboom Group. The footwall of the Hartbees River Thrust is represented by the Brakwater Metamorphic Suite. Within the gneisses of the Brakwater Metamorphic Suite, bodies of impure marble are found as part of the Kameel Puts Formation. The Bushmanland Subprovince is divided into three terranes known as the Aggeneys-, Okiep- and Garies Terranes. The study area falls within the Aggeneys Terrane which consists of para- and orthogneisses, granulites and granitoids. The Aggeneys Terrane is subdivided into the following lithostratigraphic subdivisions: - Droëboom Group north of Vogelstruislaagte shear zone; and - Bushmanland Group to the south (characterised by a quartzite-schist-banded iron-formation association, overlain by pink gneiss that originated from an arkosic, thyolitic or granitic protolith). Numerous stratiform deposits and vein deposits were identified within the Bushmanland Subprovince: - The De Tuin Noord Ag-Pb-Cu-Zn deposit; - The Adjoining Geelvloer Pb-Zn-Cu-Au-Ag deposit; - The Grootriet iron deposit; - The De Uitkyk Boven De Kalkgaten W deposit; and - The Pypklip West F deposit.	The Bushmanland Terrane lies west of the Kakamas Terrane and south of the Richterveld Terrane. The eastern boundary is defined by the Hartbees River Thrust, while the northern boundary is defined by the Groothoek Thrust and the Wortel Belt. This terrane lies on an Eburnean basement and its domains are made of deformed supracrustal volcano-sedimentary sequences intruded by granitoids. The Bushmanland Terrane is characterised by pink gneiss characteristic of the Hoogoor Suite. The Bushmanland Terrane is divided into three age groups. - The reworked Kheisian strata include the Gladkop Suite (fine-grained granodiorite-granite) in the Steinkopf area and the Achab Gneiss (a megacrystic granitoid) in the Pofadder area. Associated xenoliths of amphibolite, calc-silicates and quartzites are found in both areas. - The young, deformed supracrustal and plutonic rocks occur in the Bushmanland Terrane as several discontinuous east-west trending belts dominated by quartzofeldspatic gneiss, metavolcanic rocks with a composition of rhyolite to dacite, quartzite and mica-sillimanite schist or cordierite-rich gneiss. - Some of the suites of syn- and late-tectonic Namaquan intrusive rocks include: 1. The TÓubep Suite (~1200 Ma): West of Kenhardt consisting of late-tectonic granitoids and metabasite; and 2. The Nouzees Complex and Wortel Suite (~1060 – 1030 Ma): Plug- and sill-like basic plutonic intrusions southeast and northwest of Pofadder, that form clusters consisting of olivine-bearing metapyroxenites.

Table 2-2 (continued): Description of the regional geology, structural geology and metamorphism.

	Bushmanland Subprovince **(**Boelema, 1994; Eglington, 2006; Hartnady *et al.*, 1985; Joubert, 1974, 1981, 1986; Moen, 2007; Stowe, 1986; Tankard *et al.*, 1982; Thomas *et al.*, 1994; Visser, 1998**)**	**Bushmanland Terrane** **(**Cornell *et al.*, 2006; Moore *et al.*, 1990; SACS, 1980; Thomas *et al.*, 1994**)**
Structural geology and Metamorphism	The Bushmanland subprovince has been subjected to deformation events: F_1, F_2, F_3, F_4 and shear deformation. F_1 – Exemplified by intrafolial folds with disjointed limbs and sharp hinge zones, as well as consistently discontinuous bending of banded rocks. F_2 – The main phase known for its economic importance. Exemplified by thrusting towards the southwest and south a variety of folds with large amplitudes and short wavelengths with dominant mineral lineation parallel to the axes of the folds. Post-F_2 and pre-F_3 thrusts west of Kenhardt are recognised by ultramylonite, mylonite, blastomylonite and calc-silicate gneiss. F_3 - The development of large, open flexural-slip type folds and brachystructures resulting in movement and shearing along existing S_2 foliation planes. New foliation obliques and flexural-slip thrusts developed which resulted in pegmatite emplacement. F_4 – Exemplified by monoclonal folds with associated shear zones and fractures, together with associated pegmatites and quartz veins. The monoclinical structures between Kakamas and Kenhardt are overfolded with associated reverse faults that branched from shear zones. Later shear deformation – Some of the most pronounced shearing is associated with conjugate shears like the Steenbok Shear Zone, the Pofadder Lineament (with its Rooidam and Rozynenbosch Shears) which are regarded as D_4 fractures, the Ratelpoort Shear Zone and the Buffels River Shear Zone.	The Bushmanland Terrane is associated with two major tectonic episodes: D_2 and D_3. The deformation event D_1 was found in the metasedimentary xenoliths at Aggeneys and in the Gladkop Suite. Speculations of the presence of pre-1800 Ma supracrustal sediments were based on this theory, which led to the correlation of D_1 structures with deformation in the Richtersveld Subprovince. A heterogeneous, sub-horizontal fabric parallel to the axial planes of east-trending folds was produced by the D_2 deformation event, which dominates regionally and ended around 1060 Ma. The Bushmanland Terrane is characterised by a metamorphic grade that ranges from upper amphibolite facies, occurring in the north, north-east and south of the terrane, to upper granulite facies which occur in an east north-east trending belt in the south. The upper amphibolite facies have typical pressures and temperatures of 4 kbar and 650 - 700°C, whilst that of the upper granulite facies is 5 – 7 kbar and 830°C.

Table 2-2 (continued):Description of the regional geology, structural geology and metamorphism.

	Bushmanland Subprovince (Eglington, 2006)	**Bushmanland Terrane** (Cornell *et al.*, 2006)
Metamorphic history	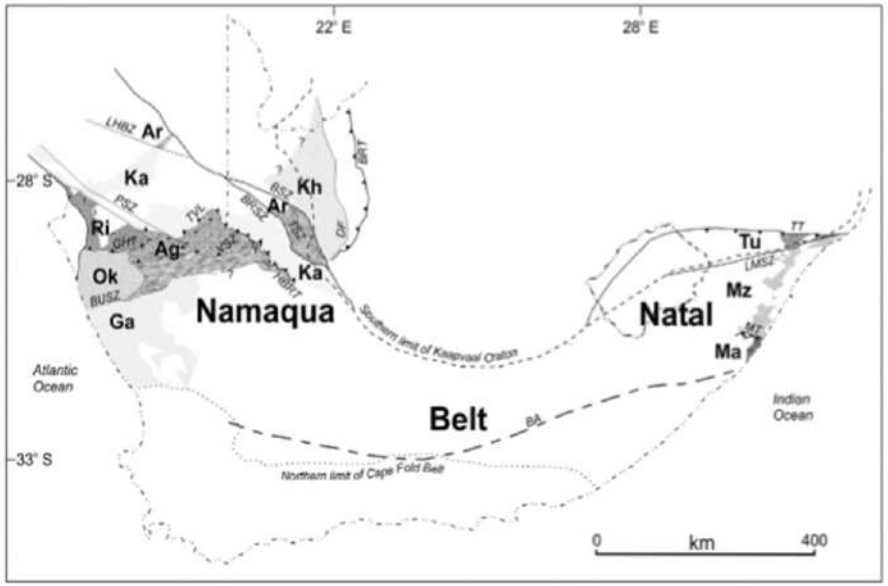 Figure 2-1: Regional extent of the Namaqua-Natal Belt with respect to sub-provinces and terranes comprising the belt (Eglington, 2006). **Ri** – Richtersveld sub-province; **Bushmanland sub-province: Ag** – Aggeneys terrane, **Ga** – Garies terrane, **Ok** – Okiep terrane; **Gordonia sub-province: Ar** – Areachap terrane, **Ka** – Kakamas terrane; **Kh** – Kheis sub-province; **Natal sub-province: Ma** – Margate terrane, **Mz** – Mzumbe terrane, **Tu** – Tugela terrane. **Thrusts, faults and shear zones: BA** – Beattie anomaly, **BRSZ** – Bovenrugzeer shear zone, **BRT** – Blackridge thrust, **BSZ** – Brakbosch shear zone, **BUSZ** – Buffels **River shear zone: DF** – Dabep fault, **GHT** – Groothoek thrust, **HBRT** – Hartbees River thrust, **LHBZ** – Lord Hill Boundary Zone, **LMSZ** – Lilani-Matigulu shear zone, **MT** – Melville thrust, **PSZ** – Pofadder shear zone, **TSZ** – Trooilapspan shear zone, **TT** – Tugela thrust, **TVL** – Tantalite Valley line, **VSZ** – Vogelstruislaagte shear zone.	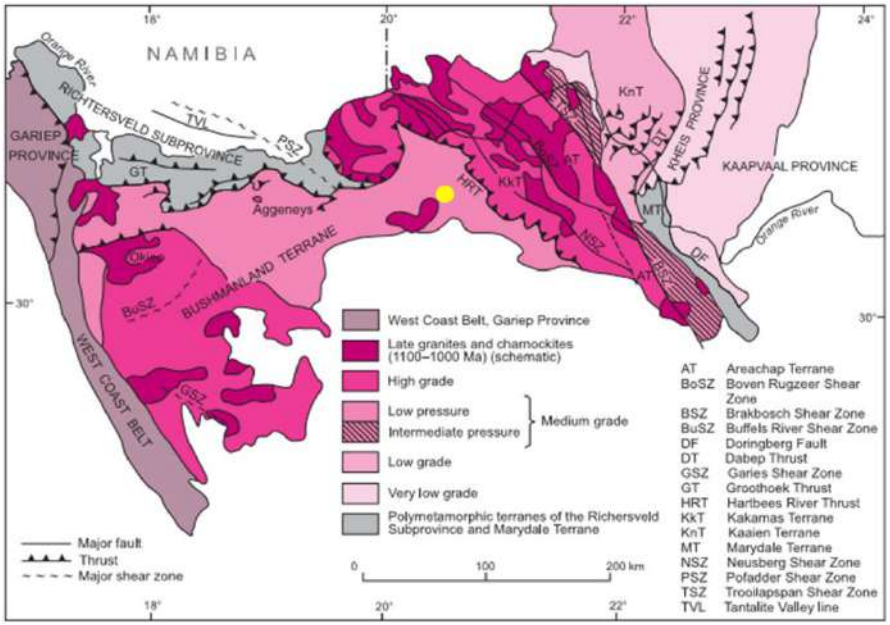 Figure 2-2: Map indicating metamorphism in the Namaqua Sector and the Kaapvaal Craton (Cornell *et al.*, 2006). [The locality of the study area is indicated in yellow (Figure 2-2)].

2.2.3 Cenozoic Deposits

2.2.3.1 Calcretes

The distribution of pedogenic deposits depends on the climate of the area. De Martonne (1926) proposed a method that was used to identify five climate zones in South Africa in order to establish aridity index values. Figure 2-3 illustrates the aridity index map of South Africa which divides the country into arid, semi-arid, dry sub-humid, moist sub-humid and humid zones.

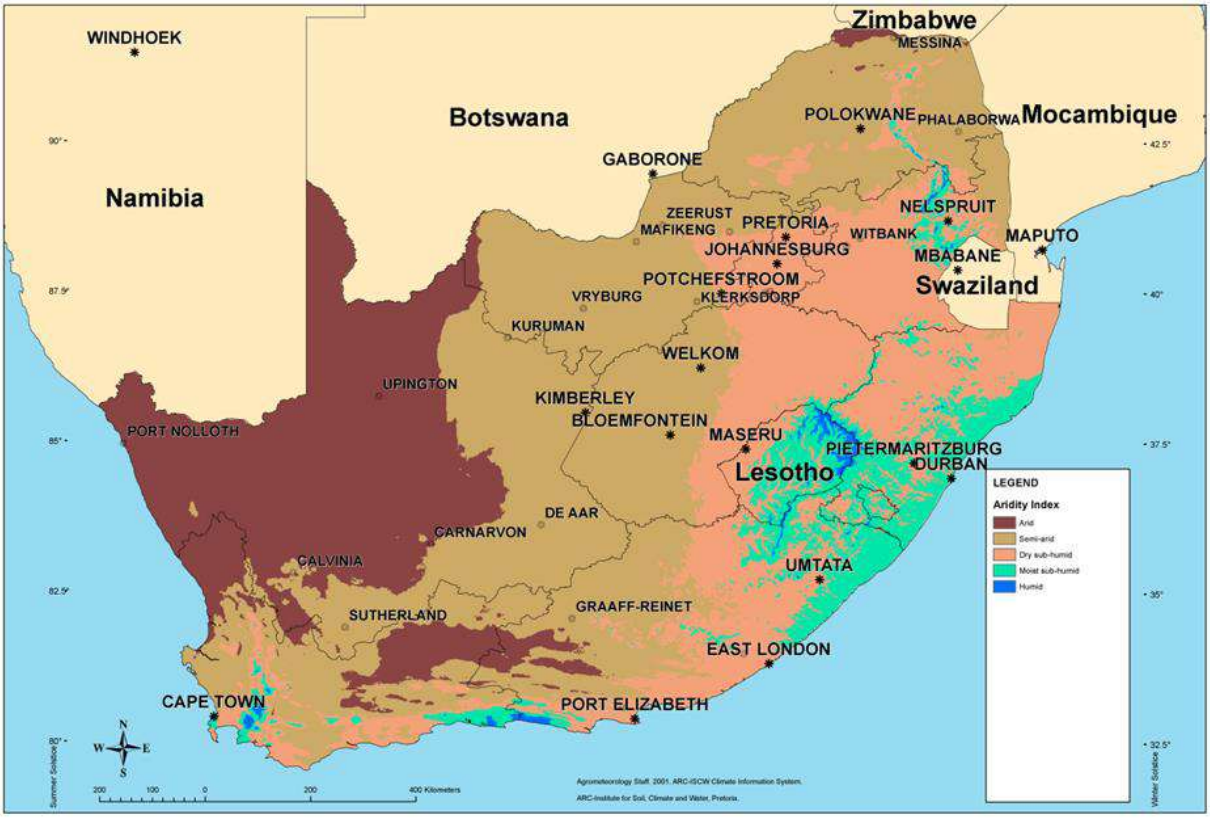

Figure 2-3: Aridity index map of South Africa (Spatial temporal evidence for planning South Africa, 2016).

Weinert (1980) proposed a modified approach, the N-value ($N = 12E_J / P_a$), which represents the ratio of evaporation during the warmest month (E_J) to the annual precipitation (P_a). This value indicates the effect of climate on weathering. Figure 2-4 illustrates the distribution of pedogenic material according to the N-value. Decomposition occurs in areas with an N-value of less than 5 (typically more humid regions of southern Africa) whereas areas with an N-value of more than 5 (more arid environments) is dominated by disintegration hence physical weathering (Weinert, 1980; Weinert, 1984).

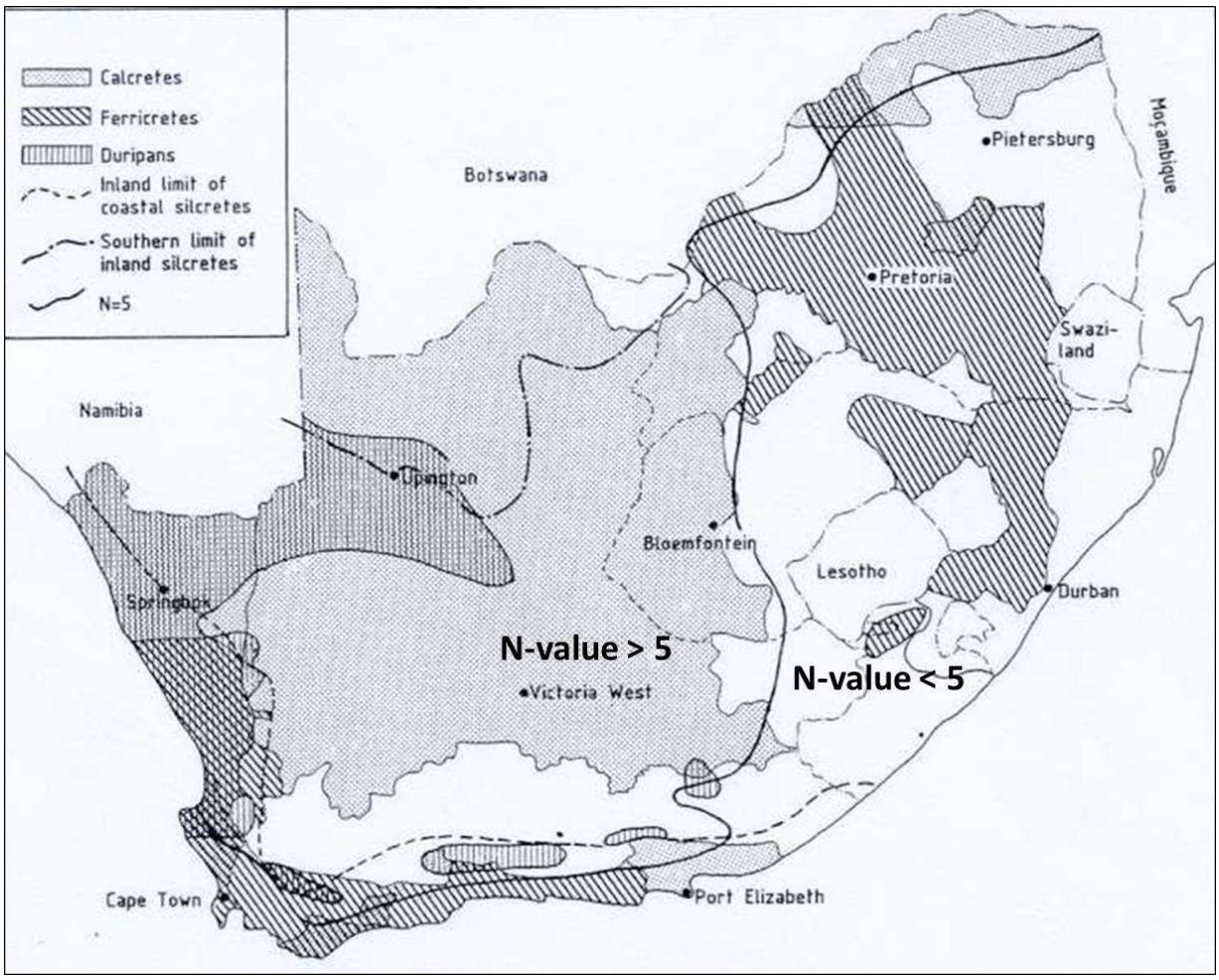

Figure 2-4: The distribution of pedogenic material according to the Weinert N-value (Weinert, 1980).

According to Netterberg (1969), a calcrete is an unconsolidated material cemented or replaced by calcium carbonate which could be classified as residual soil, alluvium, weathered rock or colluvium. The calcretes in South Africa are divided into age-groups varying from pre-Pliocene, Pliocene, Middle Pleistocene (First Intermediate), Upper Pleistocene (Second Intermediate) and Recent (Haddon, 2005; Netterberg, 1969). Calcretes are classified as either pedogenic or non-pedogenic depending on the process of formation (Nash & McLaren, 2003). According to Nash and McLaren (2003) the vertical distribution of calcium carbonate in soil, which in return is influenced by the present parent material and climate (Netterberg, 1969), is responsible for the formation of pedogenic calcretes. Non-pedogenic calcretes on the other hand, differ depending on the geomorphological setting and are not dependant on climate.

The calcretes found within this study area were classified as pedogenic Kalahari calcretes (Watts, 1980). The Kalahari calcretes formed due to the leaching of lime in soils that show a decrease in compaction with an increase in soil depth. Soil texture is one of the main factors that influence the development of calcretes as coarser textures leads to better infiltration. Sources for calcium

carbonate include weathering of primary minerals (for instance plagioclase), solution after extensive shallow flooding, laterally migrating soil water and wind-transported calcareous dust that leach into the soil (Khadkikar *et al.*, 1998; Mabbutt, 1977).

2.2.3.2 Terrestrial sand deposits

According to Hurter (2016) the main aeolian deposits in South Africa are the Namib sediments and the Kalahari sands. The Namib sand sea stretches from the Kuiseb River in the north up to the Gariep River in the south. According to Thomas and Wiggs (2012) the Namib Sand Sea sediments are transported through aeolian and fluvial processes and are redistributed in the Pofadder region of the Northern Cape of South Africa.

However, the Kalahari sediments stretch from the northern parts of South Africa up to the Congo and were redistributed in the mid-Pleistocene Period (Von M Harmse & Hatting, 2012). According to Von M Harmse and Hatting (2012) Kalahari sediments have been redistributed to the south as far as the Vaal River in the North-West Province.

2.3 Soil

Soil forms the intermedium between geology and vegetation and has an extensive influence on plant ecology and diversity. According to McDonald *et al.* (1996) and Shen *et al.* (2000) soil properties are highly dependent on environmental factors like geology, climate and topography. Hence an interrelationship between geology, soil, climate and topography in accordance with species composition exist.

2.3.1 Soil forming processes and factors (pedogenesis)

Physical, chemical and biological processes of wind, water, mineralogy and biological factors result in the production of aggregates of unconsolidated minerals or particles known as soil (Winegardner, 1995). The chemical-, physical-, and mineralogical properties of parent material reflect the underlying soil (Cottle, 2004), however, according to Birkeland (1984) [cited by Cottle, 2004] it is only in the early stages of soil formation and under arid conditions that the influence of parent material is reflected optimally.

According to the Agricultural Research Council (Land Type Survey Staff, 1991) weathering is the process of geological decomposition (chemical weathering) or disintegration (physical weathering) that occurs resulting in the formation of residual soil. Erosion on the other hand is defined as the movement of particles, resulting in the formation of transported soils.

Based on the information obtained from Brink (1985) it is evident that the soils found within the study area are of mixed origin, i.e. residual, alluvial and aeolian (transported) as well as

pedogenic. The general soil types and land types occurring within the site and surrounding area are described in Chapter 5.

2.3.1.1 Residual Soil

Physical weathering, also known as mechanical disintegration, is the main cause of weathering (soil formation) in arid environments. Based on the descriptions given by Leeder (1982) and Boggs (2011) the following physical factors are considered the main agents of physical weathering:

- Thermal Pressure or Insolation weathering

During the day rocks heat up and expand while contracting during cooler evenings. This causes physical stress leading to the weakening and crumbling of the rock. Thermal pressure weathering is common in arid environments for instance the desiccation cracks on Dwyka Tillite floors.

- Exfoliation

Exfoliation is experienced when pressure is released during abrasion, causing the rock to crack parallel to the land surface like the exfoliation of gneiss.

- Salt weathering

Hydration, heating and crystal growth are the main mechanisms through which salt weathering operates. Salt crystal growth generates internal pressure leading to granular disintegration. Salt weathering is common in semi-arid regions or along coastlines, where salt domes are a common phenomenon in saline depression.

- Freeze thaw weathering

Water enters the pores and cracks of rocks. As it freezes the water expands by approximately 9% forcing the cracks and pores to also expand. Eventually these rocks are broken into smaller fragments. The size of the broken fragments depends primarily on the presence of microfractures and other microstructures.

- Flora and Fauna

Roots penetrate the cracks of rocks causing them to breakup into smaller fragments and make space for microbial activity to fill the micro pores, consequently contributing to the weathering process. Animals create underground tunnels accelerating erosion processes, allowing more

water infiltration and microbial activity which has a major composite and integrated effect on weathering.

- Abrasion

Wind, water and ice are the mechanisms through which abrasion weathering operates.

Physical weathering is considered a weathering mechanism that breaks rocks into smaller fragments. As a result, minimal changes will take place with respect to mineral composition therefore the resultant soil will mainly consist of primary rock forming minerals. Some minerals are more stable while other is more prone to weathering (Department of Public Works, 2007). Figure 2-5 illustrates the stability of minerals with respect to weatherability.

Weathering rates are site specific, depend on both physical and chemical processes and are strongly influenced by climatic conditions. Soils of varying thickness form over weathered bedrock as a result of subaerial weathering. Subaerial physical weathering generally gives rise to silicate minerals including quartz and feldspar as well as various rock fragments.

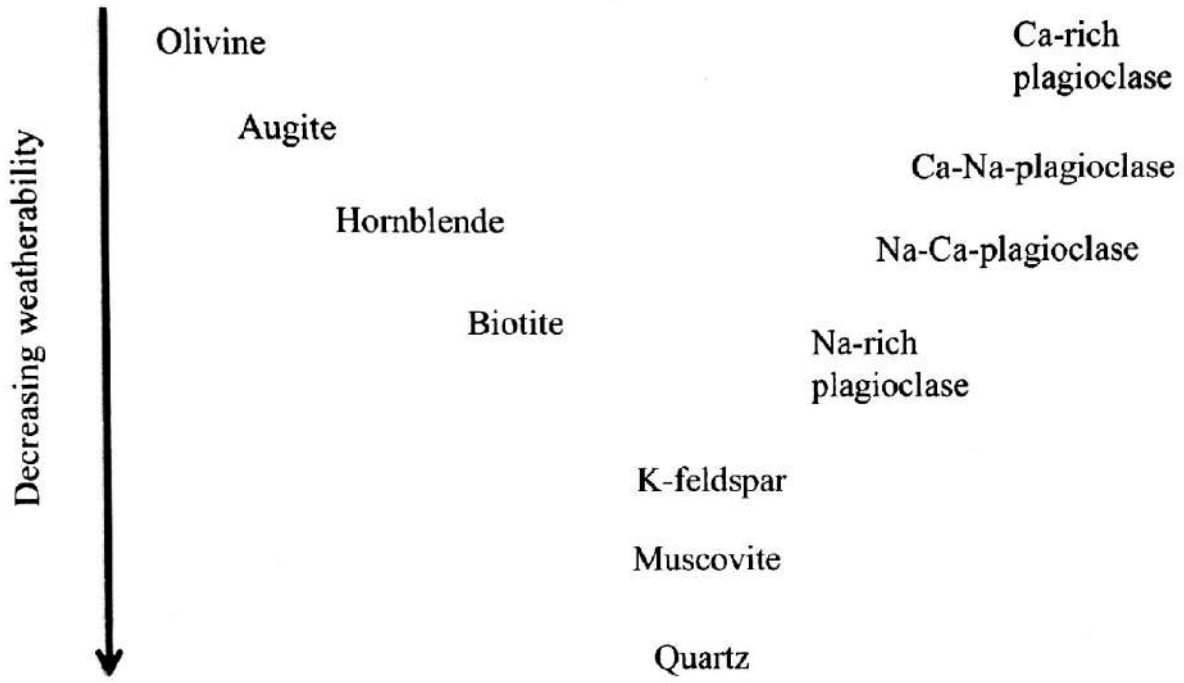

Figure 2-5: Goldich weathering sequence (Goldich, 1938).

2.3.1.2 Transported Soil

According to Beckedahl *et al.* (1988), southern Africa is exposed to extensive and diverse soil erosion controlled by both the nature of environmental processes as well as the response of the environment to edaphic conditions. The transport path of soil is determined by mineral composition, particle size distribution (PSD), and the velocity of the transportation medium (Boggs, 2011). Therefore, the type of transported soil will be determined by the type of erosion and will be governed by all interrelated environmental factors. Typical examples of transported soils with associated soil properties are:

- Aeolian: Mostly sandy soils.
- Alluvial: Dominated by silty and clay soils in low lying areas with sub-angular to round pebbles. Pebbles with attrition marks are common.
- Colluvium: Large rock fragments in poorly sorted young soils with weak structure.
- Glaciers: Soils from glaciers tend to have more silt fractions also known as loess with loose rock fragments.

Soil erosion is influenced by a combination of factors including climate, geology, topography, soil characteristics and vegetation. Figure 2-6 illustrates the interrelationship between environmental processes that governs soil erosion.

Based on the illustration in Figure 2-6 it is evident that there exists an interrelationship between environmental factors contributing to soil erosion. Differences between the environmental factors contributing to soil erosion will also result in different types of erosion processes as illustrated in Table 2-3.

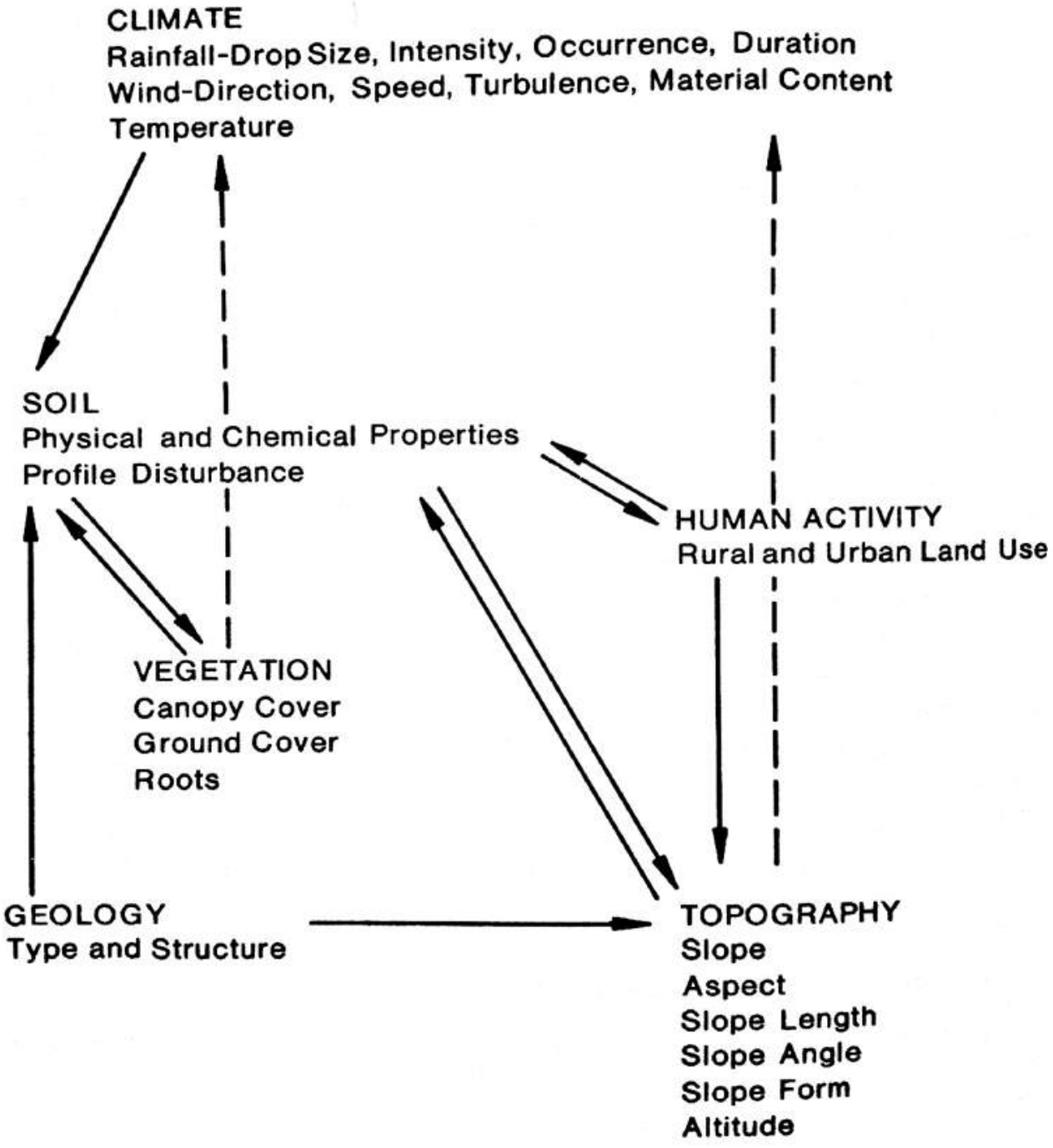

Figure 2-6: Interactions between environmental factors in the soil erosion process (Beckedahl *et al.*, 1988).

Table 2-3: Different types and classes of soil erosion (SARRCUS, 1981).

Type of erosion	Severity class of erosion	Description and remarks
1. Erosion caused by water		
Sheet (surface) *Uniform removal of surface soil*	None apparent Slight Moderate Severe & Very severe	No visible sign of erosion on air-photo. Level of management appears to be high. Areas of light-tone observed on air-photos. Erosion deduced from poor cover, sediment deposits and plant pedestals. Eroded areas obvious on air-photos. Plant cover very poor and sediment deposits extensive. Associated with small rills. Sheet erosion of such severity always associated with rills and gullies. Much or all of the A-horizon has been removed.
Rill *Removal of soil in small channels or rivulets, mainly on arable land.*	None apparent Slight Moderate Severe Very severe	As for sheet erosion Small, shallow (< 0.1 m) rills present but not readily observed on air-photos. Rills of considerable depth (0.1 to 0.3 m) and intensity usually observed on air-photos. An abundance of deep rills (< 0.5 m) easily observed on air-photos. Subsoil may be exposed. Large well-defined rills but may be crossed by farm machinery. Associated with gully erosion.
Gully (donga) *Removal of soil in large channels or gullies by concentrated runoff from large catchment areas.*	None apparent Slight Moderate Severe Very severe	As for sheet erosion. Clearly observed on air-photos and usually up to 1 m deep. Cannot be crossed by farm machinery. Intricate pattern of deep gullies (1 to 3 m) exposing entire soil profile in places. Many 'islands' of topsoil remain. Landscape dissected and truncated by large (3 to 5 m deep) gullies. 25% - 50% of area unproductive. Large and deep (> 5m) gullies have totally denuded over 50% of the area.
Landslide *Soil mass slumps downwards, leaving vertical scarp.*	Five class ratings also apply to these types of erosion but are seldom used.	Usually visible in air-photos. Oversaturation causes soil mass to slide downslope leaving a vertical scarp at the top. Catchment area normally absent.
Terracette *Step-like formation on steep slopes*		Easily observed on air-photos. Usually associated with steep slopes (> 15%) in high rainfall areas. Aggravated by trampling.
Creep *Gradual viscous movement of the soil mass down slope.*		A natural phenomenon which may be observed in mountain areas. Recognition aided by observation of other features. No readily observed on air-photos.
Streambank *Undercutting and slumping in of stream and river banks.*		Occurs on outer curves of streams and rivers where fast-flowing water undercuts the banks. May or may not be seen on air-photos.
2. Erosion caused by wind		
Wind *Sandy material (> 85% sand) removed by suspension, saltation and creep during strong winds.*	None apparent	Seldom observed in well vegetated and humid areas where clayey soils predominate.
	Slight	Not readily observed on air-photos. Field checks show evidence of removal and deposition and loamy soils (15-35% clay and 65-85% sand) may predominate.
	Moderate	Easily observed on air-photos. Sand deposited against obstructions and small dunes are formed. Soils are mostly sandy (< 15% clay and > 85% sand).
	Severe	Large parallel sand dunes observed on air-photos. Vegetation is sparse and soils very sandy (< 10% clay).
	Very severe	Over 50% of the area rendered unproductive by so-called 'blow-outs' and deposition of sand.

2.3.1.3 Pedogenic Soils

The formation of soil (pedogenesis) depends primarily on the parent material and its resistance to weathering, the influence of climate, biota, relief and topography as well as time. Jenny (1941) developed an equation to express these factors:

$$\text{Soil} = f\,(cl, o, r, pm, t)$$

Where *f* is a function, *cl* is climate, *o* is organisms (fauna and flora), *r* is relief (topography), *pm* is parent material and *t* is time. In recent time it is accepted to also include the “a” factor known as the anthropogenic factor. In some cases, it would be difficult to distinguish between the “a” factor and the “o” factor but there are well defined boundaries where both can exist in the same process.

The main pedogenic processes are identified as follows:

- Laterization

Laterization dominates in tropical and subtropical environments, characterised by high temperatures and elevated levels of precipitation. These areas are typically dominated by excessive weathering, accommodated with eluviation and leaching of essential nutrients (excluding iron and aluminium). Acidic soil is the result of intensive leaching (Pidwirny, 2006).

- Podzolization

Podzolization is associated with the removal of iron and aluminium compounds, clay minerals and humus from topsoil horizon by organic leachate solutions (with acidic characteristics) in humid but cold climates (Pidwirny, 2006).

- Calcification

Calcification dominates in semi-arid environments and is associated with the upward movement of calcium carbonate, by means of capillary movement when evapotranspiration rates are higher than precipitation rates (Pidwirny, 2006).

- Salinization

The process of salinization is similar to that of calcification; however, salinization occurs in drier environments resulting in the precipitation of salt either at or near the soil surface (Pidwirny, 2006).

- Glerization

Glerization can be described as the accumulation of organic material in the topsoil horizons, with subsoil horizons typically characterised by a gley horizon as a result of the chemical reduction of iron. Glerization is associated with poor drainage in moist and cold climates (Pidwirny, 2006).

2.3.2 The influence of soil properties on vegetation composition and species richness

The high level of plant speciation in South Africa is related to gene flow limiting factors (including geographical isolation, phenology, ethology and sterility barrier) as well as factors that manages disruptive selection (Linder, 2003). Soil has an enormous influence on the vegetation structure and composition as well as the species richness of an area (Tilman, 1982). Variations in resource requirements between species also contribute to differences in species composition. According to Austin (2002) and Pausas *et al.* (2003) soil properties can either have a direct effect or a resource effect on vegetation. Direct effect refers to soil properties that have a physiological effect on the growth of plants, whereas resource effect refers to the availability of resources, for instance nutrients and moisture that are crucial for survival.

In nature the relationship between plant richness and environmental factors can be described as a hump-shaped relationship. The survival rate of plant species is considered low with limited resource availability resulting in low plant richness. However, as resource availability increases plant richness also increases up to a point where the most adaptive and competitive species become dominant. This will result in the decrease of less-competitive species causing a decline in plant richness (Austin, 1982; Grime, 1979, Huston, 1979; Tilman, 1988).

2.3.2.1 Soil physical properties

- Soil Water Content

Environmental factors operate in conjunction with an integrated system contributing to plant composition and species richness. Soil water content is one of the most important limited resources in the semi-arid regions of South Africa (Cody, 1989). Soil moisture availability is determined by precipitation, temperature, soil texture, elevation and topography. No clear relationship has been shown for plant richness and moisture availability. However, positive correlations between plant richness and rainfall have been reported in previous studies by Knight *et al.* (1982), O'Brien (1993) as well as Richerson and Lum (1980). Long term plant available water in the sub-surface (root zone) contributes to species composition and richness (Dengler *et al.*, 2012; Dúbravková *et al.*, 2010; Michálková, 2007; Reitalu *et al.*, 2014). For instance, soil with a clay texture and a moderate to high infiltration rate will support more plants; therefore, the area will obtain a higher plant density and consist of plant species with deep root systems. In semi-arid

areas it is common to find palaeo drainage systems. With regards to soil composition these palaeo drainage systems do not differ from the adjacent area, however, due to differences in soil water content they contain typical shrubby plant species whilst the adjacent areas consist of grassland.

- Surface Crusting

Soil crusting is considered yet another limiting factor. It reflects soil characteristics like soil texture, mineralogy, organic material, electrical conductivity as well as exchangeable sodium percentage (Frenkel *et al.*, 1978; Laker, 2004; Morin *et al.*, 1981). The formation of soil crusts has a negative influence on plant growth and species richness by means of limiting water movement in soil, increasing soil erosion and runoff and restricting the germination of seeds (Hillel, 2004; Singer *et al.*, 1982).

2.3.2.2 Soil chemical properties (as well as the function of plant nutrients)

Soil chemical properties contribute to both the direct effects and resource effects exerted on plants, for instance the relationship between pH and nutrient availability. In acidic conditions ions like Al^{3+}, Cu^{2+}, Ni^{2+} and Fe^{2+}/Fe^{3+} become toxic to plants while essential nutrients like Ca^{2+}, Mg^{2+}, P^{3-} and K^{+} are captured in forms unavailable for plant uptake (Wolf, 2000). Alkaline soils usually show deficiencies in N^{3-}, Fe^{2+}/Fe^{3+}, Cu^{2+}, Zn^{2+}, and K^{+} (Marschner, 1986). The Fertilizer Society of South Africa (FSSA, 2007) describes the function of both micro-elements and macro-elements within plants as follows:

- Nitrogen

Nitrogen contributes to photosynthesis as well as the growth and reproduction of plants. Nitrogen is taken up in a nitrate (NO_3^-) form but is found in plant amino acids, adenosine triphosphate (ATP), adenosine diphosphate (ADP), deoxyribonucleic acid (DNA), protein and phospholipids as NH_2 (FSSA, 2007).

- Phosphorus

Phosphorus is immobile in plants and contributes to photosynthesis, all growth processes, reproduction, and the maintenance of plant genetic identity. The availability of phosphorus is restricted to a pH of less than 6 (FSSA, 2007).

- Potassium

Potassium contributes to the transportation of nitrogen within the plant. It promotes photosynthesis, is associated with the regulation of stomata, and is used for the translocation of starch (FSSA, 2007).

- Magnesium

Magnesium forms the centre of the chlorophyll molecule therefore magnesium is considered essential for photosynthesis (FSSA, 2007).

- Calcium

Calcium can be found in the middle lamella of the cell wall (as calcium pectate) and is considered immobile in plants. It also promotes the production of protein and cell growth (FSSA, 2007).

- Sulphur

Sulphur in the form of sulphate (SO_4^{-2}) forms part of amino acids which are considered the building blocks of proteins therefore, sulphur also plays a role in plant growth (FSSA, 2007).

- Zinc

Zinc is involved in the activation of enzymes, the formation of chlorophyll and growth hormones and regulates the pH within cell liquids (FSSA, 2007).

- Manganese

Manganese enables enzyme activity and iron metabolism and are considered important for photosynthesis and oxidation reduction reactions within plants (FSSA, 2007).

- Copper

Copper acts as catalyst for various oxidation processes and forms part of the respiration process. Iron can be found in the enzymes and certain proteins contributing to chlorophyll production and oxidation-reduction processes (FSSA, 2007).

- Boron

Boron is known for improving cell differentiation and contributes to pectin and lignin synthesis (FSSA, 2007).

- Molybdenum

Molybdenum is important for the reduction of nitrates during photosynthesis (FSSA, 2007).

2.4 Climate

Climate is considered as one of the main attributing environmental factors determining vegetation composition and species richness (Cottle, 2004). It contributes to soil formation as well as soil moisture content and soil temperature regimes. With respect to soil formation, it not only determines the mode of weathering but also the weathering rate. The aridity index as well as the N-value as discussed in section 2.2.3.1. are used to describe the effect of climate on weathering.

Climate also influences vegetation composition and species richness. According to Cottle (2004) vegetation growth rates increase with increasing humidity and temperature. Two of the most important attributes in accordance with climate contributing to plant growth is moisture availability and exposure to radiation or sunlight. Different plant species have different preferences and limitations with regards to radiation and moisture requirements.

Based on evidence found of fossilised plant material in the marsh sediments of the Northern Cape (Partridge, 1998) it was concluded that the climatic conditions during the Cretaceous Period was humid and warm. However, during the late Cretaceous Period as well as the beginning of the Palaeocene climate changed to more arid conditions. With the initiation of a drier period came the formation of calcretes, dorbanks and silcretes in the western parts of South Africa together with a shrub dominated vegetation (Maud, 2012; McCarthy & Rubidge, 2005; Partridge *et al.*, 2006).

Aridity in the western regions of southern Africa is intensified by the cold Benguela Current, adjacent to the west coast (Wilkinson, 1988). According to Lancaster (1979) global climate changes resulted in fluctuating aridity conditions during the Quaternary Period. Based on information gathered by Wilkinson (1988), the degree of vegetation cover in the semi-arid regions of southern Africa is controlled by the low rainfall along the lower Gariep River valley and the west coast as well as the temperature maxima in west-central Kalahari. Moisture content is limited while radiation exposure is extensive; therefore, these regions are dominated by plant species adapted to these environmental limitations.

2.5 Topography

Topography can be defined by four major topographic factors known as slope, geometry (length and angle), aspect, and elevation. Variations in these primary topographic factors will result in distinct microclimatic conditions with unique secondary topographic properties (solar radiation, moisture, and temperature). According to McCune and Kean (2002), aspect is important as it

determines the insolation of the soil surface. Slope influences solar radiation, moisture and temperature. Warmer temperatures and a higher degree of solar radiation are associated with steeper slopes with a decrease in soil moisture due to increased surface runoff (Bennie *et al.*, 2008). Based on previous research (Austin, 2002; Bennie *et al.*, 2008; Burke *et al.*, 1989; Coblentz & Keating, 2008; Coblentz & Riitters, 2004; Hofer *et al.*, 2008; Rietkerk *et al.*, 2002; Zhao *et al.*, 2010) these microclimatic conditions will result in vegetation differences with respect to distribution, biodiversity and species richness. The general relief is affected by geological structures while the lithological units have more specific influences on relief due to differing weatherability (Cottle, 2004).

According to Wilkinson (1988) the majority of all landscapes in the arid and semi-arid regions of southern Africa, including the Karoo- and Namib deserts as well as the Kalahari- and Namib dunes, follow the shield and platform morpho-structural pattern. These areas are known to be old with minimal altitudinal differentiation. One of its most important characteristic features is the lack of topographically induced climatic contrasts. As discussed in Chapter 1 the topography of the study area is relatively homogenous with minimal climatic variations.

2.6 Anthropogenic Influence

Anthropogenic influences are considered important attributes for habitat diversity and soil erosion. Most regions of southern Africa are susceptible to soil erosion and changes in natural habitats with respect to anthropogenic influences. According to Ellis and Swift (1988) [cited by Siebert *et al.*, 2003] ecosystems in the semi-arid regions are event-driven. Therefore, highly degraded ecosystems will not recover with the decrease of stress loads. It was also stated that if the disturbance is due to anthropogenic influences (only in extreme cases), vegetation will not be able to recover.

Natural vegetation has been subjected to various anthropogenic influences including livestock grazing, cultivation, burning, field or woodland management as well as the development of infrastructure [for instance the major economic development of solar facilities in the Northern-Cape Province (Department of Environmental Affairs, 2014)]. According to Cottle (2004) modification of land by anthropogenic influences over the past 10 000 years have resulted in more distinct differences between areas of varying geology.

2.7 Vegetation

According to Cowling and Roux (1987) variations in vegetation growth form is governed by environmental factors including geology, soil properties, topography, climate as well as anthropogenic influences. One of the most important objectives in ecological studies is to explain

and understand the spatial distribution of vegetation communities, species richness and biodiversity (Guisan & Zimmerman, 2000).

For optimal growth and reproduction vegetation requires essential nutrients. Each species has different preferences and limits of tolerance for different environmental factors therefore the amount, variety and availability of environmental factors control species composition.

The area under investigation (semi-arid Bushmanland region) falls within the Nama Karoo Biome. The Nama Karoo Biome is the second largest biome in South Africa and is considered as topographically homogenous with altitudinal differences in most parts between 1000 m and 1400 m. This biome is considered as grass and dwarf shrub dominated with grasses occurring more commonly in sandy soils. The Nama Karoo contains some invasive species including *Opuntia aurantiaca* and *Prosopis glandulosa* with less than 1% of its total area considered conserved (Bezuidenhout, 2009).

Acocks (1953) sub-divided the vegetation of South Africa into different veld types based on botanical composition and practical utilization. Mucina and Rutherford (2006) reclassified all veld types based on vegetation distribution, species dominance, land features, geology, soil and climate.

According to Yeaton and Esler (1990) as well Esler and Cowling (1993), competition in the arid and semi-arid environments of southern Africa exists among perennial shrubs and between perennial shrubs and annuals. Based on the classification of Mucina and Rutherford (2006) it was concluded that the proposed study area comprises mainly the Bushmanland Arid Grassland, the Bushmanland Sandy Grassland and the Bushmanland Basin Shrubland.

- Bushmanland Arid Grassland

The Bushmanland Arid Grassland is characterised by irregular plains dominated by *Stipagrostis* species. In some regions the vegetation structure is altered by low shrubs of *Salsola.* Species that are considered as endemic to the Bushmanland Arid Grassland include *Dinteranthus pole-evansii, Larryleachia dinteri, L. marlothii, Ruschia kenhardtensis, Lotononis oligocephala* and *Nemesia maxi. Tridentea dwequensis* is considered as the only biogeographically important taxon within this veld type (Mucina & Rutherford, 2006).

- Bushmanland Sandy Grassland

The Bushmanland Sandy Grassland is characterised by sandy grassland plains dominated by *Stipagrostis* and *Schmidtia* species. There is also a common occurrence of drought-resistant

shrubs and after rainfall the display of ephemeral spring flora including *Grielum humifusum* and *Gazania lichtensteinii* (Mucina & Rutherford, 2006).

- Bushmanland Basin Shrubland.

The Bushmanland Basin Shrubland is characterised by irregular plains dominated by shrubs including *Rhigozum, Salsola, Pentzia* and *Eriocephalus*, as well as different *Stipagrostis* grass species. After rainfall *Gazania* and *Leysera* species may appear. Some species that are considered as endemic to the Bushmanland Basin Shrubland include *Cromidon minutum, Omithogalum bicornutum* and *O. ovatum subsp. oliverorum.* As in the Bushmanland Arid Grassland *Tridentea dwequensis* is considered the only biogeographically important taxon for the Bushmanland Basin Shrubland (Mucina & Rutherford, 2006).

The vegetation of an area can be divided into plant communities and habitats. According to Mueller-Dombois (1984) the purpose for the classification of plant communities is to categorise vegetation patterns and to explain ecological relationships. Mueller-Dombois (1984) also stated that the classification of plant communities is based on vegetation differences as well as its surrounding environment. Siebert *et al.* (2003) stated that a clear relationship between environmental factors and plant communities exist.

Based on the description given by Odum (1971) a habitat can be defined as the place where an organism lives, together with the available resources and present conditions that result in the survival of that organism. According to Morrison *et al.* (1992), different vegetation types are supported by different environmental conditions which can be described as a habitat.

2.8 Summary

Based on previous research (Körner, 2000), climate change has the most prominent influence on arid and semi-arid environments. Therefore, to better understand ecological changes, it is important to first understand the relationship between vegetation and both biotic and abiotic factors. It has been stated that plant community composition and structure (Connell, 1983; Fowler, 1986; Goldberg and Barton, 1992; Schoener, 1983), their compositional determining factors (Callaway, 1995) and variations between communities (Goldberg and Novoplansky, 1997; Goldberg *et al.,* 1999) depend primarily on the interactions between different species as well as the interaction between vegetation and environmental factors. Hence, the key forces behind vegetation community composition are the intra- and interspecific interactions between species and the environment (Went, 1942).

CHAPTER 3

MATERIALS AND METHODS

Various techniques and methods were used for the fulfilment of the proposed research aims and objectives as set out in Chapter 1 (section 1.3) to obtain information with respect to this multidisciplinary approach. This Chapter presents all these techniques and methods in an orderly manner. The study was conducted in four phases:

- Phase I: Mapping with satellite imagery;
- Phase II: Surveying for identification, description, and classification purposes;
- Phase III: Sampling and analyses; and
- Phase IV: Interpretations and correlations.

3.1 Phase I: Mapping with satellite imagery

During the first phase aerial photography was utilised to identify characteristic mapping units. Whether these mapping unit characteristics were identified based on their vegetation composition, soil properties or geological features will be established by means of phases two and three. For practical reasons Google Earth (2016) was used to divide the study area into characteristic mapping units (consult Chapter 4 section 4.1 for more information), according to the principles of parametric terrain evaluation as described by Mitchell (1977). Google Earth is a medium-resolution satellite-imaging system. It uses geostationary satellites moving at the same speed as planet Earth and provides imagery with a typical pixel size of 4 km at the equator (Hill *et a*l., 2005).

A total of ten mapping units (referred to as mapping unit A – J) were identified based on corresponding characteristics visible on satellite imagery. Each mapping unit consists of various sub-units depending on locality (consult Table A-1 in Annexure A for location and description of mapping units and sub-units). The first site visit took place on 3 July 2016 where the mapping unit characteristics were verified and assessed.

3.2 Phase II: Surveying for identification, description and classification purposes

3.2.1 Vegetation

The plant identification survey was conducted from 8 July 2016 until 1 August 2016. The site was revisited in March 2017 (after rainfall) where additional plant identification took place.

As illustrated in Figure 3-1, this area falls within the very late summer rainfall region. It is advised by Driver *et al.* (2009) that floristic surveys in this region be conducted between October and April. However, according to meteorological statistics from the South African Weather Services (Weather Bureau, 2016) (see Chapter 1, section 1.5.5.) the annual rainfall for this area, from 1992 up to 2015, was between 140 mm and 250 mm per annum. The data obtained during the survey in 2016 and the additional observations made during the final site visit in March 2017 are considered as adequate for this study. However, the timing of the plant identification survey in 2016 had an effect on the results.

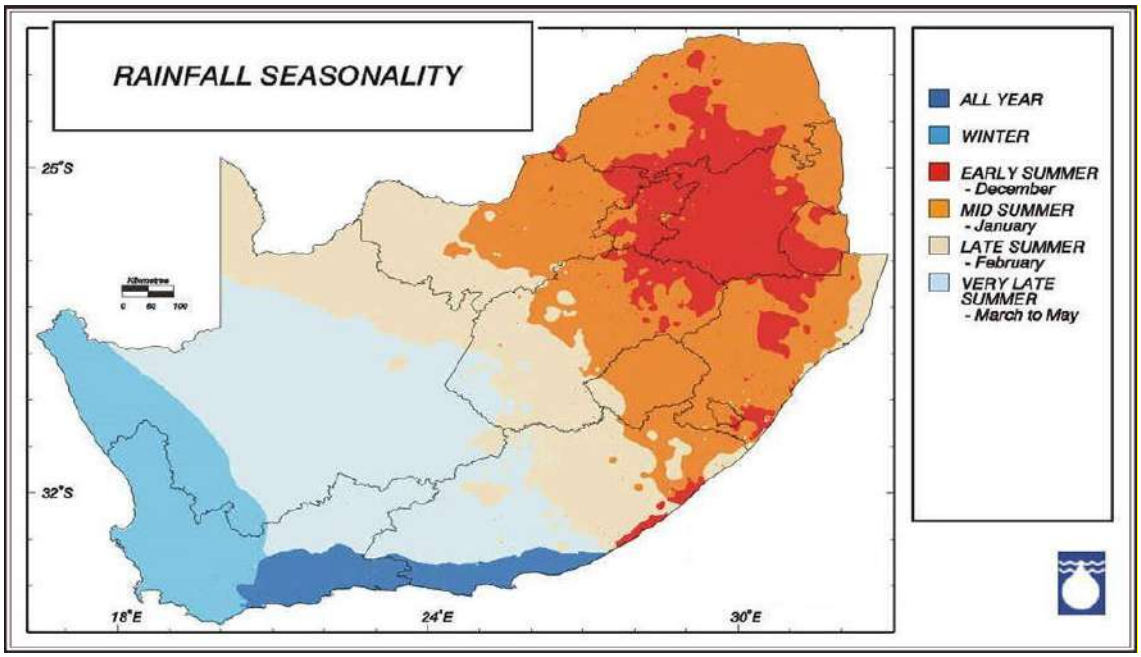

Figure 3-1: Map indicating the rainfall seasonality in South Africa (Schulze, 1997).

According to Hill *et al*. (2005) for natural vegetation classification a minimum of five quadrats must be recorded for the whole site. A minimum of five representative sub-units per mapping unit was identified (except for mapping unit A, F and I). Mapping unit A and I consisted of only two sub-units each, whilst only two sub-units of mapping unit F was situated within the boundaries of the study area. Therefore, two sub-units were identified for mapping unit A, I and F respectively.

The size of the quadrats depends on the vegetation type present (Greenwood, 2006; Hill, *et al.*, 2005). For grasslands a 4 m by 4 m quadrat is recommended whereas a 10 m by 10 m quadrat is recommended for shrubby areas (Hill, *et al.*, 2005). Due to the combination of vegetation types on this site, it was decided that the size of the quadrats be kept at a consistent 10 m by 10 m.

To obtain information with respect to species composition, habitats and community assemblage quadrats were randomly placed within each identified representative sub-unit (a total of 41 quadrats). A quantitative collection method was used to record data with respect to the presence, absence and quantity of species.

Within each quadrat all plant species were identified and quantified [up to species level and according to Germishuizen & Meyer (2003)] with the help of plant identification guides (Fish, 2015; Van Oudtshoorn, 2012; Van Wyk, 2011). Plant species that could not be identified on site were either pressed in a plant press (Figure 3-2) or kept in dry paper bags and taken to the herbarium (AP Goossens Herbarium, North-West University) for identification.

Figure 3-2: Photograph of a standard plant press (University of Florida Herbarium, 2015).

After plant identification and quantification each plant was classified according to a hierarchical system of identification and nomenclature, which is based on a criterion of physiognomy and growth form.

3.2.2 Soil

Minimal information was obtained from the Agricultural Research Council (Land Type Survey Staff, 2003) which entails the division of land into land types, typical terrain cross sections and dominant soil types for each terrain unit. Land types are identified based on similarity in soil distribution patterns, terrain, and climate.

Soil description and classification took place from 8 July 2016 until 1 August 2016. The site was visited again in March 2017 where additional observations were made. The localities identified for soil surveying corresponds with the localities of the plant identification survey. Within each identified quadrat a soil auger was used to drill holes up to a maximum depth in order to make soil description and classification possible.

The morphological, chemical and physical properties (at field level) of each soil horizon were described according to the guidelines set out by the Agricultural Research Council (Land Type Survey Staff, 1991). (Consult Figure A-1 in Annexure A for explanation of soil description categories, and Figure A-2 in Annexure A to view the standard soil description form).

The Binomial System (MacVicar *et al.*, 1977) was used for soil classification, because the original land type surveys were conducted with this system. A re-classification was done using the Taxonomic System (Soil Classification Working Group, 1991) in order to interpret and re-classify the soil data with respect to soil families. Soil was classified according to a hierarchical system incorporating classification categories (Figure 3-3). The classification categories used in this study for the purpose of soil descriptions are described as follows:

- Soil Order: At the highest level, soil order refers to the genesis of Natural Soils (Soil Classification Working Group, 2018).

- Soil Group: The clustering of soil forms based on distinctive topsoil horizons or distinctive subsoil horizons. Albeit not recognised by the South African Soil Classification System (Soil Classification Working Group, 1991), numerous studies (Brummer, 2015; Fanourakis, 1991; Schmidhuber, 2015; Von M Harmse & Hatting, 1985) have made use of the classification of soil groups as described by Fey (2010) and the IUSS Working Group WRB (2006).

- Soil Form: Defined by a vertical sequence of diagnostic horizons soil form is recognised by either a typical topsoil horizon and an indurated horizon, two diagnostic subsoil horizons or a single diagnostic horizon with a depth of 1.5 m (Soil Classification Working Group, 2018).

- Soil Family: Describing characteristic soil properties soil family is differentiated within soil form (Soil Classification Working Group, 2018).

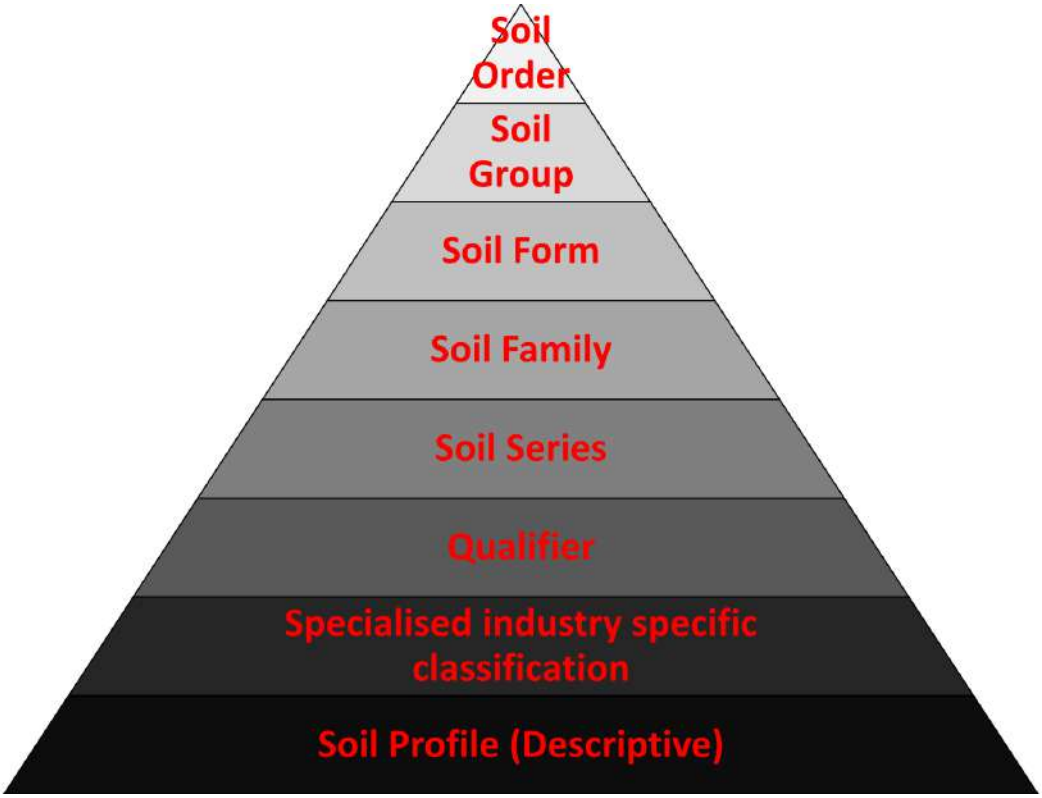

Figure 3-3: Schematic illustration of classification categories as described by the Soil Classification Working Group (2018).

3.2.3 Geology

Based on the aims and objectives of this study as well as the geological complexity of this site a randomised survey approach was used for geological surveying. Each geological outcrop observed on the study area was identified and mapped by means of a GPS (Garmin Etrex 20), while a compass was used to take field measurements.

3.3 Phase III: Sampling and Analysis

3.3.1 Vegetation

3.3.1.1 Statistical Analyses

Quantitative floristic data for each mapping unit and representative sub-unit were consolidated in a database (Excel spreadsheet). For statistical analysis PRIMER 6 (2012) was used to determine the similarity in species composition of different localities. Sites were grouped according to Bray-Curtis dissimilarities by means of non-metric multidimensional scaling (NMDS) analyses in order to obtain community assemblages based on species composition. According to Holland (2008), one of the advantaged of NMDS is its unrestricted ordination ability which is based on species space measures. To visualize relationships among sampling locations, NMDS provides two-

dimensional plots presenting similar sites closer together and dissimilar sites further apart. According to Clarke and Warwick (2001), stress values can be interpreted as follows: i) stress ≤ 0.05 gives an excellent representation with no prospect of misinterpretation; ii) stress ≤ 0.1 represents a good ordination; iii) stress ≤ 0.2 gives a potentially useful ordination; and iv) stress > 0.3 is considered a poor ordination, difficult to interpret.

The first step was applying PERMANOVA to determine whether the groupings of Bray-Curtis were significantly different. PERMANOVA is considered as a multivariate analysis of variance technique where the permutation of the dissimilarity matrix determines the significance of data. In order to reduce the influence of common species a square root transformation of species data was performed (Anderson, 2001; Botha, *et al.*, 2016). Similarity Percentage Analysis (SIMPER) analyses were applied to the data in Paleontological Statistics software (PAST) (Hammer *et al.,* 2011) to establish which species contributed most to the variations between different mapping units (Clarke, 1993).

3.3.2 Soil

3.3.2.1 Sample Collection

The sample collection localities correspond to the localities where soil descriptions and classifications were conducted (Figure 5-1). At each locality one sample was collected for every soil horizon. A total of 60 soil samples were collected (samples marked G1 – G60). For additional descriptive information soil profile photographs were obtained from the geotechnical soil survey of MSc student Linde Tshilate (University of Venda, 2017).

3.3.2.2 Soil Sample Preparation

The first step of sample preparation was to air-dry or oven dry the samples not exceeding 40 °C. To ensure that no compounds are fixated or released the samples were kept out of direct sunlight. Soils were then crushed and passed through a 2.0 mm sieve as prescribed by the Non-Affiliated Soil Analysis Work Committee (1990).

The fraction smaller than 2.0 mm were sent to Eco-Analytica Laboratory, Potchefstroom for the analyses of different chemical properties (pH, electrical conductivity, exchangeable cations, cation exchangeable capacity, phosphorus, and anion concentration) as well as physical properties (particle size distribution). This standard soil preparation method was used for all soil samples (Non-Affiliated Soil Analysis Work Committee, 1990).

3.3.2.3 Chemical Analyses

- pH (H_2O)

The pH can be described as the negative logarithm to the base 10 of the activity of H^+ ions. When soluble cations with a higher affinity for adsorption displace adsorbed H^+ ions, pH will decrease (Non-Affiliated Soil Analysis Work Committee, 1990).

This method was applied on a suspension with a ratio of 1.0:2.5 soil/water. Standard buffer solutions with a pH of 4.01, 7.01 and 10.1 were used for the calibration of the pH meter. To ensure accuracy the pH meter was calibrated every hour. To start 10 g (≤ 2.0 mm) dried soil was placed in a glass beaker and 25 cm^3 de-ionised water was added. The contents were stirred for 5 seconds by using a glass rod and left to rest for 50 minutes. Thereafter, the contents were stirred again and left to rest for another 10 minutes. Finally, the sample was tested with a calibrated pH meter (Non-Affiliated Soil Analysis Work Committee, 1990).

- pH (KCl)

In order to measure the activity of the hydrogen ions 1 mol/dm^3 KCl was used to create a soil suspension. Standard buffer solutions of pH 4.01, 7.01 and 10.1 were used for the calibration of the pH meter. To ensure accuracy the pH meter was calibrated every hour. To start 10 g (≤ 2 mm) dried soil was placed in a glass beaker and 25 cm^3 KCl solution (1 mol/dm^3) were added. (To create the KCl solution 74.5 g KCl was added to 1 dm^3 de-ionised water.) The contents were stirred for 5 seconds by using a glass rod and left for 50 minutes to rest. The contents were stirred again and left for another 10 minutes. Finally, the sample was tested with a calibrated pH meter (Non-Affiliated Soil Analysis Work Committee, 1990).

- Electrical conductivity (EC) of the saturation extract

Electrical conductivity (EC) can be described as the ability of a soil to conduct electricity, hence the measurement of the amount of salts present in a soil solution. EC is measured in units of MilliSiemens per meter (mS/m). The EC measurements were conducted according to the standard method of the Non-Affiliated Soil Analysis Work Committee (1990) based on the saturated paste extract.

During dry seasons soil EC values will be higher in comparison with rainy seasons due to the precipitation of salts on the surface. During rainy seasons salts will be leached and diluted. EC measurements can be used to estimate salinity pollution, categorise the hazard of saline soils and to estimate leaching requirements for saline soils (Non-Affiliated Soil Analysis Work Committee, 1990).

- Cation exchange capacity (CEC) and exchangeable cations

According to Sparks (2003) ion exchange can be defined as the interchange between ions in solution and ions within the boundary layer between the charged surface of the soil and the solution. Therefore, CEC is the soils ability to adsorb cations by means of sources like clay minerals, organic matter and amorphous minerals. By determining the CEC and exchangeable cations of a soil, one can establish the nutrient status of that soil (Non-Affiliated Soil Analysis Work Committee, 1990).

All the soil samples were tested according to the standard method described by the Non-Affiliated Soil Analysis Work Committee (1990). Ammonium Acetate (1 mol/dm^3, pH 7) were used as extractant for exchangeable and water-soluble cations. The adsorbed cations can be displaced by a salt solution like potassium chloride after the exchange complex has been saturated with index cations. Steam distillation was applied to separate the ammonia which was then taken as equal to the CEC of the soil (Non-Affiliated Soil Analysis Work Committee, 1990).

- Anion concentration analyses

All the soil samples were tested for Cl^-, NO_3^- and SO_4^{2-} according to the standard saturated paste method described by the Non-Affiliated Soil Analysis Work Committee (1990). To start 250 g (≤ 2 mm) dried soil was placed in an applicable container and de-ionised water was added. The paste was then mixed with a spatula. An acceptable amount of de-ionised water was added until the paste flowed freely without any excess water collecting. The paste was then left for one hour and then filtered with a vacuum filtration. For this procedure a Buchner or Richards funnel were used equipped with a Whatman No. 50 filter paper (180 mm diameter). The collected filtrate was filtered until clear and tested for anions (Daniell, 2014; Metson, 1961).

3.3.2.4 Physical Analyses

- Particle Size Distribution (PSD)

The solid phase of a soil comprises of soil particles clustered together as aggregates. The term particle size distribution (PSD) is used to express the proportions of different particle sizes that a soil contains. The first step was to determine the mass of the sample. The sample was passed through a 2.0 mm sieve after crushing the aggregates in a porcelain mortar. The mass of the fraction > 2.0 mm was then expressed as a percentage of the entire sample, where after the mass of the fraction ≤ 2.0 mm was determined. For the removal of cementing and/or flocculation compounds, pre-treatments were used depending on the properties of the sample. These pre-treatments included the removal of carbonates, the removal of siliceous cementing agents, the removal of organic matter as well as the removal of iron oxides. The sand fraction was determined

by means of the sieve method, while the silt and clay fractions were determined with the sedimentation or pipette method (Non-Affiliated Soil Analysis Work Committee, 1990). Table 3-1 presents the particle size standards as described by the Non-Affiliated Soil Analysis Work Committee (1990).

Table 3-1: Grain size limits (Non-Affiliated Soil Analysis Work Committee, 1990).

Class	Diameter (mm)	Method of separation
Gravel	> 2	sieve
Coarse sand	2,0 - 0,5	sieve
Medium sand	0,5 - 0,25	sieve
Fine sand	0,25 - 0,106	sieve
Very fine sand	0,106 - 0,05	sieve
Coarse silt	0,05 - 0,02	sedimentation
Fine silt	0,02 - 0,002	sedimentation
Clay	< 0,002	sedimentation

The data obtained from the particle size distribution analyses were further processed by means of soil texture classification as described by USDA-NRCS (2017).

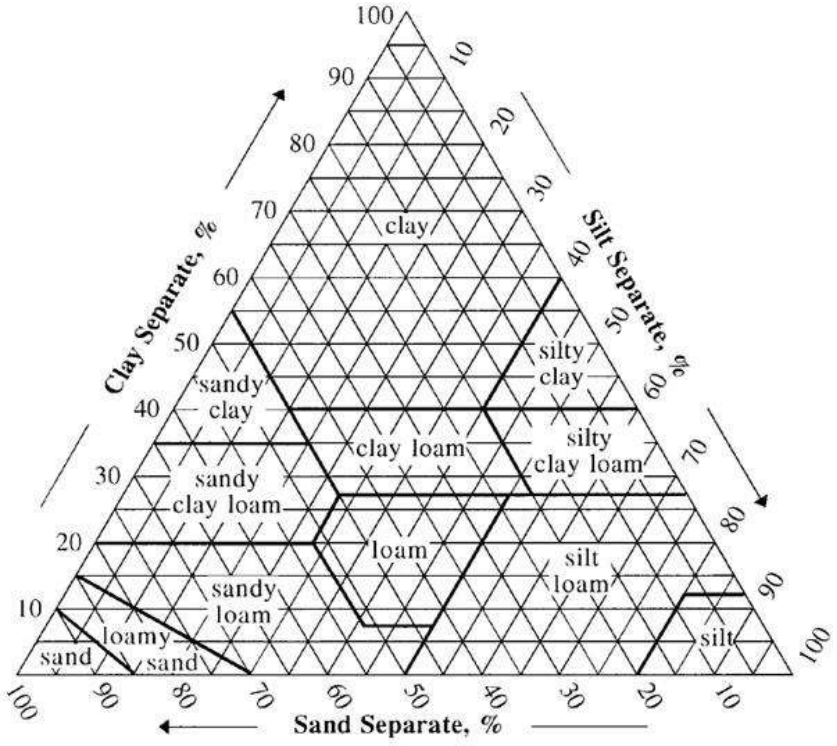

Figure 3-4: A trilinear diagram used for soil texture classification (USDA-NRCS, 2017).

This trilinear diagram is only intended for soil fractions ≤ 2.0 mm. Soil fractions sand, silt and clay are presented on the three apexes with a fractional percentage scale along each side.

3.3.3 Geology

3.3.3.1 Sample Collection

Based on the aims and objectives of this study geological samples were collected for identification purposes. A total of three samples were collected for mineralogical analyses.

3.3.3.2 Mineralogical Analyses

Thin sections were prepared for mineral and rock identification. A diamond saw was used to remove all visible weathering surfaces from the samples. In order to flatten rock surfaces, diamond-impregnated polishing wheels were used to polish the samples. Using epoxy resin each flattened sample was glued to a frosted glass slide. Excess sample was removed from the glass slide with the help of a Struers Accutom-50 precision cut-off machine after a waiting period of 12 hours. The final step in sample preparation was grinding and polishing the sample up to a thickness of 30 microns (Kruger, 2017; Nesse, 2004).

3.4 Phase IV: Interpretations and Correlations

Methodologies used during this phase focused on the identification of certain correlations between vegetation, soil and geology. The basic concept of correlation is based on spatial autocorrelation. Spatial autocorrelation can be defined as the measurement of sample similarity for a specific variable as a function of spatial distance (Diniz-Filho *et al.*, 2003; Griffith, 1987; Legendre, 1993; Sokal & Oden, 1978). A generalization exists, stating that the values of samples taken in close proximity are generally more uniform than those taken further apart. (Cliff & Ord, 1973; Lichstein *et al.,* 2002; Liebhold *et al.*, 1993; Rossi *et al.*, 1992). The application of spatial autocorrelation in geographical ecology is profound, with reference to latitudinal gradients in species richness (Badgley & Fox, 2000), spatial patterns within plant communities (Leduc *et al.*, 1992), associations between regional and local species richness (Bini *et al.*, 2000; Fox *et al.*, 2000) as well as spatial co-existence (Koenig, 1998, 1999). However, spatial autocorrelation contradicts the assumption of independence. The main aim of this study is to determine whether correlations between the vegetation, soil and geology in the semi-arid Bushmanland region of South Africa exist. Therefore, the need for comprehensive statistical analysis is limited, eliminating the problem of independence assumptions to some degree (Liebhold *et al.*, 1993). In Chapter 7 landscape-level relationships were examined by means of typical surface pattern analysis (Legendre, 1993).

3.4.1 Method 1

The first method consisted of the construction of correlation maps (overlay method) based on the older method of trend-surface analysis. Trend-surface analysis expresses variables as a function of sample localities. It makes use of lines to represent the recognition, isolation, and measurement of trends. This method was used due to its simplicity in order to obtain trend lines and spatial structure from the environmental data obtained (Agterberg, 1964; Chayes & Suzuki, 1973; Student, 1914; Unwin, 1979). After the construction of correlation maps, information obtained from these maps were used to construct correlation matrix diagrams to illustrate the relationship between geology and vegetation, soil and vegetation as well as geology and soil respectively. The correlation matrix diagrams were used for the identification of two-tier correlations and establishing the degree of correlation.

3.4.2 Method 2

The second method was based on the concept of areal interpolation (Maantay *et al.*, 2007). Areal interpolation can be described as the re-aggregation of data into new geographic zones through the application of spatial algorithms. This technique rests on the perception that the estimated quantity at the intersecting zone is proportional to that proportion of the source zone (Eicher & Brewer, 2001; Fisher & Longford, 1996; Flowerdew & Green, 1992; Goodchild & Lam, 1980; Langford *et al.,* 1991; Tapp, 2010).

To exert this areal interpolation technique the concept of a block count methods was applied (Griffith *et al.*, 2003; Loveland *et al.,* 2002). Based on the recommendations provided by O'Neill *et al.* (1996) a grid consisting of 100 m by 100 m blocks was placed over the vegetation, soil and geology maps respectively (see Figure 3-5 for example).

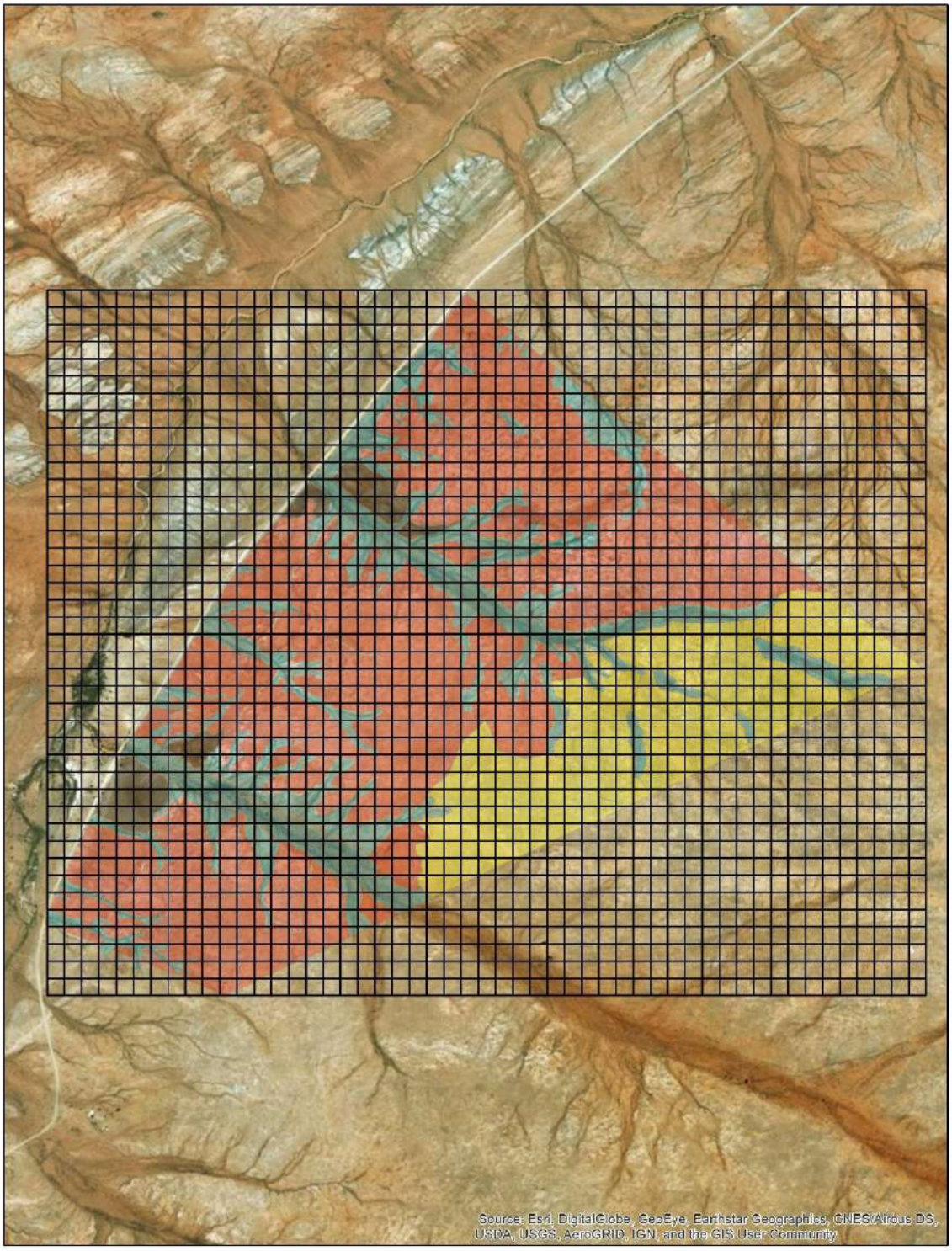

Figure 3-5: Example of the block count method used to identify three-tier correlations (this example illustrates the plant community map).

Please note that for the identification of three-tier correlations plant communities were used instead of vegetation habitats due to statistical analysis supporting the identification of these plant communities. At each intersection point (total of 988 intersection points) the plant community, soil group and geological lithostratigraphical unit was recorded (for instance P1S3G1). Table 3-2 illustrates the codes used for these descriptions.

Table 3-2: Description codes of three-tier correlations.

Plant Communities		Soil Groups		Geological Units	
P1	*Rhigozum trichomum – Stipagrostis namaquensis* Shrubland	S1	Silicic (*Oudtshoorn, Knersvlakte*)	G1	Alluvial and aeolian sandy material.
P2	*Calobota spinescens – Stipagrostis fastigiata* Grassland	S2	Calcic (*Etosha, Addo, Brandvlei, Coega*)	G2	Surficial calcrete deposits with occasional gneiss outcrops.
P3	*Stipagrostis ciliate – Stipagrostis obuse* Shrubby Grassland	S3	Cumilic (*Oakleaf, Augrabies, Dundee*)	G3	Granitoids: Gneiss > Metaquartzite > pegmatite.
P4	*Salsola tuberculate – Stipagrostis obtuse* Shrubby Grassland	S4	Lithic (*Mispah*)	G4	Metaquartzite outcrops.
				G5	Gypsic deposits.

Each intersection point represents 1.0 ha polygons. After recording all the combinations within the study area, the total representation percentages of each correlation were calculated.

CHAPTER 4

VEGETATION IDENTIFICATION, CLASSIFICATION AND MAPPING

This chapter presents the results of Phase I: Mapping with satellite imagery to create characteristic mapping units. It also presents Phase II: Surveying for identification, description and classification purposes and Phase III: Sampling and analyses, with respect to the vegetation survey as described in Chapter 3. The objective of Chapter 4 was therefore to reflect on species composition, habitat description and plant community classification in order to construct maps and visually present potential correlations between vegetation, soil and geology.

4.1 Mapping with satellite imagery

As mentioned in Chapter 3 aerial photography (Google Earth, 2016) was used during the first phase to divide the study area into characteristic mapping units according to the principles of parametric terrain evaluation, as described by Mitchell (1977). Figure 4-1 illustrates the different mapping units as well as sub-units that were identified (consult Table A-1 in Annexure A for localities and descriptions of mapping units and sub-units).

A total of ten mapping units (referred to as mapping units A – J) were identified based on corresponding characteristics visible on satellite imagery. Each mapping unit consists of various sub-units depending on locality.

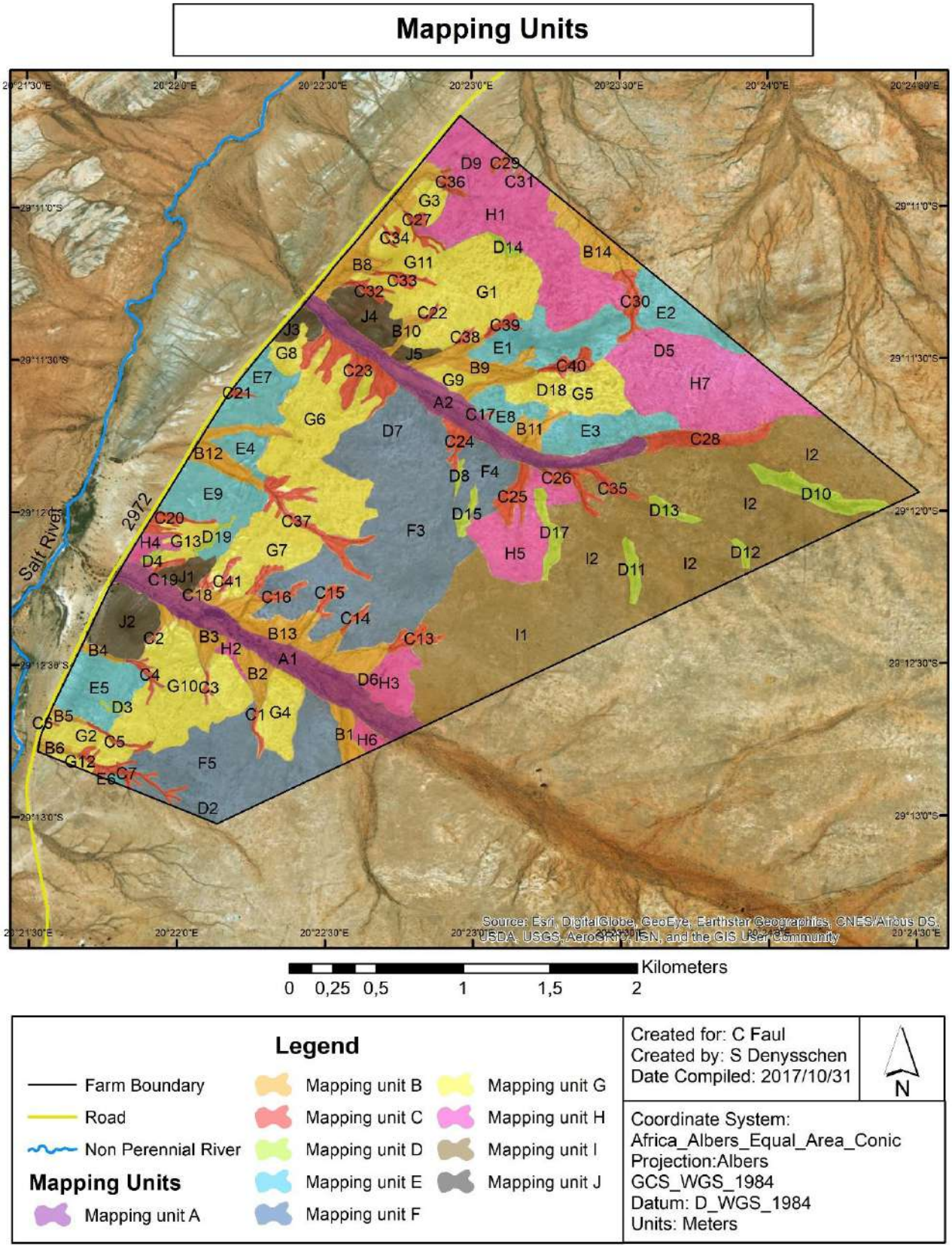

Figure 4-1: Mapping units and sub-units identified for the study area (Google Earth, 2016).

4.2 Vegetation identification, classification and mapping

An integrated nested approach was followed to describe the vegetation of this study area. The applicable biomes and veld types were described according to Mucina & Rutherford (2006) (see Chapter 2 section 2.7). Species composition of the area was determined based on a floristic approach (Driver *et al.,* 2009) followed by vegetation habitat descriptions based on species composition data. Consequently, statistical data were utilised to classify and describe plant communities.

4.2.1 Species Composition Structure

Vegetation survey localities in accordance with the associated mapping units are illustrated Figure 4-2.

To establish species composition all plant species within the 41 selected quadrats were identified up to species level according to Germishuizen and Meyer (2003) and counted. Table 4-1 illustrates the number (*n*) of plant species as well as the percentage of individuals per family for each identified mapping unit.

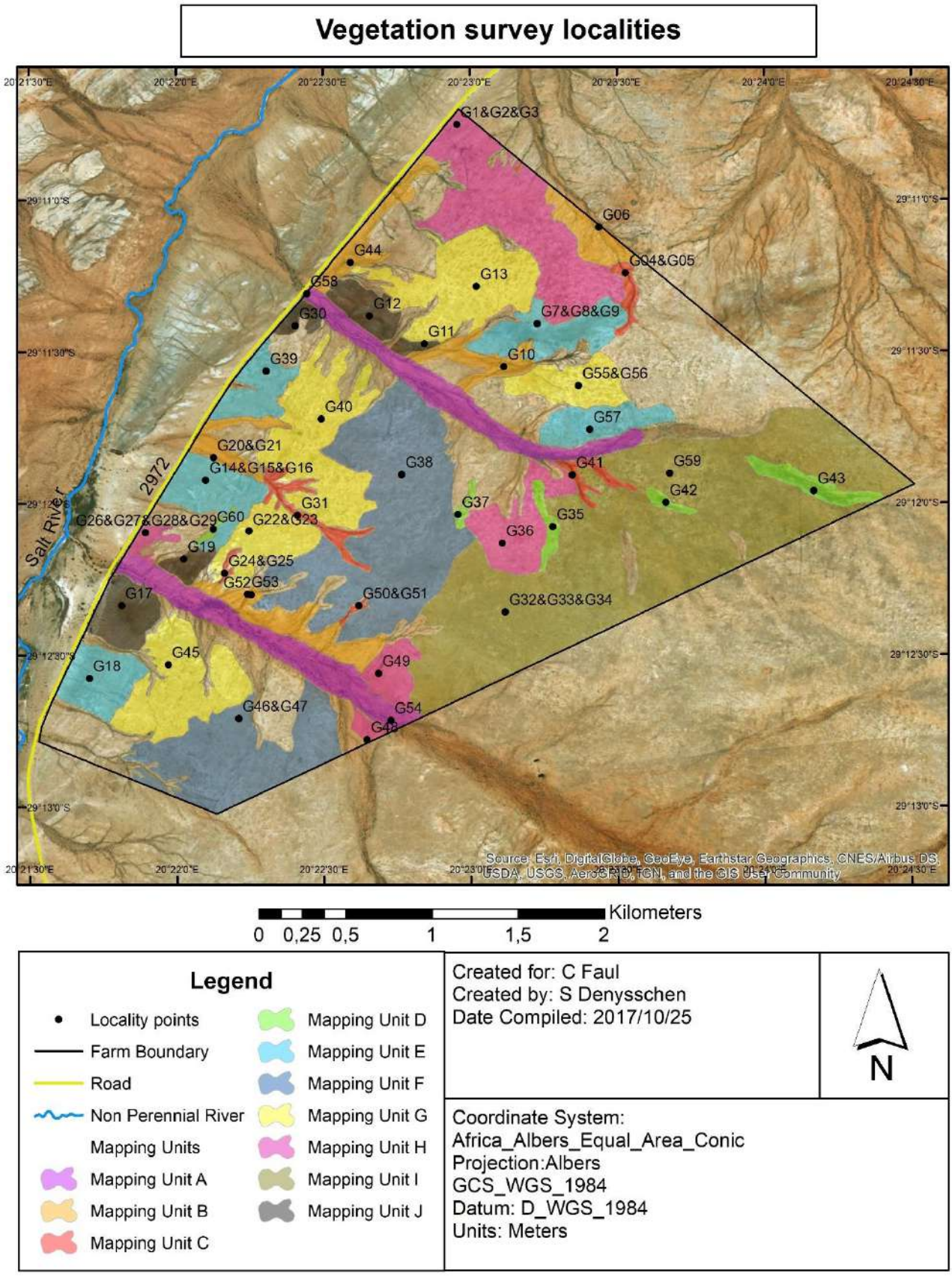

Figure 4-2: Map indicating the vegetation survey localities (Google Earth, 2016).

Table 4-1: Number (*n*) of plant species and percentage of individuals per family for each mapping unit (mu).

Plant families	mu-A		mu-B		mu-C		mu-D		mu-E	
	Species (*n*)	Individuals %	Species (*n*)	Individuals %	Species (*n*)	Individuals %	Species (*n*)	Individuals %	Species (*n*)	Individuals %
Poaceae	8	78,34	7	55,13	8	62,31	5	80,88	4	72,87
Chenopodiaceae	0	0,00	2	1,38	2	3,81	1	0,50	2	5,02
Fabaceae	1	0,50	1	0,25	2	0,76	1	0,80	0	0,00
Asteraceae	2	14,11	1	3,50	2	2,40	1	2,90	3	0,20
Zygophyllacea	1	2,77	1	0,13	2	0,87	1	0,50	2	2,11
Asparagaceae	1	0,00	0	0,00	0	0,00	0	0,00	1	0,05
Bignoniaceae	0	0,00	1	32,75	1	25,16	1	7,81	1	0,65
Scrophulariaceae	0	0,00	1	0,25	2	1,09	1	0,50	1	0,25
Solanaceae	1	1,51	1	0,13	2	1,63	2	1,80	1	0,10
Lopiocarpaceae	0	0,00	1	6,00	1	1,31	1	0,20	1	0,05
Acanthaceae	0	0,00	1	0,25	0	0,00	1	1,10	1	0,10
Aizoaceae	1	2,52	0	0,00	1	0,11	1	2,70	1	0,15
Mesembryanthemaceae	1	0,25	1	0,13	1	0,54	2	0,30	1	18,41
Apocynaceae	0	0,00	1	0,13	0	0,00	0	0,00	1	0,05

Table 4-1 (continued):Number (*n*) of plant species and percentage of individuals per family for each mapping unit (mu).

Plant families	mu-F		mu-G		mu-H		mu-I		mu-J	
	Species (*n*)	Individuals %	Species (*n*)	Individuals %	Species (*n*)	Individuals %	Species (*n*)	Individuals %	Species (*n*)	Individuals %
Poaceae	2	85,15	4	87,98	6	94,13	3	99,66	3	92,78
Chenopodiaceae	1	2,30	2	1,37	2	0,86	1	0,14	2	1,53
Fabaceae	0	0,00	1	0,20	2	0,27	0	0,00	1	1,90
Asteraceae	2	0,18	1	0,13	2	1,24	0	0,00	2	1,17
Zygophyllacea	1	0,18	2	0,13	1	0,11	0	0,00	1	0,73
Asparagaceae	0	0,00	1	0,07	0	0,00	0	0,00	1	0,15
Bignoniaceae	0	0,00	0	0,00	0	0,00	0	0,00	1	0,51
Scrophulariaceae	0	0,00	1	0,46	1	0,48	0	0,00	1	0,36
Solanaceae	1	0,09	1	0,26	2	0,27	1	0,14	1	0,15
Lopiocarpaceae	0	0,00	0	0,00	1	0,05	0	0,00	1	0,15
Acanthaceae	0	0,00	1	0,07	1	0,05	0	0,00	1	0,58
Aizoaceae	0	0,00	0	0,00	1	0,38	1	0,07	0	0,00
Mesembryanthemaceae	1	12,11	1	9,34	2	2,05	0	0,00	0	0,00
Apocynaceae	0	0,00	0	0,00	1	0,11	0	0,00	0	0,00

Refer to Figures 4-3 and 4-4 for a visual representation of vegetation data summarised in Table 4-1. Figure 4-3 provides a visual description of the biodiversity of each mapping unit with respect to the contribution of plant families and plant species.

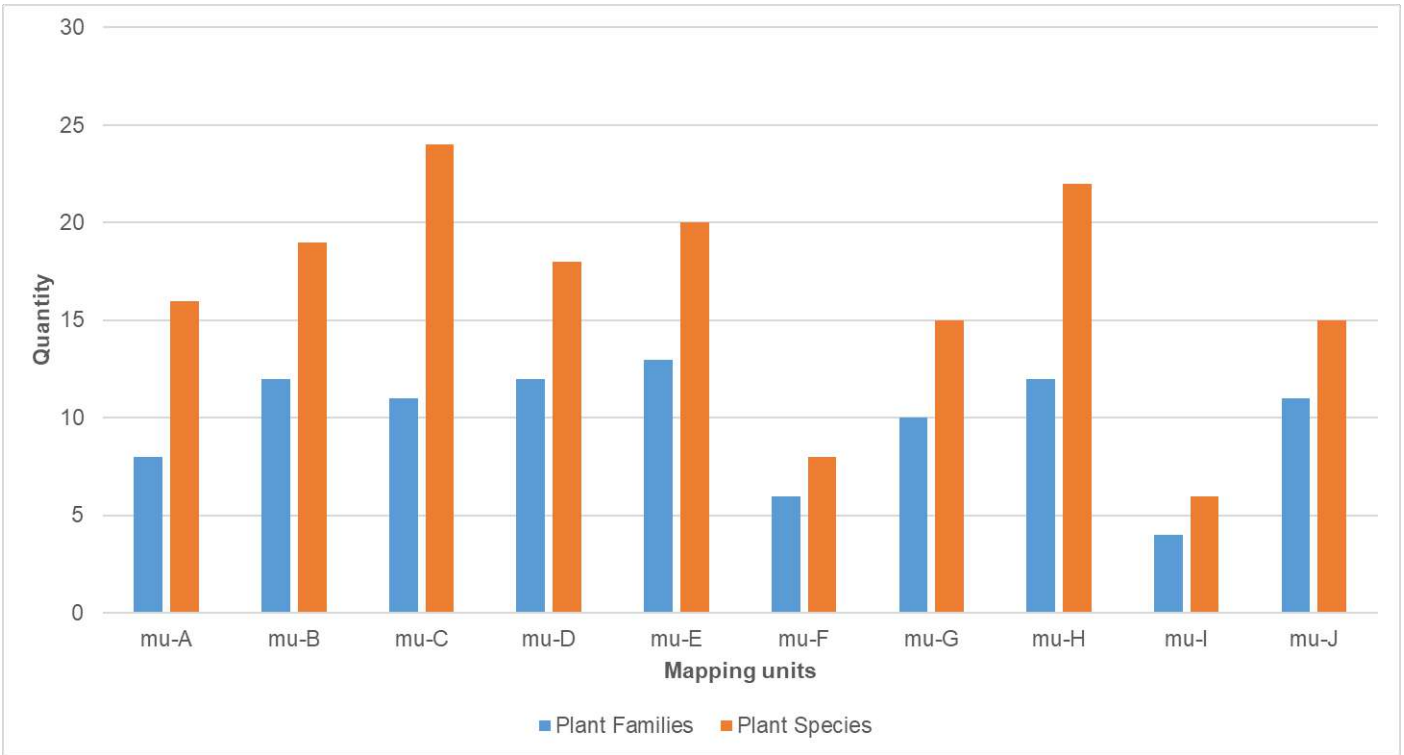

Figure 4-3: A comparison of the number of plant families and plant species present within each mapping unit.

Results presented in Figure 4-3 suggest that mapping unit C has the highest plant diversity, while mapping unit I has the lowest diversity. However, with respect to plant family contribution mapping unit E revealed higher phylogenetic diversity than mapping unit I which revealed the lowest.

Figure 4-4 illustrates the family dominance within each mapping unit. This data was used to categorise the different mapping units into habitat types (see section 4.2.4.).

Figure 4-4: Visual representation of family dominance per mapping unit.

All mapping units were dominated by the grass family (Poaceae) with varying sub-dominant families being revealed for each mapping unit (Figure 4-4). Poaceae (78.34%) and Asteraceae (14.11%) dominated mapping unit A. Mapping unit B was dominated by Poaceae (55.13%) with Bignoniaceae (32.75%) being the second most dominant plant family. Similarly, for mapping unit C [Poaceae (62.31%); Bignoniaceae (25.16%)] and D [Poaceae (80.88%); Bignoniaceae (7.81%)]. Mapping unit E [Poaceae (72.87%); Mesembryanthemaceae (18.41%)], F [Poaceae (85.15%); Mesembryanthemaceae (12.11%)] and G [Poaceae (87.98%); Mesembryanthemaceae (9.34%)] were co-dominated by Mesembryanthemaceae. Poaceae was considered the dominant plant family for mapping units H (94.13%), I (99.66%) and J (92.78%). This information was further analysed for the identification and description of habitats.

4.2.2 Plant assemblages

Significant variation in plant diversity was observed which may be attributed to variations in species composition (Hooper & Vitousek, 1997; Burns *et al.,* 2009). Non-Metric Multi-Dimensional Scaling (NMDS) ordinations based on Bray Curtis Dissimilarity Indices were applied to establish where these compositional changes occurred. Figure 4-5 illustrates the NMDS analysis for the different mapping units based on species composition.

NMDS analysis revealed clustering in a two-dimensional space. The stress factor of 0.18 suggests a useful ordination (Clarke & Warwick, 2001). Clear distinction in plant species composition were observed between the drainage systems (mapping unit A, B, C and D), metaquartzites (mapping unit J) and grassland systems (mapping unit F, G, H and I), bare patches (mapping unit E) were variously associated depending on the surrounding vegetation. The grassland plots revealed a much tighter clustering than that of the metaquartzites or drainage systems.

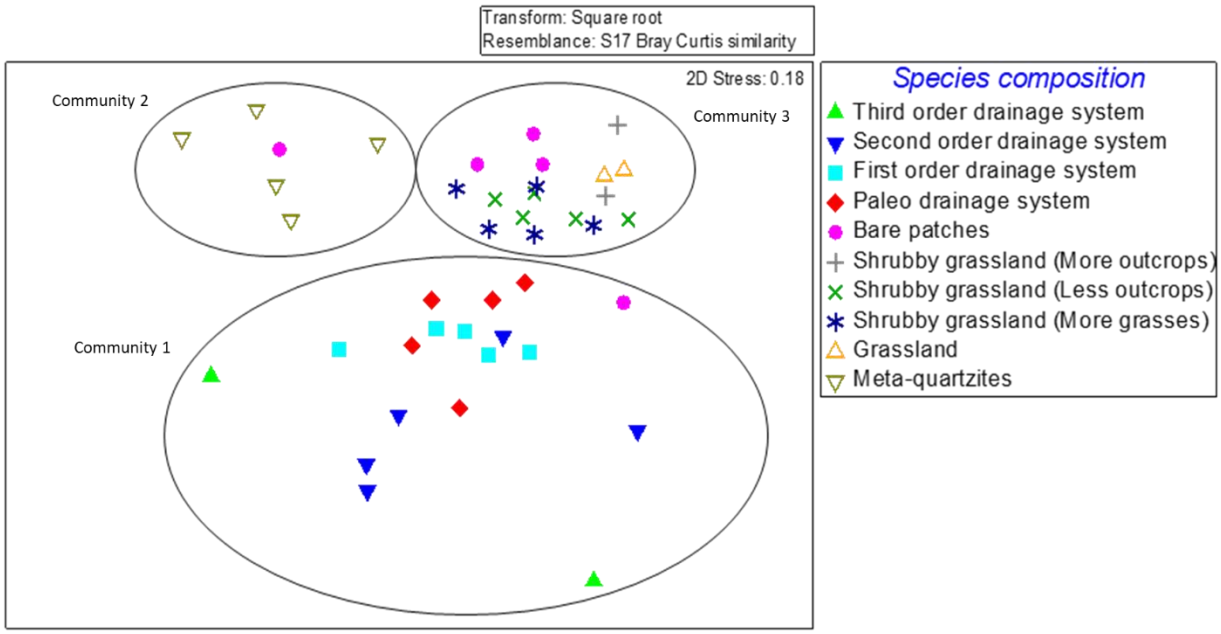

Figure 4-5: Non-metric multidimensional scaling (NMDS) analyses for different mapping units, based on species composition.

Significant differences in species composition between mapping units were confirmed with PERMANOVA analyses. Table 4-2 summarises PERMANOVA analysis of species composition and species richness between different mapping units.

Table 4-2: PERMANOVA analyses of the species composition and species richness between mapping units.

Resource	Source	*df*	SS	MS	F	*p*
Total species	Species composition	9	41544	4616	4,3552	0,01
Species	s.e.	31	32856	1059,9	4,3552	0,001

s.e., standard error; d*f*, degree of freedom; SS, sum of squared differences; MS, mean square; F, whether variability between mapping units is significantly different, i.e. higher F-values means greater significant differences; *p*, *p*-values below a certain threshold ($p < 0.05$) indicates significant differences between mapping units.

Significant differences between mapping units were confirmed with a pseudo-F value of 4.3552 and a *p*-value of 0.001 in coordination with the NMDS analyses.

4.2.3 Contributing Plant Species

Three communities were identified based on the NMDS analysis (Figure 4-5). Community 1 comprised of mapping units A, B, C and D. Community 2 comprised of mapping units E and J, whilst community 3 consisted of mapping units E, F, G, H and I.

Similarity Percentage Analysis (SIMPER) analyses were applied to the data in Paleontological Statistics software (PAST) (Hammer *et al.,* 2011) to establish which species contributed most to the variations between different mapping units (Clarke, 1993). Refer to Annexure B for SIMPER results indicating the top fifteen plant species responsible for variations between mapping units. For descriptive purposes, only the main variations in species composition between communities were described.

Considering differences in species composition between community 1 and community 2, the formar is characterised by *Stipagrostis namaquensis*, *Stipagrostis ciliata var. ciliata, Eragrostis lehmanniana var. lehmanniana, Eriocephalus ambiguus* and *Rhigozum trichotomum*, whereas community 2 is characterised by *Stipagrostis obtusa* and *Stipagrostis fastigiata*.

Differences between community 1 and community 3 were attributable to *Stipagrostis namaquensis*, *Eragrostis lehmanniana var. lehmanniana*, *Rhigozum trichotomum* and *Stipagrostis fastigiata* which characterised community 1, whilst community 3 is characterised by *Stipagrostis obtusa*, *Aridaria noctiflora*, *Stipagrostis ciliata var. ciliata* and *Salsola barbata*.

Considering differences between community 2 and community 3, community 2 was characterised by *Stipagrostis fastigiata, Calobota spinescens, Stipagrostis obtusa* and *Eriocephalus ambiguus* whereas community 3 was characterised by *Stipagrostis obtusa, Aridaria noctiflora, Stipagrostis ciliata var. ciliata, Salsola barbata* and *Salsola tuberculata.*

However, some species co-dominance was revealed between different communities. After eliminating these species, the following diagnostic plant species for each community were identified:

- *Stipagrostis namaquensis, Eragrostis lehmanniana var. lehmanniana* and *Rhigozum trichotomum* were diagnostic species for community 1 (Drainage systems).
- *Stipagrostis fastigiata* and *Calobota spinescens* were diagnostic species for community 2 (Meta-quartzites).
- *Aridaria noctiflora, Salsola barbata* and *Salsola tuberculata* were diagnostic species for community 3 (Grassland system).

4.2.4 Habitat Description

Habitats were identified based on biodiversity attributes as well as vegetation composition and plant structure. The data described in section 4.2.1 in accordance with field observations were used to identify different habitats. The study area is divided into three main habitats as illustrated in Table 4-3.

All habitats were dominated by the grass family (Poaceae), however, differences in vegetation structure were observed. The Grassland had typical deeper soils (except in mapping unit J) with occasional geological outcrops, while the Shrubby Grassland had occasional deep soils with more abundant geological outcrops and rock fragments (lag deposit) on the surface. The Drainage Systems differed from consisting of only sediments to not having any soil consisting of only pegmatite outcrops. Vegetation habitats were identified and described based on the principles as given by Kent (2012). Figure 4-6 illustrates the distribution of the different vegetation habitats within the study area.

Table 4-3: Description of identified habitats.

Habitat	Sub-division	Mapping units (mu)	Vegetation Type	Soil Forms Taxonomic System (Soil Classification Working Group *et al.*, 1991)	Dominating Geology	Images
Grassland		mu-H mu-I mu-J	These areas are dominated by Poaceae, with variations in growth structure. Grass species from mu-I tend to have of a large growth structure comparing to that of mu-H. The grasses from mu-J have the smallest growth structure. Mu-H and mu-I are dominated by *Stipagrostis obtuse* and *Stipagrostis cilliata*, whilst mu-J is dominated by *Stipagrostis obtuse*. The sub-units of mu-J, situated in the north-western segment of the study area, contain a protected plant species known as *Lithops julii subsp. fulleri var. fullerii* (Driver *et al.*, 2009).	The dominant soil forms include: - Mispah - Addo - Oakleaf Mu-H is dominated by Addo and Oakleaf soil forms indicating neocutanic, neocarbonate and soft carbonate properties (typically deeper soils). Mu-I is dominated by Addo soil forms, whereas mu-J is dominated by Mispah soil forms. A Mispah soil form is characterised by a shallow A horizon overlying hard rock. Due to limited root penetration growth structure development is limited resulting in a smaller plant growth structure.	The south-eastern segment (mu-I) as well as some localities to the north-west of the study area (mu-H) consist of surficial calcrete deposits with occasional gneiss outcrops. Mu-J is characterised by prominent metaquartzite outcrops.	   *Photographs taken by Faul C. (2017).*

Table 4-3 (continued): Descriptions of identified habitats.

Habitat	Sub-division	Mapping units (mu)	Vegetation Type	Soil Forms Taxonomic System (Soil Classification Working Group *et al.*, 1991)	Dominating Geology	Images
Shrubby Grassland		mu-E mu-F mu-G	These areas are dominated by Poaceae with sub-dominant plant family Mesembryanthemaceae. It contains a variety of grass species combined with shrubs and rocky outcrops (which contains no vegetation). The dominating species are *Stipagrostis obtuse, Stipagrostis cilliata* (smaller growth structure in the shrubby grassland than in the grassland) and *Aridaria noctiflora*. The north-eastern segment of this habitat contains a population of *Hoodia gordonii* listed as a protected species. Other protected species that occur in this habitat are *Avonia albissima, Euphorbia spinea* and *Lithops julii subsp. fulleri var. fullerii.*	The dominant soil forms include: - Brandvlei - Coega - Augrabies - Addo - Etosha Mu-E is dominated by Brandvlei, Coega and Augrabies soil forms, whilst mu-F consist of Addo soil forms. Addo and Etosha soil forms dominate mu-G. All these soils can be categorised as calcic soils with high concentrations of carbonates.	The north-western segment of the study area consists of abundant outcrops (granitoids) with the following order of abundancy: Gneiss > metaquartzite > pegmatite > surficial calcrete deposits.	 *Photographs taken by Faul C. (2017).*

Table 4-3 (continued): Descriptions of identified habitats.

Habitat	Sub-division	Mapping units (mu)	Vegetation Type	Soil Forms Taxonomic System (Soil Classification Working Group *et al.*, 1991)	Dominating Geology	Images
Shrubby Grassland	*Bare Patches*	mu-E	These bare patches have a very sparse vegetation cover. **The reason for their development is still unclear.** Where vegetation are present, species like *Salsola barbata*, *Salsola tuberculate*, *Lycium oxycarpum*, *Pteronia mucronate*, *Lycium bosciifolium* and *Eriocephalus ambiguus* dominates.	The soil can be described as a fine silty material. The dominating soil forms are: - Addo - Mispah Even though there are Mispah soil forms present within these bare patches, the lack of vegetation is not a result of limiting soil depth. The majority of these bare patches consist of calcareous Addo soil forms.	The geology corresponds to that of the shrubby grassland. The north-western segment of the study area consists of abundant outcrops (granitoids) with the following order of abundancy: Gneiss > metaquartzite > pegmatite > surficial calcrete deposits.	   *Photographs taken by Faul C. (2017).*

Table 4-3 (continued): Descriptions of identified habitats.

Habitat	Sub-division	Mapping units (mu)	Vegetation Type	Soil Forms Taxonomic System (Soil Classification Working Group *et al.*, 1991)	Dominating Geology	Images
Drainage systems	*Stream Order 3*	mu-A	Drainage systems with stream order 3 are dominated by Poaceae with a sub-dominant plant family Asteraceae. The area is dominated by *Stipagrostis namaquensis, Stipagrostis cilliata and Eriocephalus ambiguus.*	Dominating soil forms: - Dundee Identified by the presence of stratified alluvium.	Alluvial and aeolian sandy material.	
	Stream Order 2	mu-B	Drainage systems with stream order 2 are dominated by Poaceae with sub-dominant plant family Bignoniaceae. These areas are dominated by *Stipagrostis namaquensis, Stipagrostis obtuse and Rhigozum trichotomum.*	Dominating soil forms: - Dundee - Augrabies - Oakleaf - Knersvlakte	Alluvial and aeolian sandy material.	
	Stream Order 1	mu-C	Drainage systems with stream order 1 are dominated by Poaceae with sub-dominant plant family Bignoniaceae. These areas are dominated by *Stipagrostis cilliata, Stipagrostis obtuse and Rhigozum trichotomum.*	Dominating soil forms: - Oakleaf - Oudtshoorn	Less sediments and more pegmatite outcrops.	

Table 4-3 (continued): Descriptions of identified habitats.

Habitat	Sub-division	Mapping units (mu)	Vegetation Type	**Soil Forms** Taxonomic System (Soil Classification Working Group *et al.*, 1991)	Dominating Geology	Images
Drainage systems	*Paleo drainage systems*	mu-D	These areas are dominated by Poaceae with sub-dominant plant family Bignoniaceae. Dominant plant species for this area include *Stipagrostis cilliata, Stipagrostis obtuse* and *Rhigozum trichotomum.*	Dominating soil forms: - Addo Typically characterised by deeper, calcareous soils.	Alluvial and aeolian sandy material.	 *Photographs taken by Faul C. (2017).*

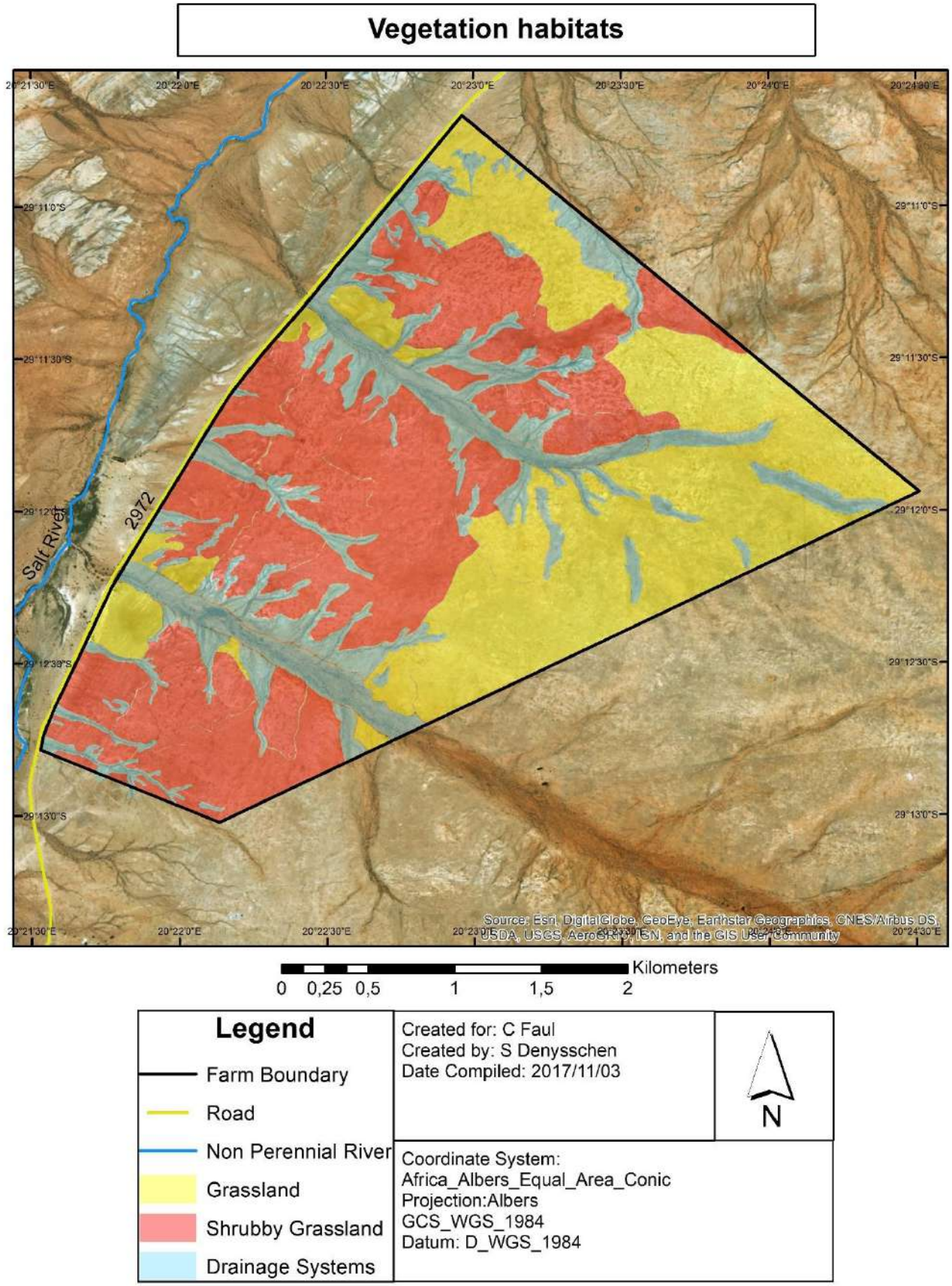

Figure 4-6: Map indicating the vegetation habitats of the study area (Google Earth, 2016).

The area consisted mainly of Grassland and Shrubby Grassland. All the localities where Mispah forms were identified are associated with a Grassland habitat that differed in structural composition comparing to the rest of the habitat. The Drainage Systems had a unique species composition and were associated with Dundee and Oakleaf soil forms.

4.2.5 Classification of Plant Communities

Plant communities were classified based on the numerical classification systems as described by Whittaker (1978a), by using statistical data [refer to the NMDS analyses (Figure 4-5)] in corporation with field observations. Plant communities will not be described based on species dominance [the term “dominant species” refers to the most conspicuous species with the highest frequency (Whittaker, 1978b)], but rather based on the diagnostic species, which makes each community unique.

Data analyses (see Figure 4-5) and additional field observations resulted in the identification of four plant communities that could be grouped into three major community units:

1. *Rhigozum trichotomum – Stipagrostis namaquensis* Shrubland
2. *Calobota spinescens – Stipagrostis fastigiata* Grassland
3. *Stipagrostis obtusa* Shrubby Grassland
    3.1. *Stipagrostis ciliata – Stipagrostis obtusa* Shrubby Grassland
    3.2. *Salsola tuberculata – Stipagrostis obtusa* Shrubby Grassland

The description of the identified plant communities is as follows:

1. *Rhigozum trichotomum – Stipagrostis namaquensis* Shrubland

The *Rhigozum trichotomum – Stipagrostis namaquensis* Shrubland is strongly associated with current (mapping units A, B and C) and palaeo drainage systems (mapping unit D), and contains the Drainage Systems habitat. It consists of either shallow soils (Augrabies, Oakleaf and Knersvlakte soil forms) with prominent geological outcrops, or deep alluvial and aeolian sandy material (Dundee soil forms). This community is situated on the Bushmanland Terrane of the Namaqua-Natal Metamorphic Complex (Cornell *et al.*, 2006).

Stipagrostis namaquensis, Eragrostis lehmanniana, Rhigozum trichotomum, Stipagrostis obtusa, Stipagrostis ciliata, Eriocephalus ambiguus and *Stipagrostis fastigiata* are considered characteristic to this community. The diagnostic species for this community include the shrub *Rhigozum trichotomum* and the grasses *Stipagrostis namaquensis* and *Eragrostis lehmanniana.*

2. *Calobota spinescens – Stipagrostis fastigiata* Grassland

The *Calobota spinescens – Stipagrostis fastigiata* Grassland is strongly associated with metaquartzite outcrops (mapping unit J) in close proximity to the north-western boundary of the study area, and contains the Grassland habitat. This area is dominated by Mishap soil forms which is characterised by shallow soils that limit root development giving rise to plants with smaller growth structures. The area consists of prominent metaquartzite outcrops forming part of the Bushmanland Terrane within the Namaqua-Natal Metamorphic Province (Cornell *et al.*, 2006).

Stipagrostis obtusa, *Stipagrostis fastigiata*, *Calobota spinescens* and *Eriocephalus ambiguus* are considered characteristic to this community, while the grass *Stipagrostis fastigiata* and the shrub *Calobota spinescens* are considered diagnostic for this community.

3. *Stipagrostis obtusa* Shrubby Grassland

This community is characterised by *Stipagrostis obtusa*, *Aridaria noctiflora*, *Stipagrostis ciliata*, *Salsola barbata* and *Salsola tuberculata*. The *Stipagrostis obtusa* Shrubby Grassland consists of two sub-communities:

3.1. *Stipagrostis ciliata – Stipagrostis obtusa* Shrubby Grassland

This sub-community is situated in the south-eastern segment of the study area and occurs in deeper calcic soils where Addo and Oakleaf soil forms dominate. These areas consist of surficial calcrete deposits with occasional gneiss outcrops. Even though this sub-community is identified as a Shrubby Grassland it consists mainly of grass species and contains the Grassland habitat (mapping unit I). However, according to NMDS analyses it is categorised together with *Salsola tuberculata – Stipagrostis obtusa* Shrubby Grassland due to the dominance of *Stipagrostis obtusa* in both sub-communities. The diagnostic species for this sub-community include the grasses *Stipagrostis obtusa* and *Stipagrostis ciliata*.

3.2. *Salsola tuberculata – Stipagrostis obtusa* Shrubby Grassland

This sub-community is situated in the north-western segment of the study area and occurs in shallow soils known as Brandvlei, Coega, Augrabies, Addo and Etosha soil forms. It contains the Shrubby Grassland habitat which are made of mapping units E, F, G and H. These areas consist of abundant outcrops (granitoids) with the following order of abundancy: Gneiss > metaquartzite > pegmatite > surficial calcrete deposits. The diagnostic species for this sub-community includes the shrubs *Salsola barbata* and *Salsola tuberculata* and the succulent *Aridaria noctiflora*. According to the Northern Cape Nature Conservation Act (9 of 2009) four species within this sub-community are considered as protected. These species include *Hoodia gordonii, Avonia albissima, Euphorbia spinea* and *Lithops julii subsp. fulleri var. fullerii.*

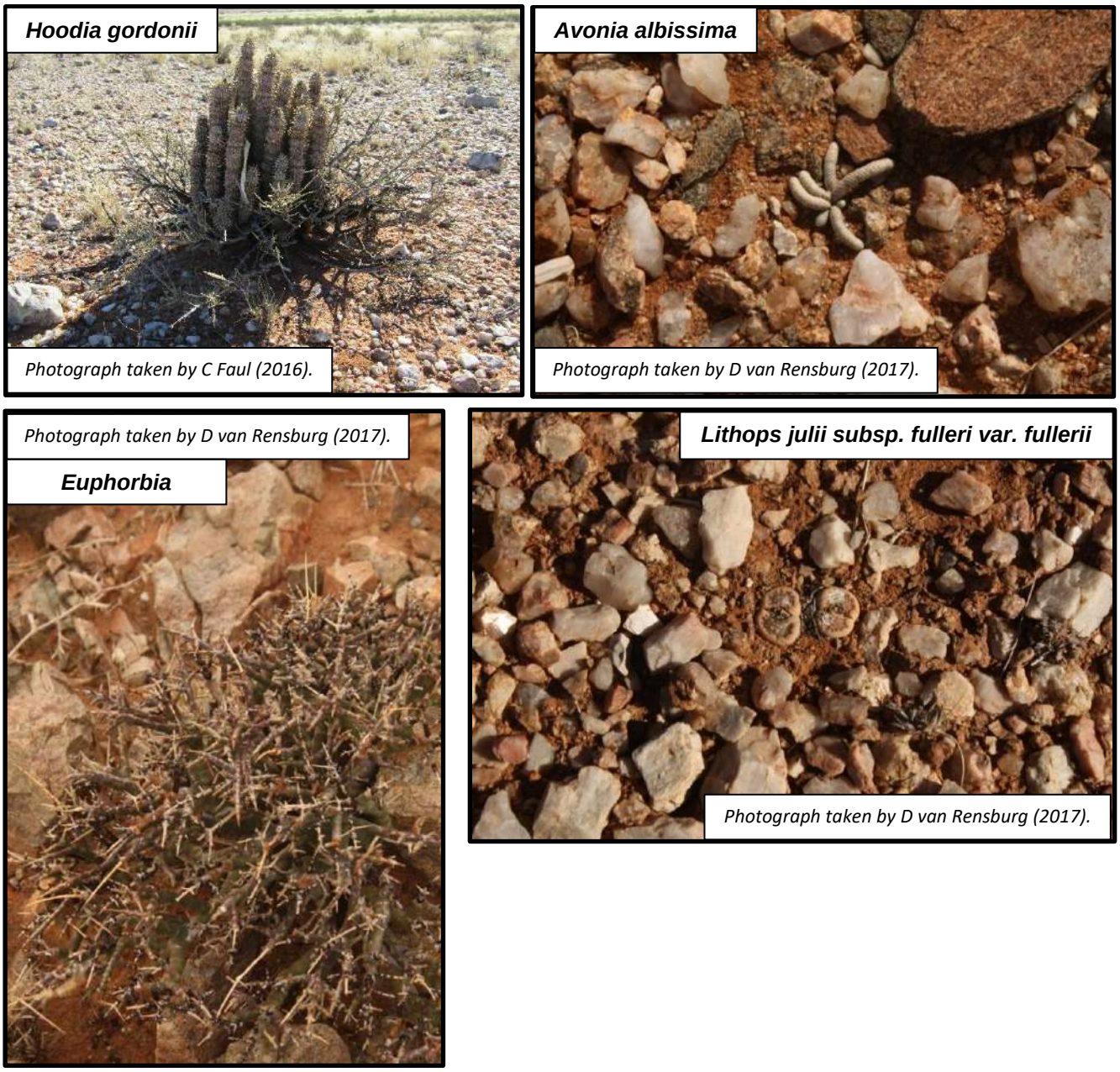

Figure 4-7: Photographs of protected plant species according to the Nature Conservation Act (9 of 2009).

A map was constructed (Figure 4-8) to illustrate the distribution of the classified plant communities and sub-communities within the study area.

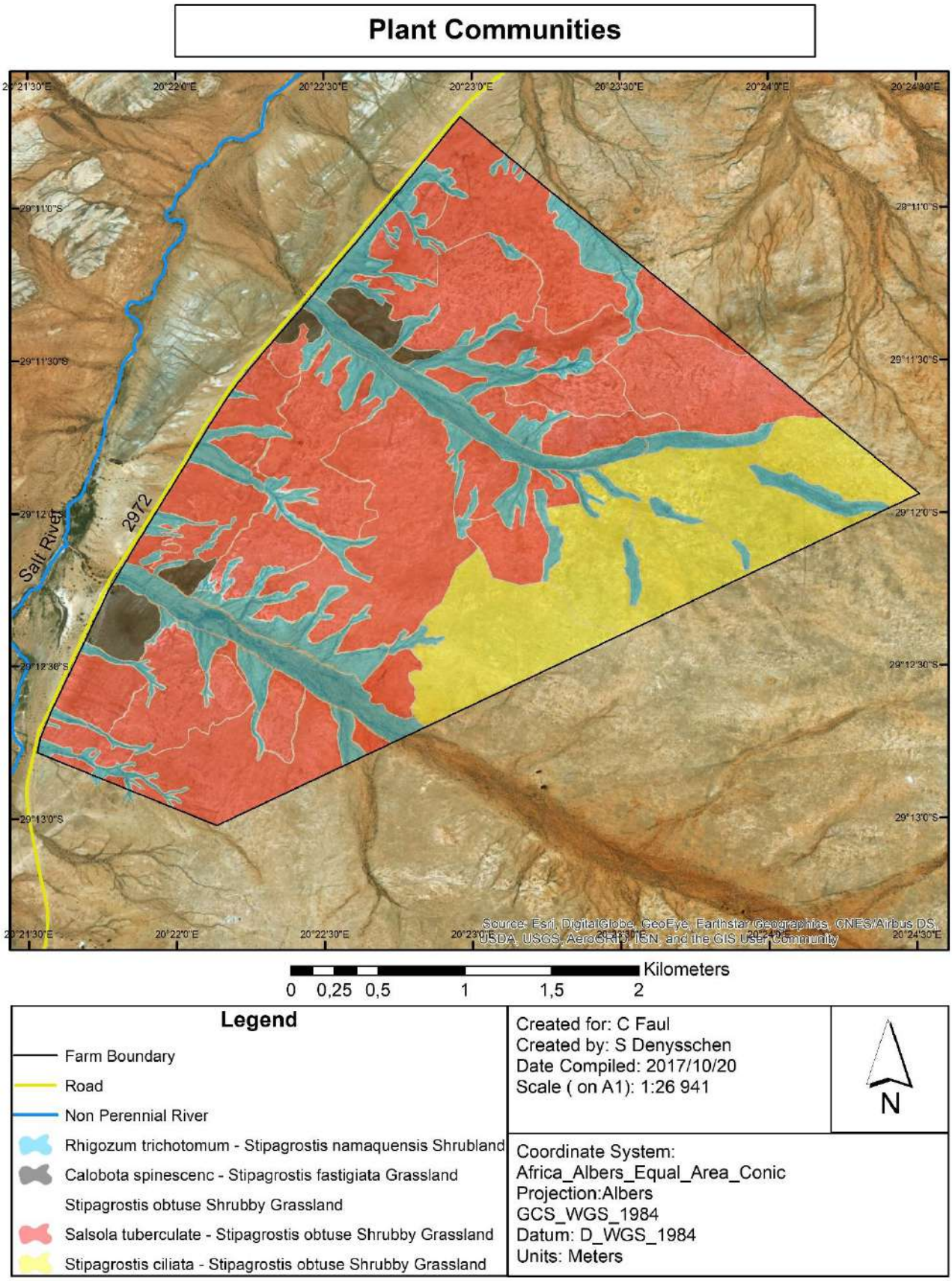

Figure 4-8: Map indicating the plant communities and sub-communities of the study area (Google Earth, 2016).

The area was mainly occupied by *Stipagrostis obtusa* Shrubby Grassland, which was divided into two sub-communities, *Salsola tuberculata – Stipagrostis obtusa* Shrubby Grassland in the north-west and *Stipagrostis ciliata – Stipagrostis obtusa* Shrubby Grassland in the south-east. All the localities where Mispah forms were identified were associated with *Calobota spinescens – Stipagrostis fastigiata* Grassland. The drainage systems had a unique species composition and were classified as *Rhigozum trichotomum – Stipagrostis namaquensis* Shrubland.

4.3 Basic Conclusion

Based on the aims and objectives of this study, plant communities and habitats were identified and classified accordingly to construct maps for correlation purposes. There existed a strong correlation between plant community *Rhigozum trichotomum – Stipagrostis namaquensis* Shrubland and the Drainage Systems habitat. Partial correlations were revealed between *Salsola tuberculata – Stipagrostis obtusa* Shrubby Grassland and the Shrubby Grassland habitat, and also between *Stipagrostis ciliata – Stipagrostis obtusa* Shrubby Grassland and the Grassland habitat. Refer to Chapter 7 for additional information regarding the role of plant communities in the correlation relationship between vegetation, soil and geology.

CHAPTER 5

SOIL IDENTIFICATION, CLASSIFICATION AND MAPPING

This chapter presents Phase II: Surveying for identification, description and classification purposes, and Phase III: Sampling and analyses with respect to the soil survey as described in Chapter 3. The purpose of Chapter 5 is therefore to reflect all soil data collected, in order to construct maps to visualise any possible correlations between vegetation, soil and geology.

5.1 Land Type Data

A predictive soil mapping approach was followed due to low soil variability and restrictive climatic conditions relating to agricultural potential. Note that since the information obtained from the land type survey is of a reconnaissance nature, only the general dominance of the soils in the landscape can be provided and not the actual area of occurrence within a specific land type. Land type data was obtained from the Agricultural Research Council (Land Type Survey Staff, 2003) and entails the division of land into land types, typical terrain cross sections and dominant soil types for each terrain unit (consult Annexure C Figure C-1 for more information). A land type can be defined as an area with similar climate, topography and soil distribution patterns.

One land type (Ag3) dominates the entire study area. According to the Land Type Survey Staff (2003), 40% of land type Ag3 consists of freely drained, shallow (< 300 mm deep), red, eutrophic, apedal soils with yellow-brown soils comprising less than 10% of this land type. The average depth of all soils is 280.5 mm. Approximately 77% of land type Ag3 consist of soils with a depth of ≤ 300 mm (depth class D1), whereas 12.5% consist of soil with a depth of 901 mm to 1200 mm (depth class D4). The average topsoil clay percentage of land type Ag3 is 10.7%. Around 88.5% of land type Ag3 consist of loamy sand soils (clay class C2) with an average clay percentage of 6.1% to 15% in the topsoil, whilst 1% consist of sandy loam soils (clay class C3) with an average clay percentage of 15.1% to 25% in the topsoil (Land Type Survey Staff, 2003).

The soils of land type Ag3 can be divided into three soil classes. Table 5-1 illustrates the different soil classes, description of soil classes, soil forms and percentage occupancy of each soil class within land type Ag3.

Table 5-1: Description of soil classes within land type Ag3 (Land Type Survey Staff, 2003).

Soil Classes	Description	Soil Form	Percentage occupancy
S2	Freely drained, structureless soils.	Hutton, Clovelly, Griffen, Shortlands, Oakleaf.	58,3%
S13	Lithic soil (shallow soils on hard weathering rocks).	Mispah, Glenrosa.	31,2%
S16	Non-soil land classes	Pans, rivers, stream beds, erosion structures, marshes, reclaimed land, dunes, gravel, etc.	0,5%

Approximately 58.3% of land type Ag3 consists of freely drained, structureless soils, whereas 31.2% consist of characteristic lithic soils. A small part (0.5%) of land type Ag3 is occupied by structures like pans, rivers, stream beds, erosion structures, marshes, reclaimed land, dunes and gravel.

5.2 Soil Description and Classification

Soil survey localities in accordance with the associated mapping units are illustrated in Figure 5-1. A total of 41 localities were selected for soil description and classification purposes.

The morphological, chemical, and physical properties (at field level) of each soil horizon were described according to the guidelines set out by the Agricultural Research Council (Land Type Survey Staff, 1991). (Consult Figure A-1 in Annexure A for explanation of soil description categories, and Figure A-2 in Annexure A to view the standard soil description form). The Binomial System (MacVicar *et al.*, 1977) was used for soil classification, because the original land type surveys were conducted with this system. A re-classification was done using the Taxonomic System (Soil Classification Working Group, 1991) in order to interpret and re-classify the soil data with respect to soil families. Soil was classified according to a hierarchical system incorporating classification categories. The classification categories used in this study for the purpose of soil descriptions include soil order, soil group, soil form and soil family. All soil description data, as well as soil classification per mapping unit are illustrated in Figure 5-2.

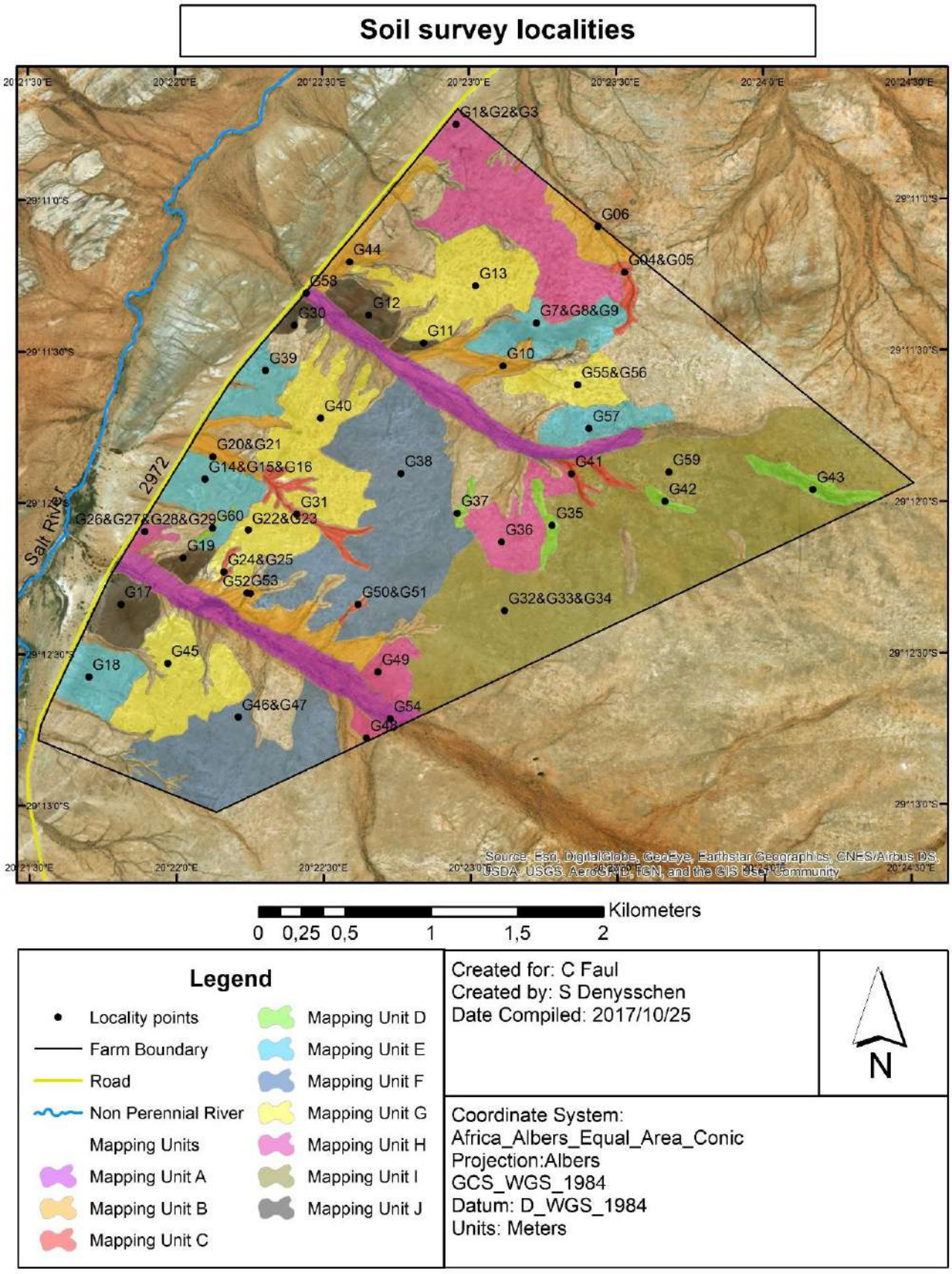

Figure 5-1: Map indicating the soil survey localities in accordance with the associated mapping units (Google Earth, 2016).

MAPPING UNIT A

Mapping Unit	Horizon	Texture class	Depth (mm)	Clay %	Sand grade	Dry colour	Moist colour	Mottles		Lime		Structure			Coarse fragments	
								OCC	COL	OCC	Type	GRA	Size	Type	Type	%
A1	A	co	0-600	0-15	co	2,5YR 6/8	2,5YR 5/8	N/A	N/A	N/A	N/A	A	c	SG	G	90
A2	A	co	0-800	0-15	co	2,5YR 6/8	2,5YR 5/8	N/A	N/A	N/A	N/A	A	c	SG	G	90

Mapping Unit	Parent material	Efficient Depth (mm)	Terrain Unit	Depth limiting material
A1	Transported material (Quartz)	600	5	Soil with low consistency.
A2	Transported material (Quartz)	200	5	Soil with low consistency.

Mapping Unit	Sample No.	Coordinates		Initial Weight (g)	Weight after (g)		
		Latitude	Longitude		Coarse (> 2 mm)	Fine (< 2 mm)	Total
A1	G54	29°12'42,9"S	20°22'43,7"E	2714	1166	1519	2685
A2	G58	29°11'18,5"S	20°22'26,7"E	1500	742	750	1492

Mapping Unit	Diagnostic Soil Horizon	Soil Form	Soil Family	WRB Reference Soil Group	USDA Soil Taxonomy
A1	Stratified alluvium	Dundee	Marico 2110	Fluvisols	Inceptisols – Fluventic variants
A2	Stratified alluvium	Dundee	Marico 2110	Fluvisols	Inceptisols – Fluventic variants

Mapping unit A1 – *Photograph taken by Faul C. (2017).*

Figure 5-2: Soil description and classification (Fey, 2010; IUSS Working Group WRB, 2006; Land Type Survey Staff, 1991; MacVicar *et al.*, 1977; Soil Classification Working Group, 1991; Soil Survey Staff, 1999).

MAPPING UNIT B

Mapping Unit	Horizon	Texture class	Depth (mm)	Clay %	Sand grade	Dry colour	Moist colour	Mottles		Lime		Structure			Coarse fragments	
								OCC	COL	OCC	Type	GRA	Size	Type	Type	%
B8	A	fi	0-400	0-15	fi	5YR 6/8	2,5YR 4/6	N/A	N/A	N/A	N/A	A	f	SG	G	20
B9	A	fi	0-400	0-15	fi	10R 5/8	10YR 5/6	N/A	N/A	s	P	A	f	SG	G	10
B12 – In riverbed	A	co	0-150	0-15	co	2,5YR 7/8	2,5YR 5/8	N/A	N/A	N/A	N/A	A	c	SG	G	20
B12 – On riverbank	A	fi	0-200	0-15	fi	2,5YR 6/8	2,5YR 5/10	N/A	N/A	N/A	N/A	A	f	SG	G	5
B13 – In riverbed	A	co	0-450	0-15	co	5YR 5/8	2,5YR 5/8	N/A	N/A	N/A	N/A	A	c	SG	G + S	80
B13 – On riverbank	A	co	0-420	0-15	co	2,5YR 5/8	5YR 5/8	N/A	N/A	N/A	N/A	A	c	SG	G + S	30
B14	A	co	0-600	0-15	co	5YR 5/8	10YR 5/6	c	Bl	N/A	N/A	A	m	SG	G	20

Mapping Unit	Parent material	Efficient Depth (mm)	Terrain Unit	Depth limiting material
B8	Quartz	200	4U	Quartz fragments
B9	Quartz	200	4L	Quartz fragments
B12 - In riverbed	Feldspar; Quartzite-schist	150	5	Calcrete; Feldspar and Quartzite-schist fragments
B12 - On riverbank	Feldspar; Quartzite-schist	200	4U	Calcrete; Feldspar and Quartzite-schist fragments
B13 - In riverbed	Quartz	350	5	Quartz outcrop
B13 - On riverbank	Quartz	300	5	Dorbank
B14	Quartz	50	4U	Dorbank

Mapping unit B14 – *Photographs taken by Faul C. (2017).*

Figure 5-2 (continued): Soil descriptions and classifications (Fey, 2010; IUSS Working Group WRB, 2006; Land Type Survey Staff, 1991; MacVicar *et al.*, 1977; Soil Classification Working Group, 1991; Soil Survey Staff, 1999).

Mapping Unit	Sample No.	Coordinates		Initial Weight (g)	Weight after (g)		
		Latitude	Longitude		Coarse (> 2 mm)	Fine (< 2 mm)	Total
B8	G44	29°11'12,3"S	20°22'35,6"E	2434	572	1852	2424
B9	G10	29°11'33,0"S	20°23'06,9"E	2609	357	2230	2587
B12 - In riverbed	G20	29°11'50,9"S	20°22'07,6"E	3271	984	2240	3224
B12 - On riverbank	G21	29°11'50,9"S	20°22'07,6"E	2505	217	2280	2497
B13 - In riverbed	G53	29°12'17,9"S	20°22'14,5"E	1756	635	1106	1741
B13 - On riverbank	G52	29°12'18,0"S	20°22'15,2"E	2826	830	1456	2286
B14	G06	29°11'05,4"S	20°23'26,3"E	2110	591	1518	2109

Mapping Unit	Diagnostic Soil Horizon	Soil Form	Soil Family	WRB Reference Soil Group	USDA Soil Taxonomy
B8	Neocutanic	Oakleaf	Caledon 1210	Acrisols Lixisols Arenosols Cambisols	Inceptisols
B9	Neo-carbonate	Augrabies	Khubus 1210	Luvisols Lixisols Arenosols Cambisols	Aridisols Inceptisols
B12 – In riverbed	Stratified alluvium	Dundee	Marico 2110	Fluvisols	Inceptisols Fluviantic variants
B12 – On riverbank	Neocutanic	Oakleaf	Caledon 1210	Acrisols Lixisols Arenosols Cambisols	Inceptisols
B13 – In riverbed	Stratified alluvium	Dundee	Marico 2110	Fluvisols	Inceptisols Fluviantic variants
B13 – On riverbank	Stratified alluvium	Dundee	Marico 2110	Fluvisols	Inceptisols - Fluviantic variants
B14	Dorbank	Knersvlakte	Bitterfontein 1000	Durisols	Typic Haplodurids Entic Durixeralfs Haplic Durixeralfs

Mapping unit B14 – *Photographs taken by Faul C. (2017).*

Mapping unit B14 – *Photographs taken by Faul C. (2017).*

Figure 5-2 (continued): Soil descriptions and classifications (Fey, 2010; IUSS Working Group WRB, 2006; Land Type Survey Staff, 1991; MacVicar *et al.*, 1977; Soil Classification Working Group, 1991; Soil Survey Staff, 1999).

MAPPING UNIT C

Mapping Unit	Horizon	Texture class	Depth (mm)	Clay %	Sand grade	Dry colour	Moist colour	Mottles		Lime		Structure			Coarse fragments	
								OCC	COL	OCC	Type	GRA	Size	Type	Type	%
C14	A	me	0-400	0-15	me	5YR 6/8	5YR 5/8	N/A	N/A	N/A	N/A	A	m	SG	G	10
	B	me	400-600	0-15	me	7,5YR 7/4	10YR 6/8	N/A	N/A	a	P	A	m	SG	G	15
C30	A	co	0-200	0-15	co	2,5YR 5/8	2,5YR 4/8	N/A	N/A	N/A	N/A	A	c	MA	G	60
	B	co	200-590	0-15	co	5YR 4/6	10YR 5/6	N/A	N/A	N/A	N/A	M	c	CR	G+S	50
C35	A	me	0-170	0-15	me	5YR 5/8	2,5YR 4/8	N/A	N/A	N/A	N/A	A	m	SG	S	30
C37	A	co	0-200	0-15	co	2,5YR 6/8	2YR 5/8	N/A	N/A	N/A	N/A	W	c	SG	G + S	70
C41	A	me	0-300	0-15	me	7,5YR 6/6	5YR 5/8	N/A	N/A	N/A	N/A	A	f	SG	S + G	40
	B	me	300-400	0-15	me	7,5YR 7/6	5YR 68	N/A	N/A	a	P	A	f	SG	G	30

Mapping Unit	Parent material	Efficient Depth (mm)	Terrain Unit	Depth limiting material
C14	Calcrete; Feldspar; Quartz	250	4	Calcrete boulders
C30	Quartz; Feldspar	200	4	Dorbank
C35	Quartz; Feldspar	100	4	Quartz fragments
C37	Quartz; Feldspar	200	4	Quartz and calcrete boulders
C41	Calcrete; Feldspar; Quartz	200	4	Calcrete boulders

Mapping Unit	Sample No.	Coordinates		Initial Weight (g)	Weight after (g)		
		Latitude	Longitude		Coarse (> 2 mm)	Fine (< 2 mm)	Total
C14	G50	29°12'20,2"S	20°22'37,2"E	2430	395	2028	2423
	G51			1184	386	794	1180
C30	G4	29°11'14.46"S	20°23'31.74"E	2253	823	1427	2250
	G5			1353	756	591	1347
C35	G41	29°11'54,4"S	20°23'20,8"E	2616	410	2126	2536
C37	G31	29°12'02,3"S	20°22'24,7"E	3423	1137	2272	3409
C41	G24	29°12'13,7"S	20°22'09,8"E	2046	855	1193	2048
	G25			1027	499	529	1028

Figure 5-2 (continued): Soil descriptions and classifications (Fey, 2010; IUSS Working Group WRB, 2006; Land Type Survey Staff, 1991; MacVicar *et al.*, 1977; Soil Classification Working Group, 1991; Soil Survey Staff, 1999).

Mapping Unit	Diagnostic Soil Horizon	Soil Form	Soil Family	WRB Reference Soil Group	USDA Soil Taxonomy
C14	Orthic / Neocutanic	Oakleaf	Caledon 1210	Acrisols Lixisols Arenosols Cambisols	Inceptisols
C30	Neocutanic / Dorbank	Oudtshoorn	Doringbaai 1210	Durisols	Typic Petrocambids Cambidic Haplodurids
C35	Neocutanic	Oakleaf	Caledon 1210	Acrisols Lixisols Arenosols Cambisols	Inceptisols
C37	Neocutanic	Oakleaf	Caledon 1210	Acrisols Lixisols Arenosols Cambisols	Inceptisols
C41	Orthic	Oakleaf	Caledon 1210	Acrisols Lixisols Arenosols Cambisols	Inceptisols

Mapping unit C37 – *Photograph taken by Faul C. (2017).*

Mapping unit C37 – *Photograph taken by Faul C. (2017).*

Mapping unit C37 – *Photograph taken by Faul C. (2017).*

Figure 5-2 (continued): Soil descriptions and classifications (Fey, 2010; IUSS Working Group WRB, 2006; Land Type Survey Staff, 1991; MacVicar *et al.*, 1977; Soil Classification Working Group, 1991; Soil Survey Staff, 1999).

MAPPING UNIT D

Mapping Unit	Horizon	Texture class	Depth (mm)	Clay %	Sand grade	Dry colour	Moist colour	Mottles		Lime		Structure			Coarse fragments	
								OCC	COL	OCC	Type	GRA	Size	Type	Type	%
D10	A	fi	0-400	0-15	fi	5YR 5/8	5YR 5/6	N/A	N/A	N/A	N/A	A	f	SG	S	20
D13	A	fi	0-300	0-15	fi	2,5YR 5/8	5YR 5/8	N/A	N/A	N/A	N/A	A	f	SG	N/A	N/A
D15	A	fi	0-220	0-15	fi	5YR 6/8	5YR 5/8	N/A	N/A	N/A	N/A	A	m	SG	S	20
D17	A	me	0-350	0-15	me	2,5YR 6/8	2,5YR 5/6	N/A	N/A	N/A	N/A	A	m	SG	G + S	20
D19	A	fi	0-200	0-15	fi	7,5YR 6/6	10YR 6/8	N/A	N/A	s	P	A	f	SG	S	10

Mapping Unit	Parent material	Efficient Depth (mm)	Terrain Unit	Depth limiting material
D10	Feldspar; Quartzite-schist	200	4	Quartz boulders
D13	Feldspar; Quartzite-schist	300	4	Quartz boulders
D15	Feldspar; Quartzite-schist	150	4	Quartz boulders
D17	Feldspar; Quartzite-schist	200	4	Quartz boulders
D19	Feldspar; Quartzite-schist; Calcrete	200	3	Quartz and calcrete boulders

Mapping Unit	Sample No.	Coordinates		Initial Weight (g)	Weight after (g)		
		Latitude	Longitude		Coarse (> 2 mm)	Fine (< 2 mm)	Total
D10	G43	29°11'57,6"S	20°24'10,1"E	2402	278	2116	2394
D13	G42	29°11'59,9"S	20°23'39,9"E	2118	174	1943	2117
D15	G37	29°12'02,2"S	20°22'57,5"E	2326	505	1820	2325
D17	G35	29°12'04,6"S	20°23'16,8"E	2540	642	1888	2530
D19	G60	29°12'05,0"S	20°22'07,5"E	2550	253	2298	2551

Mapping Unit	Diagnostic Soil Horizon	Soil Form	Soil Family	WRB Reference Soil Group	USDA Soil Taxonomy
D10	Neocarbonate B / Soft carbonate	Addo	Spekboom 1211	Calcisols	Aridisols Inceptisols
D13	Neocarbonate B / Soft carbonate	Addo	Spekboom 1211	Calcisols	Aridisols Inceptisols
D15	Neocarbonate B / Soft carbonate	Addo	Spekboom 1211	Calcisols	Aridisols Inceptisols
D17	Neocarbonate B / Soft carbonate	Addo	Spekboom 1211	Calcisols	Aridisols Inceptisols
D19	Neocarbonate B / Soft carbonate	Addo	Spekboom 1211	Calcisols	Aridisols Inceptisols

Figure 5-2 (continued): Soil descriptions and classifications (Fey, 2010; IUSS Working Group WRB, 2006; Land Type Survey Staff, 1991; MacVicar *et al.*, 1977; Soil Classification Working Group, 1991; Soil Survey Staff, 1999).

Figure 5-2 (continued): Soil descriptions and classifications (Fey, 2010; IUSS Working Group WRB, 2006; Land Type Survey Staff, 1991; MacVicar *et al.*, 1977; Soil Classification Working Group, 1991; Soil Survey Staff, 1999).

MAPPING UNIT E

Mapping Unit	Horizon	Texture class	Depth (mm)	Clay %	Sand grade	Dry colour	Moist colour	Mottles		Lime		Structure			Coarse fragments	
								OCC	COL	OCC	Type	GRA	Size	Type	Type	%
E1	A	fi	0-300	0-15	fi	5YR 6/8	7,5YR 5/8	N/A	N/A	s	P	W	f	MA	G+S	60
	Transition	fi	300-850	0-15	fi	10R 7/4	10YR 7/4	N/A	N/A	a	P	W	f	MA	G+S	50
	B	fi	850-1650	0-15	fi	10R 7/3	10YR 7/3	N/A	N/A	a	P	W	f	MA	G	70
E3	A	fi	0-200	0-15	fi	5YR 6/8	5YR 5/6	N/A	N/A	N/A	N/A	A	f	SG	G + S	90
E5	A	fi	0-350	0-15	fi	7,5YR 7/6	7,5YR 5/8	N/A	N/A	a	P	A	f	SG	G	50
E7	A	fi	0-600	0-15	fi	7,5YR 6/8	5YR 5/8	N/A	N/A	s	P	A	f	SG	G	50
E9	A	fi	0-300	0-15	fi	7YR 6/8	5YR 6/8	N/A	N/A	c	P	A	f	SG	G+S	50
	Transition	fi	300-400	0-15	fi	10YR 8/4	7YR 7/6	N/A	N/A	a	P	A	f	SG	G+S	40
	B	fi	400-1100	0-15	fi	10YR 8/3	10YR 7/6	N/A	N/A	a	P	A	f	SG	G	30

Mapping Unit	Parent material	Efficient Depth (mm)	Terrain Unit	Depth limiting material
E1	Calcrete; Quartzite	600	3	N/A
E3	Quartz	50	2	Calcrete boulders
E5	Calcrete; Quartz	200	3	Calcrete boulders
E7	Calcrete; Quartz	200	3	Calcrete boulders
E9	Calcrete; Quartz	200	4	Calcrete boulders

Mapping Unit	Sample No.	Coordinates		Initial Weight (g)	Weight after (g)		
		Latitude	Longitude		Coarse (> 2 mm)	Fine (< 2 mm)	Total
E1	G07	29°11'24,5"S	20°23'13,7"E	2930	1411	1203	2614
	G08			1950	1084	794	1878
	G09			2067	1166	884	2050
E3	G57	29°11'45,4"S	20°23'24,4"E	3462	1602	1362	2964
E5	G18	29°12'34,5"S	20°21'42,2"E	2621	1070	1631	2701
E7	G39	29°11'33,8"S	20°22'18,4"E	2745	378	2363	2741
E9	G14	29°11'55,3"S	020°22'06,0"E	2992	729	2174	2903
	G15			1033	379	641	1020
	G16			2891	1280	1580	2860

Figure 5-2 (continued): Soil descriptions and classifications (Fey, 2010; IUSS Working Group WRB, 2006; Land Type Survey Staff, 1991; MacVicar *et al.*, 1977; Soil Classification Working Group, 1991; Soil Survey Staff, 1999).

Mapping Unit	Diagnostic Soil Horizon	Soil Form	Soil Family	WRB Reference Soil Group	USDA Soil Taxonomy
E1	Orthic Soft carbonate	Brandvlei	Grootvloer 1000	Calcisols	Aridisols Inceptisols
E3	Orthic with underlying hardpan carbonate	Coega	Nabies 1000	Calcisols	Aridisols Inceptisols
E5	Orthic / Neocarbonate B	Augrabies	Khubus 1210	Luvisols Lixisols Arenosols Cambisols	Aridisols Inceptisols
E7	Orthic with underlying hardpan carbonate	Coega	Nabies 1000	Calcisols	Aridisols Inceptisols
E9	Orthic Soft carbonate	Brandvlei	Grootvloer 1000	Calcisols	Aridisols Inceptisols

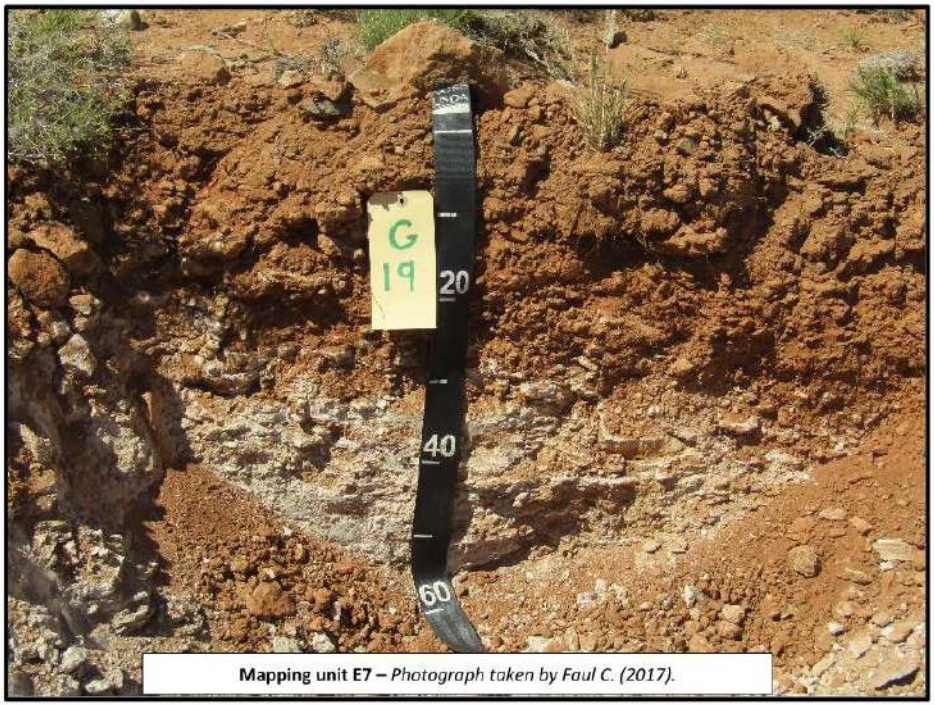

Mapping unit E7 – *Photograph taken by Faul C. (2017).*

Mapping unit E3 – *Photograph taken by Faul C. (2017).*

Figure 5-2 (continued): Soil descriptions and classifications (Fey, 2010; IUSS Working Group WRB, 2006; Land Type Survey Staff, 1991; MacVicar *et al.*, 1977; Soil Classification Working Group, 1991; Soil Survey Staff, 1999).

MAPPING UNIT F

Mapping Unit	Horizon	Texture class	Depth (mm)	Clay %	Sand grade	Dry colour	Moist colour	Mottles		Lime		Structure			Coarse fragments	
								OCC	COL	OCC	Type	GRA	Size	Type	Type	%
F3	A	me	0-100	0-15	me	7,5 YR 6/6	7,5YR 5/8	N/A	N/A	N/A	N/A	A	m	SG	S	50
F5	A	fi	0-400	0-15	fi	5YR 6/8	2,5YR 5/8	N/A	N/A	s	P	A	f	SG	G	30
	B	fi	400-600	0-15	fi	7,5YR 7/6	10YR 7/8	N/A	N/A	a	P	A	f	SG	G	10

Mapping Unit	Parent material	Efficient Depth (mm)	Terrain Unit	Depth limiting material
F3	Quartzite	50	3U	Calcrete boulders
F5	Calcrete	200	4	Calcrete boulders

Mapping Unit	Sample No.	Coordinates		Initial Weight (g)	Weight after (g)		
		Latitude	Longitude		Coarse (> 2 mm)	Fine (< 2 mm)	Total
F3	G38	29°11'54,3"S	20°22'46,0"E	1913	645	1020	1665
F5	G46	29°12'42.48"S	20°22'12.67"E	2776	641	2129	2770
	G47			1992	857	1118	1975

Mapping Unit	Diagnostic Soil Horizon	Soil Form	Soil Family	WRB Reference Soil Group	USDA Soil Taxonomy
F3	Neocarbonate B / Soft carbonate	Addo	Spekboom 1211	Carcisols	Aridisols Inceptisols
F5	Neocarbonate B / Soft carbonate	Addo	Spekboom 1211	Carcisols	Aridisols Inceptisols

Figure 5-2 (continued): Soil descriptions and classifications (Fey, 2010; IUSS Working Group WRB, 2006; Land Type Survey Staff, 1991; MacVicar *et al.*, 1977; Soil Classification Working Group, 1991; Soil Survey Staff, 1999).

Figure 5-2 (continued): Soil descriptions and classifications (Fey, 2010; IUSS Working Group WRB, 2006; Land Type Survey Staff, 1991; MacVicar *et al.*, 1977; Soil Classification Working Group, 1991; Soil Survey Staff, 1999).

MAPPING UNIT G

Mapping Unit	Horizon	Texture class	Depth (mm)	Clay %	Sand grade	Dry colour	Moist colour	Mottles		Lime		Structure			Coarse fragments	
								OCC	COL	OCC	Type	GRA	Size	Type	Type	%
G1	A	fi	0-200	0-15	fi	2,5YR 6/6	5YR 6/6	N/A	N/A	a	P	A	f	SG	G+S	40
G5	A	fi	0-70	0-15	fi	5YR 5/6	2,5YR 5/6	N/A	N/A	N/A	N/A	A	f	SG	G	30
	A continue	fi	70-150	0-15	fi	5YR 5/6	2,5YR 5/6	N/A	N/A	N/A	N/A	A	f	SG	G + S	70
G6	A	fi	0-200	0-15	fi	7,5YR 6/6	5YR 5/6	N/A	N/A	s	P	A	f	SG	S + G	60
G7	A	fi	0-200	0-15	fi	7,5YR 6/6	5YR 6/8	N/A	N/A	s	P	A	f	SG	S + G	50
	B	fi	200-600	0-15	fi	7,5YR 7/6	5YR 6/6	N/A	N/A	a	P	A	f	SG	S + G	50
G10	A	fi	0-130	0-15	fi	7,5YR 6/6	10YR 6/6	N/A	N/A	a	P	A	f	SG	S + G	70

Mapping Unit	Parent material	Efficient Depth (mm)	Terrain Unit	Depth limiting material
G1	Calcrete; Quartz	100	3	Calcrete boulders
G5	Quartz	70	3	Calcrete boulders
G6	Calcrete; Quartz; Feldspar	100	3L	Quartz & feldspar fragments
G7	Calcrete; Quartz; Feldspar	100	3U	Calcrete boulders
G10	Calcrete	50	3	Calcrete boulders

Mapping Unit	Sample No.	Coordinates		Initial Weight (g)	Weight after (g)		
		Latitude	Longitude		Coarse (> 2 mm)	Fine (< 2 mm)	Total
G1	G13	29°1'17,1"S	20°23'01,3"E	2353	688	1651	2339
G5	G55	29°11'36,8"S	20°23'22,1"E	2311	595	1715	2310
	G56			2324	980	1249	2229
G6	G40	29°11'43,3"S	20°22'29,6"E	2217	968	1239	2207
G7	G22	29°12'05,4"S	20°22'14,8"E	2516	1095	1355	2450
	G23			2208	1151	948	2099
G10	G45	29 12'31,8"S	20 21'58,3"E	2936	1220	1647	2867

Figure 5-2 (continued): Soil descriptions and classifications (Fey, 2010; IUSS Working Group WRB, 2006; Land Type Survey Staff, 1991; MacVicar *et al.*, 1977; Soil Classification Working Group, 1991; Soil Survey Staff, 1999).

Mapping Unit	Diagnostic Soil Horizon	Soil Form	Soil Family	WRB Reference Soil Group	USDA Soil Taxonomy
G1	Neocarbonate B / Soft carbonate	Addo	Spekboom 1211	Carcisols	Aridisols Inceptisols
G5	Neocutanic / Soft carbonate	Etosha	Tuli 1211	Calcisols Luvisols Lixisols	Aridisols
G6	Neocarbonate B / Soft carbonate	Addo	Spekboom 1211	Carcisols	Aridisols Inceptisols
G7	Neocarbonate B / Soft carbonate	Addo	Spekboom 1211	Carcisols	Aridisols Inceptisols
G10	Neocarbonate B / Soft carbonate	Addo	Spekboom 1211	Carcisols	Aridisols Inceptisols

Mapping unit G5 – *Photograph taken by Faul C. (2017).*

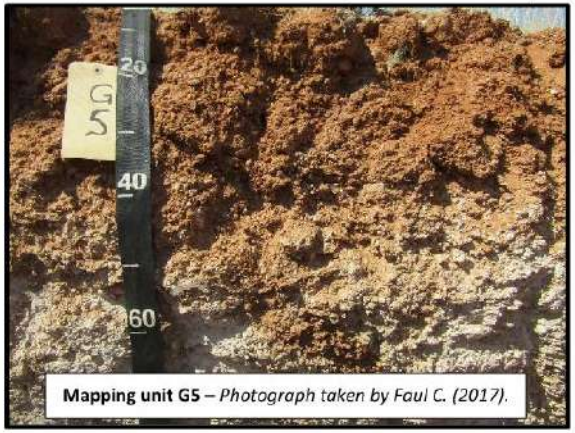

Mapping unit G5 – *Photograph taken by Faul C. (2017).*

Mapping unit G1 – *Photograph taken by Faul C. (2017).*

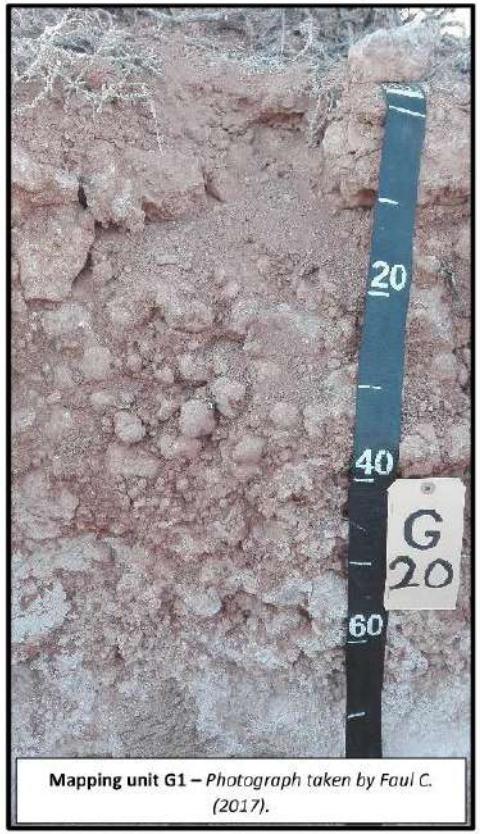

Mapping unit G1 – *Photograph taken by Faul C. (2017).*

Figure 5-2 (continued): Soil descriptions and classifications (Fey, 2010; IUSS Working Group WRB, 2006; Land Type Survey Staff, 1991; MacVicar *et al.*, 1977; Soil Classification Working Group, 1991; Soil Survey Staff, 1999).

MAPPING UNIT H

Mapping Unit	Horizon	Texture class	Depth (mm)	Clay %	Sand grade	Dry colour	Moist colour	Mottles		Lime		Structure			Coarse fragments	
								OCC	COL	OCC	Type	GRA	Size	Type	Type	%
H1	A	fi	0-470	0-15	fi	7,5YR 6/6	2,5 YR 4/6	N/A	N/A	a	P	A	f	SG	G	50
	B continue	fi	470-960	0-15	fi	10YR 8/2	7,5 YR 6/4	N/A	N/A	a	P	A	f	SG	G	50
	B continue	fi	960-1062	0-15	fi	2,5Y 8/4	7,5YR 5/6	N/A	N/A	a	P	A	f	SG	G	50
H3	A	me	0-400	0-15	me - co	5YR 5/8	2,5YR 4/8	N/A	N/A	N/A	N/A	M	m - c	CR	G	10
H4	A	fi	0-200	0-15	fi	7,5YR 7/6	5YR 6/8	N/A	N/A	c	P	A	f	SG	G	10
	B	fi	200-400	0-15	fi	7,5YR 6/6	5YR 6/6	N/A	N/A	a	P	A	f	SG	G	10
	B continue	fi	400-1200	0-15	fi	7,5YR 8/6	5YR 7/8	N/A	N/A	a	P	A	f	SG	G	10
	B continue	fi	1200-1500	0-15	fi	7,5YR 8/6	5YR 7/8	N/A	N/A	a	P	A	f	SG	G	10
H5	A	me	0-150	0-15	me	5YR 6/8	5YR 5/8	N/A	N/A	N/A	N/A	A	m	SG	S + G	60
H6	A	fi	0-450	0-15	fi	5YR 5/8	2,5YR 5/6	N/A	N/A	s	P	A	f	SG	G	10

Mapping Unit	Parent material	Efficient Depth (mm)	Terrain Unit	Depth limiting material
H1	Quartzite; calcrete; feldspar	100	3	Quartz and calcrete fragments
H3	Quartz; feldspar	200	4	Quartz and calcrete fragments
H4	Quartz; calcrete; feldspar	200	3U	N/A
H5	Quartz; feldspar	100	3	Calcrete boulders
H6	Quartz; calcrete	200	4	Hard rock

Mapping Unit	Sample No.	Coordinates		Initial Weight (g)	Weight after (g)		
		Latitude	Longitude		Coarse (> 2 mm)	Fine (< 2 mm)	Total
H1	G01	29°10'45,1"S	20°22'57,4"E	2582	1405	1161	2566
	G02			2566	1333	1227	2560
	G03			2360	1210	1148	2358
H3	G49	29°12'33,6"S	20°22'41,2"E	2620	559	2040	2599
H4	G26	29°12'05,7"S	20°21'53,7"E	2246	597	1631	2228
	G27			2161	845	1307	2152
	G28			2464	1189	1245	2434
	G29			1312	692	611	1303
H5	G36	29°12'07,9"S	20°23'06,5"E	2615	868	1743	2611
H6	G48	29°12'46.65"S	20°22'38.82"E	2311	547	1757	2304

Figure 5-2 (continued): Soil descriptions and classifications (Fey, 2010; IUSS Working Group WRB, 2006; Land Type Survey Staff, 1991; MacVicar *et al.*, 1977; Soil Classification Working Group, 1991; Soil Survey Staff, 1999).

Mapping Unit	Diagnostic Soil Horizon	Soil Form	Soil Family	WRB Reference Soil Group	USDA Soil Taxonomy
H1	Neocarbonate B / Soft carbonate	Addo	Spekboom 1211	Carcisols	Aridisols Inceptisols
H3	Neocutanic	Oakleaf	Caledon 1210	Acrisols Lixisils Arenosols Cambisols	Inceptisols
H4	Neocarbonate B / Soft carbonate	Addo	Spekboom 1211	Carcisols	Aridisols Inceptisols
H5	Hard rock	Mispah	Myhill 1100	Leptosols	Entisols
H6	Neocutanic	Oakleaf	Caledon 1210	Acrisols Lixisils Arenosols Cambisols	Inceptisols

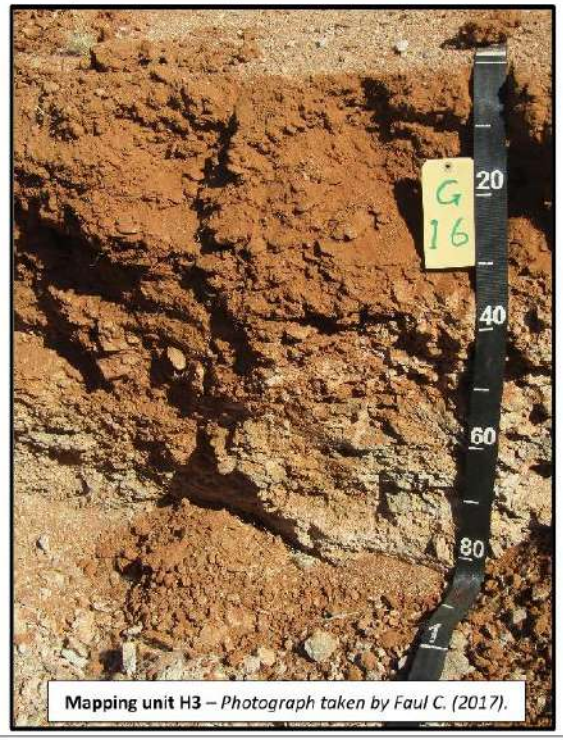

Mapping unit H3 – *Photograph taken by Faul C. (2017).*

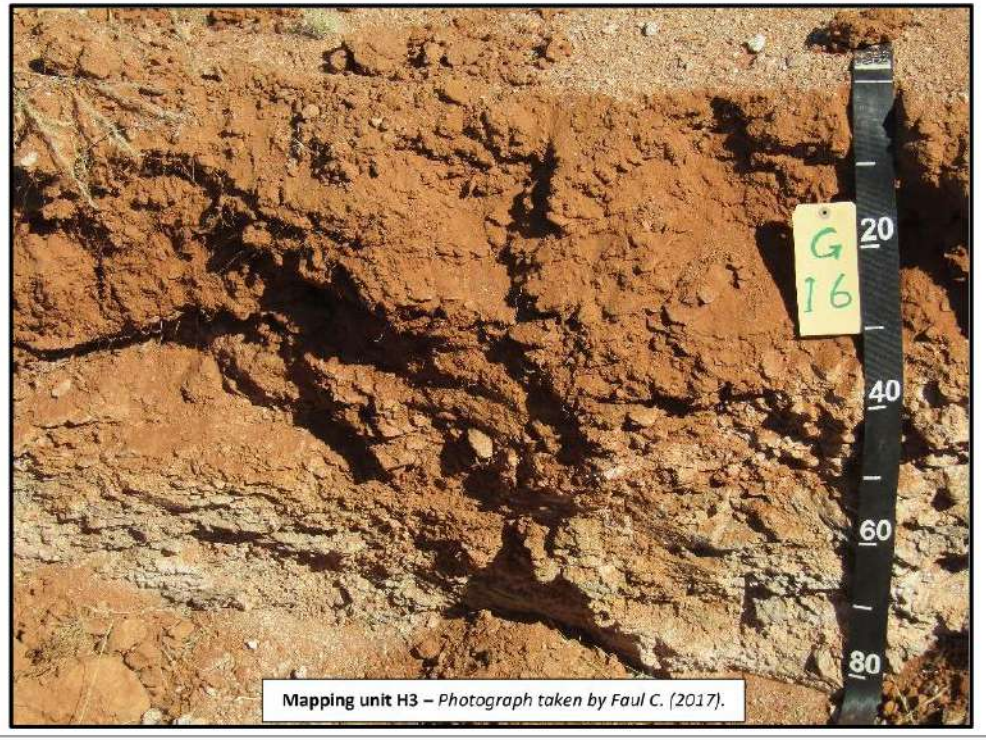

Mapping unit H3 – *Photograph taken by Faul C. (2017).*

Figure 5-2 (continued): Soil descriptions and classifications (Fey, 2010; IUSS Working Group WRB, 2006; Land Type Survey Staff, 1991; MacVicar *et al.*, 1977; Soil Classification Working Group, 1991; Soil Survey Staff, 1999).

MAPPING UNIT I

Mapping Unit	Horizon	Texture class	Depth (mm)	Clay %	Sand grade	Dry colour	Moist colour	Mottles		Lime		Structure			Coarse fragments	
								OCC	COL	OCC	Type	GRA	Size	Type	Type	%
I1	A	me	0-250	0-15	me	2,5YR 5/8	5YR 5/8	f	Bl	c	NP	W	m	G	G + S	30
	Transition	fi	250-350	0-15	fi	5YR 6/6	10YR 6/8	N/A	N/A	a	P	A	f	SG	G	30
	B	fi	350-450	0-15	fi	7,5YR 8/3	10YR 7/4	N/A	N/A	a	P	A	f	SG	G	30
I2	A	fi	0-200	0-15	fi	7,5YR 6/6	7,5YR 5/8	N/A	N/A	s	P	A	f	SG	S	10

Mapping Unit	Parent material	Efficient Depth (mm)	Terrain Unit	Depth limiting material
I1	Calcrete; Quartz; Feldspar	200	3	Rock fragments
I2	Calcrete; Quartz; Feldspar	200	4	Calcrete boulders

Mapping Unit	Sample No.	Coordinates		Initial Weight (g)	Weight after (g)		
		Latitude	Longitude		Coarse (> 2 mm)	Fine (< 2 mm)	Total
I1	G32	29°12'21,5"S	20°23'07,1"E	3327	1058	2254	3312
	G33			1360	601	749	1350
	G34			996	484	507	991
I2	G59	29°11'54,1"S	20°23'40,7"E	2678	528	2143	2671

Mapping Unit	Diagnostic Soil Horizon	Soil Form	Soil Family	WRB Reference Soil Group	USDA Soil Taxonomy
I1	Neocarbonate B / Soft carbonate	Addo	Spekboom 1211	Carcisols	Aridisols Inceptisols
I2	Neocarbonate B / Soft carbonate	Addo	Spekboom 1211	Carcisols	Aridisols Inceptisols

Figure 5-2 (continued): Soil descriptions and classifications (Fey, 2010; IUSS Working Group WRB, 2006; Land Type Survey Staff, 1991; MacVicar *et al.*, 1977; Soil Classification Working Group, 1991; Soil Survey Staff, 1999).

Mapping unit I1 – *Photograph taken by Faul C. (2017).*

Mapping unit I2 – *Photograph taken by Faul C. (2017).*

Figure 5-2 (continued): Soil descriptions and classifications (Fey, 2010; IUSS Working Group WRB, 2006; Land Type Survey Staff, 1991; MacVicar *et al.*, 1977; Soil Classification Working Group, 1991; Soil Survey Staff, 1999).

MAPPING UNIT J

Mapping Unit	Horizon	Texture class	Depth (mm)	Clay %	Sand grade	Dry colour	Moist colour	Mottles		Lime		Structure			Coarse fragments	
								OCC	COL	OCC	Type	GRA	Size	Type	Type	%
J1	A	fi	0-150	0-15	fi	5YR 5/6	5YR 5/8	N/A	N/A	s	P	A	f	SG	S + G	80
J2	A	fi	0-50	0-15	fi	5YR 5/6	5YR 5/8	N/A	N/A	N/A	N/A	A	f	SG	S	30
J3	A	fi	0-10	0-15	fi	2,5YR 5/8	2YR 5/6	N/A	N/A	N/A	N/A	A	f	SG	N/A	N/A
J4	A	fi	0-150	0-15	fi	5YR 6/8	5YR 5/6	N/A	N/A	N/A	N/A	A	f	SG	G+S	80
J5	A	fi	0-190	0-15	fi	2,5YR 5/8	2,5YR 4/8	N/A	N/A	N/A	N/A	A	f	SG	G+S	40

Mapping Unit	Parent material	Efficient Depth (mm)	Terrain Unit	Depth limiting material
J1	Quartzite	50	2	Meta-quartzite
J2	Quartzite	50	2	Meta-quartzite
J3	Quartzite	10	2	Meta-quartzite
J4	Quartzite	100	3U	Meta-quartzite
J5	Quartzite	100	3U	Meta-quartzite

Mapping Unit	Sample No.	Coordinates		Initial Weight (g)	Weight after (g)		
		Latitude	Longitude		Coarse (> 2 mm)	Fine (< 2 mm)	Total
J1	G19	29°12'10,9"S	20°22'01,5"E	2590	871	1603	2474
J2	G17	29°12'20,1"S	20°21'48,8"E	2456	919	1520	2439
J3	G30	29°11'24,85"S	20°22'24,3"E	1183	92	1094	1186
J4	G12	29°11'22,9"S	20°22'39,5"E	3354	1143	1682	2825
J5	G11	29°11'28,4"S	20°22'50,7"E	6060	1578	1638	3216

Mapping Unit	Diagnostic Soil Horizon	Soil Form	Soil Family	WRB Reference Soil Group	USDA Soil Taxonomy
J1	Hard rock	Mispah	Carnavon 1200	Leptosols	Entisols
J2	Hard rock	Mispah	Myhill 1100	Leptosols	Entisols
J3	Hard rock	Mispah	Myhill 1100	Leptosols	Entisols
J4	Hard rock	Mispah	Myhill 1100	Leptosols	Entisols
J5	Hard rock	Mispah	Myhill 1100	Leptosols	Entisols

Figure 5-2 (continued): Soil descriptions and classifications (Fey, 2010; IUSS Working Group WRB, 2006; Land Type Survey Staff, 1991; MacVicar *et al.*, 1977; Soil Classification Working Group, 1991; Soil Survey Staff, 1999).

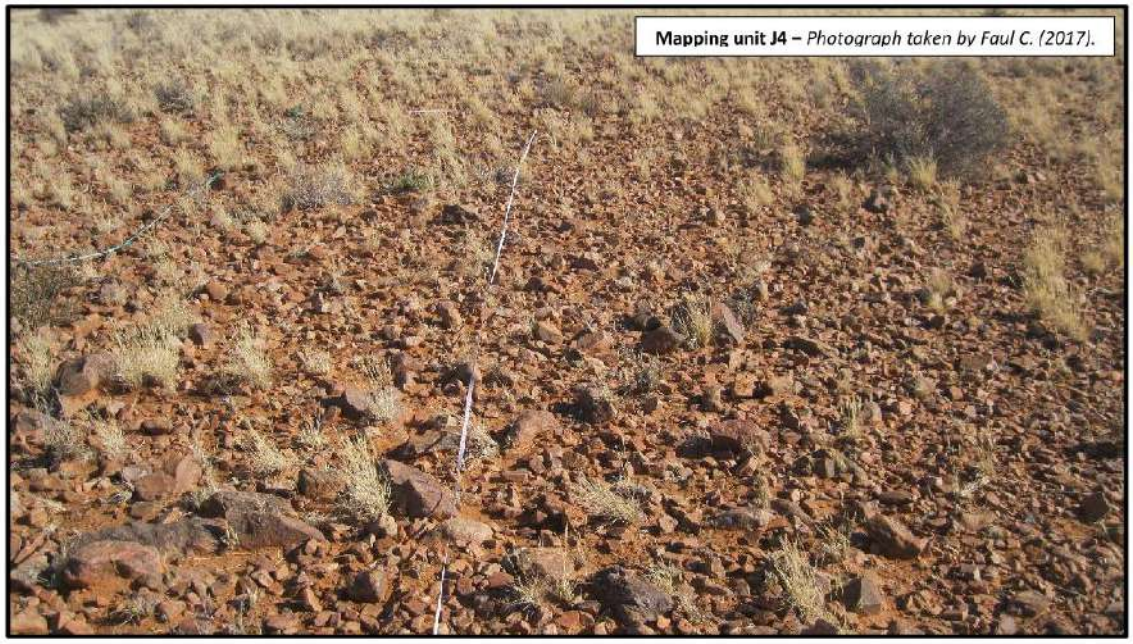

Figure 5-2 (continued): Soil descriptions and classifications (Fey, 2010; IUSS Working Group WRB, 2006; Land Type Survey Staff, 1991; MacVicar *et al.*, 1977; Soil Classification Working Group, 1991; Soil Survey Staff, 1999).

Soil description data and field observations were utilised for soil classification purposes (Land Type Survey Staff, 1991; MacVicar *et al.*, 1977; Soil Classification Working Group, 1991). The classification system of the WRB Reference Soil Group (IUSS Working Group WRB, 2006) as well as that of USDA Soil Taxonomy (Soil Survey Staff, 1999) was used for further classification.

As illustrated in Figure 5-2 a total of ten soil forms and eleven soil families were identified accordingly. The identified soil forms include Dundee, Oakleaf, Augrabies, Knersvlakte, Oudtshoorn, Addo, Brandvlei, Coega, Etosha and Mispah.

These soil forms were grouped into four individual soil groups known as silicic soils, calcic soils, cumulic soils and lithic soils (Fey, 2010; IUSS Working Group WRB, 2006). Each soil group is discussed (Table 5-2 – Table 5-5) based on description, properties, morphology, and genesis. According to the observations and information discussed in Figure 5-2, as well as the information obtained in Tables 5-2 to 5-5 a map was constructed illustrating all soil forms within the study area (Figure 5-3).

Table 5-2: Discussion of silicic soil group and associated soil forms on this site (Fey, 2010; Soil Classification Working Group, 1991).

Soil group	Concept	Identification	Soil Forms	Description	Properties	Morphology	Genesis
Silicic	Silica enrichment; arid	Dorbank	Oudtshoorn (Doringbaai 1210) Knersvlakte (Bitterfontein 1000)	Silicic soils are defined by their characteristic surface horizon where the silica becomes mobile during weathering under arid conditions and precipitates as a laminar or massive dorbank in the subsurface horizon.	Silicic soils are considered as active, currently forming soils with no slaking properties. Silicic soils are found in level or gently sloping erosion terraces typically originating from colluvial or alluvial parent material. A neocutanic B horizon is typically identified by its presence beneath a diagnostic A horizon or an E horizon, present in unconsolidated material that does not qualify as stratified alluvium or regic sand. A dorbank is typically identified by its extreme hardness, massive or platy structure and silica cementation.	Silicic soils are typically medium to coarse textured with platy or massive features and are considered as well to moderately drained. These soils have a typical abrupt upper boundary with the overlying material. There may be an occurrence of accessory cements which includes calcium carbonate and possibly iron oxide. On this site, the Oudtshoorn form had a red, non-bleached B-horizon with no luvic properties. Therefore, this soil form was classified as a Oudtshoorn form with soil family Doringbaai 1210. The Knersvlakte form had no free lime within the A-horizon and was therefore classified as a Knersvlakte form with soil family Bitterfontein 1000.	The texture of the overlying material determines the depth of the dorbank, with lower clay content giving raise to deeper dorbanks. For this part of South Africa dorbanks originate due to the presence of silica enrichment together with regular atmospheric additions of sodium in dust, combined with hydrolysis and high tempos of evaporation. Within the Oudtshoorn form the B-horizon may be unrelated to the underlying dorbank. The B-horizon may also be affected by pedoturbation or addition of material. The Knersvlakte form is characteristically shallow and found in areas where material removal through wind or water erosion took place.

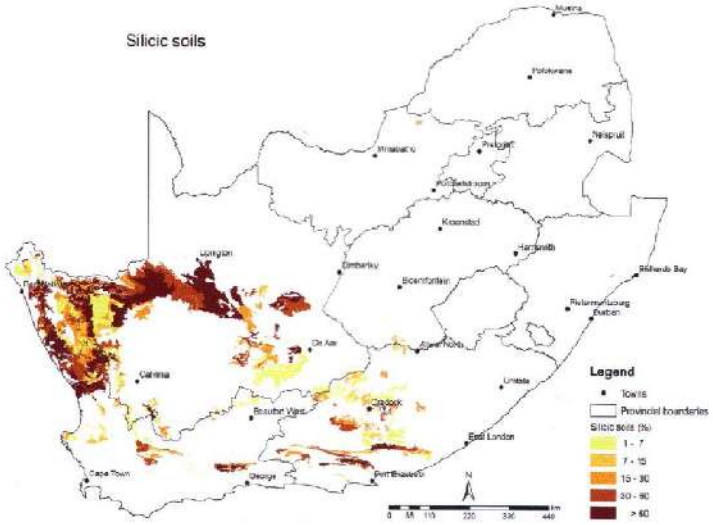

Silicic soils in South Africa, where the abundance classes refer to the estimated percentages within the land type (Fey, 2010).

Table 5-3: Discussion of calcic soil group and associated soil forms on this site (Fey, 2010; Soil Classification Working Group, 1991).

Soil group	Concept	Identification	Soil Forms	Description	Properties	Morphology	Genesis
Calcic	Carbonate or gypsum, enrichment; arid	Soft or hardpan carbonate or gypsic horizon	Etosha (Tuli 1211) Addo (Spekboom 1211) Brandvlei (Grootvloer 1000) Coega (Nabies 1000)	Calcic soils are defined by their characteristic surface horizon. In arid environments evaporation tempos are high and calcium will consequently remain behind to form a cemented soil. However, less intense aridity (in comparison with silicic soils) is needed for calcium retention.	The formation of calcic soils is due to the progressive accumulation of calcium from neocarbonate to soft to hardpan carbonate. The colour and morphology of calcic soils is a result of the composition of the carbonates. With respect to parent material, structure development and occurrence, a neocarbonate B horizon is similar to a neocutanic B horizon. However, unlike the neocutanic B horizon a neocarbonate B horizon contains calcium carbonate. A soft carbonate contains large amounts of carbonates in various forms, hence the morphology of the carbonates give rise to its characteristics. A hardpan carbonate is cemented by carbonates and identified as a solid pedon.	Calcic soils typically have well developed topsoil with crumb or granular structure and a pale brown colour. With the presence of elevated amounts of exchangeable magnesium, the structure becomes massive or platy. The colour of the subsoil depends on the parent material and may vary from brown to yellow to red. In arid environments the orthic A-horizon may have properties like crusts, bleaching and desert pavement. On this site the Etosha form had a red, non-luvic B-horizon with no signs of wetness. Therefore, this soil form was classified as a Etosha form with soil family Tuli 1211. The Addo form also had a red, non-luvic B-horizon with no signs of wetness and was classified as a Addo form with soil family Spekboom 1211. The Brandvlei form showed no signs of wetness and was classified as a Brandvlei form with soil family Grootvloer 1000. The Coega form had a non-calcic A-horizon and was classified as a Coega form with soil family Nabies 1000.	Calcic soils are considered as extremely old and polygenetic. Calcite precipitation result as CO_2 pressure and soil water levels decrease, causing increased ionic concentrations. pH levels also play an important role in the precipitation or dissolution of calcite. The origin of calcic soils may be internal or external, thus originating from the soil parent material or from outside sources for instance dust. Arid and semi-arid climate is an important factor controlling the distribution of calcic soils.

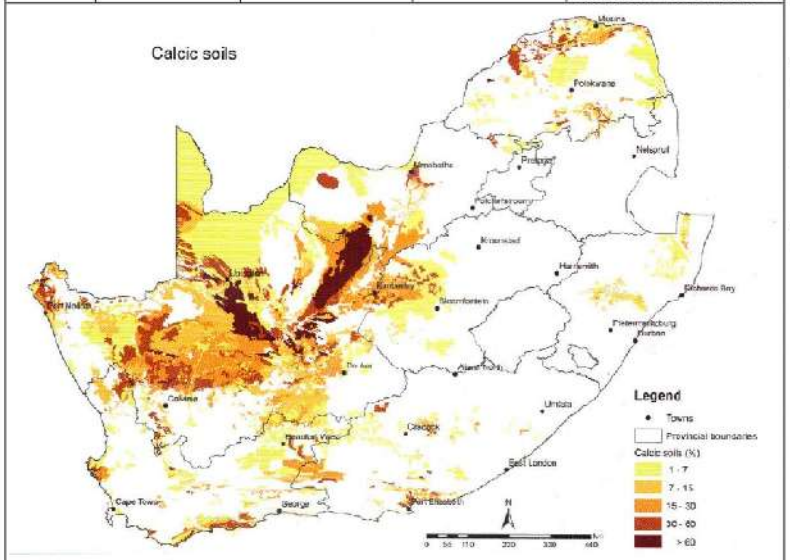

Calcic soils in South Africa, where the abundance classes refer to the estimated percentages within the land type (Fey, 2010).

Table 5-4: Discussion of cumulic soil group and associated soil forms on this study area (Fey, 2010; Soil Classification Working Group, 1991).

Soil group	Concept	Identification	Soil Forms	Description	Properties	Morphology	Genesis
Cumulic	Young soil (colluvial, alluvial, aeolian).	Neocutanic or neocarbonate B, regic sand, deep E or stratified alluvium	Oakleaf (Caledon 1210) Augrabies (Khubus 1210) Dundee (Marico 2110)	Cumulic soils are youthful and formed in recent, unconsolidated, natural deposits such as colluvium, alluvium or aeolian sediments. Cumulic soils typically identify concave foot slopes and valley basins.	The Oakleaf form is weakly altered having higher clay content with increasing depth. The Augrabies form is weakly altered having higher carbonate concentrations. The Dundee form is known to be negligibly altered in fluvic conditions. Soil families can be classified based on features like surface bleaching, reddening of soil colour, clay lamellae in the E-horizon, clay illuviation, presence of carbonates or signs of wetness. Stratified alluvium is typically unconsolidated with minimal pedogenic differentiations formed by depositional processes.	The Oakleaf form has neocutanic properties which has similar structural properties as an apedal B horizon but differs from the apedal B horizon in terms of colour. One of the properties used to identify a neocutanic horizon is the bleaching of the overlying A horizon. On this site the Oakleaf form were characterised by a red B-horizon with no luvic properties. Therefore, this soil form was classified as a Oakleaf form, with soil family Caledon 1210. The Augrabies form has neocutanic properties; however it also has a neocarbonate B horizon. On this site the Augrabies form were characterised by a red B-horizon with no luvic properties. Therefore, this soil form was classified as a Augrabies form, with soil family Khubus 1210. The Dundee form is identified based on the dominance of stratified alluvium. On this site the Dundee form were characterised by red stratified alluvium with no signs of wetness and no carbonates present within the first 1500 mm. Therefore, this soil form was classified as a Dundee form, with soil family Marico 2110.	The Dundee form is typically restricted to floodplains. The red colour is an indication of sufficient aeration for sufficient iron oxide preservation. No clear stratification was observed, indicating a gradual accumulation of sediments. The Oakleaf form was initially identified to describe the concept of developing pedogenesis in unconsolidated material. Variations in colour can be observed based on localities, faunal activity, clay illuviation as well as the degree of structure development.

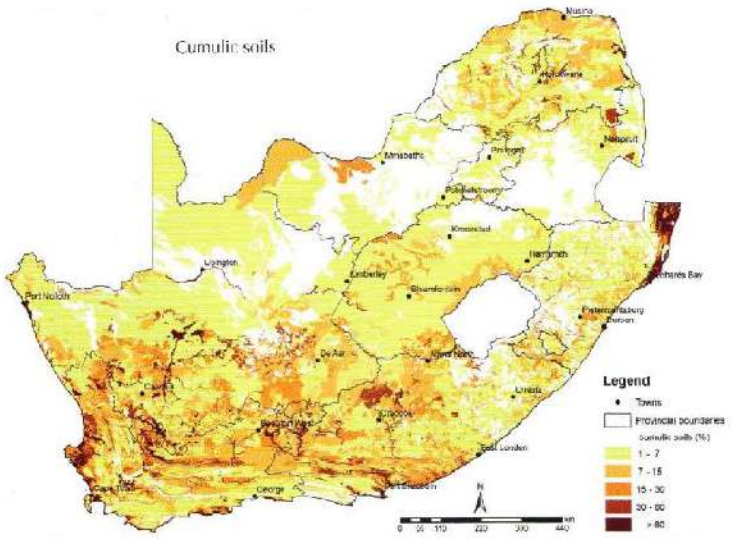

Cumulic soils in South Africa, where the abundance classes refer to the estimated percentages within the land type (Fey, 2010).

Table 5-5: Discussion of lithic soil group and associated soil forms on this site (Fey, 2010; Soil Classification Working Group, 1991).

Soil group	Concept	Identification	Soil Forms	Description	Properties	Morphology	Genesis
Lithic	Young soil on weathered rock	Lithocutanic B or hard rock	Mispah (Myhill 1100) Mispah (Carnavon 1200)	Lithic soils are youthful, typically identifying convex crests and steep slopes. The Mispah form is characterised by an orthic A overlying hard rock.	Lithic soils are characterised by their affinity with the underlying parent rock. Hard rock can be described as a continuous rock layer, not changing colour in wet conditions. A lithocutanic B horizon gradually changes into weathered rock and show some correlation with the parent material.	The tongues of topsoil into saprolite is an indication of clay movement. It is also possible to find horizontally discontinuous pockets of well-formed ped within the lithocutanic B which may cause confusion regarding the properties of the pedocutanic and the prismacutanic B horizon. On this site the majority of the soil forms were characterised by a non-bleached A horizon with no carbonates present. In this case the soil form was classified as a Mispah form with soil family Myhill 1100. However, there were one locality where calcium carbonate was present alternating the classification to a Mispah form, with soil family Carnavon 1200.	There is a strong correlation between the occurrence of lithic soils and climate determined by vegetation cover, vegetation root penetration and consequently erosion tempos. Lithic soils dominate in arid environments due to the domination of natural erosion over weathering. Due to the nature of natural reactions, lithic soils are ideal for studying the transformation from primary to secondary minerals.

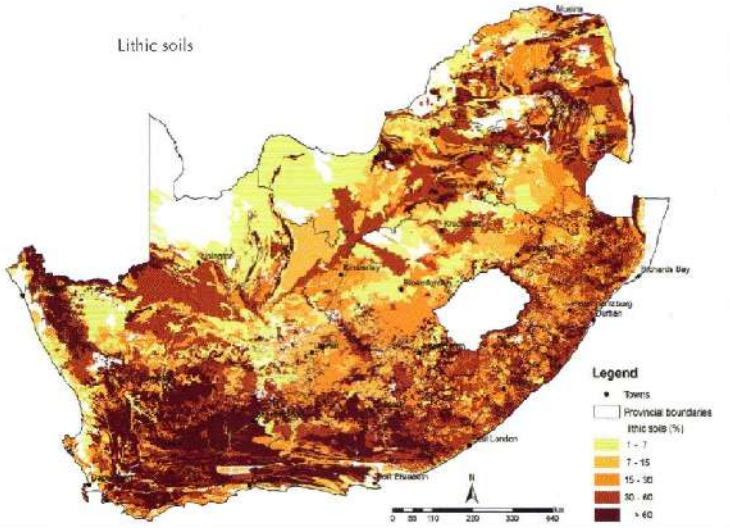

Lithic soils in South Africa, where the abundance classes refer to the estimated percentages within the land type (Fey, 2010).

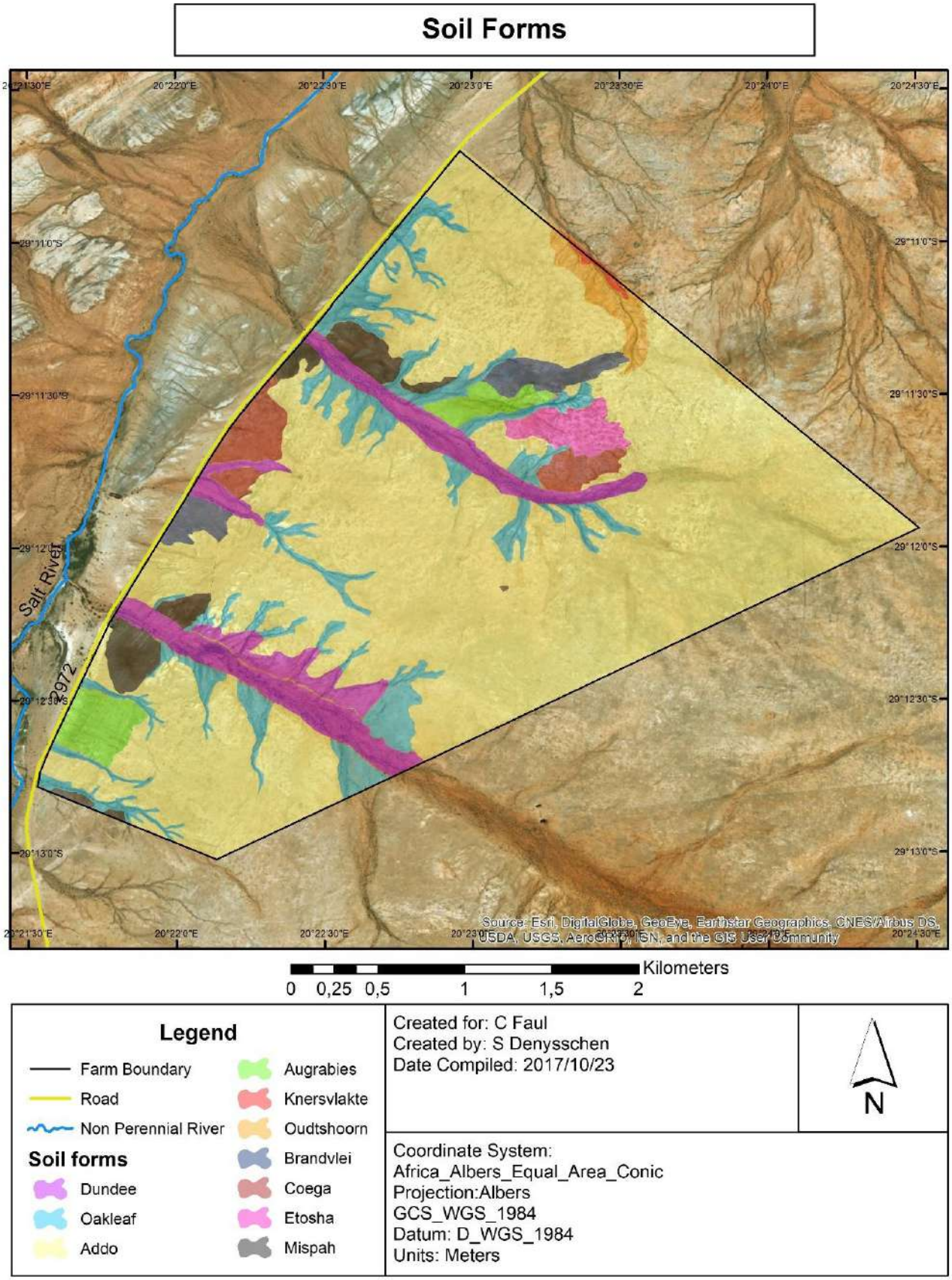

Figure 5-3: Map indicating the soil forms for the study area (Google Earth, 2016).

As discussed in Chapter 2 (see Section 2.2.3.1.), this area falls within the arid climate zone according to the aridity index (De Martonne, 1926) and in accordance with the Weinert N-value (Department of Public Works, 2007; Weinert, 1980, 1984). With reference to Table 5-2 to Table 5-5, it is clear that all these soil forms are associated with arid climate conditions. Figure 5-3 illustrates the distribution of the different soil forms within the study area. The largest part of the area is occupied by calcic soils (Augrabies, Addo, Brandvlei, Coega and Etosha). All the localities where Mispah forms were identified are associated with geological outcrops. The drainage systems on site were associated with Dundee and Oakleaf soil forms indicating depositional and in this case fluvial activities.

5.3 Soil Analyses

Soil analyses were conducted based on the methods as described in Chapter 3 (Section 3.3.2.). The soil data was used to establish meaningful differences between samples from different localities which could possibly correlate with geological differences or variation in vegetation.

5.3.1 Chemical Analyses

The results discussed in this section include pH, electrical conductivity, exchangeable cations, cation exchangeable capacity, phosphorus and anion concentration.

5.3.1.1 pH

The pH is used to measure soil acidity or alkalinity by means of indicating the activity of the hydrogen ion (H^+) and hydroxyl ion (OH^-) in a water solution (Hazelton & Murphy, 2007). A neutral pH was the norm for this site with some localities excluded from this statement. Nine of the 60 samples had an alkaline pH (H_2O) value of more than 9. According to Hazelton and Murphy (2007), the solubility and plant availability of nitrogen, calcium, magnesium, manganese, copper, zinc and aluminium is negatively influenced by a pH (H_2O) higher than 9.

Of these nine samples five belonged to the Addo soil form, two belonged to the Oakleaf soil form, while one formed part of the Augrabies soil form, and one formed part of the Dundee soil form. The Addo and Augrabies forms are known for their distinct calcareous soil horizons justifying the alkalinity of the samples. However, the Dundee and Oakleaf forms are not known for having calcareous soil horizons. These samples were obtained within prominent drainage systems. The transportation of calcareous material from another source, whether through aeolian or alluvial processes, would explain the alkalinity at these three localities. Consult Annexure C, Figure C-2 and Figure C-3 for results.

5.3.1.2 Electrical Conductivity (EC)

According to the Fertilizer Society of South Africa (2007), soils with an EC higher than 400 mS/m and an exchangeable sodium percentage lower than 15% are classified as saline soils. On this site eight samples corresponded to this criterion (Figure 5-4). Of these eight samples five belonged to the Addo soil form, one was part of the Knersvlakte soil form, one was part of the Coega soil form and one was part of the Dundee soil form.

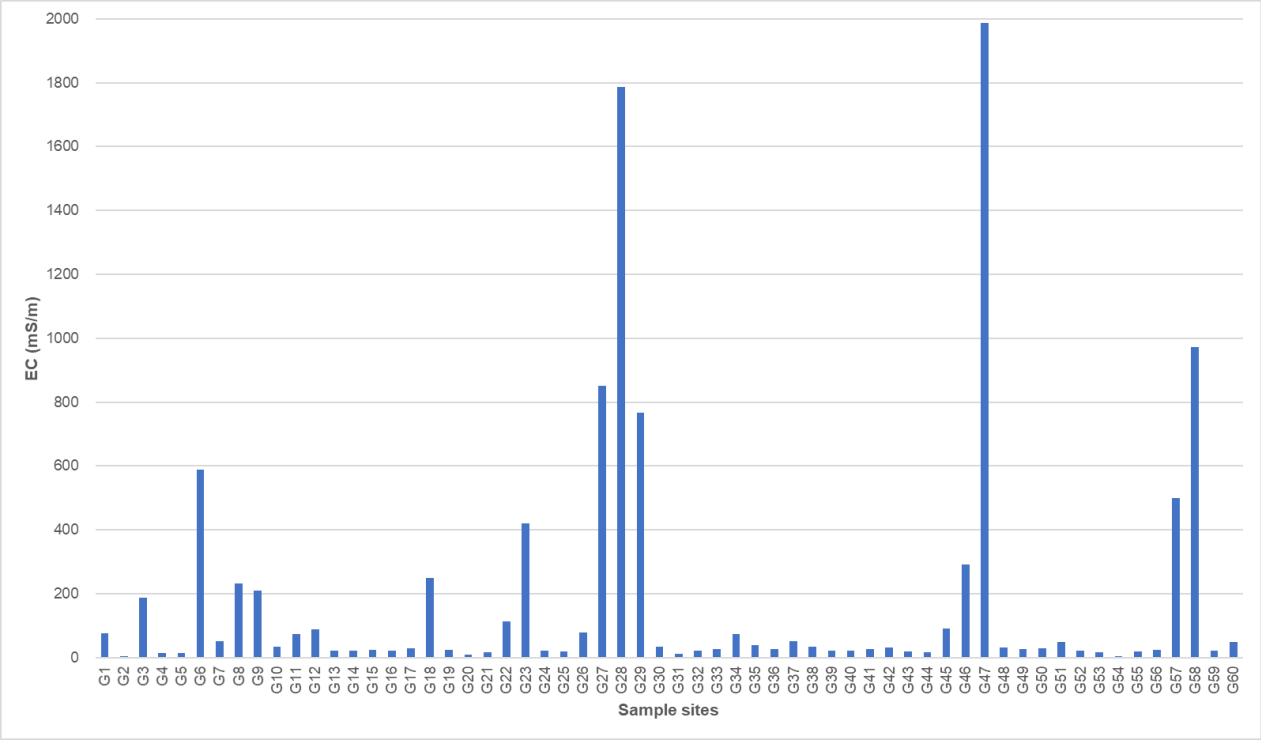

Figure 5-4: Electrical conductivity (mS/m) of all 60 soil samples obtained during the soil survey.

Although these soils have nothing in common with respect to their physical properties, all these samples were collected from low-lying localities. During precipitation events water infiltrates the soil and dissolves additional solutes. As the water moves to the low-lying areas it transports the solutes with it (Hillel, 2004). Therefore, soils in areas with lower elevation revealed increased EC values.

5.3.1.3 Cation Exchange Capacity (CEC)

The cation exchangeable capacity (CEC) is the soil's capacity to hold and exchange cations and to buffer changes in pH, available nutrients as well as structural changes (Hazelton & Murphy, 2007). Table 5-6 illustrates the different CEC ratings as described by Metson (1961) [cited by Hazelton and Murphy, 2007].

Table 5-6: Ratings for cation exchange capacity (Metson, 1961) [cited by Hazelton & Murphy, 2007].

*, soils with CEC less than three are often low in fertility and susceptible to soil acidification.

Rating	CEC cmol (+)/kg
Very low	<6*
Low	6–12
Moderate	12–25
High	25–40
Very high	>40

Figure 5-5 depicts the CEC values for all 60 samples and illustrates the different rating categories as described by Metson (1961) [cited by Hazelton & Murphy, 2007].

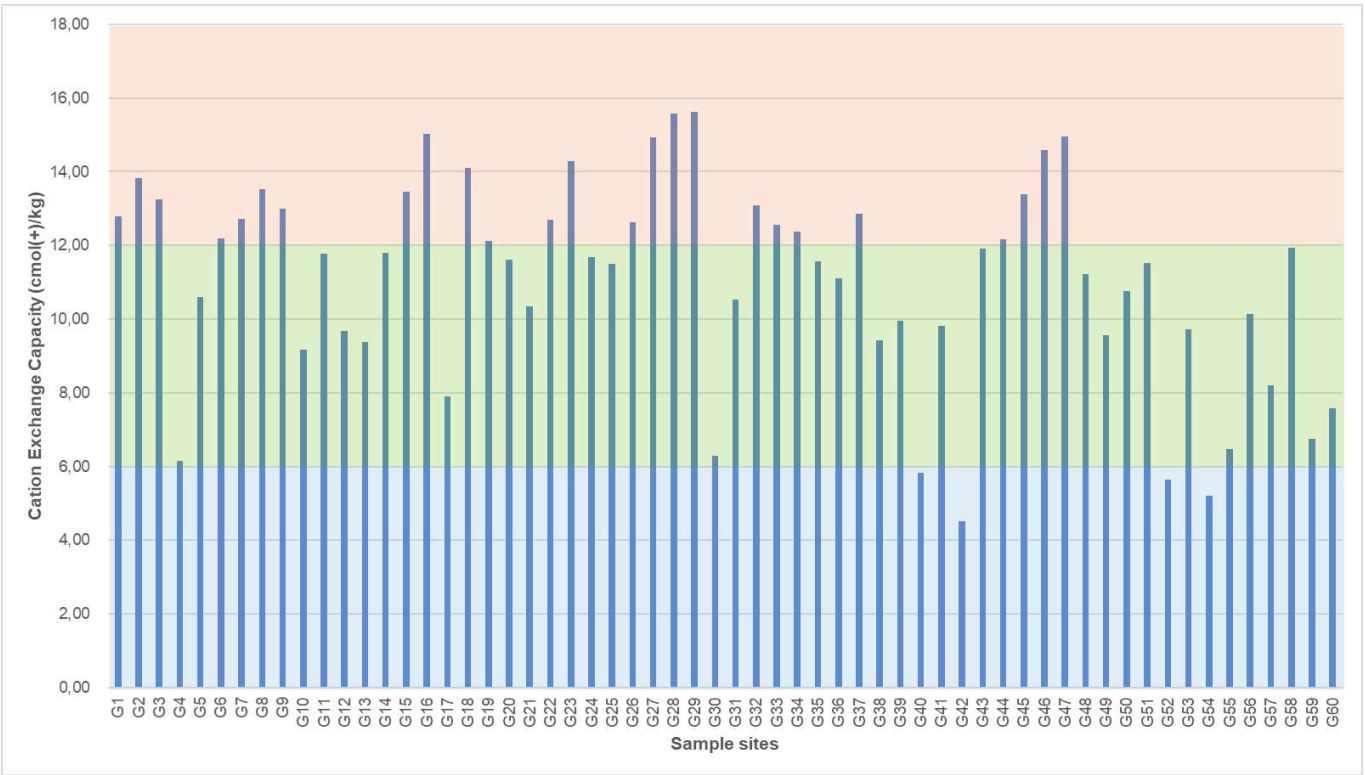

Figure 5-5: Cation Exchange Capacity [cmol(+)/kg] of all 60 samples obtained during the soil survey.

According to Figure 5-5, most of the samples revealed low CEC values. Sample G28 [15.58 cmol(+)/kg] and G29 [15.62 cmol(+)/kg] had the highest CEC values, comparing to sample G42 [4.50 cmol(+)/kg] whom had the lowest. The highest and lowest values were from samples obtained from Addo soil forms. No correlation seems to exist between CEC and soil form as CEC values varied from very low, low and moderate for Addo soil forms. All these samples were

scattered across the area therefore no apparent associations were identified between CEC and locality.

The differences in CEC could be due to topographical differences with lower areas obtaining more accumulated clay particles, transported by either aeolian or fluvial processes, therefore resulting in higher CEC values.

5.3.1.4 Exchangeable Cations

Exchangeable cations are important for plant vitality. According to Abbott (1989) [cited by Hazelton & Murphy, 2007] as well as Emerson and Bakker (1973) [cited by Hazelton & Murphy, 2007], high concentrations of sodium and magnesium leads to increased dispersion while high concentrations of sodium and calcium leads to lower dispersion. Table 5-7 illustrates the different levels of exchangeable cations.

Table 5-7: Levels of exchangeable cations [cmol(+)/kg] (Metson, 1961) [cited by Hazelton & Murphy, 2007].

Cation	Very low	Low	Moderate	High	Very high
Na	0–0.1	0.1–0.3	0.3–0.7	0.7–2.0	>2
K	0–0.2	0.2–0.3	0.3–0.7	0.7–2.0	>2
Ca	0–2	2–5	5–10	10–20	>20
Mg	0–0.3	0.3–1.0	1–3	3–8	>8

Consult Annexure C, Figure C-4 to Figure C-8 for results. According to Figure C-4, the majority of all soil samples had very low sodium concentrations. Sample G31 (Oakleaf soil form) had the lowest sodium concentration [0.00 cmol(+)/kg], whereas sample G58 (Dundee soil form) had the highest sodium concentration [7.85 cmol(+)/kg].

The majority of all soil samples had moderate potassium concentrations (see Figure C-5). Samples G4, G20, G31, G53 and G54 [0.01 cmol(+)/kg] had the lowest potassium concentrations compared to sample G7 [0.97 cmol(+)/kg] with the highest. Low potassium concentrations were obtained from Dundee, Oakleaf and Oudtshoorn soil forms, while high potassium concentrations were obtained from the A horizon of a Brandvlei soil form.

According to Figure C-6 moderate to high calcium concentrations were the norm. Sample G54 [0.51 cmol(+)/kg] had the lowest calcium concentration, whilst sample G9 [17.87 cmol(+)/kg] had the highest calcium concentration. The lowest value (sample G54) were obtained from a Dundee soil form, with the highest value (sample G9) obtained from the B horizon of a Brandvlei soil form.

Most of the soil samples had low magnesium concentrations (Figure C-7). Sample G20 [0.11 cmol(+)/kg] had the lowest magnesium concentration, comparing to sample G12 [2.99 cmol(+)/kg] with the highest. The lowest value (sample G20) was obtained from a Dundee soil form, while the highest value (sample G12) was obtained from a Mispah soil form. The dominating geology in the areas where the Mispah soil forms were identified was metaquartzite. An association between metaquartzites and elevated magnesium concentrations for this area were identified.

The Ca:Mg ratio (Figure C-8) is typically used to identify calcium or magnesium deficiencies. Of all 60 samples four were identified as low calcium, six as balanced and nine as low magnesium. The remaining 41 samples were identified as magnesium deficient. There was however no correlation between the Ca:Mg ratio and soil forms or topographical variations.

To conclude, the soils of this area have very low concentrations of sodium, low concentrations magnesium, moderate concentrations potassium and moderate to high concentrations calcium. Therefore, higher concentrations of exchangeable calcium are available for uptake by plants. The concentrations of exchangeable magnesium are too low for magnesium toxicity in vegetation.

5.3.1.5 Total Macro Element Concentrations

According to the Fertilizer Society of South Africa (2007) the total macro element concentrations in soil are important for plant growth and vitality. The total macro element concentrations will be discussed according to the thresholds as described by the Fertilizer Society of South Africa (2007). Consult Annexure C Figure C-9 to Figure C-13 for results.

Figure C-9 illustrates that the largest part of all soil samples had a moderate to high calcium concentration, which can be explained by the dominance of surficial calcrete deposits. The samples with low calcium concentrations were typically from Dundee soil forms obtained within the main drainage systems. These soil forms are known for their stratified alluvial horizons with minimal clay and dominant sand fractions.

Moderate magnesium concentration was the norm (Figure C-10), with samples from Mispah and Knersvlakte soil forms being the only exceptions. The high magnesium concentrations within these soil forms can be explained by the presence of magnesium-rich metaquartzites and a dorbank horizon.

According to Figure C-11 moderate potassium concentration was considered standard for this site. High potassium concentrations were found in samples from Mispah, Brandvlei and Addo soil forms. All these samples were obtained from A-horizons, indicating the transportation of potassium-rich material from a different source or directed from the outcrop. Low potassium

concentrations were found in samples from Dundee and Brandvlei soil forms collected from different drainage systems suggesting the leaching of potassium.

The majority of all soil samples had low sodium concentrations (Figure C-12). Samples obtained next to the north-western boundary of the study area (in close proximity with the Salt River) revealed high sodium concentrations in contrast with the rest of the samples.

According to Figure C-13 low to moderate phosphorus concentration was considered standard for this site.

5.3.1.6 Total Anion Concentrations

Consult Annexure C, Figure C-14 to Figure C-16 for results. According to Figure C-14 and Figure C-15 all soil samples revealed low chloride and sulphate concentrations, apart from sample G28, G47 and G58 obtained from both a Dundee and Addo soil form, in close proximity with the north-western boundary of the study area. These high chloride- and sulphate concentrations correlate with the increasing salt content nearing the Salt River. Therefore, it can also be predicted that the salts in and next to the Salt River are composed of NaCl as well as Na_2SO_4.

Nitrate concentrations are influenced by rainfall, the time of sampling as well as the depth over which the sample is taken (Hazelton & Murphy, 2007). According to Figure C-16, all soil samples revealed low nitrate concentrations except for sample G2, G8 and G9. Sample G2 was obtained from an Addo soil form next to the north-western boundary of the study area. Samples G8 and G9 formed part of one of two identified Brandvlei soil forms. The reason for these high nitrate concentrations is still unclear.

5.3.2 Physical Analyses

5.3.2.1 Particle Size Distribution

The amount of gravel, sand, silt and clay within a soil are described by particle size distribution and determines the properties of a soil. According to the Non-Affiliated Soil Analysis Work Committee (1990), soil particles can be divided into different size ranges. Figure C-17 (see Annexure C) illustrates the particle size distribution curves of all 60 soil samples. Variations with respect to particle size distribution occurred across the entire area. Well graded, poorly sorted soils seemed to be the norm for this area. Figure 5-6 illustrates the particle size distribution curves of the samples that showed meaningful differences.

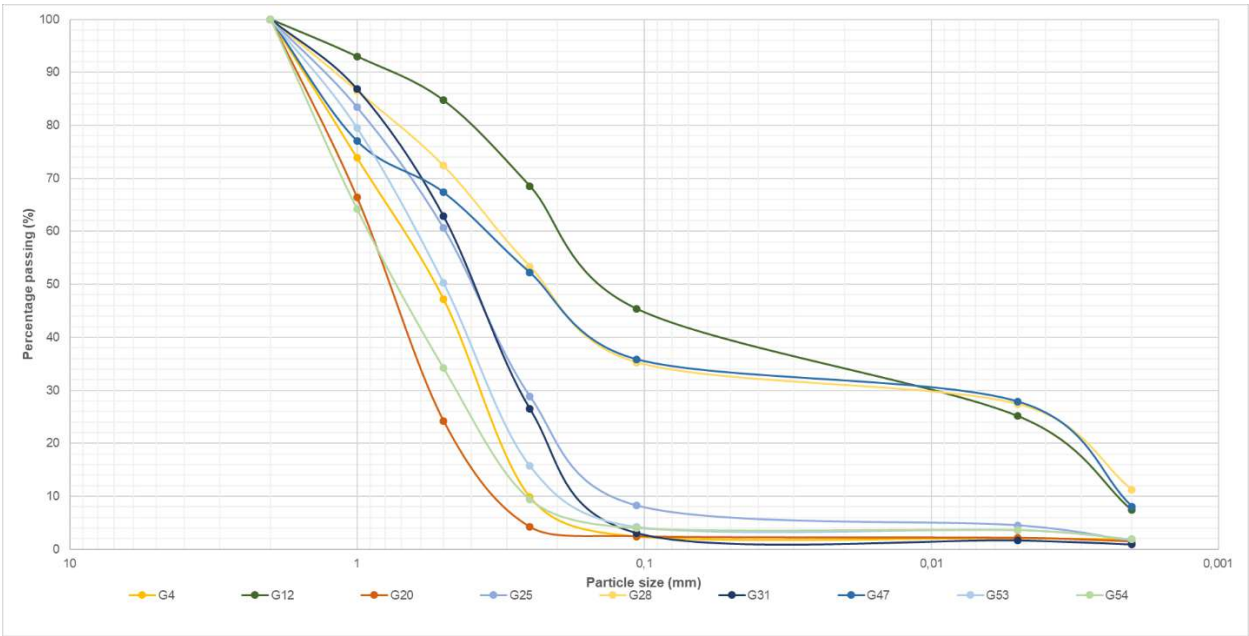

Figure 5-6: Particle size distribution (PSD) curve of samples with meaningful differences.

Samples G4, G20, G25, G31, G53 and G54, obtained from Dundee and Oakleaf soil forms within drainage systems, were dominated by sandy particles with minimal clay and silt. Clay and silt particles have either been removed during flash flood events or illuviation. Samples G12, G28 and G47 obtained from Mispah or Addo soil forms (B-horizon) consisted of clay, silt and very fine sand. The particle size distribution of an Addo soil form can be explained by the presence of large amounts of powdery calcium carbonate within the B horizon.

The USDA Soil Texture Calculator (USDA-NRCS, 2014) (http://www.nrcs.usda.gov/wps/portal/nrcs/detail/soils/survey/?cid=nrcs142p2_054167) was used to calculate the texture classes of all 60 samples. A total of 39 samples were classified as sandy soils compared to the 19 loamy sandy soils. Two samples were classified as sandy loamy soils. No correlation could be identified between soil texture and soil form, locality or topography. However, it was found that the two samples identified as sandy loam (G28 and G47) were identified as part of Addo soil forms, both showed high EC values, high Cl^- concentrations, some of the highest CEC values, some of the highest exchangeable calcium and total sodium concentrations as well as low magnesium concentration. These are typical examples of soils of mixed origin, therefore no clear explanation for these similarities can be provided.

5.4 Basic Conclusion

Based on the aims and objectives of this study soils were identified and classified in order to construct a soil form map for correlation purposes. Chemical and physical analysis was conducted to indicate the differences between soil forms and establish the relationship between soil properties and specified correlations.

The soils from this area are typical dry arid soils of mixed origin (alluvial, aeolian, residual as well as pedogenic). The calcrete material dominates in the most soils with a thickness limited to less than one meter. A-horizons are typically thin with signs of alluvial and aeolian transportation. To the north-western segment of the study area, soils tend to become much shallower and in some areas gypsic deposits are visible. The drainage systems are typically associated with cumulic soils.

Consult Chapter 7 for more information regarding the function of soil in an integrated relationship between vegetation, soil and geology.

CHAPTER 6

GEOLOGICAL IDENTIFICATION, DESCRIPTION AND MAPPING

This chapter presents the results of Phase II: Surveying for identification, description, and classification purposes, as well as Phase III: Sampling and analyses, with respect to the geological survey as described in Chapter 3. Therefore, the purpose of Chapter 6 is to reflect all geological data collected in order to construct a geological map of the study area.

6.1 Geological identification, description and mapping

The study area falls within the geological province known as the Bushmanland Terrane which forms part of the Namaqua Sector within the Namaqua-Natal Metamorphic Province. The Namaqua-Natal Metamorphic Province is a large area of contiguous structural fabric which formed during a tectonic metamorphic event. The Bushmanland Terrane covers approximately 60 600 km^2 and is known as the largest crustal block in the Namaqua Sector. It is comprised of granitic gneisses (~2000 Ma), supracrustal rocks of amphibolite to granulite grade (1600 – 1200 Ma) and granitoids (1200 – 1000 Ma). The Groothoek Thrust and Wortel Belt form the northern boundary of the Bushmanland Terrane, and the Hartbees River Thrust the eastern boundary (Cornell *et al.*, 2006).

The Bushmanland Terrane is divided into three age groups known as the Kheisian strata (1700 – 2050 Ma), the young, deformed supracrustal and plutonic rocks (1200, 1600 and ~1900) and the syn-tectonic and late-tectonic Namaquan intrusive rocks (Cornell *et al.*, 2006; Moore *et al.*, 1990; SACS, 1980; Thomas *et al.*, 1994).

This particular area of interest lies south-west of the Kaapvaal Craton and west of the Hartbees River Thrust (see Chapter 2, Figure 2-2). Based on the aims and objectives of this study as well as the geological complexity of the site, a randomised survey approach was used for geological identification. Figure 6-1 illustrates the localities of identified geological outcrops.

All geological localities (Figure 6-1), field descriptions and photographs are illustrated in Figure 6-2. These localities and descriptions were used to construct a geological map of the area (Figure 6-4).

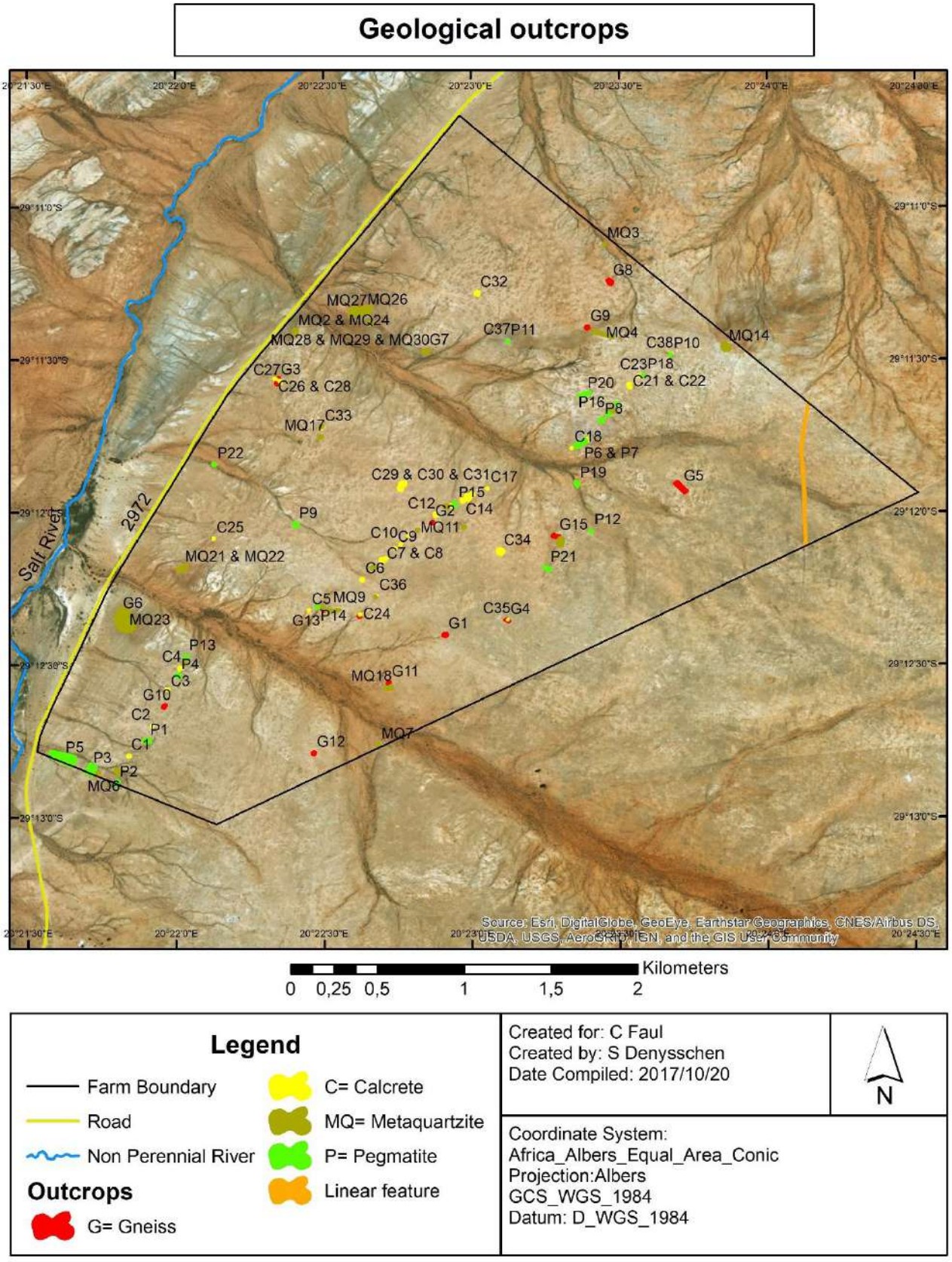

Figure 6-1: Map indicating the localities of identified geological outcrops (Google Earth, 2016).

MAPPING UNIT A

Mapping Unit	Coordinates		Geological Identification	Properties
	Latitude	Longitude		
A1	29°12'42,9" S	20°22'43,7" E	No visible outcrops.	Mixture of aeolian and fluvial sedimentary deposits.
A2	29°11'18,5" S	20°22'26,7" E	No visible outcrops.	Mixture of aeolian and fluvial sedimentary deposits.

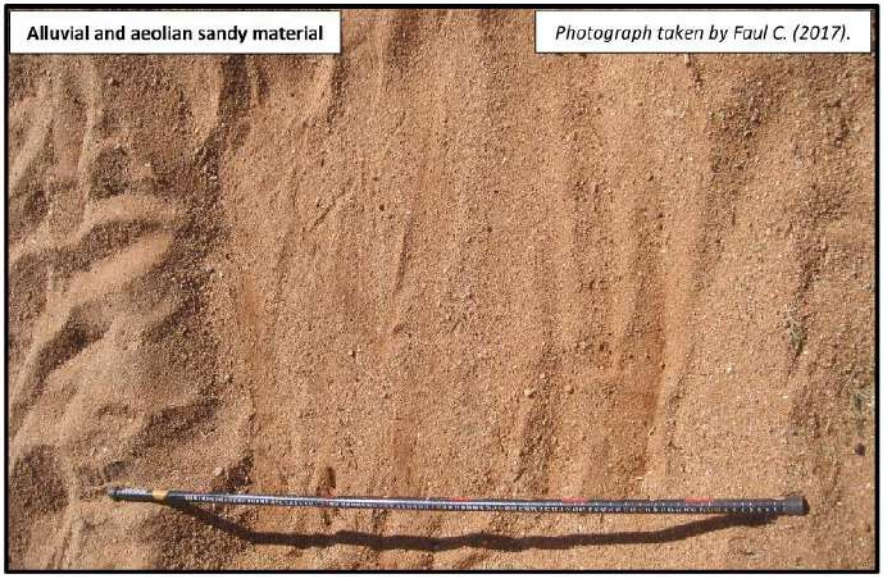

Figure 6-2: Geological identification and description.

MAPPING UNIT B

Mapping Unit	Coordinates		Geological Identification	Properties
	Latitude	Longitude		
B6	29°12'49,1"S	20°21'38,4"E	Pegmatite outcrop **(P5 in Figure 6-1).**	No properties recorded.
B8	29°11'12.3" S	20°22'35.6" E	No visible outcrops.	Small fragments of hydrothermal quarts and plagioclase present on the surface. Mixture of aeolian and fluvial sedimentary deposits.
B9	29°11'33.0" S	20°23'06.9" E	No visible outcrops.	Mixture of aeolian and fluvial sedimentary deposits.
B12-In riverbed	29°11'50.9" S	20°22'07.6" E	No visible outcrops.	Mixture of aeolian and fluvial sedimentary deposits.
B12-On riverbank	29°11'50.8" S	20°22'07.6" E	No visible outcrops.	Mixture of aeolian and fluvial sedimentary deposits.
B12	29°11'50.6" S	20°22'7.83" E	Pegmatite outcrop **(P22 in Figure 6-1).**	More weathered than in other localities.
B13-In riverbed	29°12'17.9" S	20°22'14.5" E	No visible outcrops.	Mixture of aeolian and fluvial sedimentary deposits.
B13-On riverbank	29°12'18.0" S	20°22'15.2" E		
B14	29°11'05.4" S	20°23'26.3" E	No visible outcrops.	Dorbank visible on the north-eastern side of the study area.
	29°11'07,4" S	20°23'27,0" E	Metaquartzite outcrop **(MQ3 in Figure 6-1).**	No properties recorded.

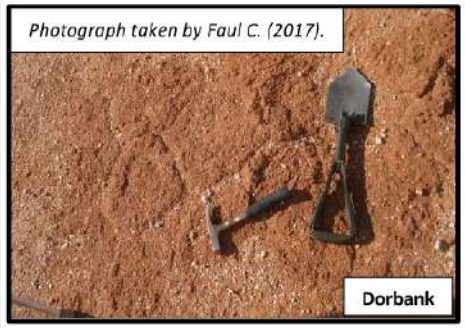

Figure 6-2 (continued): Geological identification and description.

MAPPING UNIT C

Mapping Unit	Coordinates		Geological Identification	Properties
	Latitude	Longitude		
C7	29°12'50,9" S	20°21'48,1" E	Metaquartzite outcrop (**MQ5 in Figure 6-1**).	No properties recorded.
	29°12'51,6" S	20°21'43,9" E	Metaquartzite outcrop (**MQ6 in Figure 6-1**).	No properties recorded.
C14	29°12'20.2" S	20°22'37.2" E	No visible outcrops.	Small fragments of hydrothermal quarts and plagioclase present on the surface. Mixture of aeolian and fluvial sedimentary deposits.
	29°12'20.1" S	20°22'37.3" E	Calcrete outcrop (**C24 in Figure 6-1**).	Total outcrop is approximately 4 m by 4 m in diameter.
	29°12'20.5" S	20°22'37.2" E	Gneiss outcrop (**G14 in Figure 6-1**).	Total outcrop is approximately 4 m by 4 m in diameter. No strike or dip visible.

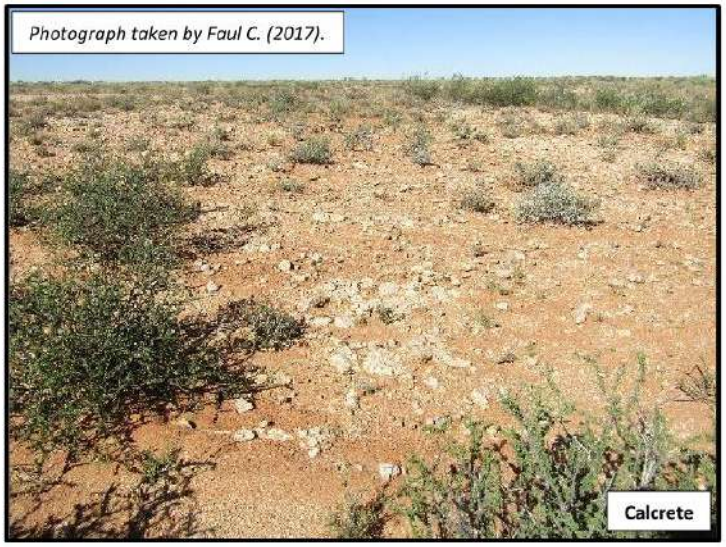

Figure 6-2 (continued): Geological identification and description.

Mapping Unit	Coordinates		Geological Identification	Properties
	Latitude	Longitude		
C15	29°12'19,4" S	20°22'31,5" E	Metaquartzite outcrop (**MQ9 in Figure 6-1**).	No properties noted.
	29°12'18,8" S	20°22'29,6" E	Gneiss outcrop (**G13 in Figure 6-1**).	Total outcrop is approximately 10 m by 10 m in diameter. The strike was measured as 140° with a dip of 60° SW.
	29°12'18,7" S	20°22'28,9" E	Pegmatite outcrop (**P14 in Figure 6-1**).	No properties noted.
C30	29°11'19.68"S	20°23'31.51"E	No visible outcrops.	Small fragments of hydrothermal quarts and plagioclase present on the surface. Mixture of aeolian and fluvial sedimentary deposits.
C35-In riverbed	29°11'54.4" S	20°23'20.8" E	No visible outcrops.	Small fragments of hydrothermal quarts and plagioclase present on the surface. Mixture of aeolian and fluvial sedimentary deposits.
C35-On riverbank	29°11'54.4" S	20°23'20.8" E		
C35	29°11'54.6" S	20°23'21.4" E	Pegmatite outcrop (**P19 in Figure 6-1**).	Total outcrop is approximately 4 m by 4 m in diameter. No strike or dip visible.
C37-In riverbed	29°12'02.3" S	20°22'24.7" E	No visible outcrops.	Hydrothermal quarts boulders present on the surface.
C37-On riverbank	29°12'02.3" S	20°22'24.7" E		
C37	29°12'02.3" S	20°22'24.5" E	Pegmatite outcrop (**P9 in Figure 6-1**).	The length of the outcrop is 1 m in a WSW (240°) to a ENE (60°) direction. The width is 40 cm perpendicular to the length.
C41-In riverbed	29°12'13.7" S	20°22'09.8" E	No visible outcrops.	Hydrothermal quarts and plagioclase fragments present on the surface, with underlying calcrete boulders.
C41-On riverbank	29°12'13.7" S	20°22'09.8" E		

Figure 6-2 (continued): Geological identification and description.

MAPPING UNIT D

Mapping Unit	Coordinates		Geological Identification	Properties
	Latitude	Longitude		
D5	29°11'29,1" S	20°23'40,5" E	Calcrete outcrop **(C38 in Figure 6-1)**.	No properties recorded.
			Pegmatite outcrop (**P10 in Figure 6-1**).	No properties recorded.
D10	29°11'57.6" S	20°24'10.1" E	No visible outcrops.	Mixture of aeolian and fluvial sedimentary deposits.
D13	29°11'59.9" S	20°23'39.9" E	No visible outcrops.	Mixture of aeolian and fluvial sedimentary deposits.
D15	29°12'02.2" S	20°22'57.5" E	No visible outcrops present.	Mixture of aeolian and fluvial sedimentary deposits.
	29°11'57,2" S	20°22'59,3" E	Calcrete outcrop **(C15 & C16 in Figure 6-1)**.	Total outcrop is approximately 25 m by 25 m in diameter.
	29°12'03,0" S	20°22'58,4" E	Metaquartzite outcrop **(MQ19 & MQ20 in Figure 6-1)**.	The length of the outcrop is approximately 40 m in a ESE (120°) to a WNW (300°) direction. The width is 12 m perpendicular to the length.
D17	29°12'04.6" S	20°23'16.8" E	No visible outcrops.	Boulders present underneath the orthic A horizon.
	29°12'04.9" S	20°23'17.5" E	Pegmatite outcrop (**P21 in Figure 6-1**).	The length of the outcrop is approximately 43 m in a S (170°) to a N (350°) direction. The width is 28 m perpendicular to the length.

Figure 6-2 (continued): Geological identification and description.

Mapping Unit	Coordinates		Geological Identification	Properties
	Latitude	Longitude		
D17	29°12'06.2" S	20°23'18.1" E	Metaquartzite outcrop (**MQ15 in Figure 6-1**).	The length of the outcrop is approximately 23 m in a E (74°) to a W (254°) direction. The width is 17 m perpendicular to the length. The strike was noted as 112°, with a 60° dip to the north.
	29°12'04,8" S	20°23'16,6" E	Gneiss outcrop (**G15 in Figure 6-1**).	No properties recorded.
D19	29°12'05.0" S	20°22'07.5" E	No visible outcrops.	Mixture of aeolian and fluvial sedimentary deposits.
	29°12'05.2" S	20°22'07.7" E	Calcrete outcrop (**C25 in Figure 6-1**).	The length of the outcrop is approximately 10 m in a S (170°) to a N (340°) direction. The width is 5 m perpendicular to the length.

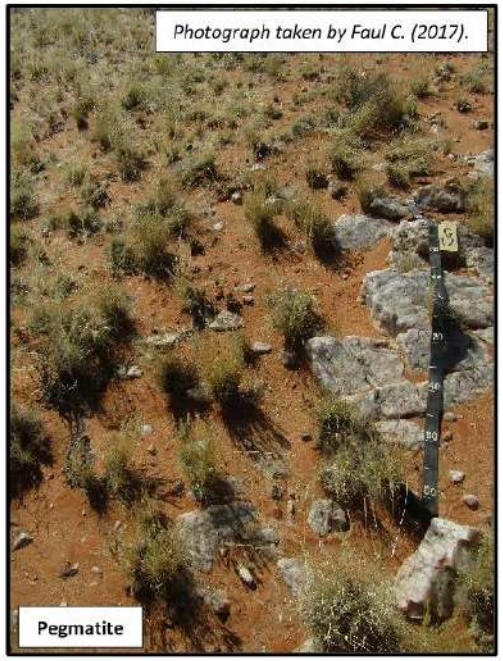

Figure 6-2 (continued): Geological identification and description.

MAPPING UNIT E

Mapping Unit	Coordinates		Geological Identification	Properties
	Latitude	Longitude		
E1	29°11′24.5″ S	20°23′13.9″ E	No visible outcrops.	Calcrete boulders present on surface, as well as smaller fragments of hydrothermal quartz and plagioclase.
	29°11′26.4″ S	20°23′07.4″ E	Pegmatite outcrop (**P11 in Figure 6-1**).	No properties recorded.
			Calcrete outcrop (**C37 in Figure 6-1**).	No properties recorded.
	29°11′25.1″ S	20°23′26.7″ E	Metaquartzite outcrop (**MQ4 in Figure 6-1**).	The length of the outcrop is approximately 115 m in a E (110°) to a W (290°) direction. The width is 2 m perpendicular to the length. The strike was noted as 110°, with a 60° dip to the west.
	29°11′23.8″ S	20°23′23.5″ E	Gneiss outcrop (**G9 in Figure 6-1**).	Total outcrop is approximately 4 m by 4 m in diameter. No strike or dip visible.
E2	29°11′27.5″ S	20°23′51.6″ E	Metaquartzite outcrop (**MQ14 in Figure 6-1**).	No properties recorded.
	29°11′35,5″ S	20°23′32,1″ E	Calcrete outcrop (**C21 & C22 in Figure 6-1**).	No properties recorded.
	29°11′33,3″ S	20°23′33,9″ E	Calcrete outcrop (**C23 in Figure 6-1**).	Total outcrop is approximately 6 m by 6 m in diameter.
	29°11′29,1″ S	20°23′40,5″ E	Calcrete outcrop (**C38 in Figure 6-1**) and pegmatite outcrop (**P10 in Figure 6-1**).	No properties recorded.
	29°11′33,2″ S	20°23′35,1″ E	Pegmatite outcrop (**P18 in Figure 6-1**).	No properties recorded.
E3	29°11′45.4″ S	20°23′24.4″ E	No visible outcrops.	Calcrete boulders present on surface, as well as smaller fragments of hydrothermal quartz and plagioclase.
	29°11′47.5″ S	20°23′20.3″ E	Calcrete outcrop (**C18 in Figure 6-1**).	No properties recorded.

Figure 6-2 (continued): Geological identification and description.

Mapping Unit	Coordinates		Geological Identification	Properties
	Latitude	Longitude		
E3	29°11'45.9" S	20°23'23.5" E	Calcrete outcrop (**C19 & C20 in Figure 6-1**).	No properties recorded.
	29°11'47.1" S	20°23'21.4" E	Pegmatite outcrop (**P6 & P7 in Figure 6-1**).	No properties recorded.
	29°11'41.9" S	20°23'26.5" E	Pegmatite outcrop (**P8 in Figure 6-1**).	No properties recorded.
E5	29°12'34.5" S	20°21'42.2" E	No visible outcrops.	Calcrete boulders present on surface, as well as smaller fragments of hydrothermal quartz and plagioclase.
E6	29°12'52.8" S	20°21'48.0" E	Pegmatite outcrop (**P2 in Figure 6-1**).	No properties recorded.
E7	29°11'33.8" S	20°22'18.4" E	No visible outcrops.	Mixture of aeolian and fluvial sedimentary deposits.
	29°11'33.7" S	20°22'20.1" E	Calcrete outcrop (**C26 & C28 in Figure 6-1**).	Total outcrop is approximately 5 m by 5 m in diameter.

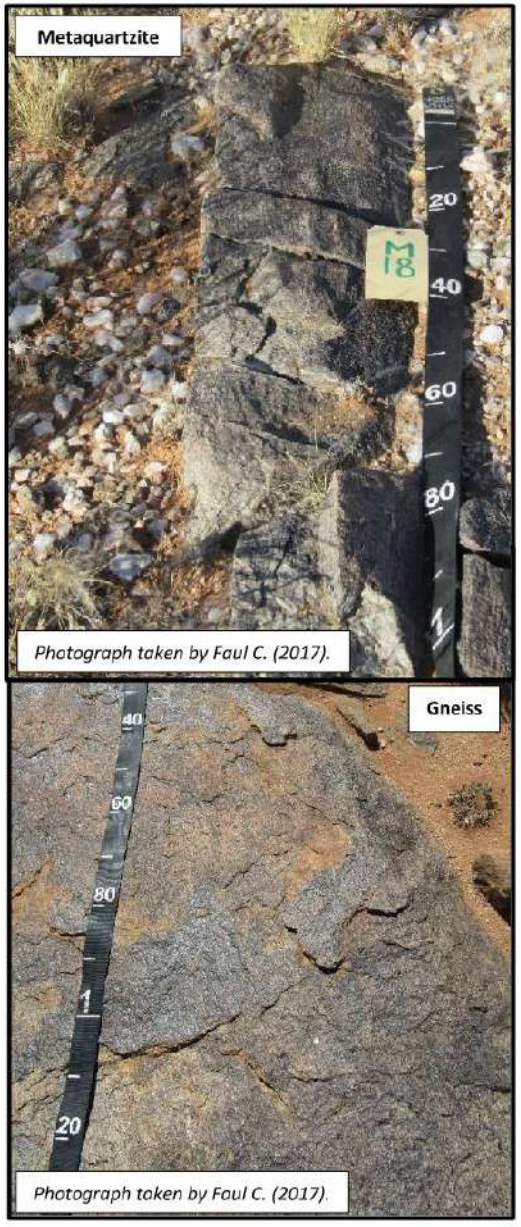

Figure 6-2 (continued): Geological identification and description.

Mapping Unit	Coordinates		Geological Identification	Properties
	Latitude	Longitude		
E7	29°11′34.3″ S	20°22′21.2″ E	Gneiss outcrop (**G3 in Figure 6-1**).	The length of the outcrop is approximately 40 m in a N (10°) to a S (190°) direction. The width is 20 m perpendicular to the length.
	29°11′34.3″ S	20°22′21.2″ E	Calcrete outcrop (**C27 in Figure 6-1**).	The length of the outcrop is approximately 17 m in a SSE (150°) to a NNW (330°) direction. The width is 5 m perpendicular to the length.
	29°11′33.4″ S	20°22′18.4″ E	Calcrete outcrop (**C39 in Figure 6-1**).	No properties recorded.
E9	29°11′55.3″ S	20°22′06.0″ E	No visible outcrops.	Calcrete boulders present on surface, as well as smaller fragments of hydrothermal quartz and plagioclase.

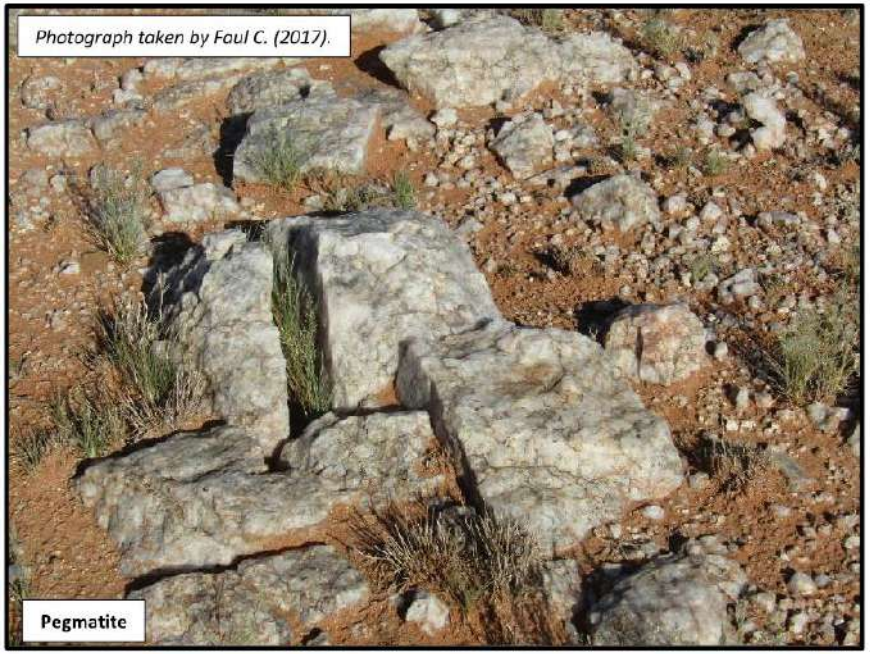

Figure 6-2 (continued): Geological identification and description.

MAPPING UNIT F

Mapping Unit	Coordinates		Geological Identification	Properties
	Latitude	Longitude		
F3	29°11'54.3" S	20°22'46.0" E	No visible outcrops.	Fragments of hydrothermal quartz on surface.
	29°11'54.5" S	20°22'46.1" E	Calcrete outcrop (**C29 in Figure 6-1**).	Total outcrop is approximately 4 m by 4 m in diameter.
	29°11'54.6" S	20°22'45.9" E	Calcrete outcrop (**C30 in Figure 6-1**).	Total outcrop is approximately 3 m by 3 m in diameter.
	29°11'55.4" S	20°22'45.5" E	Calcrete outcrop (**C31 in Figure 6-1**).	Total outcrop is approximately 3 m by 3 m in diameter.
	29°12'09,5" S	20°22'41,9" E	Calcrete outcrop (**C7 & C8 in Figure 6-1**).	Total outcrop is approximately 15 m by 15 m in diameter.
	29°12'07,1" S	20°22'44,4" E	Calcrete outcrop (**C9 in Figure 6-1**).	Total outcrop is approximately 1 m by 1 m in diameter.
	29°12'06,3" S	20°22'45,6" E	Calcrete outcrop (**C10 in Figure 6-1**).	Total outcrop is approximately 2 m by 2 m in diameter.
	29°12'04,7" S	20°22'47,2" E	Calcrete outcrop (**C11 in Figure 6-1**).	Total outcrop is approximately 1 m by 1 m in diameter.
	29°12'00,5" S	20°22'52,7" E	Calcrete outcrop (**C12 in Figure 6-1**).	Total outcrop is approximately 2 m by 2 m in diameter.
	29°11'58,9" S	20°22'55,5" E	Calcrete outcrop (**C13 in Figure 6-1**).	Total outcrop is approximately 3 m by 3 m in diameter.
	29°12'16,6" S	20°22'40,6" E	Calcrete outcrop (**C36 in Figure 6-1**) and Metaquartzite outcrop (**MQ21 in Figure 6-1**).	No properties recorded.

Figure 6-2 (continued): Geological identification and description.

Mapping Unit	Coordinates		Geological Identification	Properties
	Latitude	Longitude		
F3	29°12'13,3" S	20°22'37,8" E	Calcrete outcrop (**C6 in Figure 6-1**).	Total outcrop is approximately 30 m by 2 m in diameter.
	29°12'19,4" S	20°22'31,5" E	Metaquartzite outcrop (**MQ9 in Figure 6-1**).	No properties recorded.
	29°12'10,9" S	20°22'40,1" E	Metaquartzite outcrop (**MQ10 in Figure 6-1**).	No properties recorded.
	29°12'03,5" S	20°22'49,0" E	Metaquartzite outcrop (**MQ11 in Figure 6-1**).	No properties recorded.
	29°11'59,1" S	20°22'55,0" E	Metaquartzite outcrop (**MQ12 in Figure 6-1**).	No properties recorded.
	29°12'02,0" S	20°22'52,0" E	Gneiss outcrop (**G2 in Figure 6-1**).	No properties recorded.
F4	29°11'57,8" S	20°22'58,2" E	Calcrete outcrop (**C14 in Figure 6-1**).	Total outcrop is approximately 4 m by 4 m in diameter.
	29°11'57,2" S	20°22'59,3" E	Calcrete outcrop (**C15 & C16 in Figure 6-1**).	Total outcrop is approximately 25 m by 25 m in diameter.
	29°11'55,4" S	20°23'03,2" E	Calcrete outcrop (**C17 in Figure 6-1**).	Total outcrop is approximately 1 m by 1 m in diameter.
	29°11'58,4" S	20°22'56,7" E	Pegmatite outcrop (**P15 in Figure 6-1**).	No properties recorded.
F5	29°12'40.4" S	20°22'12.4" E	No visible outcrops.	Fragments of hydrothermal quartz and plagioclase on surface.
	29°12'47,4" S	20°22'27,9" E	Gneiss outcrop (**G12 in Figure 6-1**).	Total outcrop is approximately 4 m by 4 m in diameter.

Figure 6-2 (continued): Geological identification and description.

MAPPING UNIT G

Mapping Unit	Coordinates		Geological Identification	Properties
	Latitude	Longitude		
G1	29°11'17.1" S	20°23'01.2" E	Calcrete outcrop (**C32 in Figure 6-1**).	No properties recorded.
G5	29°11'36.8" S	20°23'22.1" E	No visible outcrops.	Fragments of calcrete, hydrothermal quartz and plagioclase on surface.
	29°11'40,7" S	20°23'27,8" E	Pegmatite outcrop (**P16 in Figure 6-1**).	Total outcrop is approximately 10 m by 10 m in diameter.
	29°11'38,7" S	20°23'29,5" E	Pegmatite outcrop (**P17 in Figure 6-1**).	Total outcrop is approximately 1 m by 1 m in diameter.
	29°11'36,9" S	20°23'22,9" E	Pegmatite outcrop (**P20 in Figure 6-1**).	The length of the outcrop is approximately 60 m in a SE (140°) to a NW (320°) direction. The width is 4 m perpendicular to the length.
	29°11'39,8" S	20°23'28,5" E	Metaquartzite outcrop (**MQ13 in Figure 6-1**).	No properties recorded.
G6	29°11'43.3" S	20°22'29.6" E	No visible outcrops.	Fragments of calcrete, hydrothermal quartz and plagioclase on surface.
	29°11'43.3" S	20°22'29.6" E	Metaquartzite outcrop (**MQ16 in Figure 6-1**).	The length of the outcrop is approximately 15 m in a ENE (76°) to a WSW (256°) direction. The width is 3 m perpendicular to the length.
	29°11'43.3" S	20°22'29.6" E	Calcrete outcrop (**C33 in Figure 6-1**).	The length of the outcrop is approximately 5 m in a ENE (76°) to a WSW (256°) direction. The width is 2 m perpendicular to the length.
	29°11'45,2" S	20°22'29,4" E	Metaquartzite outcrop (**MQ17 in Figure 6-1**).	No properties recorded.

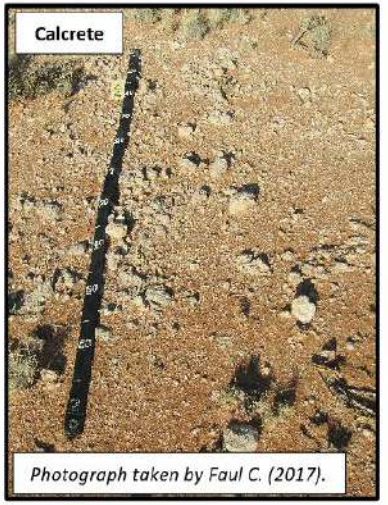

Photograph taken by Faul C. (2017).

Photograph taken by Faul C. (2017).

Figure 6-2 (continued): Geological identification and description.

Mapping Unit	Coordinates		Geological Identification	Properties
	Latitude	Longitude		
G7	29°12'05.4" S	20°22'14.8" E	No visible outcrops.	Fragments of calcrete, hydrothermal quartz and plagioclase on surface.
G10	29°12'31.8" S	20°21'58.3" E	No visible outcrops.	Fragments of calcrete, hydrothermal quartz and plagioclase on surface.
	29°12'34,8" S	20°21'58,3" E	Calcrete outcrop (**C3 in Figure 6-1**).	Total outcrop is approximately 5 m by 5 m in diameter.
	29°12'30,6" S	20°22'00,8" E	Calcrete outcrop (**C4 in Figure 6-1**).	Total outcrop is approximately 5 m by 5 m in diameter.
	29°12'42,0" S	20°21'55,1" E	Calcrete outcrop (**C2 in Figure 6-1**).	Total outcrop is approximately 4 m by 4 m in diameter.
	29°12'29,7" S	20°22'01,5" E	Metaquartzite outcrop (**MQ8 in Figure 6-1**).	No properties recorded.
	29°12'38,1" S	20°21'57,7" E	Gneiss outcrop (**G10 in Figure 6-1**).	No properties recorded.
	29°12'28,5" S	20°22'02,0" E	Pegmatite outcrop (**P13 in Figure 6-1**).	No properties recorded.
	29°12'44,9" S	20°21'54,0" E	Pegmatite outcrop (**P1 in Figure 6-1**).	No properties recorded.
	29°12'32,0" S	20°22'32,0" E	Pegmatite outcrop (**P4 in Figure 6-1**).	No properties recorded.
G12	29°12'51,1" S	20°21'42,4" E	Pegmatite outcrop (**P3 in Figure 6-1**).	No properties recorded.
	29°12'49,1" S	20°21'38,4" E	Pegmatite outcrop (**P5 in Figure 6-1**).	No properties recorded.

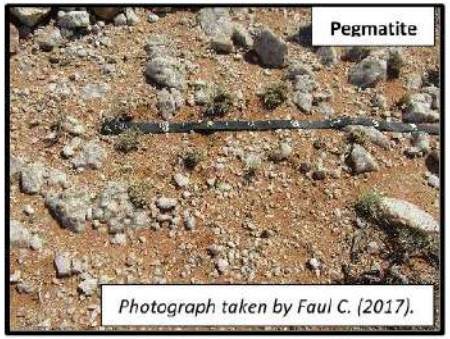

Figure 6-2 (continued): Geological identification and description.

MAPPING UNIT H

Mapping Unit	Coordinates		Geological Identification	Properties
	Latitude	Longitude		
H1	29°10'45.3" S	20°22'57.3" E	No visible outcrops.	Fragments of calcrete, hydrothermal quartz, orthoclase, and plagioclase on surface.
	29°11'14,8" S	20°23'28,1" E	Gneiss outcrop (**G8 in Figure 6-1**).	No properties recorded.
H3	29°12'33.6" S	20°22'41.2" E	No visible outcrops.	Fragments of calcrete, hydrothermal quartz, orthoclase, and plagioclase on surface.
	29°12'34.5" S	20°22'43.1" E	Metaquartzite (**MQ18 in Figure 6-1**).	The length of the outcrop is approximately 10 m in a ENE (80°) to a WSW (260°) direction. The width is 3 m perpendicular to the length.
	29°12'33.6" S	20°22'43.2" E	Gneiss outcrop (**G11 in Figure 6-1**).	Total outcrop is approximately 25 m by 25 m in diameter.
H4	29°12'05.7" S	20°21'53.7" E	No visible outcrops.	Fragments of calcrete, hydrothermal quartz, orthoclase, and plagioclase on surface.
H5	29°12'07.9" S	20°23'06.5" E	No visible outcrops.	Fragments of calcrete, hydrothermal quartz, orthoclase, and plagioclase on surface. Various calcrete outcrops in the surrounding area.
	29°12'07.8" S	20°23'05.8" E	Calcrete outcrop (**C34 in Figure 6-1**).	Total outcrop is approximately 30 m by 30 m in diameter.
H6	29°12'48.5" S	20°22'28.5" E	No visible outcrops.	Fragments of calcrete, hydrothermal quartz, orthoclase, and plagioclase on surface.
	29°12'45,7" S	20°22'40,9" E	Metaquartzite outcrop (**MQ7 in Figure 6-1**).	No properties recorded.

Figure 6-2 (continued): Geological identification and description.

MAPPING UNIT I

Mapping Unit	Coordinates		Geological Identification	Properties
	Latitude	Longitude		
I1	29°12′21.5″ S	20°23′07.1″ E	No visible outcrops.	Some orthoclase and quartz fragments on surface.
	29°12′21.3″ S	20°23′07.2″ E	Gneiss outcrop (**G4 in Figure 6-1**).	The length of the outcrop is approximately 2 m in a SE (132°) to a NW (312°) direction. The width is 30 cm perpendicular to the length. The strike is noted as 132° with a 40° dip in a north-eastern direction.
	29°12′24,2″ S	20°22′54,6″ E	Gneiss outcrop (**G1 in Figure 6-1**).	No properties recorded.
I2	29°11′54.1″ S	20°23′40.7″ E	No visible outcrops.	Some orthoclase and quartz fragments on surface.
	29°11′55.1″ S	20°23′42.6″ E	Gneiss outcrop (**G5 in Figure 6-1**).	The length of the outcrop is approximately 10 m in a SSE (150°) to a NNW (330°) direction. The width is 3 m perpendicular to the length.
	29°12′03,8″ S	20°23′24,3″ E	Pegmatite outcrop (**P12 in Figure 6-1**).	The strike is noted as 120° (ESE) with a 60° dip in a north-eastern direction.

Photograph taken by Faul C. (2017).

Photograph taken by Faul C. (2017).

Figure 6-2 (continued): Geological identification and description.

MAPPING UNIT J

Mapping Unit	Coordinates		Geological Identification	Properties
	Latitude	Longitude		
J1	29°12'10.9" S	20°22'01.5" E	Metaquartzite outcrops.	No properties recorded.
	29°12'11.1" S	20°22'01.1" E	Metaquartzite outcrop (**MQ21 in Figure 6-1**).	The strike is noted as 116° (ESE) with an 82° dip in a south-eastern direction.
	29°12'10.7" S	20°22'01.9" E	Metaquartzite outcrop (**MQ22 in Figure 6-1**).	Mylonite in metaquartzite.
J2	29°12'20.1" S	20°21'48.5" E	Metaquartzite outcrops.	No properties recorded.
	29°12'20.1" S	20°21'48.7" E	Metaquartzite outcrop (**MQ23 in Figure 6-1**).	The strike is noted as 91° (E) with an 45° dip in a south-eastern direction.
	29°12'20,1" S	20°21'48,5" E	Gneiss outcrop (**G6 in Figure 6-1**).	No properties recorded.
J3	29°11'24.4" S	20°22'24.3" E	Metaquartzite (**MQ24 in Figure 6-1**).	The strike is noted as 50° (NE) with an 50° dip in a south-eastern direction.
	29°11'24.8" S	20°22'24.3" E	Metaquartzite outcrop (**MQ2 in Figure 6-1**).	No properties recorded.
J4	29°11'22.9" S	20°22'39.5" E	Metaquartzite outcrops (**MQ1 & MQ25 in Figure 6-1**).	No properties recorded.
	29°11'20.3" S	20°22'38.3" E	Metaquartzite outcrop (**MQ26 in Figure 6-1**).	No properties recorded.
	29°11'20.6" S	20°22'36.1" E	Metaquartzite outcrop (**MQ27 in Figure 6-1**).	No properties recorded.
J5	29°11'28.4" S	20°22'50.7" E	Metaquartzite outcrop (**MQ28 in Figure 6-1**).	No properties recorded.
	29°11'28.5" S	20°22'50.8" E	Gneiss outcrop (**G7 in Figure 6-1**).	No properties recorded.
	29°11'28.6" S	20°22'51.0" E	Metaquartzite outcrop (**MQ29 in Figure 6-1**).	The strike is noted as 128° (NE) with an 40° dip in a south-eastern direction.
	29°11'28.4" S	20°22'51.0" E	Metaquartzite outcrop (**MQ30 in Figure 6-1**).	The strike is noted as 118° (ENE) with an 52° dip in a south-eastern direction.

Figure 6-2 (continued): Geological identification and description.

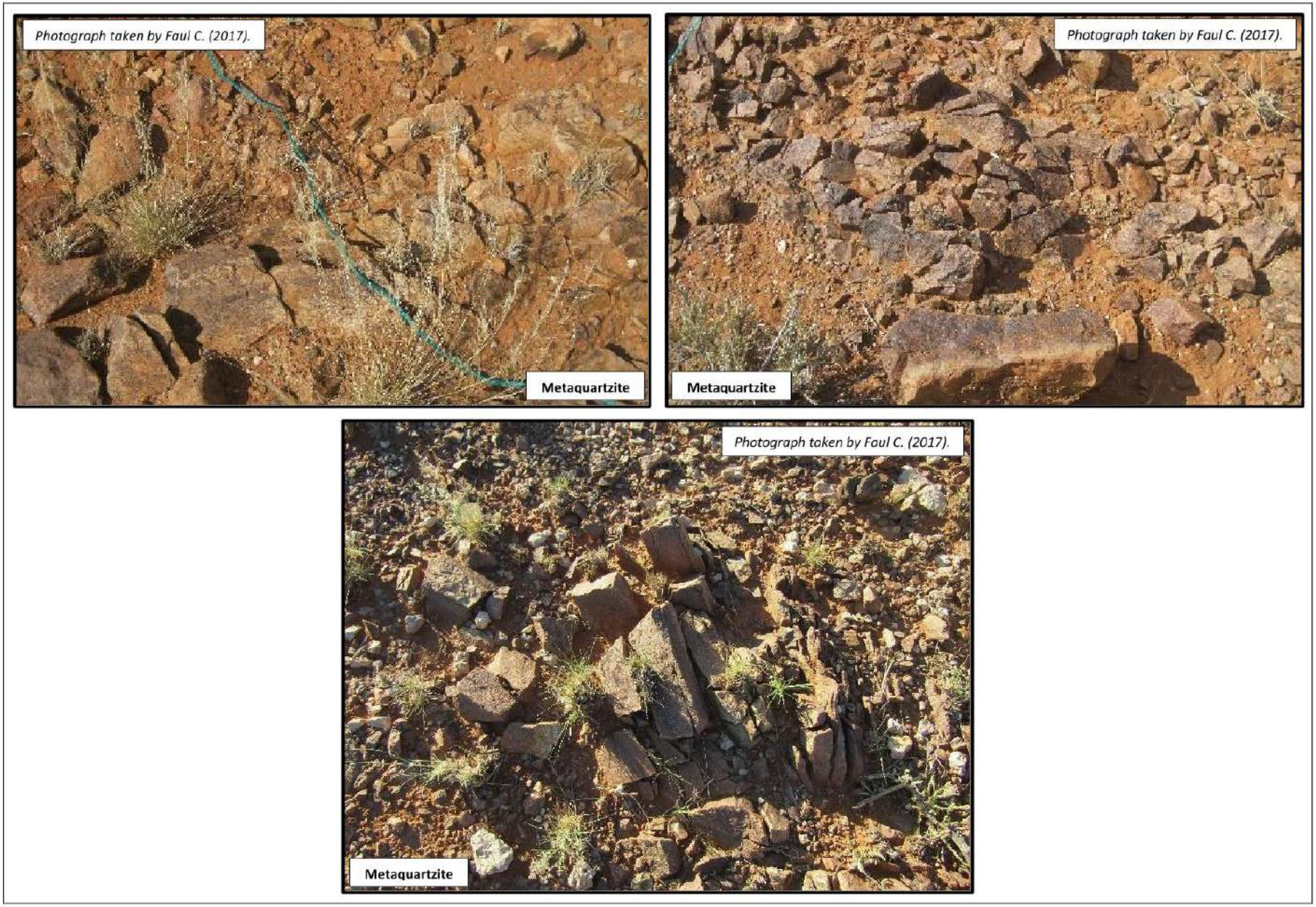

Figure 6-2 (continued): Geological identification and description.

McClung (2006) constructed a lithostratigraphic column (Figure 6-3) of the Aggeneys Terrane which forms part of the Bushmanland Group. This lithostratigraphy corresponds to that of the study area to some extent.

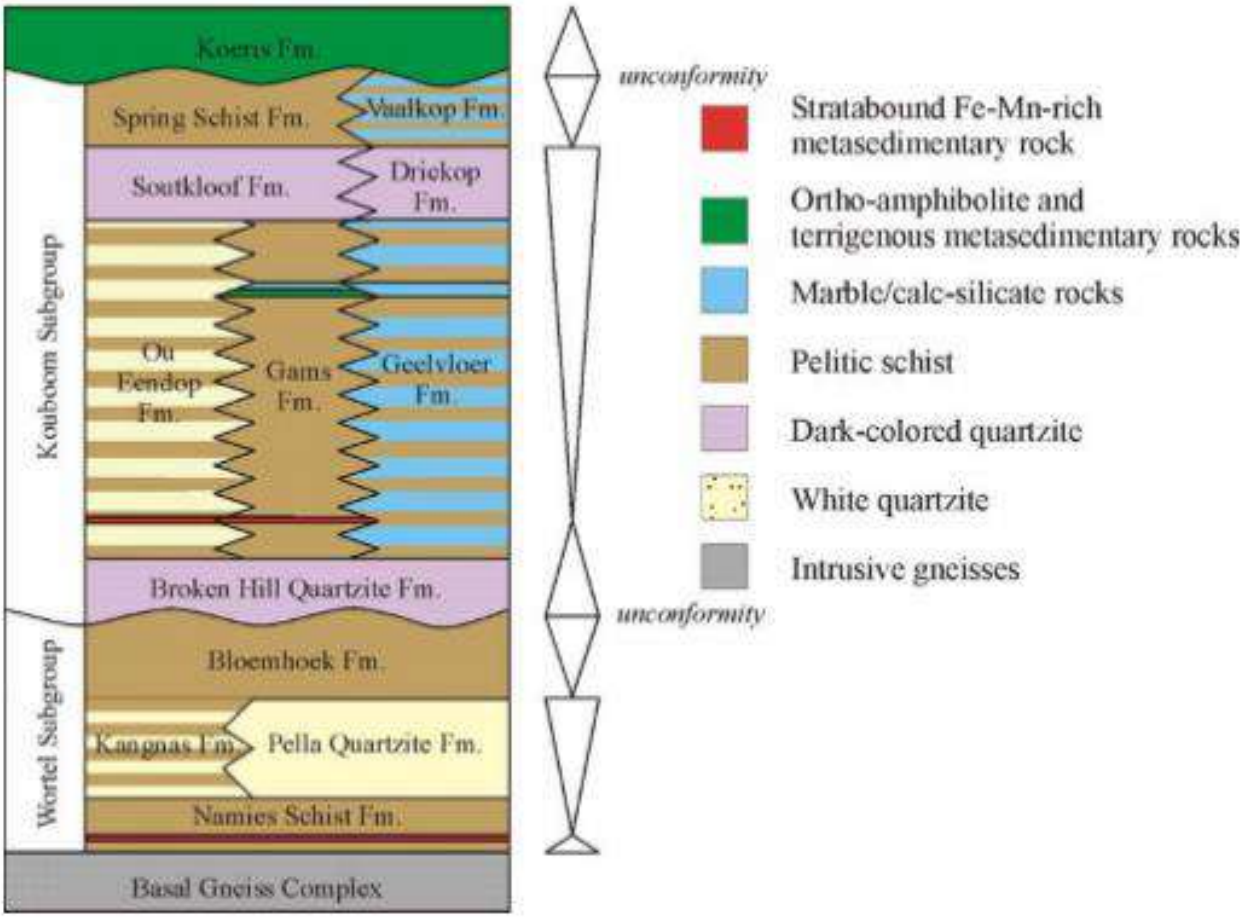

Figure 6-3: Lithostratigraphic subdivision of the Aggeneys Terrane within the Bushmanland Group (McClung, 2006).

Based on the information obtained during the geological survey, as well as information gathered from previous research (see Chapter 2, section 2.2. and Figure 6-3) a lithostratigraphic column was constructed for this area.

Table 6-1: Lithostratigraphic column of the study area (Bailie *et al.*, 2007; Colliston *et al.*, 2008; Cornell *et al.*, 2009; Cornell *et al.*, 2006; Eglington, 2006; Haddon, 2005; McClung, 2006; Reid *et al.*, 1997; Von M Harmse & Hatting, 2012; Watts, 1980).

Ma	Group	Subgroup	Formation	Intrusive Rocks	Lithological Description	Epoch	Period	Era	Eon	Ma
0 - 0.01	Kalahari Group				Kalahari calcrete, sandy material of mixed origin, lag deposit and gypsic deposits	Holocene	Quaternary	Cenozoic	Phanerozoic	0 – 0.01
0.01 – 1.6					Kalahari calcrete, sandy material of mixed origin, and lag deposit	Pleistocene				0.01 – 1.6
1.6 – 5.0					Kalahari calcrete (soft, hard bank, nodular, tabular)	Pliocene	Tertiary			1.6 – 5.0
~ 1130	Bushmanland Group	Kouboom Subgroup	Vaalkop Formation		Biotite-gneisses.			Mokolian	Proterozoic	900 - 2050
			Driekop Formation		Metagreywacke comprised of grey quartzite.					
			Geelvloer Formation		Biotite-schist hosting calc-silicate and carbonate rich rocks. Emplacement of pegmatites.					
			Broken Hill Quartzite Formation		Typical purplish-red to dark grey glassy quartzite and metaquartzite.					
~1640		Wortel Subgroup	Namies Schist Formation		Calc-silicate gneiss, biotite-rich schist, quartzite and metaquartzite.					
~ 1650				Hoogoor Suite	Pink gneiss					
1700-2050				Achab Gneiss	Migmatitic leucogneiss					

Each lithological unit within this lithostratigraphic column is described according to its age, physical properties, chemical properties as well as distribution where applicable.

- **Basement granitic gneiss**

Basement granitic gneisses dominate throughout the entire study area, with an Rb-Sr model age of 1650 - 2050 Ma. This lithostratigraphic unit is considered a typical east-west trending structural formation with minor folding. In some cases, the gneiss is deeply weathered with adjacent outcrop of fresh gneiss close by (see Figure 6-2, Mapping Unit I). These leucocratic gneisses could be derived from pre-tectonic intrusive granite and is commonly referred to as granitic gneisses. It is also possible that the south-eastern extension of the Pofadder shear zone or one of its subsidiary zones could have an influence on the deep weathering; however, no research supports this assumption. The concordant to semi-concordant red-brown weathered gneiss is considered quartzofeldspatic and referred to as the Pink Gneisses of the Hoogoor Suite, underlain by Achab Gneiss (Bailie *et al.*, 2007; Boelema, 1994; Colliston *et al.*, 2008; Cornell *et al.*, 2009; Cornell *et al.*, 2006; McClung, 2006; Reid *et al.*, 1997).

- **Metaquartzite and quartzite schist (near vertical)**

Metaquartzite are recorded at several outcrops and bedrock exposures (see Figure 6-2 Mapping Unit J). The best examples are the grey-blue metaquartzite on the north-eastern boundary as well as the south-western boundary of the study area. On the south-eastern boundary metaquartzite becomes quartzite schist. In isolated cases, it appears to be associated with calc-silicates with a near vertical dip and an east-west strike. Primary sedimentary features (such as graded bedding) are preserved in the metaquartzites. Contact metamorphic minerals for instance hydrothermal quartz veins are present on the contact zones and bedding planes associated with hydrothermal enrichment. Small porphyroblasts (2 mm – 4 mm in diameter) are present in some metaquartzites (Bailie *et al.*, 2007; Boelema, 1994; Colliston *et al.*, 2008; Cornell *et al.*, 2009; Cornell *et al.*, 2006; McClung, 2006; Reid *et al.*, 1997).

- **Pegmatites**

The pegmatites form part of the 450 km long Vioolsdrif-Kenhardt pegmatite belt. A variety of minerals including feldspar, muscovite and quartz are exploited on the pegmatite belt, but no mining or exploration activities occur within this area. The length of these pegmatites can vary between meters to kilometres and are dominated by quartz-rich centres in most cases. The more resistant quartz-rich varieties form positive land scape reliefs. Quartz is also the dominant mineral in the thin lag deposit on surface at numerous localities (Cornell *et al.*, 2006). Plagioclase and orthoclase, as well as muscovite clusters are abundant within pegmatites. A model age of 1000 – 945 Ma are given for the pegmatites (Cornell *et al.*, 2006).

- **Cenozoic calcrete**

The calcrete found in this area were classified as pedogenic Kalahari calcrete (Watts, 1980). It appears as thin layers on the surface or as bedrock below the sandy alluvium. Thickness varies from centimetres up to one meter. Calcrete are often referred to as pedogenic duricrust (Haddon, 2005), and are found in this area as different types including hardbank, soft, nodular, powdery and long tabular. (Brink, 1985; Chen *et al.*, 2002; Cornell *et al.*, 2006; Haddon, 2005; Hurter, 2016).

- **Transported sandy soils of mixed origin**

This material has no distinct properties of a typical residual, alluvial or aeolian soil and is therefore classified as soil of mixed origin. This material developed from alluvial periodic flash floods of extensive sheet wash, aeolian spells during extensive dry periods as well as through weathering of the underlying or nearby bedrock and outcrops (Brink, 1985). These soils, with an average thickness of 30 cm to 80 cm, dominate the south-eastern plains and have a dominant grass cover. The north-western outcrop area is covered with a much thinner soil layer with an average thickness of 8 cm. The texture of the soil ranges from a silty sand to a sand (Brink, 1985).

- **Lag deposits**

A lag deposit develops where soil and larger rock fragments are mixed (typical soils of mixed origin) and exposed to the surface, wind removes the finer soil particles and the stony component remain. On this site, the lag deposit is much more pronounced in the north-western part where the rocky material is close to surface. The local residual rock fragments dominate these lag deposits i.e. quartz and feldspar from the pegmatites and to a lesser extent from the metaquartzites. The lag deposits on the metaquartzites are dominated by the grey-blueish and sometimes greenish glassy components of the metaquartzite (Hurter, 2016).

- **Alluvial sandy material in drainage systems**

The three main drainage systems on the site are dominated by sandy material with a thickness of up to one meter and a width of up to hundred meters. Small tributaries have thin and narrow deposits. The texture is dominated by sand with minor fragments larger than 2 mm.

- **Gypsic material**

Gypsic material is common in dry, semi-desert environments in the western parts of South Africa. The origin of the sulphates could have derived from the sulphide mineralised local rocks including calc-silicates or from the H_2S rich fog from the coast (Cornell *et al.*, 2006). Gypsic material was

found only at the south-eastern boundary of the study area, mixed with calcareous material directly overlying weathered gneiss. A strong sulphuric odour was present in old borrow pits.

All the above-mentioned information and observations were used to construct a geological map (Figure 6-4) of the study area.

Due to the geological complexity and diversity as well as the lack of geological outcrops with respect to the size of the study area it was not possible to construct a detailed geological map. However, based on Figure 6-4 it is clear that there is a distinct difference between the north-western segment and the south-eastern segment of the study area.

The north-western part of the study area consists of granitoids with the following order of abundancy: Gneiss > metaquartzite > pegmatite > surficial calcrete deposits. The granitic gneisses are considered the oldest (1650 - 2050 Ma) lithostratigraphic unit (Cornell *et al.*, 2006; Reid *et al.*, 1997), while the metaquartzites were deposited approximately 1130 – 1640 Ma ago (Bailie *et al.*, 2007; Colliston *et al.*, 2008; McClung, 2006). Surficial calcrete deposits with occasional gneiss outcrops dominate the south-eastern part of the study area. These calcretes were deposited during the Cenozoic Era and are considered as relatively young (0 – 5 Ma) (Hurter, 2016; Watts, 1980) The drainage systems consist of alluvial and aeolian sandy material (0 – 1.6 Ma old), while gypsic deposits coexist with a calcareous mixture (1 – 0.01 Ma) (Von M Harmse & Hatting, 2012) (See Figure 6-4).

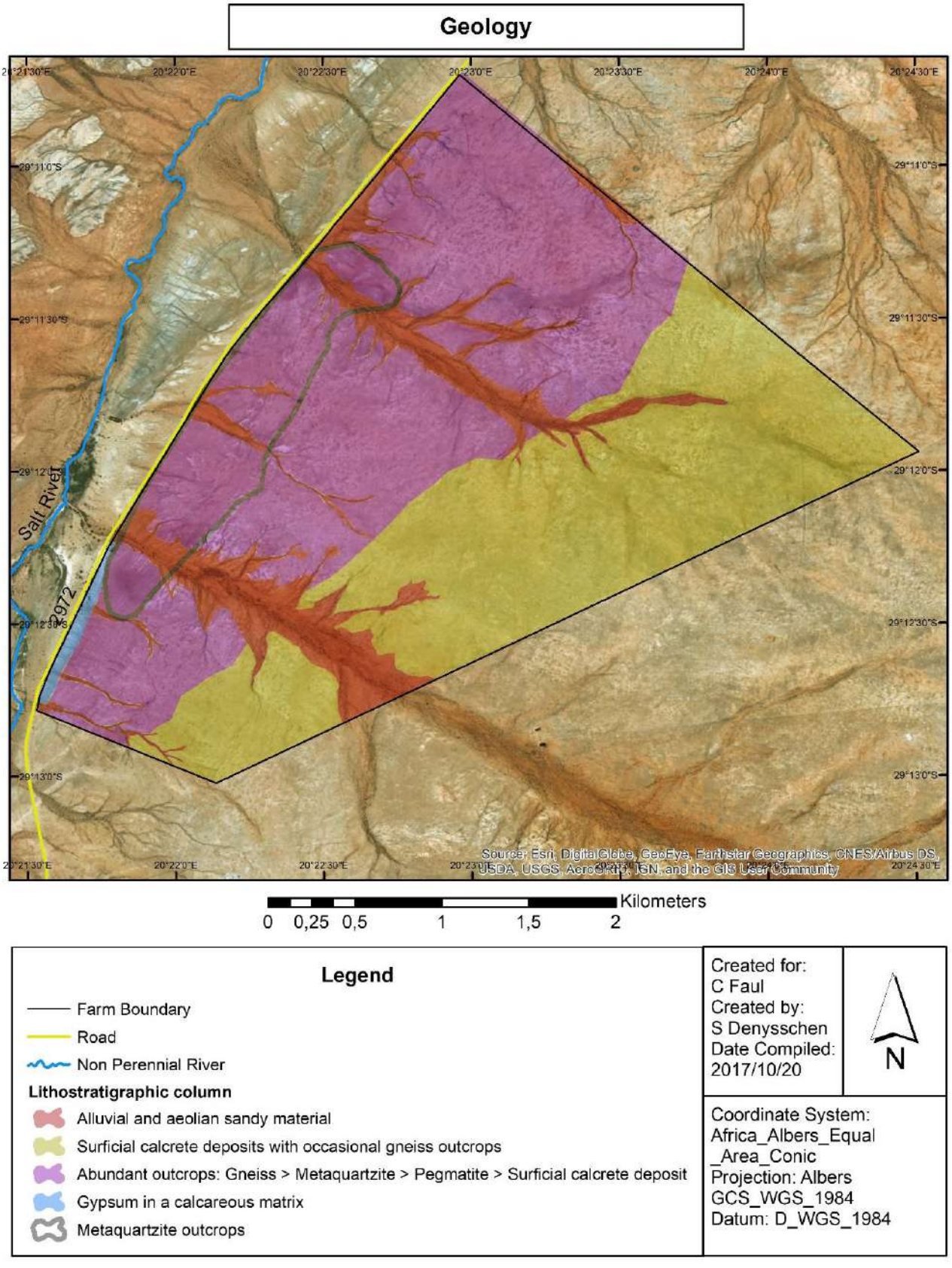

Figure 6-4: Geological map of the study area (Google Earth, 2016).

6.2 Petrography

Based on the aims and objectives of this study geological samples were only collected for identification purposes.

6.2.1 Field Appearance

All three samples (S1 S2 and S3) obtained in the north-western segment of the area, were identified as gneiss forming part of either the Achab Gneisses or the Hoogoor Suite. Local gneiss had a prominent greyish colour in some localities (Achab Gneiss), while other localities displayed reddish-brown colours (Hoogoor Suite).

Samples S1 and S2 are well foliated and gneissosity is visible due to the alternating layers of quartzofeldspatic minerals and biotite. These samples possess a strong magnetic signature caused by an abundance of magnetite inclusions. Foliation in sample S3 is not as prominent as in S1 and S2. Magnetite inclusions is absent in sample S3 however, it contains quartz veins perpendicular to the foliation of the gneiss. In general, the gneissic rocks show a south-east to south south-east trend.

6.2.2 Petrography

These rocks are given a foliated appearance by the minerals biotite and magnetite which is elongated with a preferred orientation and exhibits a hypidioblastic grain shape. Quartz is the main constituent of the rock and has a xenoblastic grain shape. Plagioclase was identified as a fine-grained groundmass surrounding biotite exhibiting polysynthetic twinning with associated sericite.

Epidote and magnetite was present in sample S1. Epidote is known as a secondary product that forms during the process of chloritisation of biotite (Eggleton & Banfield, 1985). This is proof of retrograde metamorphism. Magnetite is elongated in the same direction than biotite. Photomicrographs of sample S1, S2 and S3 are illustrated in Figure 6-5, Figure 6-6 and Figure 6-7 respectively.

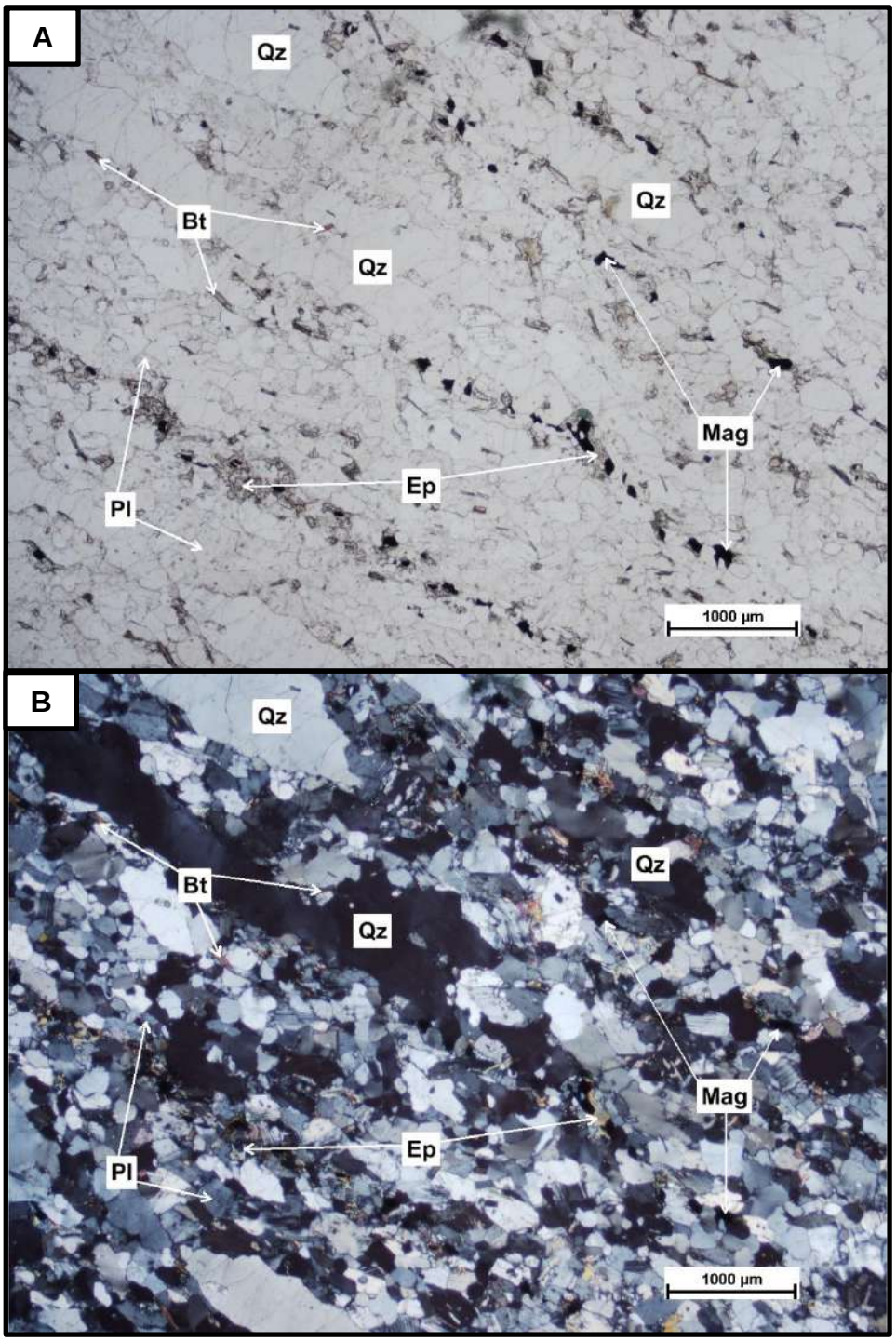

Figure 6-5: Photomicrograph of gneiss (Sample S1). (A) Minerals that make up the majority of the gneiss can be seen using plane polarised light (PPL): quartz, biotite, plagioclase, epidote, and magnetite. Note foliation. (B) Same as A, using crossed polarised light (XPL).

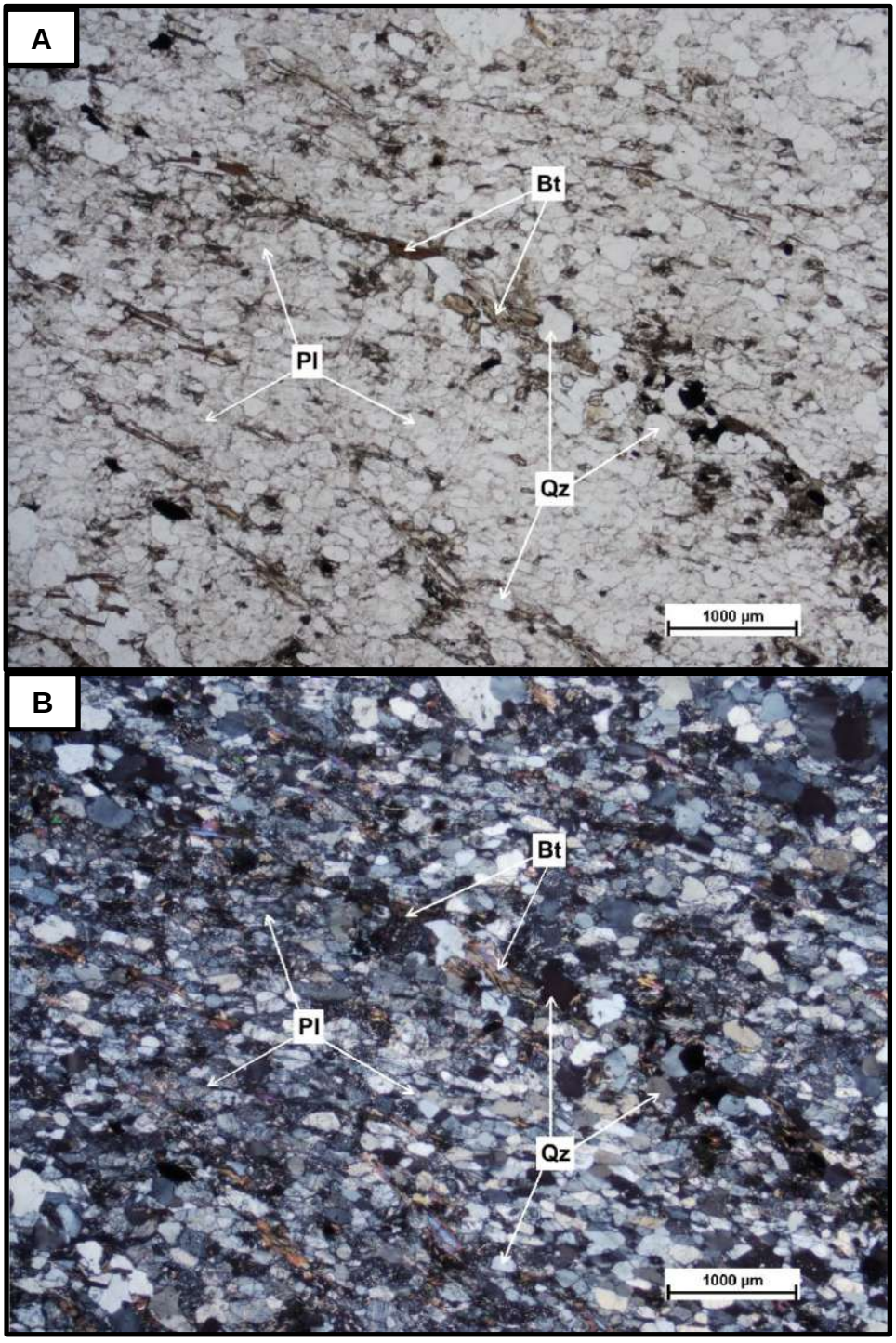

Figure 6-6: Photomicrograph of gneiss (Sample 2). (A) Minerals that make up the majority of the gneiss can be seen using plane polarised light (PPL): quartz, biotite, and plagioclase. Note foliation. (B) Same as A, using crossed polarised light (XPL).

As illustrated in Figure 6-5 and Figure 6-6, gneiss (Samples 1 and 2) consists of mainly quartz, plagioclase, and biotite with accessory epidote and magnetite. Both samples have a gneissic foliation.

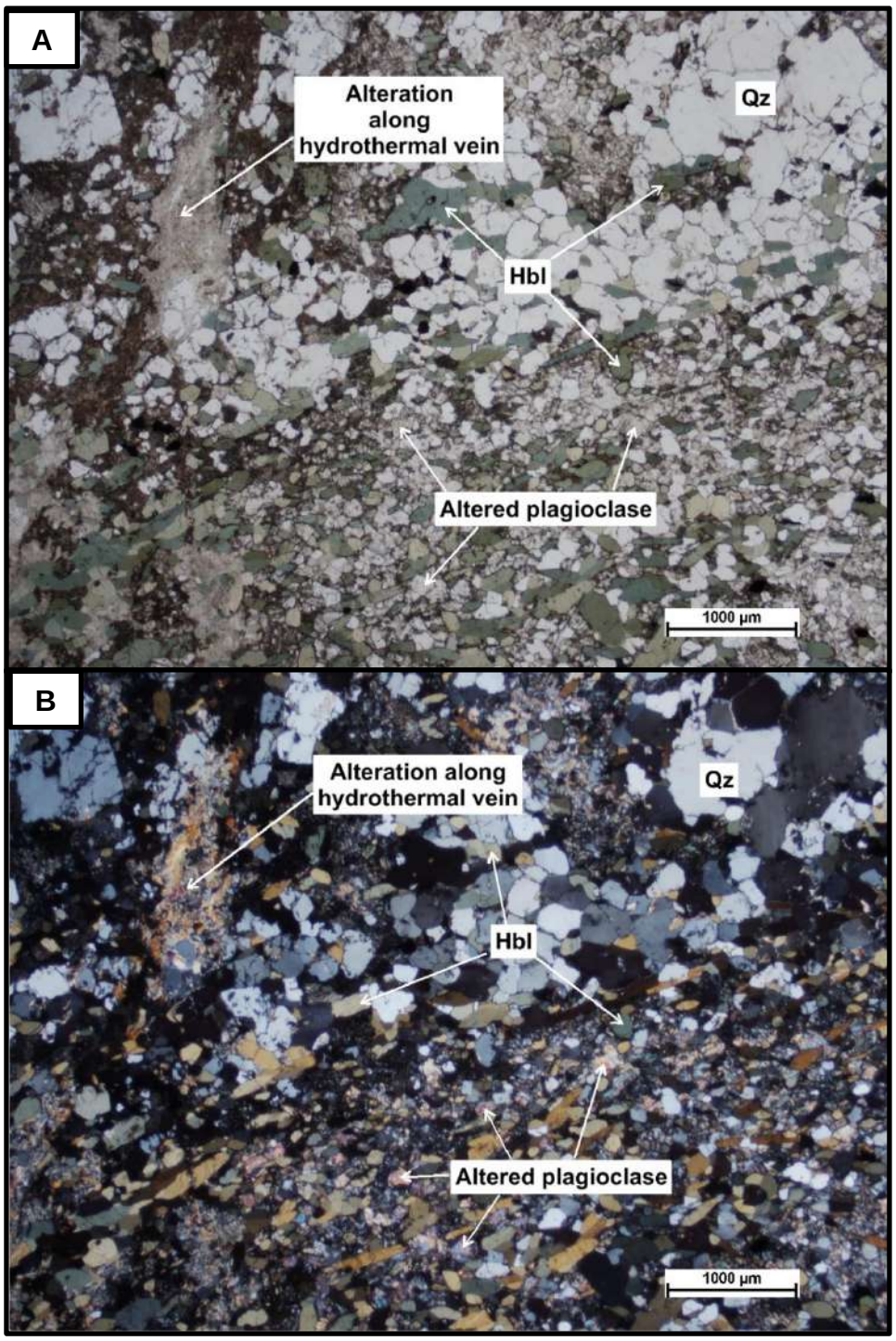

Figure 6-7: Photomicrograph of gneiss (Sample S3). (A) Minerals that make up the majority of the gneiss can be seen using plane polarised light (PPL): quartz, hornblende, and plagioclase. Note alteration along the hydrothermal vein. (B) Same as A, using crossed polarised light (XPL).

As illustrated in Figure 6-7, gneiss (sample S3) consists of mainly quartz, plagioclase and hornblende. The sample has a granoblastic texture with a poorly developed gneissic foliation. Hornblende is responsible for the foliated appearance due to its elongated, xenoblastic grain shape with a preferred orientation. Quartz and plagioclase are considered the main constituents

of the rock, with plagioclase identified as a fine-grained groundmass surrounding hornblende. Alteration along the hydrothermal vein which is sub-perpendicular to the foliation is also visible in S3.

6.3 Basic Conclusion

Based on the aims and objectives of this study, geological outcrops were identified and described in order to construct a geological map for correlation purposes. The north-western segment of the study area consists of granitoids with the following order of abundancy: Gneiss > metaquartzite > pegmatite > surficial calcrete deposits. Surficial calcrete deposits with occasional gneiss outcrops dominate the south-eastern segment of the study area. The drainage systems consist of alluvial and aeolian sandy material. Gypsic deposits, coexisting with a calcareous mixture, occur in closed proximity to the north-western boundary of the study area.

Consult Chapter 7 for more information regarding the function of geology in an integrated relationship between vegetation, soil and geology.

.

CHAPTER 7

CORRELATIONS RESULTS AND DISCUSSIONS

In environmental studies and specifically ecological studies it is common to find geographical patchiness varying in scale (Legendre, 1993). When the relationship between vegetation and substrata of a specific area is well understood, and one is familiarised with the vegetation type and pedological as well as lithological patterns of this area, a correlation between the vegetation and the corresponding substrata can be identified. This identification method is of economic importance due to the amount of information gathered through a basic surficial reconnaissance survey. Consult Chapter 3 section 3.4 for more information regarding this methodology. In this chapter landscape relationships will be examined by means of typical surface pattern analysis (Legendre, 1993). The purpose of Chapter 7 is therefore to create a type of data base that can be used for future studies in the semi-arid Bushmanland region of South Africa.

7.1 Method 1

The first method consists of the construction of correlation maps (overlay method) based on the older method of trend-surface analysis. After the construction of correlation maps, information obtained from these maps is used to construct correlation matrix diagrams in order to identify two-tier correlation combinations as well as the degree of correlation.

7.1.1 Geology and Vegetation

According to Malos (2011), plant communities and habitats are considered important in applied studies such as geological surveys. Schlesinger (1996) conducted a study where it was found that a calcareous substrate in the semi-arid regions of Navada and New Mexico correlates with typical grassland habitats whereas an acidic substrate in the same environment correlates with typical scrubland habitats.

Due to the geological complexity of this study area it was not possible to construct a detailed geological map. However, distinct differences were observed with the north-western segment of the study area consisting of abundant outcrops (granitoids) with the following order of abundancy: Gneiss > metaquartzite > pegmatite. The south-eastern segment consists of surficial calcrete deposits with occasional gneiss outcrops. The drainage systems are composed of alluvial and aeolian sandy material. Two additional geological units, metaquartzite outcrops and gypsic deposits, were identified, both occurring next to the north-western boundary of the study area.

Plant communities were identified based on diagnostic species rather than species dominance. Data analyses and additional field observations resulted in the identification of four different plant communities that can be grouped into three major community units:

1. *Rhigozum trichotomum – Stipagrostis namaquensis* Shrubland

This plant community is characterised by *Stipagrostis namaquensis, Eragrostis lehmanniana, Rhigozum trichotomum, Stipagrostis obtusa, Stipagrostis ciliata, Eriocephalus ambiguus* and *Stipagrostis fastigiata*. The diagnostic species for this community includes *Rhigozum trichotomum, Stipagrostis namaquensis* and *Eragrostis lehmanniana.*

2. *Calobota spinescens – Stipagrostis fastigiata* Grassland

Stipagrostis obtusa, *Stipagrostis fastigiata*, *Calobota spinescens* and *Eriocephalus ambiguus* characterises this plant community, while *Stipagrostis fastigiata* and *Calobota spinescens* are considered diagnostic species.

3. *Stipagrostis obtusa* Shrubby Grassland

3.1. *Stipagrostis ciliata – Stipagrostis obtusa* Shrubby Grassland

The diagnostic species for this sub-community include *Stipagrostis obtusa* and *Stipagrostis ciliata*.

3.2. *Salsola tuberculata – Stipagrostis obtusa* Shrubby Grassland

The diagnostic species for this sub-community include *Salsola barbata, Salsola tuberculata* and *Aridaria noctiflora*.

Figure 7-1 illustrates the two-tier correlation between the geological units and plant communities of the study area, and Table 7-1 visually illustrates the degree of correlation.

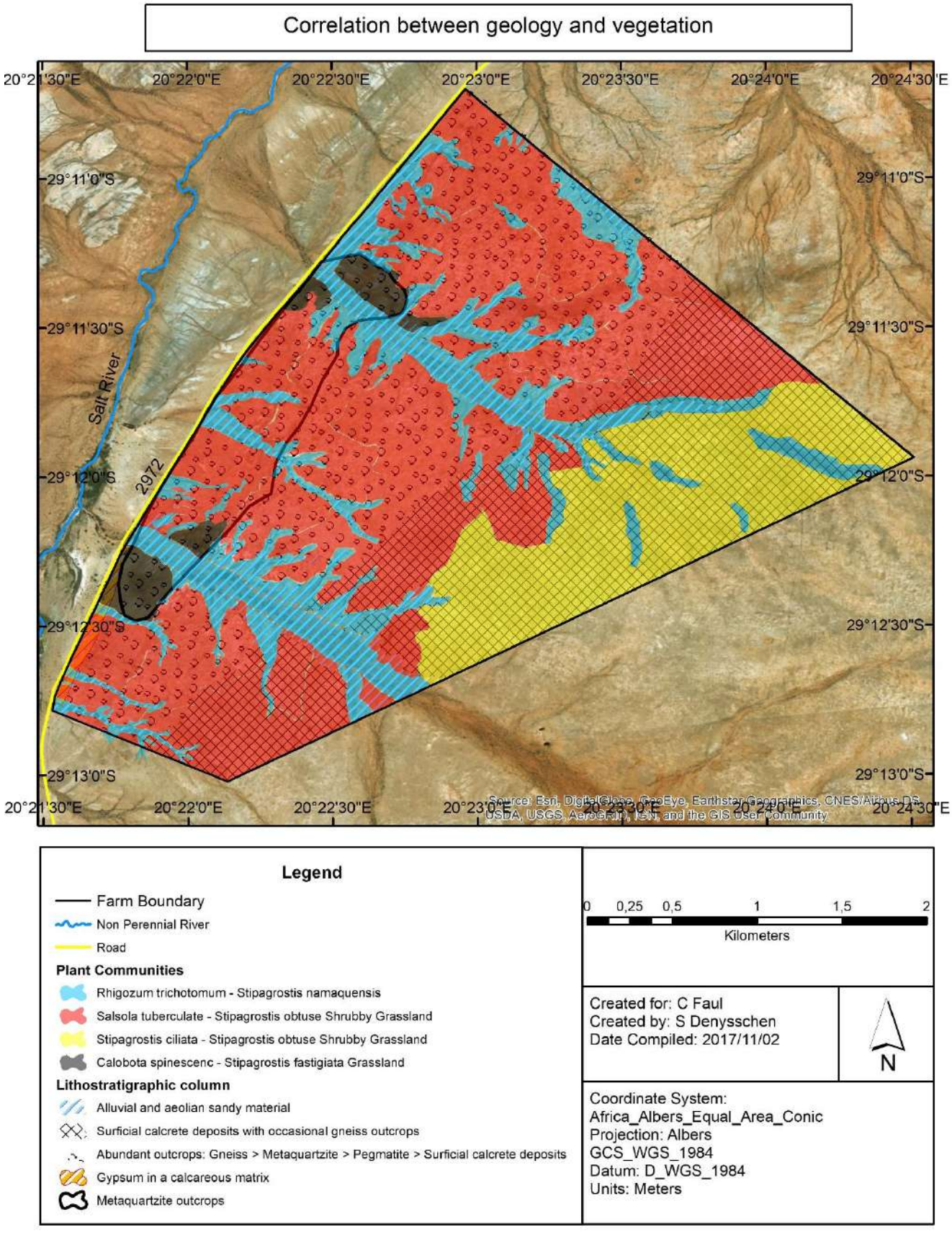

Figure 7-1: Correlation map indicating the relationship between the geological units and plant communities (Google Earth, 2016).

Table 7-1: Correlation matrix diagram illustrating the degree of correlation between the geological units and plant communities.

Correlations				
Geology	**Plant Communities**			
Gypsic Deposits	1	2	3.1	3.2
Alluvial and aeolian sandy material	1	2	3.1	3.2
Surficial calcrete deposits with occasional gneiss	1	2	3.1	3.2
Granitoids: Gneiss > metaquartzite > pegmatite	1	2	3.1	3.2
Metaquartzite outcrops	1	2	3.1	3.2

Degree of correlation
Excellent correlation
Good correlation
Poor correlation
No correlation

Plant Communities
1) *Rhigozum trichomum – Stipagrostis namaquensis* Shrubland
2) *Calobota spinescens – Stipagrostis fastigiata* Grassland
3) *Stipagrostis obtuse* Shrubby Grassland
3.1) *Stipagrostis ciliate – Stipagrostis obuse* Shrubby Grassland
3.2) *Salsola tuberculate – Stipagrostis obtuse* Shrubby Grassland

The *Rhigozum trichotomum – Stipagrostis namaquensis* Shrubland is strongly associated with drainage systems, therefore correlating with alluvial and aeolian sandy material. The *Calobota spinescens – Stipagrostis fastigiata* Grassland is strongly associated with the metaquartzite outcrops next to the north-western boundary of the study area. The *Stipagrostis ciliata – Stipagrostis obtusa* Shrubby Grassland occurs in the south-eastern segment of the study area, dominated by surficial calcrete deposits with occasional gneiss outcrops. The *Salsola tuberculata – Stipagrostis obtusa* Shrubby Grassland occurs in the north-western segment of the study area, consisting of granitoids associated with the gypsic and calcareous deposits.

7.1.2 Soil and Vegetation

According to Moore *et al.* (1993) environmental management is based on spatial predictions of soil-landscape processes. Tongway and Ludwig (1994) suggested that changes in soil properties accompany vegetation differences. Previous research was conducted on the correlations between soil attributes, terrain and environmental attributes, confirming that environmental information can be obtained with minimal field work at minimum cost (McKenzie & Austin, 1993; Moore *et al.*, 1993).

A total of ten soil forms and eleven soil families were identified accordingly. The identified soil forms include Dundee, Oakleaf, Augrabies, Knersvlakte, Oudtshoorn, Addo, Brandvlei, Coega, Etosha and Mispah (Soil Classification Working Group *et al.*, 1991). These soil forms are categorised into four individual soil groups known as silicic soils, calcic soils, cumulic soils and lithic soils. (Brummer, 2015; Fanourakis, 1991; Fey, 2010; IUSS Working Group WRB, 2006; Schmidhuber, 2015; Von M Harmse & Hatting, 1985).

Figure 7-2 illustrates the two-tier correlation between the soil forms and plant communities of the study area, while Table 7-2 visually illustrates the degree of correlation.

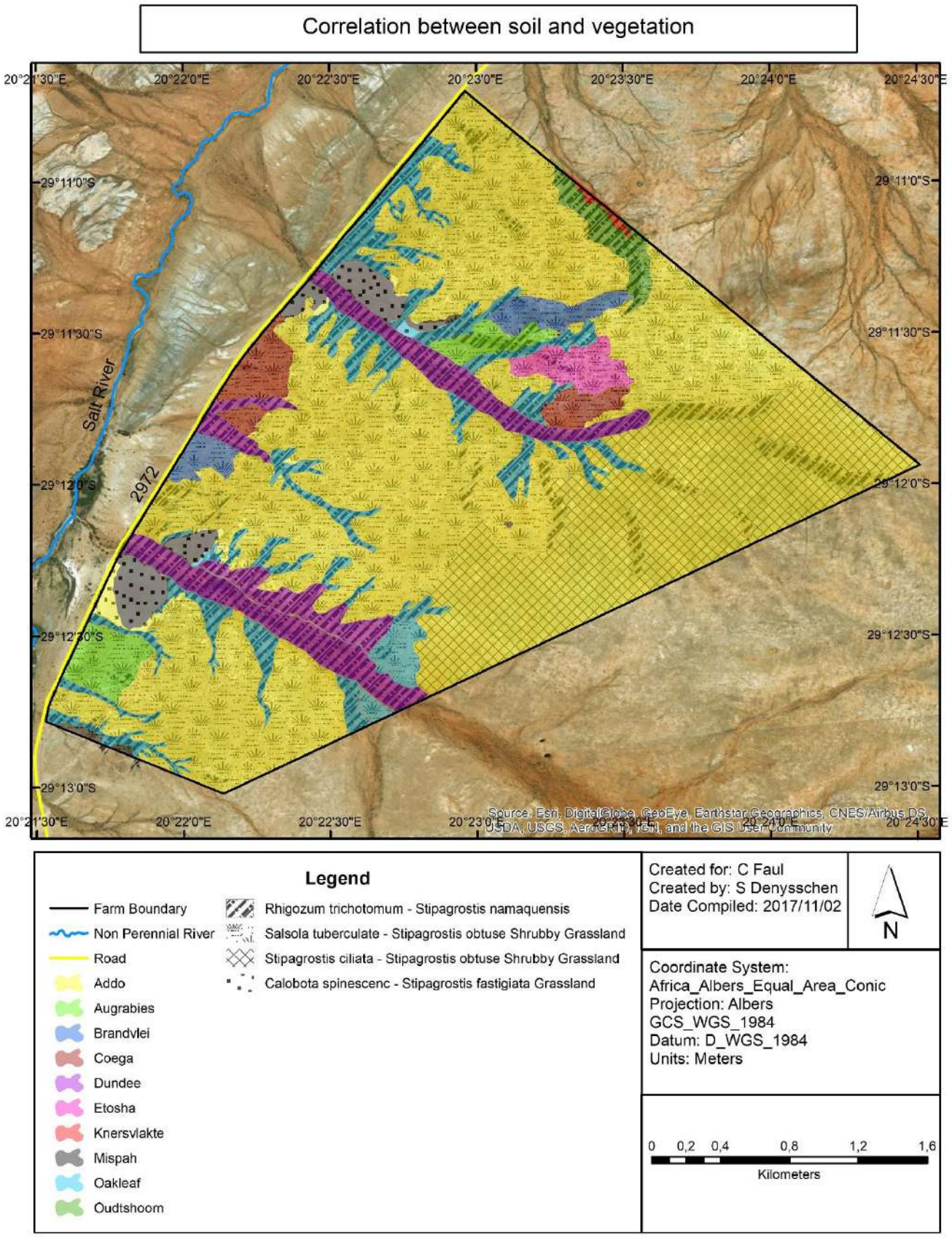

Figure 7-2: Correlation map indicating the relationship between the soil forms and plant communities (Google Earth, 2016).

Table 7-2: Correlation matrix illustrating the degree of correlation between soil forms and plant communities.

Correlations				
Soil Forms	**Plant Communities**			
Addo	1	2	3.1	3.2
Dundee	1	2	3.1	3.2
Oakleaf	1	2	3.1	3.2
Augrabies	1	2	3.1	3.2
Knersvlakte	1	2	3.1	3.2
Oudtshoorn	1	2	3.1	3.2
Brandvlei	1	2	3.1	3.2
Coega	1	2	3.1	3.2
Etosha	1	2	3.1	3.2
Mispah	1	2	3.1	3.2

Plant Communities
1) *Rhigozum trichomum – Stipagrostis namaquensis* Shrubland
2) *Calobota spinescens – Stipagrostis fastigiata* Grassland
3) *Stipagrostis obtuse* Shrubby Grassland
3.1) *Stipagrostis ciliate – Stipagrostis obuse* Shrubby Grassland
3.2) *Salsola tuberculate – Stipagrostis obtuse* Shrubby Grassland

Degree of correlation
Excellent correlation
Good correlation
Poor correlation
No correlation

A strong association between *Rhigozum trichotomum – Stipagrostis namaquensis* Shrubland and drainage systems were observed, therefore displaying an excellent correlation between this plant community and cumulic soils (Oakleaf and Dundee in this case) as well as silicic soils (Oudtshoorn and Knersvlakte). In some localities (associated with the palaeo drainage systems as described in the Chapter 4, Section 4.2.4.) this plant community also reveals a good correlation with calcic soils (Addo soil form). The *Calobota spinescens – Stipagrostis fastigiata* Grassland is strongly associated with lithic soils and in this case Mispah soil forms. The *Stipagrostis ciliata – Stipagrostis obtusa* Shrubby Grassland occurs in the south-eastern part of the study area, dominated by calcic soils (Addo soil form). The *Salsola tuberculata – Stipagrostis obtusa* Shrubby Grassland occurs in the north-western part of the study area and displays an excellent correlation with a variety of calcic soils (Brandvlei, Coega, Etosha and Addo soil forms) as well as cumulic soils (Augrabies soil form).

7.1.3 Geology and Soil

Geology can be described as an interdisciplinary field connected with disciplines including chemistry, physics, mathematics, biology, geography, meteorology, soil science, computer science and archaeology. Soil forms the intermedium between geology and vegetation and has a great influence on plant ecology and diversity. According to McDonald *et al.* (1996) and Shen *et al.* (2000) soil properties are highly dependent on environmental factors like geology, climate and topography.

Figure 7-3 illustrates the two-tier correlation between geological units and soil forms of the study area, and Table 7-3 visually illustrates the degree of correlation.

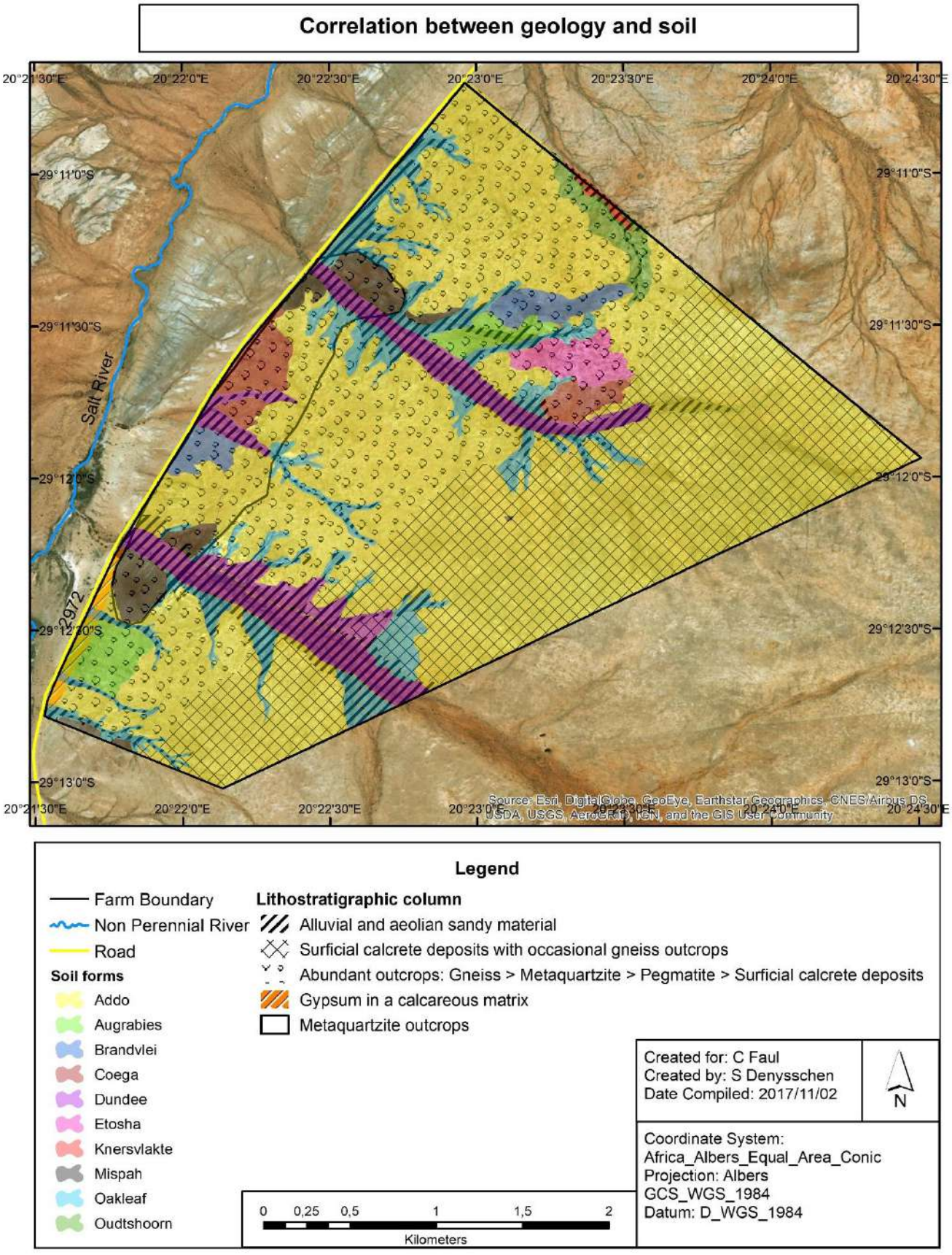

Figure 7-3: Correlation map indicating the relationship between the geological units and soil forms (Google Earth, 2016).

Table 7-3: Correlation matrix diagram illustrating the degree of correlation between geological units and soil forms.

Correlations										
Geology	**Soil Forms**									
Gypsic Deposits	Dundee	Oakleaf	Addo	Augrabies	Knersvlakte	Oudtshoorn	Brandvlei	Coega	Etosha	Mispah
Alluvial and aeolian sandy material	Dundee	Oakleaf	Addo	Augrabies	Knersvlakte	Oudtshoorn	Brandvlei	Coega	Etosha	Mispah
Surficial calcrete deposits with occasional gneiss	Dundee	Oakleaf	Addo	Augrabies	Knersvlakte	Oudtshoorn	Brandvlei	Coega	Etosha	Mispah
Granitoids: Gneiss > metaquartzite > pegmatite	Dundee	Oakleaf	Addo	Augrabies	Knersvlakte	Oudtshoorn	Brandvlei	Coega	Etosha	Mispah
Metaquatzite Outcrops	Dundee	Oakleaf	Addo	Augrabies	Knersvlakte	Oudtshoorn	Brandvlei	Coega	Etosha	Mispah

Degree of correlation
Excellent correlation
Good correlation
Poor correlation
No correlation

Alluvial and aeolian sandy material is strongly associated with drainage systems. The first order and second order drainage systems correlate with Oakleaf soil forms, whereas the third order drainage systems correlate with Dundee soil forms (cumulic soils). In the north-eastern segment of the study area, the drainage systems are associated with silicic soils (Knersvlakte and Oudtshoorn soil forms). Metaquartzite outcrops next to the north-western boundary of the study area display an excellent correlation with lithic soils (Mispah soil form). Gypsic deposits display an excellent correlation with cumulic soils (Augrabies soil form) and a good correlation with calcic soils (Addo soil form). An excellent correlation between surficial calcrete deposits with occasional gneiss outcrops and calcic soils (Addo soil form) were observed. The north-western segment of the study area consisting of granitoids are strongly associated with calcic soils (Addo, Etosha, Brandvlei, Coega soil forms) as well as cumulic soils (Augrabies soil form).

To conclude: Based on the results obtained with Method 1, Table 7-4 was constructed to illustrate the most prominent correlations between plant communities, soil forms and geological units.

Table 7-4: Most prominent correlations identified with Method 1.

Plant communities	Soil Forms	Geological Units
Rhigozum trichotomum – *Stipagrostis namaquensis* Shrubland	Dundee Oakleaf Knersvlakte Oudtshoorn	Alluvial and aeolian sandy material
Calobota spinescens – *Stipagrostis fastigiata* Grassland	Mispah	Metaquartzite Outcrops
Stipagrostis ciliata – *Stipagrostis obtusa* Shrubby Grassland	Addo	Surficial calcrete deposits with occasional gneiss outcrops.
Salsola tuberculata – *Stipagrostis obtusa* Shrubby Grassland	Augrabies Brandvlei Etosha Coega	Gypsic deposits Granitoids: Gneiss > metaquartzite > pegmatite

7.2 Method 2

The second method is based on the concept of areal interpolation (Maantay *et al.*, 2007), where the principles of a block count method is applied to identify and quantify three-tier correlation combinations. With the help of Method 2 a total of 988 intersection points was

examined and 19 three-tier correlation combinations were identified (consult Table 7-6, Figure 7-4 and Figure 7-5 for results). Table 7-5 illustrates the codes used to describe these combinations.

Table 7-5: Codes used for the description of three-tier correlation combination.

Plant Communities		**Soil Groups (Forms)**		**Geological Units**	
P1	*Rhigozum trichomum* – *Stipagrostis namaquensis* Shrubland	S1	Silicic (Oudtshoorn, Knersvlakte)	G1	Alluvial and aeolian sandy material.
P2	*Calobota spinescens* – *Stipagrostis fastigiata* Grassland	S2	Calcic (Etosha, Addo, Brandvlei, Coega)	G2	Surficial calcrete deposits with occasional gneiss outcrops.
P3	*Stipagrostis ciliata* – *Stipagrostis obtusa* Shrubby Grassland	S3	Cumulic (Oakleaf, Augrabies, Dundee)	G3	Granitoids: Gneiss > Metaquartzite > pegmatite.
P4	*Salsola tuberculata* – *Stipagrostis obtusa* Shrubby Grassland	S4	Lithic (Mispah)	G4	Metaquartzite.
				G5	Gypsic deposits.

Each intersection point represents 1.0 ha polygons. After recording all the combinations within the study area, the total representation percentages of each correlation were calculated.

The identified three-tier correlation combinations, together with the total surface coverage per combination are presented in Table 7-6, whereas Figure 7-4 and Figure 7-5 illustrate the percentage total surface occupied by each three-tier correlation combination.

Table 7-6: Three-tier correlation combinations (identified with Method 2) in association with the total surface coverage per combination.

Three-tier correlation combination	Total surface coverage per correlation (%)	Corresponding Plant Community	Corresponding Soil Group and Soil Form	Corresponding Geological Unit
P1S3G1	19.7	*Rhigozum trichotomum – Stipagrostis namaquensis* Shrubland	Cumulic (Oakleaf, Augrabies, Dundee)	Alluvial and aeolian sandy material.
P1S3G4	0.1	*Rhigozum trichotomum – Stipagrostis namaquensis* Shrubland	Cumulic (Oakleaf, Augrabies, Dundee)	Metaquartzite.
P1S2G3	0.3	*Rhigozum trichotomum – Stipagrostis namaquensis* Shrubland	Calcic (Etosha, Addo, Brandvlei, Coega)	Granitoids: Gneiss > Metaquartzite > pegmatite.
P1S3G5	0.1	*Rhigozum trichotomum – Stipagrostis namaquensis* Shrubland	Cumulic (Oakleaf, Augrabies, Dundee)	Gypsic deposits.
P1S1G3	0.6	*Rhigozum trichotomum – Stipagrostis namaquensis* Shrubland	Silicic (Oudtshoorn, Knersvlakte)	Granitoids: Gneiss > Metaquartzite > pegmatite.
P1S1G1	0.7	*Rhigozum trichotomum – Stipagrostis namaquensis* Shrubland	Silicic (Oudtshoorn, Knersvlakte)	Alluvial and aeolian sandy material.
P1S3G3	0.1	*Rhigozum trichotomum – Stipagrostis namaquensis* Shrubland	Cumulic (Oakleaf, Augrabies, Dundee)	Granitoids: Gneiss > Metaquartzite > pegmatite.
P1S2G2	2.1	*Rhigozum trichotomum – Stipagrostis namaquensis* Shrubland	Calcic (Etosha, Addo, Brandvlei, Coega)	Surficial calcrete deposits with occasional gneiss outcrops.
P1S2G4	0.3	*Rhigozum trichotomum – Stipagrostis namaquensis* Shrubland	Calcic (Etosha, Addo, Brandvlei, Coega)	Metaquartzite.
P4S2G3	29.2	*Salsola tuberculata – Stipagrostis obtusa* Shrubby Grassland	Calcic (Etosha, Addo, Brandvlei, Coega)	Granitoids: Gneiss > Metaquartzite > pegmatite.
P4S2G2	15.4	*Salsola tuberculata – Stipagrostis obtusa* Shrubby Grassland	Calcic (Etosha, Addo, Brandvlei, Coega)	Surficial calcrete deposits with occasional gneiss outcrops.
P4S2G4	6.1	*Salsola tuberculata – Stipagrostis obtusa* Shrubby Grassland	Calcic (Etosha, Addo, Brandvlei, Coega)	Metaquartzite.
P4S3G3	1.6	*Salsola tuberculata – Stipagrostis obtusa* Shrubby Grassland	Cumulic (Oakleaf, Augrabies, Dundee)	Granitoids: Gneiss > Metaquartzite > pegmatite.
P4S2G5	0.5	*Salsola tuberculata – Stipagrostis obtusa* Shrubby Grassland	Calcic (Etosha, Addo, Brandvlei, Coega)	Gypsic deposits.
P4S3G5	0.2	*Salsola tuberculata – Stipagrostis obtusa* Shrubby Grassland	Cumulic (Oakleaf, Augrabies, Dundee)	Gypsic deposits.
P4S4G4	0.2	*Salsola tuberculata – Stipagrostis obtusa* Shrubby Grassland	Lithic (Mispah)	Metaquartzite.
P2S4G4	0.6	*Calobota spinescens – Stipagrostis fastigiate* Grassland	Lithic (Mispah)	Metaquartzite.
P2S2G5	0.2	*Calobota spinescens – Stipagrostis fastigiate* Grassland	Calcic (Etosha, Addo, Brandvlei, Coega)	Gypsic deposits.
P3S2G2	19	*Stipagrostis ciliata – Stipagrostis obtusa* Shrubby Grassland	Calcic (Etosha, Addo, Brandvlei, Coega)	Surficial calcrete deposits with occasional gneiss outcrops.

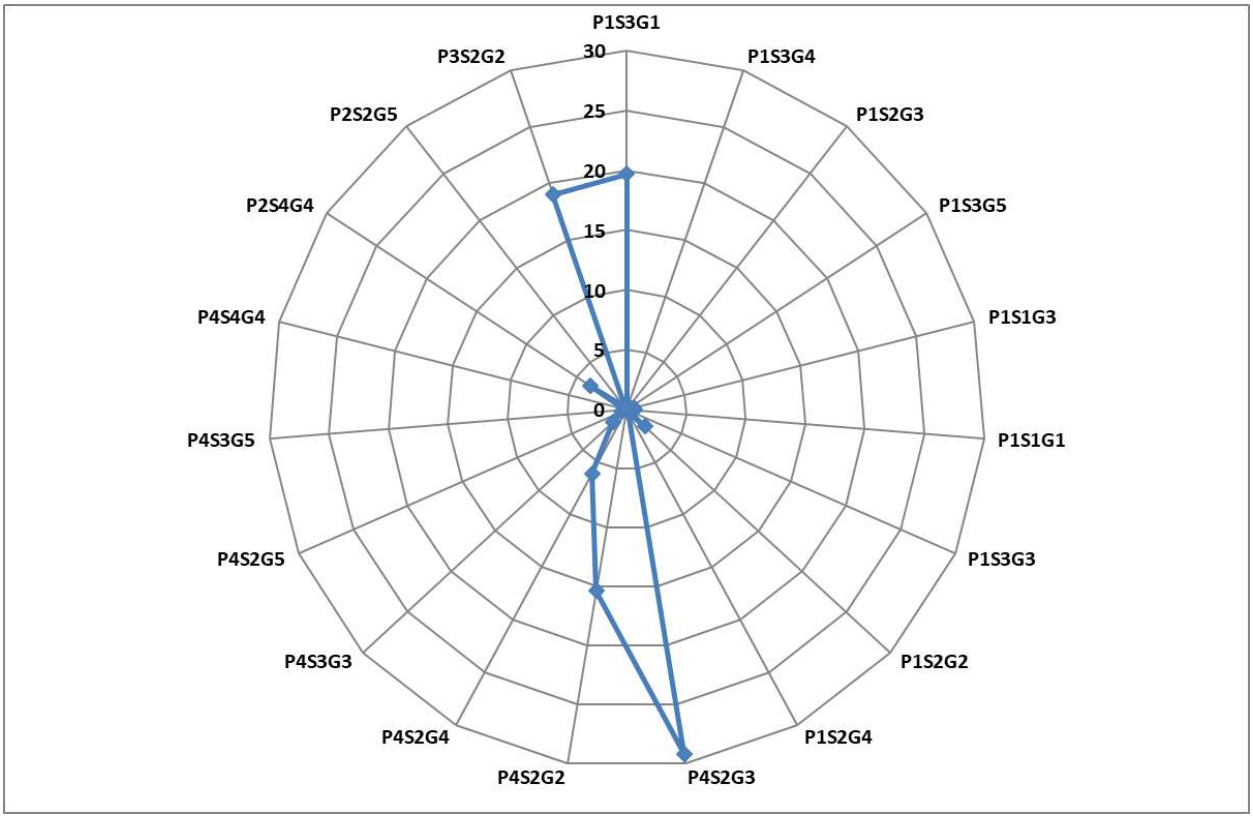

Figure 7-4: Total surface coverage per correlation.

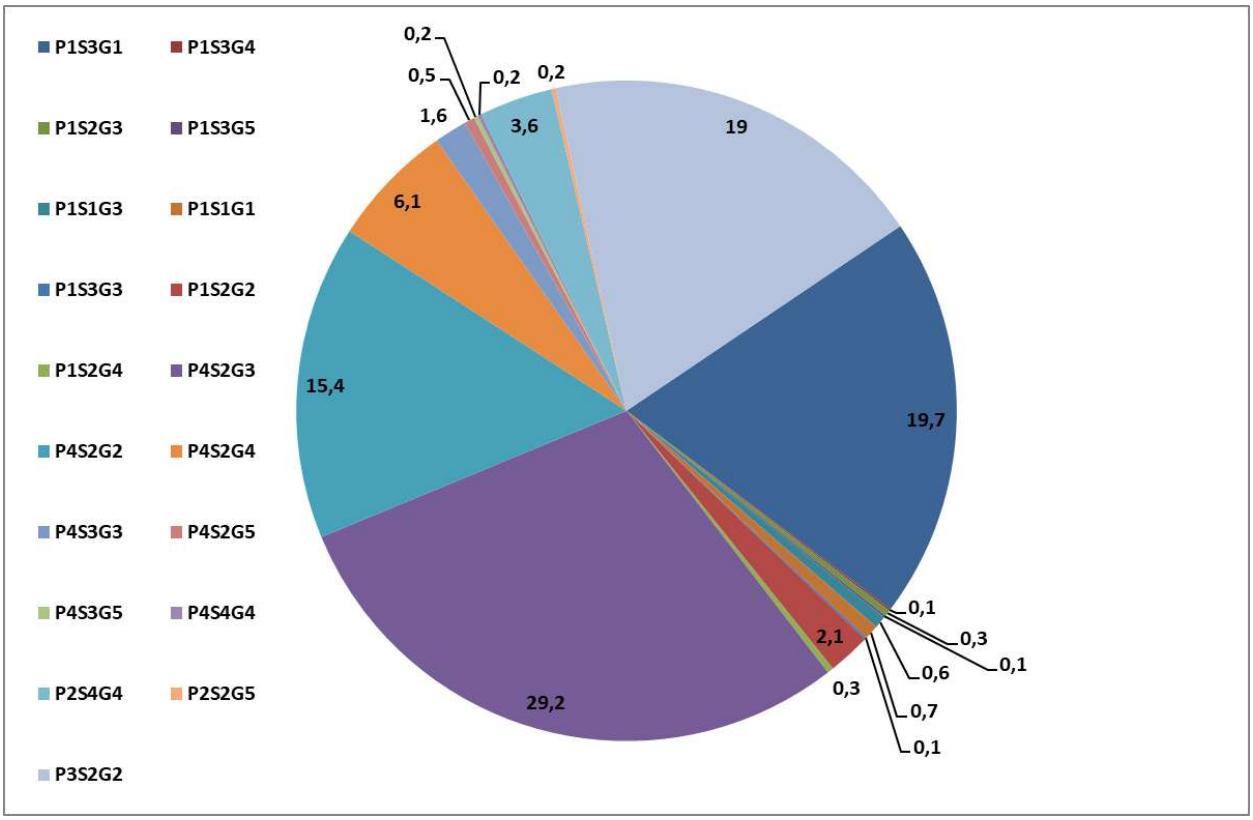

Figure 7-5: Total surface coverage per correlation.

Data presented in Figure 7-4 and Figure 7-5 confirmed that correlation combination P4S2G3 occupied the largest portion of the study area (29.2%), meaning that 29.2% of the study area consisted of granitoids with the abundancy of gneiss > metaquartzite > pegmatite, along with calcic soils dominated by *Salsola tuberculata* – *Stipagrostis obtusa* Shrubby Grassland.

The second largest combination (P1S3G1) occupied 19.7% of the study area and consisted of alluvial and aeolian sandy material, along with cumulic soils dominated by *Rhigozum trichomum* – *Stipagrostis namaquensis* Shrubland. This correlation combination is also recognised as typical drainage systems in the semi-arid Bushmanland regions of South Africa.

Occupying 19% of the study area, combination P3S2G2 were identified as the third largest correlation combination and consisted of surficial calcrete deposits with occasional gneiss outcrops. This area contains typical deeper calcic soils dominated by *Stipagrostis ciliata* – *Stipagrostis obtusa* Shrubby Grassland (grassland habitat).

Even though P4S2G3 is considered the largest correlation combination on this site, is does not mean that this correlation is the most significant. When the occurrence of correlation combinations is considered with respect to plant communities, P1 occurs in nine combinations, P4 in seven, P2 in two and P3 in one. Regarding soil forms S1 and S4 are considered most important as both occur in only two correlation combinations. With respect to geological units, G1 (two combinations) and G2 (three combinations) are considered most significant. Therefore, it can be assumed that correlation combinations P2S4G4 and P3S2G2 are considered most significant. In P2S4G4 both P2 and S4 are considered rare, whereas P3 and G2 are rare in the case of correlation combination P3S2G2.

To conclude: The most unique correlation combinations identified are the two-tier correlation between lithic soils (in this case Mispah soil form) and *Calobota spinescens* – *Stipagrostis fastigiata* Grassland as well as the two-tier correlation between surficial calcrete deposits with occasional gneiss outcrops and *Stipagrostis ciliata* – *Stipagrostis obtusa* Shrubby Grassland (identified with the help of Method 2). When comparing these plant communities with the corresponding vegetation habitats, both plant communities fall within the boundaries of the grassland habitat however differing in growth structure. *Calobota spinescens* – *Stipagrostis fastigiata* Grassland consists of a typical small vegetation structure and low density (but high frequency), whilst *Stipagrostis ciliata* – *Stipagrostis obtusa* Shrubby Grassland consists of a typical larger vegetation structure and high density (but low frequency).

CHAPTER 8

CONCLUSION

Predictive associations between quantitative environmental variables have been investigated in numerous studies (Odeh *et al.*, 1994; McKenzie & Austin, 1993). Spatial interpolation is esteemed for the prediction of variables at unsampled locations. Interpolation methods including co-kriging have been developed to estimate the characteristics of environmental variables by using secondary variables (Kalivas *et al.*, 2002). However, these predictive associations are not always comprehensible due to the influence of environmental variables fluctuating throughout space.

In its completeness, this study identified correlations between environmental variables (vegetation, soil and geology respectively) in the semi-arid Bushmanland region of South Africa, which can be used as a guideline in future research.

8.1 Main Findings

8.1.1 Vegetation identification, description and mapping

Based on the objectives of this study, plant communities and habitats were identified and classified accordingly to constructed maps for correlation purposes. The area consisted of three habitats identified as Grassland, Shrubby Grassland and Drainage Systems. All habitats were dominated by the grass family (Poaceae) however, differences in vegetation structure were observed. The Grassland had typical deeper soils (except in mapping unit J) with occasional geological outcrops, whereas the Shrubby Grassland contained occasional deep soils with more abundant geological outcrops and lag deposits. The Drainage Systems differed from consisting of only sediments to containing merely pegmatite outcrops.

Data analyses (refer to Figure 4-5) and additional field observations resulted in the identification of three plant communities and two sub-communities. The area was mainly occupied by *Stipagrostis obtusa* Shrubby Grassland, which was divided into two sub-communities, *Salsola tuberculata – Stipagrostis obtusa* Shrubby Grassland in the north-west and *Stipagrostis ciliata – Stipagrostis obtusa* Shrubby Grassland in the south-east. All the localities where Mispah soil forms were identified were associated with *Calobota spinescens – Stipagrostis fastigiata* Grassland. The drainage systems consisted of a unique species composition and were classified as *Rhigozum trichotomum – Stipagrostis namaquensis* Shrubland.

8.1.2 Soil identification, classification and mapping

To comply with the aims and objectives of this study, soils were identified and classified in order to construct a map based on soil forms and soil groups for correlation purposes. Chemical and physical analysis were conducted to indicate the differences between soil forms and to establish the relationship between these soil properties and specified correlations.

The soils from this area are typical dry arid soils of mixed origin (alluvial, aeolian, residual as well as pedogenic). The largest part of the area is occupied by calcic soils (Augrabies, Addo, Brandvlei, Coega and Etosha). Calcrete material dominates in most soils with a thickness limited to less than one meter. A-horizons are typically thin with signs of alluvial and aeolian transportations. In the north-western segment of the study area soils tend to become much shallower and in some areas gypsic deposits are visible. All the localities where Mispah soil forms were identified are associated with geological outcrops. Drainage systems on site were associated with Dundee and Oakleaf soil forms (cumulic soils) indicating depositional and in this case fluvial activities.

With respect to soil analyses no clear association between soil form and soil chemical analyses could be identified, however, a relationship between some chemical properties and topography were implied. Regarding soil physical properties a clear association appeared between soil form and particle size distribution, with Dundee and Oakleaf soil forms consisting of a more sandy texture, while calcic soils appeared loamy.

8.1.3 Geological identification, description and mapping

To comply with the aims and objectives of this study, geological outcrops were identified and mapped for correlation purposes. The north-western segment of the study area consists of granitoids with the following order of abundancy: Gneiss > metaquartzite > pegmatite > surficial calcrete deposits. The granitic gneisses are considered the oldest (1650 - 2050 Ma) lithostratigraphic unit (Cornell *et al.*, 2006; Reid *et al.*, 1997), whereas metaquartzites were deposited approximately 1130 – 1640 Ma ago (Bailie *et al.*, 2007; Colliston *et al.*, 2008; McClung, 2006). Surficial calcrete deposits with occasional gneiss outcrops dominate the south-eastern segment. These calcretes were deposited during the Cenozoic Era and are considered as relatively young (0 – 5 Ma) (Hurter, 2016; Watts, 1980). The drainage systems consist of alluvial and aeolian sandy material (0 – 1.6 Ma old), whereas gypsic deposits coexist with a calcareous mixture (1 – 0.01 Ma) (Von M Harmse & Hatting, 2012).

8.2 Correlations between vegetation, soil and geology

8.2.1 Method 1

Method 1 was used to construct correlation maps (overlay method) based on the trend-surface analysis method. After the construction of correlation maps, information obtained from these maps was used to construct correlation matrix diagrams in order to identify two-tier correlation combinations as well as the degree of correlation. Table 7-5 illustrates the most prominent correlations between plant communities, soil forms and geological units.

8.2.2 Method 2

Method 2 was based on the concept of areal interpolation (Maantay *et al.*, 2007), where the principles of a block count method was applied to identify and quantify three-tier correlation combinations. Method 2 investigated a total of 988 intersection points where 19 three-tier correlation combinations were identified (Table 7-6).

The most unique correlation combinations identified are the two-tier correlation between lithic soils (in this case Mispah soil form) and *Calobota spinescens – Stipagrostis fastigiata* Grassland as well as the two-tier correlation between surficial calcrete deposits with occasional gneiss outcrops and *Stipagrostis ciliata – Stipagrostis obtusa* Shrubby Grassland. When comparing these plant communities with corresponding vegetation habitats, both plant communities fall within the boundaries of the grassland habitat however differing in growth structure. *Calobota spinescens – Stipagrostis fastigiata* Grassland consists of a typical small vegetation structure and low density (but high frequency), whilst *Stipagrostis ciliata – Stipagrostis obtusa* Shrubby Grassland consists of a typical larger vegetation structure and high density (but low frequency).

To conclude: Correlations between vegetation, soil and geology in the semi-arid Bushmanland region of South Africa were confirmed during this study. A three-tier correlation between grassland vegetation, calcic soils and surficial calcrete deposits is typical for the semi-arid Bushmanland region. Drainage systems in this part of South Africa are associated with shrubs and grasses (in particular *Rhigozum trichotomum* which dominates these areas) as well as cumulic soils.

Environmental correlations can be used for spatial prediction if environmental variables are limited to a minimum. It is also important to note that the correlation strength between the variables under investigation, will determine the success of environmental correlation.

8.3 Recommendations for future research

During the course of this project, some valuable observations were made that requires further research to be resolved:

- Better understanding and in-depth investigation of the geology of the Bushmanland Terrane.
- Characterisation of the properties that governs the identified correlations.
- Investigation regarding the contribution of climate to the specific vegetation and soil formation processes in the semi-arid Bushmanland.
- The interactive development of predictive models for spatial prediction, with respect to vegetation, soil and geology in the semi-arid Bushmanland region of South Africa.

REFFERENCES

Abbott, T. S. 1989. BCRI soil testing methods and interpretation. Rydalmere: NSW Agriculture and Fisheries.

Acocks, J.P.H. 1953. Veld Types of South Africa. 1st ed. *Memoirs of the Botanical Survey of South Africa,* 28: 1-192.

AGIS. 2007. Agricultural Geo-Referenced Information System. www.agis.agric.za Date of access: 10 June 2017.

Agterberg, F.P. 1964. Methods of trend surface analysis. *Colorado School of Mines Quarterly,* 59: 111-130.

Anderson, M.J. 2001. A new method for non-parametric multivariate analysis of variance. *Austral Ecology*, 26(1): 32 – 46.

Austin, M.P. 1982. Use of relative physiological performance value in the prediction of performance in multispecies mixtures from monoculture performance. *Journal of Ecology,* 70: 559-570.

Austin, M.P. 2002. Spatial prediction of species distribution: An interface between ecological theory and statistical modelling. *Ecological Modelling,* 157(2-3): 101-118.

Badgley, C. & Fox, D.L. 2000. Ecological biogeography of North American mammals: Species density and ecological structure in relation to environmental gradients. *Journal of Biogeography,* 27: 1437-1467.

Bailie, R., Armstrong, R. & Reid, D. 2007. The Bushmanland Group supracrustal succession, Aggeneys, Bushmanland, South Africa: Provenance, age of deposition and metamorphism. *South African Journal of Geology,* 110: 59-86.

Beckedahl, H.R., Bowyer-Bower, T.A.S., Dardis, G.F. & Hanvey, P.M. 1988. Geomorphic Effects of Soil Erosion. (*In* Moon, B.P. & Dardis, G.F. *eds.* The Geomorphology of Southern Africa. Johannesburg: Southern Book Publishers. p. 249-276).

Bennie, J., Huntleya, B., Wiltshirea, A., Hill, M.O. & Baxtera, R. 2008. Slope, aspect and climate: Spatially explicit and implicit models of topographic microclimate in chalk grassland. *Ecological Modelling,* 216: 47-59.

Bezuidenhout, H. 2009. The classification, mapping and description of the vegetation of the Rooipoort Nature Reserve, Northern Cape, South Africa. *Koedoe,* 51(1): 69-79.

Billings, W.D. 1950. Vegetation and plant growth as affected by chemical altered rocks in the Western Great Basin. *Ecology,* 31(1): 62-74.

Bini, L.M., Diniz-Filho, J.A.E., Bonfim, E.S. & Bastos, R.P. 2000. Local and regional species richness relationships in viperid snake assemblages from South America: unsaturated patterns at three different spatial scales. *Copeia*, 2000: 799-805.

Birkeland, P.W. 1984. Soils and Geomorphology. 3rd ed. New York: Oxford University Press.

Boelema, R. 1994. The metallogeny of the Upington and Kenhardt area, Northern Cape. Grahamstown: Rhodes University. (Dissertation – MSc).

Boggs, S. 2011. Principles of Sedimentology and Stratigraphy. 5th ed. USA: Pearson.

Botha, M., Siebert, S.J. & Van der Berg, J. 2016. Do arthropod assemblages fit the grassland and savanna biomes of South Africa? *Journal of Science*, 112(9/10):1-10.

Boyle, A.P., McCarthy, P.M. & Stewart, D. 1987. Geochemical control of saxicolous lichen communities on the Creggaun Gabbro, Letterfrack, Co. Galway, Western Ireland. *Lichenologist,* 19: 307-317.

Brink, A.B.A. 1985. Engineering Geology of Southern Africa. 4th ed. Pretoria: Building Publications.

Brummer, R.A. 2015. Geotechnical Properties of Pedological Soils (Volume 2). Potchefstroom: North-West University. (Mini-Dissertation - Honours).

Burke, I.C., Reiners, W.A. & Olson, R.K. 1989. Topographic control of vegetation in a mountain big sagebrush steppe. *Vegetation,* 84: 77-86.

Burns, C.E., Collins, S.L. & Smith, M.D. 2009. Plant community response to loss of large herbivores: comparing consequences in a South African and a North American grassland. Biodiversity Conservation, 18: 2327-2342.

Callaway, P.M. 1995. Positive interactions among plants. *The Botanical Review,* 61: 306-349.

Center for Brains, Minds and Machines. 2017. AAAI Spring Symposium Series. Science of Intelligence: Computational principles of natural artificial intelligence. California: Stanford University.

Chayes, F. & Suzuki, Y. 1973. Geological contours and trend surfaces: A discussion. *Journal Petrology,* 4: 307-312.

Chen, X.Y., Lintern, M.J. & Roach, I.C. 2002. Calcrete: characteristics, distribution and use in mineral exploration. Kensington: Cooperative Research Centre for Landscape Environments and Mineral Exploration.

Clarke, K.R. 1993. Non-parametric multivariate analyses of changes in community structure. *Austral Ecology,* 18(1): 117-143.

Clarke, K.R. & Warwick, R.M. 2001. Changes in marine communities: An approach to statistical analysis and interpretation. 2nd Edition. Plymouth: PRIMER-E Ltd.

Clarke, K.R. & Gorley, R.N. 2015. PRIMER v7: User Manual/Tutorial. Plymouth: PRIMER-E Ltd.

Cliff, A.D. & Ord, J.K. 1973. Spatial Autocorrelation. London: Pion Press.

Coblentz, D. & Keating, P.L. 2008. Topographic controls on the distribution of tree islands in the high Andes of south-Western Ecuado. *Journal of Biogeography,* 35: 2026-2038.

Coblentz, D. & Ritters, K.H. 2004. Topographic controls on the regional-scale biodiversity of the south-western USA. *Journal of Biogeography,* 31: 1125-1138.

Cody, M.L. 1989. Growth-form diversity and community structure in desert plants. *Journal of Arid Environments,* 17: 199-209.

Colliston. W.P., Schoch, A.E. & Praekelt, H.E. 2008. Comments on the papers by Bailie *et al.* concerning the age and deposition of the Bushmanland Group (SAJG 110, 59-86) and single zircon ages of the Aggeneys Granite Suite (SAJG 110, 87-110). *South African Journal of Geology,* 111: 133-135.

Connell, J.H. 1983. On the prevalence and relative importance of interspecific competition: Evidence from field experiments. *American Naturalist*, 122: 661-696.

Cornell, D.H., Pettersson, A., Whitehouse, M.J. & Schersten, A. 2009. A new chronostratigraphic paradigm for the age and tectonic history of the Mesoproterozoic Bushmanland Ore District, South Africa. *Economic Geology,* 104(3): 385-404.

Cornell, D.H., Thomas, R.J., Moen, H.F.G., Reid, D.L., Moore, J.M. & Gibson, R.L. 2006. The Namaqua-Natal Province (*In* Johnson, M.R., Anhaeusser, C.R. & Thomas, R.J. *eds*. The Geology of South Africa. Johannesburg: Geological Society of South Africa & Pretoria: Council for Geoscience. p. 325-380).

Cottle, R. 2004. Linking Geology and Biodiversity (*In* Cottle, R. *ed.* English Nature Research Reports. Report Number 562. Peterborough, United Kingdom: English Nature).

Cowling, R.M. & Roux, P.W. 1987. The karoo biome: A preliminary synthesis. Part 2 – vegetation and history. Pretoria: Foundation for Research Development.

Daniell, A. 2014. Geochemical monitoring of soil pollution from the MWS-5 gold tailings facility on the farm Stilfontein. Potchefstroom: North-West University. (Dissertation-MSc).

De Martonne, E. 1926. Une nouvelle fontion climatologique: L. indice daridite. La Meteorogie [Translated]. p. 449-458.

Dengler, J., Becker, T., Ruprecht, E., Szabó, A., Becker, U., Beldean, M., Bita-Nicolae, C., Dolnik, C., Gola, I., Peyrat, J., Sutcliffe, L.M.E., Turtureanu, P.D. & Ugurlu, E. 2012. *Festuco-Brometea* communities of the Transylvanian Plateau (Romania) – a preliminary overview on syntaxonomy, ecology, and biodiversity. *Tuexenia*, 32: 319-359.

Department of Environmental Affairs. 2014. Portal Mapping and Analysis Platform: Renewable Energy Applications. Updated 09/02/2018. https://dea.maps.arcgis.com/home/webmap/viewer.html?webmap=5b9c50949be74387a13400d9c283d782. Date of access: 8 April 2018.

Department of Public Works. 2007. Identification of problematic soils in Southern Africa: Technical Notes for civil and structural engineers. PW 2006/1.

Diniz-Filho, J.A.F., Bini, L.M. & Hawkins, B.A. 2003. Spatial autocorrelation and red herrings in geographical ecology. *Global Ecology & Biogeography,* 12: 53-64.

Driver, M., Raimondo, D., Maze, K., Pfab, M.F. & Helme, N.A. 2009. Applications of the Red List for conservation practitioners. (*In* Raimondo, D., Von Staden, L., Foden, W., Victor, J.E., Helme, N.A., Turner, R.C., Kamundi, D.A. & Manyama, P.A., *eds.* Red List of South African Plants. Strelitzia 25. Pretoria: South African National Biodiversity Institute. p.41-52).

Dúbravková, D., Chytrý, M., Willner, W., Illyés, E., Janišová, M. & Kállayné Szerényi, J. 2010. Dry grasslands in the Western Carpathians and the northern Pannonian Basin: A numerical classification. *Preslia,* 82: 162-221.

Eggleton, R.A. & Banfield, J.F. 1985. The alteration of granitic biotite to chlorite. *American Mineralogist,* 70: 902-910.

Eglington, B.M. 2006. Evolution of the Namaqua-Natal Belt, southern Africa – A geochronological and isotope geochemical review. *Journal of African Earth Sciences*, 46: 93-111.

Eicher, C.L. & Brewer, C.A. 2001. Dasymetric mapping and areal interpolation: Implementation and Evaluation. *Geographic Information Science,* 28(2): 125-138.

Ellis, J.E. & Swift, D.M. 1988. Stability of African pastoral systems: Alternate paradigms and implications for development. *Journal of Range Management*, 41: 450-459.

Emerson, W.W. & Bakker, A.C. 1973. The comparative effects of exchangeable calcium, magnesium and sodium on some physical properties of aggregates from subsoils of red-brown earths. 2nd ed. *Australian Journal of Soil Research*, 11: 151–157.

Environmental Systems Research Institute. 2013. ArcGIS: Release 10.2. California: Redlands.

Esler, K.J. & Cowling, R.M. 1993. Edaphic factors and competition as determinants of pattern in South Africa Karoo vegetation. *South African Journal of Botany,* 59: 287-295.

Fanourakis, G.C. 1991. Engineering soil properties from pedological data. Johannesburg: Technicon Witwatersrand. (Thesis - PhD).

Fertilizer Society of South Africa. 2007. FSSA Fertilizer Handbook. 7th ed. Lynnwoodrif, SA: MVSA.

Fey, M. 2010. Soils of South Africa. Cape Town: Cambridge University Press.

Fish, L., Mashau, A.C., Moeaha, M.J. & Nembudani, M.T. 2015. Identification guide to southern African grasses: An identification manual with keys, descriptions and distribution. Sterlitzia 36. Pretoria: South African National Biodiversity Institute.

Fisher, P. & Longford, M. 1996. Modeling sensitivity to accuracy in classified imagery: A study of areal interpolation by dasymetric mapping. *Professional Geographer,* 48(3): 299-309.

Flowerdew, R. & Green, M. 1992. Development in areal interpolation methods and GIS. *Annuals of Regional Science,* 26: 67-78.

Fowler, N. 1986 The role of competition in plant communities in arid and semiarid regions. *Annual Review of Ecology and Systematics*, 17: 89-110.

Fox, J.W., McGrady-Steed, J. & Petchey, O.L. 2000. Testing for local species saturation with nonindependent regional species pools. *Ecology Letters*, 3: 198-206.

Frenkel, H., Goertzen, J.O. & Rhoades, J.D. 1978. Effects of clay type and content, exchangeable sodium percentage, and electrolyte concentration on clay dispersion and soil hydraulic conductivity. *Soil Science Society of America Journal,* 42: 32-39.

Geringer, G.J., Botha, B.J.V., Pretorius, J.J. & Ludick, D.J. 1986. Calc-alkaline volcanism along the eastern margin of the Namaqua Mobile Belt, South Africa – a possible middle Proterozoic volcanic arc. *Precambrian Research*, 33: 139-170.

Germishuizen, G. & Meyer, N.L. 2003. Plants of southern Africa: an annotated checklist. Strelitzia 14. Pretoria: National Botanical Institute.

Goldberg, D.E. & Barton, A.M. 1992. Patterns and consequences of interspecific competition in natural communities: A review of field experiments with plants. *American Naturalist*, 139: 771-801.

Goldberg, D.E. & Novoplansky, A. 1997. On the relative importance of competition in unproductive environments. *Journal of Ecology*, 85: 409-418.

Goldberg, D.E., Rajaniemi, T., Gurevitch, J. & Stewart, O.A. 1999. Empirical approaches to quantifying interaction intensity: competition and facilitation along productivity gradients. *Ecology*, 80: 1118-1131.

Goldich, S.S. 1938. A study in rock-weathering. *Journal of Geology*, 46 (1): 17-58.

Goodchild, M. & Lam, N. 1980. Areal interpolation: A variant of the traditional spatial problem. *Geo-processing,* 1: 297-312.

Google Earth. 2016. Kakamas – Remainder of portion 4 of the farm Brypaal no. 134. 29°11'56.41" S, 20°22'55.84" E. elevation 865 m and Imagery Date 12/14/2015. http://www.google.com/earth/index.html. Date of access: 30 June 2017.

Greenwood,J.J.D. & Robinson, R.A. 2006. Principles of sampling. (*In* Sutherland, W.J. *ed.* Ecological census techniques: A handbook. 2nd ed. Cambridge: Cambridge University Press. p.11-86).

Griffith, D.A. 1987. Spatial autocorrelation: A Primer. Washington DC: Resource publications in geography. Association of American Geographers.

Griffith, J., Stehman, S.V., Loveland, T.R. 2003. Landscape trends in Mid-Atlantic and Southeastern United States ecoregions. *Environmental Management,* 32: 572-588.

Grime, J.P. 1979. Plant strategies and vegetation processes. New York: John Wiley and Sons.

Guisan, A., & Zimmerman, N.E. 2000. Predictive habitat distribution models in ecology. *Ecological Modelling*, 135: 147-186.

Haddon, I.G. 2005. The sub-Kalahari geology and tectonic evolution of the Kalahari Basin. Johannesburg: University of Witwatersrand. (Thesis – PhD).

Hammer, Ø., Harper, D.A.T. & Ryan, P.D. 2001. PAST: Paleontological Statistics software package for education and data analysis. *Palaeontologia Electronica,* 4(1):1-9. http://palaeo.electronica.org/2001_1/past/issue1_01.htm. Date of access: 15 September 2017.

Hartnady, C.J.H., Joubert, P. & Stowe, C.W. 1985. Proterozoic crustal evolution in southwestern Africa. *Episodes*, 8: 236-244.

Hazelton, P. & Murphy, B. 2007. Interpreting soil test results: What do all the numbers mean? 2nd ed. Collingwood, Australia: CSIRO Publishing.

Hill, D., Fasham, M., Tucker, G., Shewry, M. & Shaw, P. 2005. Handbook of biodiversity methods: Survey, evaluation and monitoring. Cambridge: Cambridge University Press.

Hillel, D. 2004. Introduction to Environmental Soil Physics. Oxford: Elsevier.

Hofer, G., Wagner, H.H., Herzog, F. & Edwards, P.J. 2008. Effects of topographic variability on the scaling of plant species richness in gradient dominated landscapes. *Ecography,* 31: 131-139.

Holland, S.M. 2008. Non-metric multidimensional scaling (MDS). Athens: Department of Geology, University of Georgia.

Hooper, D.U. & Vitousek, P.M. 1997. The effects of plant composition and diversity on ecosystem processes. *Science*, 277: 1302-1305.

Hurter, B. 2016. Cenozoic deposits of South Africa. Potchefstroom: North-West University. (Dissertation – MSc).

Huston, M.A. 1979. A general hypothesis of species diversity. *American Naturalist,* 113: 81-101.

Huston, M.A. 1980. Soil nutrients and tree species richness in Costa Rican forests. *Journal of Biogeography,* 7: 147-157.

IUSS Working Group WRB. 2006. World Reference Base for Soil Resources 2nd ed. World Soil Resources Report 103. Rome: FAO.

Jarvis, S.C. & Pigott, C.D. 1973. Mineral nutrition of Lychnis viscaria. *New Phytologist*, 72: 1047-1055.

Jarvis, S.C. 1974. Soil factors affecting the distribution of plant communities on the cliffs of Craig Breidden, Montgomeryshire. *Journal of Ecology,* 62(3): 721-733.

Jenny, H. 1941. The Factors of Soil Formation. New York: McGraw-Hill.

Joubert, P. 1974. The gneisses of Namaqualand and their deformation. *Geological Society of South Africa*, 77: 339-345.

Joubert, P. 1981. The Namaqualand Metamorphic Complex (*In* Hunter, D.R. *ed.* Precambrian of the Southern Hemisphere. Amsterdam: Elservier. p. 687-705).

Joubert P. 1986. The Namaqualand Metamorphic Complex - A summary in Mineral Deposits of Southern Africa. *Geological Society of South Africa*, 1&2: 1395-1420.

Kalivas, D.P., Triantakonstantis, D.P. & Kollias, V.J. 2002. Spatial prediction of two soil properties using topographic information. *Global Nest Journal,* 4(1): 41-49.

Kent, M. 2012. Vegetation Description and Data Analysis: A Practical Approach. 2nd ed. Chichester: Wiley-Blackwell.

Khadkikar, A.S., Merh, S.S., Malik, J.N., Chamyal, L.S. 1998. Calcretes in semi-arid alluvial systems: formative pathways and sinks. *Sedimentary Geology*, 116: 251-260.

Knight, R.S., Crowe, T.M. & Seigfried, W.R. 1982. Distribution and species richness of trees in southern Africa. *Journal of South African Botany,* 48: 455-480.

Koenig, W.D. 1998. Spatial autocorrelation in California land birds. *Conservation Biology,* 12: 612-620.

Koenig, W.D. 1999. Spatial autocorrelation of ecological phenomena. *Trends in Ecology and Evolution,* 14: 22-26.

Körner, C.H. 2000. Biosphere responses to CO_2 enrichment. *Ecological Applications*, 10: 1590-1619.

Kruckeberg, A. 2002. Geology and plant life. Seattle: University of Washington Press.

Kruger, W.A.J. 2017. The petrogenesis of the Winddam, Koedoesfontein, and Rietfontein intrusions, Vredefort Dome, South Africa. Potchefstroom: North-West University. (Dissertation – MSc).

Laker, M.C. 2004. Advances in soil erosion, soil conservation, land suitability evaluation and land use planning research in South Africa (1978 – 2003). *South African Journal of Plant and Soil,* 21(5): 345-368.

Lancaster, N. 1979. Quaternary environments in the arid zone of southern Africa. Environmental Studies, Occasional Paper No. 22. Johannesburg: Department of Geography and Environmental Studies, University of the Witwatersrand.

Land Type Survey Staff. 1991. A procedure for describing soil profiles. SIRI Report Number GB/A/91/67. Pretoria: Soil and Irrigation Research Institute.

Land Type Survey Staff. 2003. Land types of the map 2920 Kenhardt. *Memoirs on the Agricultural Natural Resources of South Africa*, 29.

Langford, M., Maguire, D.J. & Unwin, D.J. 1991. The areal interpolation problem: Estimating population using remote sensing in a GIS framework. (*In* Masser, I. & Blakemore, M.B. *eds.* Handling geographic information. Essex, United Kingdom: Longman Scientific and Technical. p. 55-77).

Lavers, C. & Field, R. 2006. A resource-based conceptual model of plant diversity that reassesses causality in the productivity-diversity relationship. *Global Ecology and Biogeography,* 15: 213-224.

Leduc, A., Drapeau, P., Bergeron, Y. & Legendre, P. 1992. Study of spatial components of forest cover using partial mantel tests and path-analysis. *Journal of Vegetation Science*, 3: 69-78.

Leerder, M.R. 1982. Sedimentology: Processes and Product. London: George Allen & Unwin.

Legendre, P. 1993. Spatial autocorrelation: Trouble or new paradigm? *Ecology,* 74(6): 1659-1673.

Lichstein, J.W., Simons, T.R., Shriner, S.A. & Franzreb, K.E. 2002. Spatial autocorrelation and autoregressive models in ecology. *Ecological Monographs,* 72(3): 445-463.

Liebhold, A.M., Rossi, R.E. & Kemp. W.P. 1993. Geostatistics and geographic information systems in applied insect ecology. *Annual Review Entomology,* 38: 303-327.

Linder, H.P. 2003. The radiation of the Cape flora, southern Africa. *Biological Review,* 78: 597-638.

Loveland, T.R., Sohl, T.L., Stehman, S.V., Gallant, A.L., Sayler, K.L. & Napton, D.E. 2002. A strategy for estimating the rates of recent United States land-cover changes. *Photogrammetric Engineering & Remote Sensing,* 68: 1091-1099.

Lundqvist, J. 1968. Plant cover and environment of steep hillsides in Pite Lappmark. Sweden: Almqvist and Wiksells Boktryckeri AB.

Maantay, J.A., Maroko, A.R. & Herrmann, C. 2007. Mapping Population Distribution in the Urban Environment: The Cadastral-based Expert Dasymetric System (CEDS). *Cartography and Geographic Information Science,* 34(2): 77-102.

Mabbutt, J.A. 1977. Desert Landforms. Cambridge: The MIT Press. p. 340.

MacVicar, C.N., De Villiers, J.M., Loxton, R.F., Verster, E., Lambrechts, J.J.N., Merryweather, F.R., Le Roux, J., Van Rooyen, T.H. & Von M Harmse, H.J. 1977. Soil Classification. A binomial system for South Africa. Pretoria: Department of Agriculture and Technical Services.

Malos, C.V. 2011. Correlations between geology, geomorphologic processes and rare plant species status in the Transylvanian Basin. Romania: Babes-Bolyai University. (Thesis – PhD).

Marschner, H. 1986. Mineral nutrition of higher plants. London: Academic Press.

Maud, R. 2012. Macroscale Geomorphic Evolution. (*In* Holmes, P. & Meadows, M. *eds.* Southern Africa Geomorphology, New trends and new directions. Bloemfontein: Sun Press. p. 7-21).

McCarthy, T. & Rubidge, B. 2005. The story of earth and life: A South African perspective on 4.6 billion-year journey. Cape Town: Hirt and Carter Cape. p. 333.

McClung, C.R. 2006. Basin analysis of the Bushmanland Group, Namaqualand Metamorphic Complex of the Northern Cape Province, South Africa. Johannesburg: University of Johannesburg. (Thesis – PhD).

McCune, B. & Kean, D. 2002. Equations for potential annual direct incident radiation and heat load. *Journal of Vegetation Science,* 13: 603-606.

McDonald, D.J., Cowling, R.M. & Boucher, C. 1996. Vegetation: Environment relationships on a species rich coastal mountain range in the fynbos biome. *Plant Ecology,* 123: 165-182.

McKenzie, N.J. & Austin, M.P. 1993. A quantitative Australian approach to medium and small scale surveys based on soil stratigraphy and environmental correlation. *Geoderma,* 57: 329-355.

Metson, A.J. 1961. Methods of chemical analysis for soil samples. Soil Bureau Bulletin No. 12. Wellington, New Zealand: Department of Scientific and Industrial Research. p. 168-175.

Michálková, D. 2007. Diversity of dry grasslands in the Považský Inovec Mts (Slovakia) – a numerical analysis. *Hacquetia,* 6: 61-76.

Mitchell, C.W. 1977. Terrain Evaluation: An introductory handbook to the history, principles and methods of practical terrain assessment. London: Longman Group Limited.

Moen, H.F.G. 2007. The Geology of the Upington Area. Pretoria: Council of Geoscience.

Mooney, H.A. 1966. Influence of soil type on the distribution of two closely related species of Erigeron. *Ecology,* 47: 950-958.

Moore, I.D., Gessler, P.E., Nielsen, G.A. & Petersen, G.A. 1993. Soil attribute prediction using terrain analysis. *Soil Science Society of America Journal,* 57: 443-452.

Moore, J.M., Watkeys, M.K. & Reid, D.L. 1990. The regional setting of the Aggeneys/Gamsberg base metal deposits, Namaqualand, South Africa. (*In* Spry, P.G. & Bryndzia, L.T. *eds.* Regional Metamorphism of Ore Deposits and Genetic Implications. Utrecht: VSP Publishers. p. 77-95).

Morin, J., Benyamini, Y. & Michaeli, A. 1981. The dynamics of soil crusting by rainfall impact and the water movement in the soil profile. *Journal of Hydrology,* 52: 321-335.

Morrison, M.L., Marcot, B.G. & Mannan, R.W. 1992. Wildlife habitat relationships: Concepts and applications. Madison: University of Wisconsin Press.

Mucina, L., Rutherford, M.C., Palmer, A.R., Milton, S.J., Scott, L., Lloyd, J.W., Van Der Merwe, B., Hoare, D.B., Bezuidenhout, H., Vlok, J.H.J., Euston-Brown, D.I.W., Powrie, L.W. & Dold, A.P. 2006. Nama-Karoo Biome. (*In* Mucina, L. & Rutherford, M.C., *eds*. The Vegetation of South Africa, Lesotho, and Swaziland. Strelitzia 19. Pretoria: South African National Biodiversity Institute. p. 325-347).

Mueller-Dombois, D. 1984. Classification and Mapping of Plant Communities: A review with Emphasis on Tropical Vegetation. (*In* Woodwel, G.M. *ed*. The role of terrestrial vegetation in the global carbon cycle: Measurement by Remote Sensing. New Jersey: John Wiley & Sons. p. 21-88).

Nash, D.J & McLaren, S.J. 2003. Kalahari valley calcretes: the nature, origin and environmental significance. *Quaternary International*, 111: 3-22.

Nesse, W.D. 2004. Introduction to optical mineralogy. 3rd ed. New York: Oxford University Press.

Netterberg, F. 1969. Ages of calcretes in Southern Africa. *The South African Archaeological Bulletin*, 24: 88-92.

Northern Cape Nature Conservation Act **see** South Africa.

O'Brien, E.M. 1993. Climatic gradients in woody plant species richness: Towards an explanation based on an analysis of southern Africa's woody flora. *Journal of Biogeography,* 20: 181-198.

Odeh, I.O.A., McBratney, A.B., Chittleborough, D.J., 1994. Spatial prediction of soil properties from landform attributes derived from a digital elevation model. *Geoderma,* 63: 197–214.

Odum, E.P. 1971. Fundamentals of ecology. Philadelphia: W.B. Sanders Co.

O'Neill, R.V., Hunsaker, C.T., Timmins, S.P., Jackson, B.L., Jones, K.B., Riitters, K.H. & Wickham, J.D. 1996. Scale problems in reporting landscape pattern at the region scale. *Landscape Ecology,* 11(3): 169-480.

Partridge, T.C. 1998. Of diamonds, dinosaurs and diastrophism: 150 million years of landscape evolution in southern Africa. *South African Journal of Geology,* 101(3): 167-184.

Partridge, T.C., Botha, G.A. & Haddon, I.G. 2006. Cenozoic Deposits of the Interior (*In* Johnson, M.R., Anhaeusser, C.R. & Thomas, R.J., *eds*. The Geology of South Africa. Johannesburg: Geological Society of South Africa & Pretoria: Council for Geoscience. p. 585-604).

Pausas, J.G., Carreras, J., Ferre, A. & Font, X. 2003. Coarse-scale plant species richness in relation to environmental heterogeneity. *Journal of Vegetation Science,* 14: 661-668.

Pidwirny, M. 2006. Soil Pedogenesis. *Fundamentals of Physical Geography,* 2. http://www.physicalgeography.net/fundamentals/iou.html Date of access: 1 November 2017.

Pillay, M. & Swanepoel, T. 2013. Final Scoping Report for the Gamsberg Zinc Mine and Associated Infrastructure in the Northern Cape (Environmental Resources Management). https://www.erm.com/contentassets/34e202e6c03e4c5f9f0c4338134b71e7/final-scoping-report/full-final-scoping-report-gamsberg-mine---final.pdf Date of access: 10 October 2017.

PRIMER 6 version 1.1.15, 2012, computer software, PRIMER-E Ltd.

Raina, A.K. & Gupta, M.K. 2009. Soil and vegetation studies in relation to parent material of Garhwal Himalayas, Uttarakhand (India). *Annals of Forestry,* 17(1): 71-82.

Reid, D., Smith, C.B., Watkeys, M.K., Welke, H.J. & Betton, P.J. 1997. Whole-rock radiometric age patterns in the Aggeneys-Gamsberg ore district, central Bushmanland, South Africa. *South African Journal of Geology,* 100: 11-22.

Reitalu, T., Helm, A., Pärtel, M., Benytsson, K., Gerhold, P., Rosén, E., Takkis, K., Znamenskiy, S. & Prentice, H.C. 2014. Determinants of dine-scale plant diversity in dry calcareous grasslands within the Baltic Sea region. *Agriculture, Ecosystems and Environment,* 182: 59-68.

Richerson, P.J. & Lum, K.L. 1980. Patterns of plant species diversity in California: Relation to weather and topography. *American Naturalist,* 116: 504-536.

Rietkerk, M., Boerlijst, M.C., Van Langevelde, F., Hillerislambers, R., De Koppel, J.V., Kumar, L., Prins, H.H. & De Roos, A.M. 2002. Self-organization of vegetation in arid ecosystems. *The American Naturalist,* 160(4): 524-530.

Rossi, R.E., Mulla, D.J., Journel, A.G. & Franz, E.H. 1992. Geostatistical tools for modeling and interpreting ecological spatial dependence. *Ecological Monographs,* 62: 277-314.

Sagar, R., Raghubanshi, A.S. & Singh, J.S. 2003. Tree species composition, dispersion and diversity along a disturbance gradient in a dry tropical forest region of India. *Forest Ecology and Management*, 186: 61-71.

SARRCUS (South African Regional Commission for the Conservation and Utilisation of Soil). 1981. A system for the classification of soil erosion in the SARCCUS region. Pretoria: Department of Agriculture and Fisheries.

Schlesinger, W.H., Raikes, J.A., Hartley, A.E. & Cross, A.F. 1996. On the Spatial Pattern of Soil Nutrients in Desert Ecosystems. *Ecology,* 77(2): 364-374.

Schmidhuber, B.E. 2015. Geotechnical Properties of Pedological Soils (Volume 1). Potchefstroom: North-West University. (Mini-Dissertation - Honours).

Schoener, T.W. 1983. Field experiments on interspecific competition. *American Naturalist*, 122: 240-285.

Schulze, R.E. 1997. South African Atlas of agrohydrology and climatology. Pretoria: Water Research Commission.

Shen, Z.H., Zhang, X.H. & Jin, Y.X. 2000. Gradient analysis of the influence of mountain topography on vegetation pattern. *Acta Phytoecologica Sinica,* 24(4): 430-435.

Shunqukela, T. 2014. A study of the structural geology of an area between the Neusspruit shear zone and the Brakfontein shear zone near Kakamas, Northern Cape. Cape Town: University of the Western Cape. (Thesis – PhD).

Siebert, S.J., Matthee, M. & Van Wyk, A.E. 2003. Semi-arid savanna of the Potlake Nature Reserve and surrounding areas in Sekhukhuneland, South Africa. *Koedoe,* 46(1): 29-52.

Singer, M.J., Janitzky, P. & Blackard, J. 1982. The influence of exchangeable sodium percentage on soil erodibility. *Soil Science Society of America Journal,* 46: 117-121.

Soil Classification Working Group. 1991. Soil Classification: A Taxonomic System for South Africa. Memoirs on the Agricultural Natural Resources of South Africa No. 15. Pretoria: Department of Agricultural Development.

Soil Classification Working Group. 2018. Soil Classification: A Natural and Anthropogenic System for South Africa. Pretoria: ARC-Institute for Soil, Climate and Water. (In press).

Soil Survey Staff. 1999. Soil Taxonomy. A Basic System of Soil Classification for Making and Interpreting Soil Surveys. 2nd ed. United States Department of Agriculture, Natural Resources Conservation Service, Agriculture Handbook No. 436. Washington, DC: Government Printing Office.

Sokal, R.R. & Oden, N.L. 1978. Spatial autocorrelation in biology. *Biological Journal of the Linnean Society*, 10: 199-228.

South Africa. 2011. Northern Cape Nature Conservation Act 9 of 2009.

South African Committee for Stratigraphy (SACS). 1980. Stratigraphy of South Africa. Part I. (*In* Kent, L.E. *ed.* Lithostratigraphy of the Republic of South Africa, South West Africa/Namibia and the Republics of Bophuthatswana, Transkei and Venda. Handbook of Geological Survey of South Africa. Pretoria: Department of Mineral and Energy Affairs. 8: 690).

Sparks, D.L. 2003. Environmental Soil Chemistry. 2nd ed. California: Elsevier Science.

Spatial temporal evidence for planning South Africa. 2016. Climate Indicators Aridity. http://www.stepsa.org/climate_aridity.html. Date of access: 28 July 2017.

Stowe, C.W., Hardtnady, C.J.H. & Joubert, P. 1984. Proterozoic tectonic provinces of southern Africa. *Precambrian Research*, 25: 229-231.

Stowe, C.W. 1986. Synthesis and interpretation of structures along the north-eastern boundary of the Namaqua Tectonic Province. *Geological Society of South Africa,* 89: 185-198.

Student. 1914. The elimination of spurious correlation due to position in time or space. *Biometrika*, 10: 179-181.

Tankard, A.J., Jackson, M.P.A., Erickson, K.A., Hobday, D.K., Hunter, D.R. & Minter, W.E.L. 1982. Crustal Evolution of Southern Africa. Verlag: Springer. p. 523.

Tansley, A.G. & Adamson, R.S. 1925. Studies of the vegetation of the English Chalk. *Journal of Ecology XIII,* 2: 177-223.

Tansley, A.G. & Rankin, W.M. 1911. The vegetation of calcareous soils: The sub-formation of the chalk. (*In* Tansley, A.G. *ed.* Types of British Vegetation. Cambridge: Cambridge University Press. p. 161-186).

Tapp, A.F. 2010. Areal interpolation and Dasymetric mapping methods using local ancillary data sources. *Cartography and Geographic Information Science,* 37(3): 215-228.

Non-Affiliated Soil Analyses Work Committee. 1990. Handbook of standard soil testing methods for advisory purposes. Pretoria: Soil Science Society of South Africa.

Thomas, D.S.G. & Wiggs, G.F.S. 2012. Aeolian systems. (*In* Holmes, P. & Meadows, M*. eds*. Southern Africa Geomorphology: New trends and new directions. Bloemfontein: Sun Press. p. 143-165).

Thomas, R., Agenbacht, A., Cornell, D. & Moore, J. 1994. The Kibaran of southern Africa: Tectonic evolution and metallogeny. *Ore Geology Reviews*, p. 131-160.

Tilman, D. 1982. Resources competition and community structure. Princeton: Princeton University Press.

Tilman, D. 1988. Plant strategies and the structure and dynamics of plant communities. Princeton: Princeton University Press.

Tongway, D.J. & Ludwig, J.A. 1994. Small-scale resource heterogeneity in semi-arid landscapes. *Pacific Conservation Biology*, 1: 201-208.

Toure, D., Ge, J. & Zhou, J. 2015. Spatial patterns of tree species number in relationship with the local environmental variations in karst ecosystem. *Applied Ecology and Environmental Research*, 13(4): 1035-1054.

USDA-NRCS (United States Department of Agriculture - Natural Resources Conservation Services. 2014. Soil Texture Calculator. http://www.nrcs.usda.gov/wps/portal/nrcs/detail/soils/survey/?cid=nrcs142p2_054167. Date of access: 11 August 2017.

University of Florida Herbarium. 2015. Preparation of plant specimens for deposit as herbarium vouchers, edited by Marc, S.F. & Kent, D. http://www.floridamuseum.ufl.edu/herbarium/voucher.htm Date of access: 23 August 2017.

Unwin, D. 1979. An introduction to trend surface analysis. Leicester: University of Leicester.

Van Oudtshoorn, F. 2012. Gids tot grasse van suider-Afrika. Pretoria: Briza Publikasies.

Van Wyk, B., Van Wyk, P. & Van Wyk, B.E. 2011. Fotogids tot biome van suider-Afrika. Pretoria: Briza Publikasies.

Visser, D.J.L. 1998. The geotechnical evolution of South Africa and offshore areas. Pretoria: Council of Geoscience.

Von M Harmse, H.J. & Hatting, A.M. 1985. Pedological profile classes. (*In* Brink, A.B.A. 1985. Engineering Geology of Southern Africa. 4th ed. Pretoria: Building Publications. p. 272-285).

Von M Harmse, H.J. & Hatting, A.M. 2012. The sedimentary petrology of aeolian sands in Western Free State and adjacent areas north of the Vaal River (South Africa). Potchefstroom: Platinum Press. p. 93.

Watts, N.L. 1980. Quaternary pedogenic calcretes from the Kalahari (southern Africa): Mineralogy, genesis and diagenesis. *Sedimentology*, 27: 661-686.

Weather Bureau. 2016. Total rainfall per annum for Kakamas, Kenhardt and Pofadder (1992-2015) (CTP 201607003 NWU and CTP 201703003 NWU: C. Faul Weather Data). Pretoria: Weather Bureau, Department of Environmental Affairs.

Weinert, H.H. 1980. The natural road construction materials of southern Africa. Pretoria: Academia.

Weinert, H.H. 1984. Climate and the durability of South African road aggregates. *Bulletin of the International Association of Engineering Geology*, 29(1): 463-466.

Went, E.W. 1942. The dependence of certain annual plants on shrubs in southern California deserts. *Bulletin of the Torrey Botanical Club*, 69: 100-114.

Wentworth, T.R. 1981. Vegetation on limestone and granite in the Mule Mountains, Arizona. *Journal of Ecology*, 62(2): 469-482.

Wilkinson, M.J. 1988. Arid Landscapes. (*In* Moon, B.P. & Dardis, G.F. *eds.* The Geomorphology of southern Africa. Johannesburg: Southern Book Publishers. p. 78-102).

Winegardner, D.L. 1995. An introduction to soils for environmental professionals. Florida: Lewis Publishers.

Whittaker, R.H. 1978a. Approaches to classifying vegetation. (*In* Whittaker, R.H. *ed.* Classification of plant communities. Junk: The Hague. p. 1-32).

Whittaker, R.H. 1978b. Dominance types. (*In* Whittaker, R.H. *ed*. Classification of plant communities. Junk: The Hague. p. 65-79).

Wolf, B. 2000. The fertile triangle: The interrelationship of air, water, and nutrients in maximizing soil productivity. New York: Food Products Press.

Yeaton, R.I. & Esler, K.J. 1990 The dynamics of a Succulent Karoo vegetation: A study of species association and recruitment. *Vegetation*, 88: 103-113.

Zhao, N., Yang, Y. & Zhou,X. 2010. Application of geographically weighted regression in estimating the effect of climate and site conditions on vegetation distribution in Haihe Catchment, China. *Plant Ecology,* 209: 349-359.

TABLE OF CONTENTS FOR ANNEXURES

ANNEXURE C: SOIL DATA

ANNEXURE A: BACKGROUND INFORMATION

Table A-1: Identification and description of mapping units and associated sub-units (highlighted sub-units were chosen as representative where soil and vegetation surveys were conducted).

Mapping Unit	Sub-Unit	Coordinates		Description
		Latitude	Longitude	
A	A1	29°12'27.44"S	20°22'18.62"E	Mapping unit A represents the main drainage systems (stream order three) on the site.
	A2	29°11'34.31"S	20°23'0.62"E	
B	B1	29°12'43.68"S	20°22'34.72"E	Mapping unit B represents the second order drainage systems on the site. One of the properties used to distinguish between mapping unit B and mapping unit C, is mapping unit B's characteristic red colour, and mapping unit C, not showing any. Therefore, mapping unit B was identified based on both drainage order as well as soil colour.
	B2	29°12'32.66"S	20°22'15.97"E	
	B3	29°12'24.64"S	20°22'3.23"E	
	B4	29°12'27.41"S	20°21'44.92"E	
	B5	29°12'39.77"S	20°21'38.13"E	
	B6	29°12'46.08"S	20°21'35.93"E	
	B7	29°13'4.85"S	20°21'36.57"E	
	B8	29°11'4.78"S	20°22'40.88"E	
	B9	29°11'31.99"S	20°23'0.25"E	
	B10	29°11'25.24"S	20°22'46.18"E	
	B11	29°11'44.07"S	20°23'13.50"E	
	B12	29°11'48.88"S	20°22'6.28"E	
	B13	29°12'24.23"S	20°22'22.91"E	
	B14	29°11'4.94"S	20°23'24.98"E	
C	C1	29°12'43.51"S	20°22'16.48"E	
	C2	29°12'24.18"S	20°21'55.45"E	

Table A-1 (continued): Identification and description of mapping units and associated sub-units (highlighted sub-units were chosen as representative where soil and vegetation surveys were conducted).

Mapping Unit	Sub-Unit	Coordinates		Description
		Latitude	Longitude	
C	C3	29°12'34.54"S	20°22'6.09"E	Mapping unit C represents the first order drainage systems on the site. Due to the absence of red colours, similar to mapping unit B, as well as the standard nature of drainage systems, mapping unit C was identified based on drainage order and probably vegetation composition.
	C4	29°12'33.37"S	20°21'53.78"E	
	C5	29°12'44.27"S	20°21'48.63"E	
	C6	29°12'41.42"S	20°21'34.84"E	
	C7	29°12'51.82"S	20°21'51.24"E	
	C8	29°12'50.78"S	20°21'37.16"E	
	C9	29°13'6.98"S	20°21'50.61"E	
	C10	29°13'4.93"S	20°21'40.69"E	
	C11	29°13'2.06"S	20°21'36.28"E	
	C12	29°13'13.44"S	20°21'35.86"E	
	C13	29°12'24.93"S	20°22'48.44"E	
	C14	29°12'21.35"S	20°22'36.34"E	
	C15	29°12'17.66"S	20°22'31.34"E	
	C16	29°12'14.04"S	20°22'20.27"E	
	C17	29°11'40.85"S	20°23'3.55"E	
	C18	29°12'13.48"S	20°22'6.13"E	
	C19	29°12'10.58"S	20°21'58.65"E	
	C20	29°12'2.04"S	20°22'0.86"E	

Table A-1 (continued): Identification and description of mapping units and associated sub-units (highlighted sub-units were chosen as representative where soil and vegetation surveys were conducted).

Mapping Unit	Sub-Unit	Coordinates		Description
		Latitude	Longitude	
C	C21	29°11'36.57"S	20°22'13.40"E	Mapping unit C represents the first order drainage systems on the site. Due to the absence of red colours, similar to mapping unit B, as well as the standard nature of drainage systems, mapping unit C was identified based on drainage order and probably vegetation composition.
	C22	29°11'20.73"S	20°22'51.29"E	
	C23	29°11'32.77"S	20°22'35.08"E	
	C24	29°11'46.92"S	20°22'57.05"E	
	C25	29°11'56.77"S	20°23'7.93"E	
	C26	29°11'53.40"S	20°23'15.99"E	
	C27	29°11'5.02"S	20°22'50.42"E	
	C28	29°11'45.48"S	20°23'47.96"E	
	C29	29°10'51.56"S	20°23'5.74"E	
	C30	29°11'19.68"S	20°23'31.51"E	
	C31	29°10'53.66"S	20°23'9.81"E	
	C32	29°11'16.60"S	20°22'38.78"E	
	C33	29°11'14.43"S	20°22'46.07"E	
	C34	29°11'5.67"S	20°22'43.70"E	
	C35	29°11'56.20"S	20°23'25.55"E	
	C36	29°10'55.20"S	20°22'56.23"E	
	C37	29°12'3.16"S	20°22'29.17"E	
	C38	29°11'25.35"S	20°22'58.47"E	

Table A-1 (continued): Identification and description of mapping units and associated sub-units (highlighted sub-units were chosen as representative where soil and vegetation surveys were conducted).

Mapping Unit	Sub-Unit	Coordinates		Description
		Latitude	Longitude	
C	C39	29°11'23.47"S	20°23'6.33"E	
	C40	29°11'30.72"S	20°23'19.07"E	
	C41	29°12'12.35"S	20°22'10.89"E	
D	D1	29°13'0.84"S	20°22'5.12"E	Mapping unit D showed similar properties to that of mapping unit C, however, not connected to any of the identified drainage systems. Therefore, mapping unit D represents palaeo drainage systems, and was identified based on vegetation differences.
	D2	29°12'58.22"S	20°22'6.65"E	
	D3	29°12'38.45"S	20°21'47.16"E	
	D4	29°12'8.65"S	20°21'55.36"E	
	D5	29°11'28.37"S	20°23'38.75"E	
	D6	29°12'32.56"S	20°22'41.14"E	
	D7	29°11'44.06"S	20°22'43.68"E	
	D8	29°11'53.26"S	20°22'57.36"E	
	D9	29°10'53.80"S	20°22'59.19"E	
	D10	29°11'55.72"S	20°24'10.14"E	
	D11	29°12'11.60"S	20°23'32.35"E	
	D12	29°12'8.36"S	20°23'54.39"E	
	D13	29°11'59.55"S	20°23'41.42"E	
	D14	29°11'7.44"S	20°23'6.91"E	
	D15	29°11'59.65"S	20°22'58.89"E	

Table A-1 (continued): Identification and description of mapping units and associated sub-units (highlighted sub-units were chosen as representative where soil and vegetation surveys were conducted).

Mapping Unit	Sub-Unit	Coordinates		Description
		Latitude	Longitude	
D	D16	29°10'52.21"S	20°23'8.92"E	
	D17	29°12'4.52"S	20°23'15.54"E	
E	D18	29°11'36.08"S	20°23'16.31"E	Mapping unit E represents the areas between drainage systems, identified by its slight grey colour. During the construction of these mapping units, with the help of aerial photography, it is unclear what the main cause of this typical colour is. Further fieldwork had to be done in order to establish the characteristic determining factor. .
	D19	29°12'4.63"S	20°22'7.74"E	
	E1	29°11'25.51"S	20°23'15.62"E	
	E2	29°11'20.43"S	20°23'44.63"E	
	E3	29°11'44.56"S	20°23'28.01"E	
	E4	29°11'49.21"S	20°22'12.79"E	
	E5	29°12'35.24"S	20°21'44.78"E	
	E6	29°12'57.39"S	20°21'40.54"E	
	E7	29°11'35.36"S	20°22'15.74"E	
	E8	29°11'39.93"S	20°23'7.52"E	
	E9	29°11'59.69"S	20°22'7.56"E	
F	F1	29°13'15.04"S	20°21'35.30"E	Mapping unit F represents the areas between drainage systems, identified by a lighter grey colour than that of mapping unit E. During the construction of these mapping units, with the help of aerial photography, it is unclear what the main cause of this typical colour is. Further fieldwork had to be done in order to establish the characteristic determining factor.
	F2	29°13'9.15"S	20°21'39.23"E	
	F3	29°12'1.36"S	20°22'38.17"E	
	F4	29°11'53.35"S	20°23'2.93"E	
	F5	29°12'50.60"S	20°22'4.57"E	

Table A-1 (continued): Identification and description of mapping units and associated sub-units (highlighted sub-units were chosen as representative where soil and vegetation surveys were conducted).

Mapping Unit	Sub-Unit	Coordinates		Description
		Latitude	Longitude	
F	F6	29°11'34.27"S	20°23'45.49"E	
	F7	29°13'8.23"S	20°21'51.00"E	
G	G1	29°11'16.61"S	20°22'54.87"E	Mapping unit G represents the areas between drainage systems, identified by its white colour. During the construction of these mapping units, with the help of aerial photography, it is unclear what the main cause of this typical colour is. Further fieldwork had to be done in order to establish the characteristic determining factor.
	G2	29°12'44.91"S	20°21'42.33"E	
	G3	29°10'59.55"S	20°22'51.29"E	
	G4	29°12'39.88"S	20°22'21.06"E	
	G5	29°11'35.75"S	20°23'19.58"E	
	G6	29°11'45.84"S	20°22'29.09"E	
	G7	29°12'7.53"S	20°22'18.17"E	
	G8	29°11'27.99"S	20°22'22.80"E	
	G9	29°11'33.82"S	20°22'56.62"E	
	G10	29°12'34.55"S	20°22'0.87"E	
	G11	29°11'7.94"S	20°22'46.04"E	
	G12	29°12'53.72"S	20°21'36.85"E	
	G13	29°12'6.47"S	20°22'1.70"E	
H	H1	29°11'3.38"S	20°23'10.12"E	
	H2	29°12'29.11"S	20°22'11.03"E	
	H3	29°12'33.54"S	20°22'43.74"E	

Table A-1 (continued): Identification and description of mapping units and associated sub-units (highlighted sub-units were chosen as representative where soil and vegetation surveys were conducted).

Mapping Unit	Sub-Unit	Coordinates		Description
		Latitude	Longitude	
H	H4	29°12'7.91"S	20°21'55.27"E	Mapping unit H represents the areas between drainage systems, identified by its slight brown colour. During the construction of these mapping units, with the help of aerial photography, it is unclear what the main cause of this typical colour is. Further fieldwork had to be done in order to establish the characteristic determining factor.
	H5	29°12'2.69"S	20°23'10.21"E	
	H6	29°12'43.42"S	20°22'39.51"E	
	H7	29°11'47.22"S	20°24'14.04"E	
I	I1	29°12'24.35"S	20°23'8.77"E	Mapping unit I represents the area to the south-eastern side of the site, identified by its blotched greenish colour. During the construction of these mapping units, with the help of aerial photography, it is unclear what the main cause of this typical colour is. Further fieldwork had to be done in order to establish the characteristic determining factor.
	I2	29°12'4.91"S	20°23'48.85"E	
J	J1	29°12'12.36"S	20°22'2.17"E	Mapping unit J represents the areas, identified by distinct black patches. During the construction of these mapping units, with the help of aerial photography, it is unclear what the main cause of this typical colour is. However, it was speculated that the cause of this distinct colour could be due to geological outcrops. Further fieldwork had to be done in order to establish the characteristic determining factor.
	J2	29°12'21.51"S	20°21'49.08"E	
	J3	29°11'23.10"S	20°22'24.80"E	
	J4	29°11'21.67"S	20°22'38.22"E	
	J5	29°11'29.01"S	20°22'48.74"E	

EXPLANATION OF SYMBOLS

OBSERVATION NUMBER
Personal

FORM/SERIE/FAMILY
Depends on requirement e.g. Hu36 or Hu3200 or Hu36/3200

TEXTURE CLASS
(of the A horizon for classification purposes)

fi	=	fine
me	=	medium
co	=	coarse
Sa	=	sand
Cl	=	clay
Lm	=	loam
Si	=	silt

PHASE
Phase notations where necessary

OBSERVATION TYPE
Circle correct letter

A	=	auger
C	=	cutting or pit

HORIZONS

ob	=	overburden
O	=	O horizon
A1-A2	=	A horizon
E	=	E horizon
B1-B2	=	B horizon
C	=	saprolite/uncon. mat.
G	=	G horizon
R	=	hard rock

DEPTH
Lower boundary of the horizon in mm

CLAY PERCENTAGE
Field method

SAND GRADE

fi	=	fine
me	=	medium
co	=	coarse

COLOUR
Munsell colour of the horizon (always the moist colour, optional dry colour e.g. for E and bleached A, etc.)

MOTTLES

OCC	=	OCCURANCE
f	=	few (<2%)
c	=	common (2-20%)
m	=	many (>20%)
COL	=	COLOUR
Y	=	yellow
R	=	red
BR	=	brown
Bl	=	black
G	=	grey
O	=	orange

LIME

OCC	=	OCCURANCE
s	=	sporadic
c	=	common
a	=	abundant
TYPE		
N	=	nodular
P	=	powdary
NP	=	nodular and powdary

STRUCTURE

GRA	=	GRADE
A	=	apedal
W	=	weak
M	=	medium
S	=	strong
SIZE		
f	=	fine
m	=	medium
c	=	coarse
TYPE		
SG	=	single grain
MA	=	massive
AB	=	angular blocky
SB	=	subangular blocky
GR	=	granular
CR	=	crumb
PR	=	prismatic
CO	=	columnar
PL	=	platy

COARSE FRAGMENTS

TYPE		
G	=	gravel
S	=	stones
B	=	boulders
P	=	plinthite

%
Estimated percentage of the horizon occupied by coarse fragments

DIAGNOSTIC HORIZONS

oo	=	Organic O horizon
ah	=	Humic A horizon
vc	=	Vertic A horizon
ml	=	Melanic A horizon
ot	=	Orthic A horizon
gs	=	E horizon
gh	=	G horizon
re	=	Red apedal B horizon
ye	=	Yellow-brown apedal B horizon
vr	=	Red structured B horizon
sp	=	Soft plinthic B horizon
hp	=	Hard plinthic B horizon
pr	=	Prismacutanic B horizon
ge	=	Gleycutanic B horizon
vp	=	Pedocutanic B horizon
lc	=	Lithocutanic B horizon
ne	=	Neocutanic B horizon
nc	=	Neocarbonate B horizon
pz	=	Podzol B horizon
pp	=	Podzol B horizon with
PP	=	Placic pan
rs	=	Regic sand
al	=	Stratified alluvium
db	=	Dorbank
so	=	Saprolite
sc	=	Soft carbonate horizon
hc	=	Hard carbonate horizon
ud	=	Unconsolidated material, without signs of wetness
uw	=	Unconsolidated material,
on	=	Unspecified material, with
mm	=	Man-made soil deposit
ro	=	Hard rock

PARENT MATERIAL

UN	=	Unknown
AL	=	Alluvium
AE	=	Aeolian
CO	=	Colluvium
GA	=	Gabbro
GR	=	Granite
BA	=	Basalt, dolerite
AN	=	Andesite
RH	=	Rhyolite
QS	=	Quartz sandstone
FS	=	Feldspathic sandstone
MS	=	Micaceous sandstone
SH	=	Shale
MU	=	Mudstone
SI	=	Siltstone
DO	=	Dolomite, chert
TI	=	Tillite
IR	=	Banded Ironstone
GN	=	Gneiss
SC	=	Schist
SL	=	Slate
DI	=	Diabase
BR	=	Breccia

EFFECTIVE DEPTH
Effective depth of profile for general plant growth in mm

TERRAIN UNIT

1	=	Crest
2	=	Scarp
3	=	Midslope
3U	=	Upper Midslope
3L	=	Lower Midslope
4	=	Footslope
4U	=	Upper Footslope
4L	=	Lower Footslope
5	=	Valley bottom
6	=	Terrace
7	=	Closed depression

DEPTH LIMITING MATERIAL

so	=	saprolite
hp	=	hard plinthite
R	=	rock
ge	=	gleyed material
st	=	strong structure
k	=	calcrete
sl	=	stone line

GPS (optional)
Reading of Global Positional System instrument .

In case of map reading, cross GPS text

SKETCH
Optional for e.g. landtype surveys

REMARKS
Soil features for which no provision is made, e.g. surface rock, consistance, vegetation, disturbed profile, water table, erosion and type of analysis required for the samples are noted here.

Figure A-1: Soil description categories (Land Type Survey Staff, 1991).

SURVEY _____ SURVEYER: _____ DATE: _____ PAGE: _____

Observ. no.: / Form/Serie/Family	Hor.	Depth (mm)	Clay %	Sand grade	Dry colour	Moist colour	Mottles: Occ	Mottles: Col.	Lime: Occ	Lime: Type	Structure: Gra	Structure: Size	Structure: Type	Coarse Frag.: Type	Coarse Frag.: %	Diag. hor.	Bag no.	Parent mat. / Eff. depth / Terrain unit / Depth lim. mat. / G P S Lat. / Long.
Text. class.:																		
Phase:																		
Observ. type: A C	Remarks:																	
Obsv. no.: / Form/Serie/Family																		Parent mat.: / Eff. depth: / Terrain unit: / Depth lim. mat.: / G P S Lat.: / Long.:
Text. class.:																		
Phase:	Observ. type: A C	Remarks:																
Obs. no.: / Form/Serie/Family																		Parent mat.: / Eff. depth: / Terrain unit: / Depth lim. mat.: / G P S Lat.: / Long.:
Text. class.:																		
Phase:	Observ. type: A C	Remarks:																
Obs .no.: / Form/Serie/Family																		Parent mat.: / Eff. depth: / Terrain unit: / Depth lim. mat.: / G P S Lat.: / Long:
Text. class.:																		
Phase:	Observ. type: A C	Remarks:																

Figure A-2: Standard soil description form (Land Type Survey Staff, 1991).

ANNEXURE B: VEGETATION DATA

Table B-1: Results for SIMPER, indicating the top fifteen plant species responsible for variations between mapping units A and B in the NMDS graphs.

Mapping unit A and B					
Taxon	**Av. dissim**	**Contrib. %**	**Cumulative %**	**Mean abund. A**	**Mean abund. B**
Rhigozum trichotomum	14,42	17,71	17,71	0,00	52,40
Stipagrostis namaquensis	14,06	17,27	34,98	46,50	26,20
Stipagrostis ciliata var. ciliata	11,24	13,80	48,78	46,00	7,20
Stipagrostis obtuse	10,17	12,50	61,28	21,00	42,20
Eragrostis lehmanniana var. lehmanniana	6,95	8,54	69,81	27,50	0,00
Eriocephalus ambiguus	6,57	8,07	77,88	26,00	0,00
Lophiocarpus polystachyus	2,53	3,11	80,99	0,00	9,60
Aristida adscensionis	1,97	2,42	83,41	0,00	5,60
Eragrostis annulata	1,77	2,17	85,59	7,00	0,00
Aizoon schellenbergii	1,60	1,96	89,57	5,00	0,00
Zygophyllum microcarpum	1,46	1,79	91,36	5,50	0,00
Stipagrostis fastigiata	1,42	1,74	93,10	0,00	5,40
Panicum arbusculum	1,39	1,71	94,81	5,50	0,00
Eragrostis procumbens	1,10	1,36	96,16	0,00	3,80
Lycium bosciifolium	0,76	0,93	97,09	3,00	0,00

Key to column headings: Av. Dissim, Average dissimilarity; Contrib. %, Percentage contribution of each species to the average dissimilarity; Cumulative %, Cumulative contribution percentage; Mean abund., mean abundance per mapping unit.

Table B-2: Results for SIMPER, indicating the top fifteen plant species responsible for variations between mapping units A and C in the NMDS graphs.

Mapping unit A and C					
Taxon	**Av. dissim**	**Contrib. %**	**Cumulative %**	**Mean abund. A**	**Mean abund. C**
Stipagrostis namaquensis	13,59	19,04	19,04	46,50	2,40
Stipagrostis obtuse	13,07	18,30	37,34	21,00	67,60
Rhigozum trichotomum	12,27	17,19	54,53	0,00	46,20
Eragrostis lehmanniana var. lehmanniana	6,52	9,13	63,66	27,50	0,00
Eriocephalus ambiguus	6,17	8,64	72,30	26,00	0,00
Stipagrostis ciliata var. ciliata	3,93	5,50	77,80	46,00	33,80
Eragrostis annulata	1,66	2,33	80,12	7,00	0,00
Stipagrostis fastigiata	1,63	2,28	82,40	0,00	6,60
Aizoon schellenbergii	1,47	2,06	84,46	5,00	0,00
Aristida adscensionis	1,38	1,93	86,40	0,00	5,60
Panicum arbusculum	1,30	1,83	88,22	5,50	0,00
Zygophyllum microcarpum	1,20	1,69	89,91	5,50	0,80
Salsola tuberculate	1,19	1,67	91,57	0,00	4,60
Lycium bosciifolium	0,73	1,02	93,98	3,00	0,60
Lycium oxycarpum	0,68	0,95	94,93	0,00	2,40

Key to column headings: Av. Dissim, Average dissimilarity; Contrib. %, Percentage contribution of each species to the average dissimilarity; Cumulative %, Cumulative contribution percentage; Mean abund., mean abundance per mapping unit.

Table B-3: Results for SIMPER, indicating the top fifteen plant species responsible for variations between mapping units A and D in the NMDS graphs.

Mapping unit A and D					
Taxon	**Av. dissim**	**Contrib. %**	**Cumulative %**	**Mean abund. A**	**Mean abund. D**
Stipagrostis obtuse	15,66	22,23	22,23	21,00	81,20
Stipagrostis namaquensis	13,50	19,17	41,39	46,50	4,20
Eragrostis lehmanniana var. lehmanniana	6,46	9,17	50,56	27,50	0,00
Eriocephalus ambiguus	6,10	8,67	59,23	26,00	0,00
Stipagrostis ciliata var. ciliata	6,09	8,64	67,86	46,00	52,80
Stipagrostis fastigiata	5,62	7,98	75,84	0,00	22,20
Rhigozum trichotomum	4,21	5,97	81,81	0,00	15,60
Eragrostis annulata	1,64	2,33	84,15	7,00	0,00
Aizoon schellenbergii	1,53	2,18	86,32	0,00	5,40
Panicum arbusculum	1,29	1,83	92,23	5,50	0,00
Zygophyllum microcarpum	1,28	1,82	94,05	5,50	1,00
Lycium bosciifolium	0,84	1,19	95,25	3,00	3,00
Salsola tuberculate	0,76	1,08	96,33	0,00	2,80
Aristida adscensionis	0,44	0,62	96,95	1,50	0,00
Acanthopsis disperma	0,42	0,59	97,54	0,00	2,20

Key to column headings: Av. Dissim, Average dissimilarity; Contrib. %, Percentage contribution of each species to the average dissimilarity; Cumulative %, Cumulative contribution percentage; Mean abund., mean abundance per mapping unit.

Table B-4: Results for SIMPER, indicating the top fifteen plant species responsible for variations between mapping units A and E in the NMDS graphs.

Mapping unit A and E					
Taxon	**Av. dissim**	**Contrib. %**	**Cumulative %**	**Mean abund. A**	**Mean abund. E**
Stipagrostis obtuse	36,98	43,86	43,86	21,00	249,00
Aridaria noctiflora	11,46	13,59	57,45	0,00	73,40
Stipagrostis namaquensis	8,99	10,67	68,11	46,50	10,60
Stipagrostis ciliata var. ciliata	6,48	7,68	75,80	46,00	35,20
Eragrostis lehmanniana var. lehmanniana	4,59	5,45	81,24	27,50	0,00
Eriocephalus ambiguus	4,34	5,15	86,39	26,00	0,00
Salsola barbata	2,72	3,23	89,62	0,00	11,80
Salsola tuberculate	1,47	1,74	91,36	0,00	8,20
Eragrostis annulata	1,17	1,39	92,75	7,00	0,00
Zygophyllum microphyllum	1,04	1,23	93,98	0,00	8,00
Aizoon schellenbergii	0,98	1,16	95,13	5,00	0,00
Panicum arbusculum	0,92	1,09	96,22	5,50	0,00
Zygophyllum microcarpum	0,89	1,05	97,28	5,50	0,40
Lycium bosciifolium	0,50	0,59	97,87	3,00	0,00
Rhigozum trichotomum	0,38	0,45	98,33	0,00	2,60

Key to column headings: Av. Dissim, Average dissimilarity; Contrib. %, Percentage contribution of each species to the average dissimilarity; Cumulative %, Cumulative contribution percentage; Mean abund., mean abundance per mapping unit.

Table B-5: Results for SIMPER, indicating the top fifteen plant species responsible for variations between mapping units A and F in the NMDS graphs.

Mapping unit A and F					
Taxon	**Av. dissim**	**Contrib. %**	**Cumulative %**	**Mean abund. A**	**Mean abund. F**
Stipagrostis obtuse	53,33	61,57	61,57	21,00	427,00
Aridaria noctiflora	8,82	10,19	71,75	0,00	68,50
Stipagrostis namaquensis	6,39	7,38	79,13	46,50	0,00
Stipagrostis ciliata var. ciliata	5,66	6,53	85,66	46,00	59,50
Eragrostis lehmanniana var. lehmanniana	3,40	3,93	89,59	27,50	0,00
Eriocephalus ambiguus	3,22	3,71	93,30	26,00	0,00
Salsola tuberculate	1,72	1,98	95,29	0,00	13,00
Eragrostis annulata	0,87	1,00	96,29	7,00	0,00
Zygophyllum microcarpum	0,69	0,80	97,09	5,50	0,00
Aizoon schellenbergii	0,69	0,79	97,88	5,00	0,00
Panicum arbusculum	0,68	0,79	98,67	5,50	0,00
Lycium bosciifolium	0,37	0,43	99,10	3,00	0,00
Aristida adscensionis	0,20	0,23	99,33	1,50	0,50
Setaria verticillata	0,19	0,21	99,54	1,50	0,00
Zygophyllum microphyllum	0,13	0,15	99,70	0,00	1,00

Key to column headings: Av. Dissim, Average dissimilarity; Contrib. %, Percentage contribution of each species to the average dissimilarity; Cumulative %, Cumulative contribution percentage; Mean abund., mean abundance per mapping unit.

Table B-6: Results for SIMPER, indicating the top fifteen plant species responsible for variations between mapping units A and G in the NMDS graphs.

Mapping unit A and G					
Taxon	**Av. dissim**	**Contrib. %**	**Cumulative %**	**Mean abund. A**	**Mean abund. G**
Stipagrostis obtuse	39,98	49,67	49,67	21,00	220,00
Stipagrostis namaquensis	10,19	12,66	62,33	46,50	0,60
Aridaria noctiflora	6,22	7,73	70,06	0,00	28,60
Stipagrostis ciliata var. ciliata	6,16	7,65	77,70	46,00	44,60
Eragrostis lehmanniana var. lehmanniana	5,11	6,35	84,06	27,50	0,00
Eriocephalus ambiguus	4,83	6,01	90,06	26,00	0,00
Eragrostis annulata	1,30	1,62	91,68	7,00	0,00
Aizoon schellenbergii	1,10	1,36	93,04	5,00	0,00
Panicum arbusculum	1,02	1,27	94,31	5,50	0,00
Zygophyllum microcarpum	1,02	1,26	95,58	5,50	0,20
Salsola tuberculate	0,78	0,97	96,55	0,00	3,80
Stipagrostis fastigiata	0,76	0,95	97,50	0,00	3,80
Lycium bosciifolium	0,56	0,69	98,19	3,00	0,00
Aristida adscensionis	0,33	0,41	98,60	1,50	0,00
Setaria verticillata	0,28	0,35	98,94	1,50	0,00

Key to column headings: Av. Dissim, Average dissimilarity; Contrib. %, Percentage contribution of each species to the average dissimilarity; Cumulative %, Cumulative contribution percentage; Mean abund., mean abundance per mapping unit.

Table B-7: Results for SIMPER, indicating the top fifteen plant species responsible for variations between mapping units A and H in the NMDS graphs.

Mapping unit A and H					
Taxon	**Av. dissim**	**Contrib. %**	**Cumulative %**	**Mean abund. A**	**Mean abund. H**
Stipagrostis obtuse	35,77	47,10	47,10	21,00	226,00
Stipagrostis ciliata var. ciliata	13,47	17,73	64,83	46,00	119,00
Stipagrostis namaquensis	8,88	11,68	76,51	46,50	1,00
Eragrostis lehmanniana var. lehmanniana	4,55	5,99	82,50	27,50	0,00
Eriocephalus ambiguus	4,30	5,66	88,16	26,00	0,00
Aridaria noctiflora	1,34	1,77	89,93	0,00	7,40
Eragrostis annulata	1,16	1,52	91,45	7,00	0,00
Aizoon schellenbergii	0,96	1,26	92,71	5,00	0,00
Zygophyllum microcarpum	0,94	1,23	93,94	5,50	0,00
Panicum arbusculum	0,91	1,20	95,14	5,50	0,00
Aristida adscensionis	0,53	0,70	95,84	1,50	3,00
Stipagrostis fastigiata	0,52	0,69	96,53	0,00	2,80
Lycium bosciifolium	0,50	0,66	97,19	3,00	0,40
Salsola tuberculate	0,34	0,45	97,64	0,00	2,00
Aptosimum spinescens	0,28	0,37	98,43	0,00	1,80

Key to column headings: Av. Dissim, Average dissimilarity; Contrib. %, Percentage contribution of each species to the average dissimilarity; Cumulative %, Cumulative contribution percentage; Mean abund., mean abundance per mapping unit.

Table B-8: Results for SIMPER, indicating the top fifteen plant species responsible for variations between mapping units A and I in the NMDS graphs.

Mapping unit A and I					
Taxon	**Av. dissim**	**Contrib. %**	**Cumulative %**	**Mean abund. A**	**Mean abund. I**
Stipagrostis obtuse	64,81	75,80	75,80	21,00	627,00
Stipagrostis ciliata var. ciliata	6,37	7,45	83,25	46,00	105,00
Stipagrostis namaquensis	5,33	6,23	89,48	46,50	0,00
Eragrostis lehmanniana var. lehmanniana	2,88	3,37	92,85	27,50	0,00
Eriocephalus ambiguus	2,72	3,18	96,03	26,00	0,00
Eragrostis annulata	0,73	0,86	96,89	7,00	0,00
Zygophyllum microcarpum	0,59	0,68	97,57	5,50	0,00
Panicum arbusculum	0,58	0,67	98,24	5,50	0,00
Aizoon schellenbergii	0,57	0,67	98,91	5,00	0,00
Lycium bosciifolium	0,31	0,37	99,28	3,00	0,00
Aristida adscensionis	0,17	0,20	99,48	1,50	0,00
Setaria verticillata	0,16	0,18	99,67	1,50	0,00
Salsola tuberculate	0,11	0,13	99,79	0,00	1,00
Aizoon schellenbergii	0,06	0,07	99,87	0,00	0,50
Lycium oxycarpum	0,06	0,07	99,94	0,00	0,50

Key to column headings: Av. Dissim, Average dissimilarity; Contrib. %, Percentage contribution of each species to the average dissimilarity; Cumulative %, Cumulative contribution percentage; Mean abund., mean abundance per mapping unit.

Table B-9: Results for SIMPER, indicating the top fifteen plant species responsible for variations between mapping units A and J in the NMDS graphs.

Mapping unit A and J					
Taxon	**Av. dissim**	**Contrib. %**	**Cumulative %**	**Mean abund. A**	**Mean abund. J**
Stipagrostis obtuse	40,34	45,39	45,39	21,00	233,00
Stipagrostis namaquensis	12,56	14,14	59,53	46,50	0,00
Stipagrostis ciliata var. ciliata	10,29	11,58	71,11	46,00	3,80
Eragrostis lehmanniana var. lehmanniana	5,96	6,70	77,81	27,50	0,00
Eriocephalus ambiguus	5,63	6,34	84,14	26,00	0,00
Stipagrostis fastigiata	3,23	3,64	87,78	0,00	17,20
Eragrostis annulata	1,52	1,71	89,49	7,00	0,00
Aizoon schellenbergii	1,35	1,52	91,01	5,00	0,00
Zygophyllum microcarpum	1,25	1,40	92,41	5,50	0,00
Panicum arbusculum	1,19	1,34	93,75	5,50	0,00
Calobota spinescens	1,12	1,26	95,01	0,00	5,20
Salsola barbata	0,80	0,90	95,91	0,00	3,80
Lycium bosciifolium	0,65	0,73	96,64	3,00	0,00
Acanthopsis disperma	0,48	0,54	97,80	0,00	1,60
Aristida adscensionis	0,39	0,44	98,24	1,50	0,20

Key to column headings: Av. Dissim, Average dissimilarity; Contrib. %, Percentage contribution of each species to the average dissimilarity; Cumulative %, Cumulative contribution percentage; Mean abund., mean abundance per mapping unit.

Table B-10: Results for SIMPER, indicating the top fifteen plant species responsible for variations between mapping units B and C in the NMDS graphs.

Mapping unit B and C					
Taxon	**Av. dissim**	**Contrib. %**	**Cumulative %**	**Mean abund. B**	**Mean abund. C**
Stipagrostis obtuse	13,60	23,18	23,18	42,20	67,60
Rhigozum trichotomum	13,28	22,64	45,82	52,40	46,20
Stipagrostis ciliata var. ciliata	7,87	13,42	59,23	7,20	33,80
Stipagrostis namaquensis	6,98	11,89	71,12	26,20	2,40
Lophiocarpus polystachyus	2,82	4,80	75,92	9,60	2,40
Aristida adscensionis	2,80	4,77	80,69	5,60	5,60
Stipagrostis fastigiata	2,69	4,58	85,27	5,40	6,60
Eriocephalus ambiguus	2,17	3,69	88,96	5,60	4,20
Salsola tuberculate	1,29	2,20	91,16	0,20	4,60
Eragrostis procumbens	1,20	2,05	93,20	3,80	1,60
Lycium oxycarpum	0,74	1,26	94,46	0,20	2,40
Salsola barbata	0,64	1,09	95,55	2,00	1,20
Aptosimum spinescens	0,50	0,85	96,41	0,40	1,80
Calobota spinescens	0,37	0,63	97,04	0,40	1,20
Aridaria noctiflora	0,32	0,54	97,58	0,00	1,00

Key to column headings: Av. Dissim, Average dissimilarity; Contrib. %, Percentage contribution of each species to the average dissimilarity; Cumulative %, Cumulative contribution percentage; Mean abund., mean abundance per mapping unit.

Table B-11: Results for SIMPER, indicating the top fifteen plant species responsible for variations between mapping units B and D in the NMDS graphs.

Mapping unit B and D					
Taxon	**Av. dissim**	**Contrib. %**	**Cumulative %**	**Mean abund. B**	**Mean abund. D**
Stipagrostis obtuse	15,87	23,21	23,21	42,20	81,20
Rhigozum trichotomum	12,99	19,00	42,21	52,40	15,60
Stipagrostis ciliata var. ciliata	12,86	18,81	61,02	7,20	52,80
Stipagrostis namaquensis	7,15	10,46	71,48	26,20	4,20
Stipagrostis fastigiata	5,09	7,44	78,92	5,40	22,20
Lophiocarpus polystachyus	2,58	3,78	82,69	9,60	0,40
Eriocephalus ambiguus	2,35	3,43	86,13	5,60	5,80
Aristida adscensionis	2,03	2,97	89,09	5,60	0,00
Aizoon schellenbergii	1,70	2,49	91,59	0,00	5,40
Eragrostis procumbens	1,19	1,74	93,32	3,80	1,20
Salsola tuberculate	0,84	1,22	94,54	0,20	2,80
Lycium bosciifolium	0,75	1,10	95,64	0,00	3,00
Acanthopsis disperma	0,55	0,81	96,45	0,40	2,20
Salsola barbata	0,54	0,79	97,24	2,00	0,00
Calobota spinescens	0,47	0,69	97,93	0,40	1,60

Key to column headings: Av. Dissim, Average dissimilarity; Contrib. %, Percentage contribution of each species to the average dissimilarity; Cumulative %, Cumulative contribution percentage; Mean abund., mean abundance per mapping unit.

Table B-12: Results for SIMPER, indicating the top fifteen plant species responsible for variations between mapping units B and E in the NMDS graphs.

Mapping unit B and E					
Taxon	**Av. dissim**	**Contrib. %**	**Cumulative %**	**Mean abund. B**	**Mean abund. E**
Stipagrostis obtuse	35,21	44,59	44,59	42,20	249,00
Aridaria noctiflora	12,09	15,32	59,91	0,00	73,40
Rhigozum trichotomum	9,73	12,33	72,23	52,40	2,60
Stipagrostis namaquensis	5,33	6,75	78,98	26,20	10,60
Stipagrostis ciliata var. ciliata	4,28	5,42	84,40	7,20	35,20
Salsola barbata	2,89	3,66	88,06	2,00	11,80
Lophiocarpus polystachyus	1,77	2,25	90,30	9,60	0,20
Salsola tuberculate	1,55	1,96	92,26	0,20	8,20
Aristida adscensionis	1,27	1,60	93,87	5,60	0,00
Eriocephalus ambiguus	1,11	1,40	95,27	5,60	0,20
Zygophyllum microphyllum	1,09	1,37	96,64	0,00	8,00
Stipagrostis fastigiata	0,83	1,05	97,69	5,40	1,40
Eragrostis procumbens	0,74	0,94	98,63	3,80	0,00
Aptosimum spinescens	0,18	0,22	98,86	0,40	1,00
Enneapogon desvauxii	0,16	0,20	99,06	0,80	0,00

Key to column headings: Av. Dissim, Average dissimilarity; Contrib. %, Percentage contribution of each species to the average dissimilarity; Cumulative %, Cumulative contribution percentage; Mean abund., mean abundance per mapping unit.

Table B-13: Results for SIMPER, indicating the top fifteen plant species responsible for variations between mapping units B and F in the NMDS graphs.

Mapping unit B and F					
Taxon	**Av. dissim**	**Contrib. %**	**Cumulative %**	**Mean abund. B**	**Mean abund. F**
Stipagrostis obtuse	52,87	61,00	61,00	42,20	427,00
Aridaria noctiflora	9,22	10,64	71,63	0,00	68,50
Stipagrostis ciliata var. ciliata	7,08	8,16	79,80	7,20	59,50
Rhigozum trichotomum	7,05	8,13	87,93	52,40	0,00
Stipagrostis namaquensis	3,50	4,04	91,97	26,20	0,00
Salsola tuberculate	1,77	2,04	94,01	0,20	13,00
Lophiocarpus polystachyus	1,27	1,46	95,47	9,60	0,00
Aristida adscensionis	0,84	0,97	96,44	5,60	0,00
Eriocephalus ambiguus	0,79	0,91	97,35	5,60	0,50
Stipagrostis fastigiata	0,71	0,82	98,16	5,40	0,00
Eragrostis procumbens	0,52	0,60	98,76	3,80	0,00
Salsola barbata	0,26	0,30	99,07	2,00	0,00
Zygophyllum microphyllum	0,14	0,16	99,23	0,00	1,00
Hoodia gordonii	0,14	0,16	99,39	0,00	1,00
Enneapogon desvauxii	0,11	0,13	99,52	0,80	0,00

Key to column headings: Av. Dissim, Average dissimilarity; Contrib. %, Percentage contribution of each species to the average dissimilarity; Cumulative %, Cumulative contribution percentage; Mean abund., mean abundance per mapping unit.

Table B-14: Results for SIMPER, indicating the top fifteen plant species responsible for variations between mapping units B and G in the NMDS graphs.

Mapping unit B and G					
Taxon	**Av. dissim**	**Contrib. %**	**Cumulative %**	**Mean abund. B**	**Mean abund. G**
Stipagrostis obtuse	38,24	48,94	48,94	42,20	220,00
Rhigozum trichotomum	11,11	14,22	63,16	52,40	0,00
Stipagrostis ciliata var. ciliata	7,51	9,61	72,77	7,20	44,60
Aridaria noctiflora	6,72	8,59	81,37	0,00	28,60
Stipagrostis namaquensis	5,41	6,92	88,29	26,20	0,60
Lophiocarpus polystachyus	1,97	2,52	90,81	9,60	0,00
Aristida adscensionis	1,43	1,83	92,64	5,60	0,00
Eriocephalus ambiguus	1,26	1,61	94,25	5,60	0,40
Stipagrostis fastigiata	1,17	1,50	95,75	5,40	3,80
Eragrostis procumbens	0,83	1,07	96,82	3,80	0,00
Salsola tuberculate	0,83	1,06	97,88	0,20	3,80
Salsola barbata	0,41	0,53	98,41	2,00	0,40
Aptosimum spinescens	0,29	0,37	98,77	0,40	1,40
Calobota spinescens	0,18	0,23	99,00	0,40	0,60
Enneapogon desvauxii	0,18	0,23	99,23	0,80	0,00

Key to column headings: Av. Dissim, Average dissimilarity; Contrib. %, Percentage contribution of each species to the average dissimilarity; Cumulative %, Cumulative contribution percentage; Mean abund., mean abundance per mapping unit.

Table B-15: Results for SIMPER, indicating the top fifteen plant species responsible for variations between mapping units B and H in the NMDS graphs.

Mapping unit B and H					
Taxon	**Av. dissim**	**Contrib. %**	**Cumulative %**	**Mean abund. B**	**Mean abund. H**
Stipagrostis obtuse	33,95	42,37	42,37	42,20	226,00
Stipagrostis ciliata var. ciliata	21,79	27,18	69,55	7,20	119,00
Rhigozum trichotomum	9,72	12,13	81,69	52,40	0,00
Stipagrostis namaquensis	4,73	5,90	87,59	26,20	1,00
Lophiocarpus polystachyus	1,74	2,17	89,76	9,60	0,20
Aridaria noctiflora	1,43	1,78	91,54	0,00	7,40
Aristida adscensionis	1,22	1,52	93,06	5,60	0,00
Eriocephalus ambiguus	1,19	1,48	94,54	5,60	1,60
Stipagrostis fastigiata	0,73	0,92	95,46	5,40	2,80
Eragrostis procumbens	0,73	0,91	96,36	3,80	0,00
Salsola barbata	0,40	0,50	97,61	2,00	1,20
Salsola tuberculate	0,34	0,42	98,03	0,20	2,00
Aptosimum spinescens	0,33	0,42	98,45	0,40	1,80
Aizoon schellenbergii	0,23	0,28	98,73	0,00	1,40
Calobota spinescens	0,20	0,25	98,98	0,40	0,80

Key to column headings: Av. Dissim, Average dissimilarity; Contrib. %, Percentage contribution of each species to the average dissimilarity; Cumulative %, Cumulative contribution percentage; Mean abund., mean abundance per mapping unit.

Table B-16: Results for SIMPER, indicating the top fifteen plant species responsible for variations between mapping units B and I in the NMDS graphs.

Mapping unit B and I					
Taxon	**Av. dissim**	**Contrib. %**	**Cumulative %**	**Mean abund. B**	**Mean abund. I**
Stipagrostis obtuse	64,84	72,94	72,94	42,20	627,00
Stipagrostis ciliata var. ciliata	11,05	12,43	85,37	7,20	105,00
Rhigozum trichotomum	5,89	6,63	92,00	52,40	0,00
Stipagrostis namaquensis	2,93	3,29	95,29	26,20	0,00
Lophiocarpus polystachyus	1,06	1,19	96,48	9,60	0,00
Aristida adscensionis	0,69	0,78	97,26	5,60	0,00
Eriocephalus ambiguus	0,64	0,72	97,99	5,60	0,00
Stipagrostis fastigiata	0,60	0,67	98,65	5,40	0,00
Eragrostis procumbens	0,43	0,49	99,14	3,80	0,00
Salsola barbata	0,22	0,25	99,39	2,00	0,00
Enneapogon desvauxii	0,09	0,10	99,50	0,80	0,00
Salsola tuberculate	0,09	0,10	99,60	0,20	1,00
Aizoon schellenbergii	0,06	0,07	99,67	0,00	0,50
Lycium oxycarpum	0,06	0,07	99,74	0,20	0,50
Acanthopsis disperm	0,05	0,06	99,79	0,40	0,00

Key to column headings: Av. Dissim, Average dissimilarity; Contrib. %, Percentage contribution of each species to the average dissimilarity; Cumulative %, Cumulative contribution percentage; Mean abund., mean abundance per mapping unit.

Table B-17: Results for SIMPER, indicating the top fifteen plant species responsible for variations between mapping units B and J in the NMDS graphs.

Mapping unit B and J					
Taxon	**Av. dissim**	**Contrib. %**	**Cumulative %**	**Mean abund. B**	**Mean abund. J**
Stipagrostis obtuse	39,92	52,70	52,70	42,20	233,00
Rhigozum trichotomum	13,35	17,63	70,32	52,40	1,40
Stipagrostis namaquensis	6,65	8,78	79,10	26,20	0,00
Stipagrostis fastigiata	2,96	3,91	83,01	5,40	17,20
Lophiocarpus polystachyus	2,38	3,14	86,16	9,60	0,40
Aristida adscensionis	1,90	2,51	88,67	5,60	0,00
Stipagrostis ciliata var. ciliata	1,80	2,37	91,04	7,20	3,80
Eriocephalus ambiguus	1,78	2,35	93,39	5,60	3,00
Calobota spinescens	1,16	1,53	94,92	0,40	5,20
Eragrostis procumbens	1,05	1,38	96,30	3,80	0,00
Salsola barbata	0,76	1,01	97,31	2,00	3,80
Acanthopsis disperma	0,51	0,67	97,98	0,40	1,60
Zygophyllum microphyllum	0,32	0,42	98,40	0,00	2,00
Aptosimum spinescens	0,31	0,41	98,81	0,40	1,00
Enneapogon desvauxii	0,23	0,30	99,11	0,80	0,00

Key to column headings: Av. Dissim, Average dissimilarity; Contrib. %, Percentage contribution of each species to the average dissimilarity; Cumulative %, Cumulative contribution percentage; Mean abund., mean abundance per mapping unit.

Table B-18: Results for SIMPER, indicating the top fifteen plant species responsible for variations between mapping units C and D in the NMDS graphs.

Mapping unit C and D					
Taxon	**Av. dissim**	**Contrib. %**	**Cumulative %**	**Mean abund. C**	**Mean abund. D**
Stipagrostis obtuse	12,56	26,87	26,87	67,60	81,20
Rhigozum trichotomum	8,21	17,55	44,42	46,20	15,60
Stipagrostis ciliata var. ciliata	7,46	15,95	60,37	33,80	52,80
Stipagrostis fastigiata	5,76	12,31	72,68	6,60	22,20
Eriocephalus ambiguus	1,59	3,40	76,08	4,20	5,80
Aizoon schellenbergii	1,54	3,28	79,36	0,20	5,40
Aristida adscensionis	1,40	2,99	82,35	5,60	0,00
Salsola tuberculate	1,33	2,84	85,19	4,60	2,80
Stipagrostis namaquensis	1,30	2,78	87,97	2,40	4,20
Lycium oxycarpum	0,69	1,49	89,45	2,40	0,60
Lycium bosciifolium	0,66	1,41	90,86	0,60	3,00
Eragrostis procumbens	0,63	1,34	92,20	1,60	1,20
Lophiocarpus polystachyus	0,62	1,33	93,53	2,40	0,40
Calobota spinescens	0,58	1,25	94,78	1,20	1,60
Aptosimum spinescens	0,51	1,09	95,87	1,80	1,00

Key to column headings: Av. Dissim, Average dissimilarity; Contrib. %, Percentage contribution of each species to the average dissimilarity; Cumulative %, Cumulative contribution percentage; Mean abund., mean abundance per mapping unit.

Table B-19: Results for SIMPER, indicating the top fifteen plant species responsible for variations between mapping units C and E in the NMDS graphs.

Mapping unit C and E					
Taxon	**Av. dissim**	**Contrib. %**	**Cumulative %**	**Mean abund. C**	**Mean abund. E**
Stipagrostis obtuse	28,64	43,00	43,00	67,60	249,00
Aridaria noctiflora	11,68	17,53	60,53	1,00	73,40
Rhigozum trichotomum	8,12	12,20	72,73	46,20	2,60
Stipagrostis ciliata var. ciliata	5,61	8,42	81,15	33,80	35,20
Salsola barbata	2,73	4,10	85,25	1,20	11,80
Stipagrostis namaquensis	1,88	2,82	88,06	2,40	10,60
Salsola tuberculate	1,33	2,00	90,06	4,60	8,20
Stipagrostis fastigiata	1,33	1,99	92,05	6,60	1,40
Zygophyllum microphyllum	1,08	1,62	93,67	0,40	8,00
Aristida adscensionis	0,98	1,47	95,14	5,60	0,00
Eriocephalus ambiguus	0,72	1,09	96,23	4,20	0,20
Lycium oxycarpum	0,45	0,67	96,90	2,40	0,40
Lophiocarpus polystachyus	0,41	0,61	97,51	2,40	0,20
Aptosimum spinescens	0,36	0,54	98,06	1,80	1,00
Eragrostis procumbens	0,28	0,42	98,47	1,60	0,00

Key to column headings: Av. Dissim, Average dissimilarity; Contrib. %, Percentage contribution of each species to the average dissimilarity; Cumulative %, Cumulative contribution percentage; Mean abund., mean abundance per mapping unit.

Table B-20: Results for SIMPER, indicating the top fifteen plant species responsible for variations between mapping units C and F in the NMDS graphs.

Mapping unit C and F					
Taxon	**Av. dissim**	**Contrib. %**	**Cumulative %**	**Mean abund. C**	**Mean abund. F**
Stipagrostis obtuse	47,66	63,96	63,96	67,60	427,00
Aridaria noctiflora	8,93	11,98	75,95	1,00	68,50
Rhigozum trichotomum	6,11	8,20	84,14	46,20	0,00
Stipagrostis ciliata var. ciliata	5,81	7,80	91,94	33,80	59,50
Salsola tuberculate	1,57	2,11	94,05	4,60	13,00
Stipagrostis fastigiata	0,84	1,13	95,18	6,60	0,00
Aristida adscensionis	0,71	0,96	96,14	5,60	0,00
Eriocephalus ambiguus	0,50	0,67	96,81	4,20	0,50
Lophiocarpus polystachyus	0,32	0,42	97,23	2,40	0,00
Stipagrostis namaquensis	0,31	0,42	97,66	2,40	0,00
Lycium oxycarpum	0,31	0,42	98,08	2,40	0,50
Aptosimum spinescens	0,23	0,31	98,39	1,80	0,00
Eragrostis procumbens	0,20	0,27	98,66	1,60	0,00
Salsola barbata	0,16	0,22	98,88	1,20	0,00
Calobota spinescens	0,16	0,21	99,09	1,20	0,00
Hoodia gordonii	0,13	0,18	99,27	0,00	1,00

Key to column headings: Av. Dissim, Average dissimilarity; Contrib. %, Percentage contribution of each species to the average dissimilarity; Cumulative %, Cumulative contribution percentage; Mean abund., mean abundance per mapping unit.

Table B-21: Results for SIMPER, indicating the top fifteen plant species responsible for variations between mapping units C and G in the NMDS graphs.

Mapping unit C and G					
Taxon	**Av. dissim**	**Contrib. %**	**Cumulative %**	**Mean abund. C**	**Mean abund. G**
Stipagrostis obtuse	30,68	50,49	50,49	67,60	220,00
Rhigozum trichotomum	9,53	15,68	66,16	46,20	0,00
Aridaria noctiflora	6,27	10,31	76,48	1,00	28,60
Stipagrostis ciliata var. ciliata	6,05	9,95	86,43	33,80	44,60
Stipagrostis fastigiata	1,77	2,91	89,33	6,60	3,80
Aristida adscensionis	1,09	1,79	91,13	5,60	0,00
Salsola tuberculate	1,02	1,67	92,80	4,60	3,80
Eriocephalus ambiguus	0,81	1,34	94,14	4,20	0,40
Lycium oxycarpum	0,52	0,85	94,98	2,40	0,80
Stipagrostis namaquensis	0,51	0,84	95,83	2,40	0,60
Lophiocarpus polystachyus	0,49	0,81	96,63	2,40	0,00
Aptosimum spinescens	0,42	0,70	97,33	1,80	1,40
Eragrostis procumbens	0,31	0,51	97,84	1,60	0,00
Salsola barbata	0,29	0,48	98,32	1,20	0,40
Calobota spinescens	0,27	0,45	98,77	1,20	0,60

Key to column headings: Av. Dissim, Average dissimilarity; Contrib. %, Percentage contribution of each species to the average dissimilarity; Cumulative %, Cumulative contribution percentage; Mean abund., mean abundance per mapping unit.

Table B-22: Results for SIMPER, indicating the top fifteen plant species responsible for variations between mapping units C and H in the NMDS graphs.

Mapping unit C and H					
Taxon	**Av. dissim**	**Contrib. %**	**Cumulative %**	**Mean abund. C**	**Mean abund. H**
Stipagrostis obtuse	27,60	44,92	44,92	67,60	226,00
Stipagrostis ciliata var. ciliata	15,93	25,93	70,85	33,80	119,00
Rhigozum trichotomum	8,37	13,62	84,47	46,20	0,00
Stipagrostis fastigiata	1,47	2,39	86,86	6,60	2,80
Aridaria noctiflora	1,40	2,28	89,14	1,00	7,40
Aristida adscensionis	0,96	1,57	90,71	5,60	0,00
Eriocephalus ambiguus	0,79	1,28	91,99	4,20	1,60
Salsola tuberculate	0,75	1,21	93,20	4,60	2,00
Stipagrostis namaquensis	0,50	0,81	94,90	2,40	1,00
Aptosimum spinescens	0,45	0,73	95,63	1,80	1,80
Lycium oxycarpum	0,44	0,72	96,35	2,40	0,60
Lophiocarpus polystachyus	0,41	0,66	97,02	2,40	0,20
Salsola barbata	0,33	0,54	97,55	1,20	1,20
Calobota spinescens	0,28	0,45	98,00	1,20	0,80
Eragrostis procumbens	0,28	0,45	98,45	1,60	0,00

Key to column headings: Av. Dissim, Average dissimilarity; Contrib. %, Percentage contribution of each species to the average dissimilarity; Cumulative %, Cumulative contribution percentage; Mean abund., mean abundance per mapping unit.

Table B-23: Results for SIMPER, indicating the top fifteen plant species responsible for variations between mapping units C and I in the NMDS graphs.

Mapping unit C and I					
Taxon	**Av. dissim**	**Contrib. %**	**Cumulative %**	**Mean abund. C**	**Mean abund. I**
Stipagrostis obtuse	60,21	77,89	77,89	67,60	627,00
Stipagrostis ciliata var. ciliata	7,80	10,09	87,98	33,80	105,00
Rhigozum trichotomum	5,12	6,62	94,60	46,20	0,00
Stipagrostis fastigiata	0,71	0,92	95,52	6,60	0,00
Aristida adscensionis	0,60	0,78	96,29	5,60	0,00
Salsola tuberculate	0,48	0,62	96,92	4,60	1,00
Eriocephalus ambiguus	0,45	0,59	97,51	4,20	0,00
Lophiocarpus polystachyus	0,26	0,34	97,85	2,40	0,00
Stipagrostis namaquensis	0,26	0,34	98,19	2,40	0,00
Lycium oxycarpum	0,26	0,34	98,52	2,40	0,50
Aptosimum spinescens	0,20	0,25	98,78	1,80	0,00
Eragrostis procumbens	0,17	0,22	99,00	1,60	0,00
Salsola barbata	0,14	0,18	99,18	1,20	0,00
Calobota spinescens	0,13	0,17	99,35	1,20	0,00
Aridaria noctiflora	0,11	0,15	99,50	1,00	0,00

Key to column headings: Av. Dissim, Average dissimilarity; Contrib. %, Percentage contribution of each species to the average dissimilarity; Cumulative %, Cumulative contribution percentage; Mean abund., mean abundance per mapping unit.

Table B-24: Results for SIMPER, indicating the top fifteen plant species responsible for variations between mapping units C and J in the NMDS graphs.

Mapping unit C and J					
Taxon	**Av. dissim**	**Contrib. %**	**Cumulative %**	**Mean abund. C**	**Mean abund. J**
Stipagrostis obtuse	32,98	50,27	50,27	67,60	233,00
Rhigozum trichotomum	11,18	17,05	67,32	46,20	1,40
Stipagrostis ciliata var. ciliata	7,47	11,39	78,71	33,80	3,80
Stipagrostis fastigiata	3,99	6,09	84,80	6,60	17,20
Aristida adscensionis	1,29	1,96	86,76	5,60	0,00
Eriocephalus ambiguus	1,22	1,86	88,62	4,20	3,00
Salsola tuberculate	1,08	1,65	90,27	4,60	0,40
Calobota spinescens	0,98	1,50	91,77	1,20	5,20
Salsola barbata	0,77	1,17	92,94	1,20	3,80
Lycium oxycarpum	0,62	0,95	93,89	2,40	0,40
Stipagrostis namaquensis	0,58	0,89	94,78	2,40	0,00
Lophiocarpus polystachyus	0,58	0,88	95,65	2,40	0,40
Acanthopsis disperma	0,49	0,74	96,39	0,00	1,60
Aptosimum spinescens	0,48	0,73	97,13	1,80	1,00
Zygophyllum microphyllum	0,38	0,58	97,70	0,40	2,00

Key to column headings: Av. Dissim, Average dissimilarity; Contrib. %, Percentage contribution of each species to the average dissimilarity; Cumulative %, Cumulative contribution percentage; Mean abund., mean abundance per mapping unit.

Table B-25: Results for SIMPER, indicating the top fifteen plant species responsible for variations between mapping units D and E in the NMDS graphs.

Mapping unit D and E					
Taxon	**Av. dissim**	**Contrib. %**	**Cumulative %**	**Mean abund. D**	**Mean abund. E**
Stipagrostis obtuse	27,71	43,24	43,24	81,20	249,00
Aridaria noctiflora	11,49	17,93	61,17	0,20	73,40
Stipagrostis ciliata var. ciliata	7,29	11,37	72,54	52,80	35,20
Stipagrostis fastigiata	3,65	5,70	78,24	22,20	1,40
Salsola barbata	2,75	4,28	82,52	0,00	11,80
Rhigozum trichotomum	2,56	3,99	86,51	15,60	2,60
Stipagrostis namaquensis	2,02	3,16	89,67	4,20	10,60
Salsola tuberculate	1,35	2,11	91,78	2,80	8,20
Zygophyllum microphyllum	1,04	1,62	93,40	0,00	8,00
Eriocephalus ambiguus	1,01	1,58	94,98	5,80	0,20
Aizoon schellenbergii	0,99	1,54	96,52	5,40	0,60
Lycium bosciifolium	0,49	0,77	97,29	3,00	0,00
Acanthopsis disperma	0,34	0,54	97,83	2,20	0,40
Calobota spinescens	0,26	0,41	98,24	1,60	0,00
Aptosimum spinescens	0,24	0,38	98,62	1,00	1,00

Key to column headings: Av. Dissim, Average dissimilarity; Contrib. %, Percentage contribution of each species to the average dissimilarity; Cumulative %, Cumulative contribution percentage; Mean abund., mean abundance per mapping unit.

Table B-26: Results for SIMPER, indicating the top fifteen plant species responsible for variations between mapping units D and F in the NMDS graphs.

Mapping unit D and F					
Taxon	**Av. dissim**	**Contrib. %**	**Cumulative %**	**Mean abund. D**	**Mean abund. F**
Stipagrostis obtuse	46,03	64,96	64,96	81,20	427,00
Aridaria noctiflora	8,83	12,45	77,42	0,20	68,50
Stipagrostis ciliata var. ciliata	5,79	8,17	85,59	52,80	59,50
Stipagrostis fastigiata	2,85	4,02	89,61	22,20	0,00
Rhigozum trichotomum	2,07	2,91	92,53	15,60	0,00
Salsola tuberculate	1,59	2,24	94,77	2,80	13,00
Aizoon schellenbergii	0,73	1,03	95,80	5,40	0,00
Eriocephalus ambiguus	0,71	1,00	96,80	5,80	0,50
Stipagrostis namaquensis	0,51	0,72	97,52	4,20	0,00
Lycium bosciifolium	0,36	0,51	98,03	3,00	0,00
Acanthopsis disperma	0,24	0,34	98,38	2,20	0,00
Calobota spinescens	0,20	0,28	98,66	1,60	0,00
Eragrostis procumbens	0,17	0,24	98,89	1,20	0,00
Zygophyllum microphyllum	0,13	0,19	99,08	0,00	1,00
Hoodia gordonii	0,13	0,19	99,27	0,00	1,00

Key to column headings: Av. Dissim, Average dissimilarity; Contrib. %, Percentage contribution of each species to the average dissimilarity; Cumulative %, Cumulative contribution percentage; Mean abund., mean abundance per mapping unit.

Table B-27: Results for SIMPER, indicating the top fifteen plant species responsible for variations between mapping units D and G in the NMDS graphs.

Mapping unit D and G					
Taxon	**Av. dissim**	**Contrib. %**	**Cumulative %**	**Mean abund. D**	**Mean abund.G**
Stipagrostis obtuse	29,33	51,12	51,12	81,20	220,00
Stipagrostis ciliata var. ciliata	8,08	14,09	65,21	52,80	44,60
Aridaria noctiflora	6,25	10,90	76,11	0,20	28,60
Stipagrostis fastigiata	3,89	6,79	82,90	22,20	3,80
Rhigozum trichotomum	3,24	5,65	88,55	15,60	0,00
Aizoon schellenbergii	1,17	2,04	90,59	5,40	0,00
Eriocephalus ambiguus	1,10	1,91	92,50	5,80	0,40
Salsola tuberculate	0,89	1,56	94,06	2,80	3,80
Stipagrostis namaquensis	0,81	1,42	95,48	4,20	0,60
Lycium bosciifolium	0,55	0,95	96,43	3,00	0,00
Acanthopsis disperma	0,38	0,65	97,08	2,20	0,20
Calobota spinescens	0,37	0,65	97,73	1,60	0,60
Aptosimum spinescens	0,33	0,58	98,31	1,00	1,40
Eragrostis procumbens	0,27	0,47	98,77	1,20	0,00
Lycium oxycarpum	0,22	0,38	99,16	0,60	0,80

Key to column headings: Av. Dissim, Average dissimilarity; Contrib. %, Percentage contribution of each species to the average dissimilarity; Cumulative %, Cumulative contribution percentage; Mean abund., mean abundance per mapping unit.

Table B-28: Results for SIMPER, indicating the top fifteen plant species responsible for variations between mapping units D and H in the NMDS graphs.

Mapping unit D and H					
Taxon	**Av. dissim**	**Contrib. %**	**Cumulative %**	**Mean abund. D**	**Mean abund. H**
Stipagrostis obtuse	26,53	49,51	49,51	81,20	226,00
Stipagrostis ciliata var. ciliata	13,16	24,56	74,07	52,80	119,00
Stipagrostis fastigiata	3,42	6,39	80,45	22,20	2,80
Rhigozum trichotomum	2,84	5,30	85,75	15,60	0,00
Aridaria noctiflora	1,35	2,52	88,27	0,20	7,40
Aizoon schellenbergii	0,97	1,80	90,08	5,40	1,40
Eriocephalus ambiguus	0,83	1,56	91,63	5,80	1,60
Stipagrostis namaquensis	0,77	1,44	93,07	4,20	1,00
Aristida adscensionis	0,57	1,06	94,13	0,00	3,00
Salsola tuberculate	0,55	1,03	95,16	2,80	2,00
Lycium bosciifolium	0,44	0,82	95,98	3,00	0,40
Aptosimum spinescens	0,37	0,68	96,66	1,00	1,80
Calobota spinescens	0,36	0,66	97,33	1,60	0,80
Acanthopsis disperma	0,34	0,63	97,96	2,20	0,20
Eragrostis procumbens	0,23	0,44	98,39	1,20	0,00

Key to column headings: Av. Dissim, Average dissimilarity; Contrib. %, Percentage contribution of each species to the average dissimilarity; Cumulative %, Cumulative contribution percentage; Mean abund., mean abundance per mapping unit.

Table B-29: Results for SIMPER, indicating the top fifteen plant species responsible for variations between mapping units D and I in the NMDS graphs.

Mapping unit D and I					
Taxon	**Av. dissim**	**Contrib. %**	**Cumulative %**	**Mean abund. D**	**Mean abund. I**
Stipagrostis obtuse	58,58	81,83	81,83	81,20	627,00
Stipagrostis ciliata var. ciliata	5,73	8,00	89,83	52,80	105,00
Stipagrostis fastigiata	2,40	3,35	93,17	22,20	0,00
Rhigozum trichotomum	1,73	2,41	95,59	15,60	0,00
Eriocephalus ambiguus	0,63	0,87	96,46	5,80	0,00
Aizoon schellenbergii	0,57	0,80	97,26	5,40	0,50
Stipagrostis namaquensis	0,43	0,61	97,87	4,20	0,00
Lycium bosciifolium	0,31	0,43	98,30	3,00	0,00
Salsola tuberculate	0,29	0,41	98,71	2,80	1,00
Acanthopsis disperma	0,21	0,29	99,00	2,20	0,00
Calobota spinescens	0,17	0,23	99,23	1,60	0,00
Eragrostis procumbens	0,14	0,19	99,43	1,20	0,00
Aptosimum spinescens	0,11	0,15	99,58	1,00	0,00
Lycium oxycarpum	0,11	0,15	99,73	0,60	0,50
Zygophyllum microcarpum	0,10	0,13	99,86	1,00	0,00

Key to column headings: Av. Dissim, Average dissimilarity; Contrib. %, Percentage contribution of each species to the average dissimilarity; Cumulative %, Cumulative contribution percentage; Mean abund., mean abundance per mapping unit.

Table B-30: Results for SIMPER, indicating the top fifteen plant species responsible for variations between mapping units D and J in the NMDS graphs.

Mapping unit D and J					
Taxon	**Av. dissim**	**Contrib. %**	**Cumulative %**	**Mean abund. D**	**Mean abund. J**
Stipagrostis obtuse	33,30	52,35	52,35	81,20	233,00
Stipagrostis ciliata var. ciliata	11,75	18,47	70,83	52,80	3,80
Stipagrostis fastigiata	5,16	8,12	78,94	22,20	17,20
Rhigozum trichotomum	3,66	5,76	84,70	15,60	1,40
Eriocephalus ambiguus	1,51	2,37	87,07	5,80	3,00
Aizoon schellenbergii	1,45	2,27	89,34	5,40	0,00
Calobota spinescens	1,15	1,80	91,14	1,60	5,20
Stipagrostis namaquensis	0,88	1,39	92,53	4,20	0,00
Salsola barbata	0,81	1,28	93,81	0,00	3,80
Acanthopsis disperma	0,74	1,17	94,97	2,20	1,60
Salsola tuberculate	0,71	1,11	96,08	2,80	0,40
Lycium bosciifolium	0,64	1,01	97,09	3,00	0,00
Aptosimum spinescens	0,35	0,54	97,64	1,00	1,00
Eragrostis procumbens	0,33	0,52	98,16	1,20	0,00
Zygophyllum microphyllum	0,30	0,47	98,63	0,00	2,00

Key to column headings: Av. Dissim, Average dissimilarity; Contrib. %, Percentage contribution of each species to the average dissimilarity; Cumulative %, Cumulative contribution percentage; Mean abund., mean abundance per mapping unit.

Table B-31: Results for SIMPER, indicating the top fifteen plant species responsible for variations between mapping units E and F in the NMDS graphs.

Mapping unit E and F					
Taxon	**Av. dissim**	**Contrib. %**	**Cumulative %**	**Mean abund. E**	**Mean abund. F**
Stipagrostis obtuse	24,54	55,65	55,65	249,00	427,00
Aridaria noctiflora	9,02	20,46	76,10	73,40	68,50
Stipagrostis ciliata var. ciliata	5,13	11,64	87,75	35,20	59,50
Salsola barbata	1,45	3,29	91,04	11,80	0,00
Salsola tuberculate	1,23	2,80	93,84	8,20	13,00
Stipagrostis namaquensis	1,00	2,28	96,12	10,60	0,00
Zygophyllum microphyllum	0,73	1,66	97,77	8,00	1,00
Rhigozum trichotomum	0,25	0,56	98,33	2,60	0,00
Stipagrostis fastigiata	0,16	0,35	98,68	1,40	0,00
Hoodia gordonii	0,11	0,24	98,93	0,00	1,00
Aptosimum spinescens	0,08	0,18	99,11	1,00	0,00
Aizoon schellenbergii	0,06	0,13	99,24	0,60	0,00
Aristida adscensionis	0,05	0,12	99,36	0,00	0,50
Lycium oxycarpum	0,05	0,12	99,48	0,40	0,50
Eriocephalus ambiguus	0,05	0,12	99,60	0,20	0,50

Key to column headings: Av. Dissim, Average dissimilarity; Contrib. %, Percentage contribution of each species to the average dissimilarity; Cumulative %, Cumulative contribution percentage; Mean abund., mean abundance per mapping unit.

Table B-32: Results for SIMPER, indicating the top fifteen plant species responsible for variations between mapping units E and G in the NMDS graphs.

Mapping unit E and G					
Taxon	**Av. dissim**	**Contrib. %**	**Cumulative %**	**Mean abund. E**	**Mean abund. G**
Stipagrostis obtuse	13,34	35,31	35,31	249,00	220,00
Aridaria noctiflora	11,12	29,42	64,74	73,40	28,60
Stipagrostis ciliata var. ciliata	5,90	15,60	80,34	35,20	44,60
Salsola barbata	2,17	5,73	86,07	11,80	0,40
Stipagrostis namaquensis	1,41	3,72	89,79	10,60	0,60
Salsola tuberculate	1,08	2,87	92,65	8,20	3,80
Zygophyllum microphyllum	0,92	2,43	95,09	8,00	0,20
Stipagrostis fastigiata	0,61	1,62	96,71	1,40	3,80
Rhigozum trichotomum	0,33	0,87	97,58	2,60	0,00
Aptosimum spinescens	0,24	0,63	98,21	1,00	1,40
Lycium oxycarpum	0,12	0,32	98,53	0,40	0,80
Calobota spinescens	0,09	0,24	98,77	0,00	0,60
Eriocephalus ambiguus	0,08	0,22	98,98	0,20	0,40
Aizoon schellenbergii	0,08	0,20	99,19	0,60	0,00
Zygophyllum microcarpum	0,07	0,19	99,37	0,40	0,20

Key to column headings: Av. Dissim, Average dissimilarity; Contrib. %, Percentage contribution of each species to the average dissimilarity; Cumulative %, Cumulative contribution percentage; Mean abund., mean abundance per mapping unit.

Table B-33: Results for SIMPER, indicating the top fifteen plant species responsible for variations between mapping units E and H in the NMDS graphs.

Mapping unit E and H					
Taxon	**Av. dissim**	**Contrib. %**	**Cumulative %**	**Mean abund. E**	**Mean abund. H**
Stipagrostis obtuse	14,11	32,37	32,37	249,00	226,00
Stipagrostis ciliata var. ciliata	12,67	29,07	61,44	35,20	119,00
Aridaria noctiflora	9,28	21,29	82,74	73,40	7,40
Salsola barbata	1,92	4,40	87,14	11,80	1,20
Stipagrostis namaquensis	1,33	3,06	90,19	10,60	1,00
Salsola tuberculate	1,02	2,33	92,52	8,20	2,00
Zygophyllum microphyllum	0,86	1,98	94,50	8,00	0,40
Aristida adscensionis	0,42	0,97	95,48	0,00	3,00
Stipagrostis fastigiata	0,35	0,79	96,27	1,40	2,80
Rhigozum trichotomum	0,31	0,70	96,97	2,60	0,00
Aptosimum spinescens	0,27	0,63	97,60	1,00	1,80
Eriocephalus ambiguus	0,23	0,53	98,13	0,20	1,60
Aizoon schellenbergii	0,21	0,49	98,62	0,60	1,40
Calobota spinescens	0,11	0,25	98,87	0,00	0,80
Lycium oxycarpum	0,09	0,21	99,09	0,40	0,60

Key to column headings: Av. Dissim, Average dissimilarity; Contrib. %, Percentage contribution of each species to the average dissimilarity; Cumulative %, Cumulative contribution percentage; Mean abund., mean abundance per mapping unit.

Table B-34: Results for SIMPER, indicating the top fifteen plant species responsible for variations between mapping units E and I in the NMDS graphs.

Mapping unit E and I					
Taxon	**Av. dissim**	**Contrib. %**	**Cumulative %**	**Mean abund. E**	**Mean abund. I**
Stipagrostis obtuse	35,10	67,26	67,26	249,00	627,00
Stipagrostis ciliata var. ciliata	6,67	12,78	80,05	35,20	105,00
Aridaria noctiflora	6,28	12,04	92,08	73,40	0,00
Salsola barbata	1,23	2,36	94,44	11,80	0,00
Stipagrostis namaquensis	0,88	1,69	96,12	10,60	0,00
Salsola tuberculate	0,69	1,32	97,44	8,20	1,00
Zygophyllum microphyllum	0,61	1,18	98,62	8,00	0,00
Rhigozum trichotomum	0,22	0,41	99,03	2,60	0,00
Stipagrostis fastigiata	0,13	0,26	99,29	1,40	0,00
Aizoon schellenbergii	0,08	0,16	99,44	0,60	0,50
Aptosimum spinescens	0,07	0,14	99,58	1,00	0,00
Lycium oxycarpum	0,05	0,09	99,67	0,40	0,50
Pteronia mucronata	0,03	0,06	99,73	0,40	0,00
Zygophyllum microcarpum	0,03	0,06	99,80	0,40	0,00
Acanthopsis disperma	0,03	0,05	99,85	0,40	0,00

Key to column headings: Av. Dissim, Average dissimilarity; Contrib. %, Percentage contribution of each species to the average dissimilarity; Cumulative %, Cumulative contribution percentage; Mean abund., mean abundance per mapping unit.

Table B-35: Results for SIMPER, indicating the top fifteen plant species responsible for variations between mapping units E and J in the NMDS graphs.

Mapping unit E and J					
Taxon	**Av. dissim**	**Contrib. %**	**Cumulative %**	**Mean abund. E**	**Mean abund. J**
Stipagrostis obtuse	23,20	46,72	46,72	249,00	233,00
Aridaria noctiflora	10,69	21,52	68,24	73,40	0,00
Stipagrostis ciliata var. ciliata	4,41	8,87	77,11	35,20	3,80
Salsola barbata	2,49	5,01	82,12	11,80	3,80
Stipagrostis fastigiata	2,21	4,45	86,57	1,40	17,20
Stipagrostis namaquensis	1,46	2,94	89,51	10,60	0,00
Salsola tuberculate	1,33	2,68	92,19	8,20	0,40
Zygophyllum microphyllum	1,06	2,13	94,31	8,00	2,00
Calobota spinescens	0,80	1,61	95,92	0,00	5,20
Rhigozum trichotomum	0,50	1,00	96,92	2,60	1,40
Eriocephalus ambiguus	0,39	0,79	97,71	0,20	3,00
Acanthopsis disperma	0,32	0,65	98,36	0,40	1,60
Aptosimum spinescens	0,24	0,48	98,84	1,00	1,00
Lophiocarpus polystachyus	0,08	0,17	99,01	0,20	0,40
Aizoon schellenbergii	0,08	0,17	99,17	0,60	0,00

Key to column headings: Av. Dissim, Average dissimilarity; Contrib. %, Percentage contribution of each species to the average dissimilarity; Cumulative %, Cumulative contribution percentage; Mean abund., mean abundance per mapping unit.

Table B-36: Results for SIMPER, indicating the top fifteen plant species responsible for variations between mapping units F and G in the NMDS graphs.

Mapping unit F and G					
Taxon	**Av. dissim**	**Contrib. %**	**Cumulative %**	**Mean abund. F**	**Mean abund. G**
Stipagrostis obtuse	24,01	59,93	59,93	427,00	220,00
Aridaria noctiflora	7,78	19,43	79,36	68,50	28,60
Stipagrostis ciliata var. ciliata	5,61	14,00	93,36	59,50	44,60
Salsola tuberculate	1,36	3,39	96,76	13,00	3,80
Stipagrostis fastigiata	0,43	1,08	97,84	0,00	3,80
Aptosimum spinescens	0,15	0,37	98,21	0,00	1,40
Hoodia gordonii	0,12	0,29	98,49	1,00	0,00
Zygophyllum microphyllum	0,12	0,29	98,78	1,00	0,20
Lycium oxycarpum	0,10	0,24	99,03	0,50	0,80
Eriocephalus ambiguus	0,08	0,20	99,23	0,50	0,40
Stipagrostis namaquensis	0,07	0,17	99,40	0,00	0,60
Calobota spinescens	0,07	0,17	99,57	0,00	0,60
Aristida adscensionis	0,06	0,14	99,72	0,50	0,00
Salsola barbata	0,05	0,11	99,83	0,00	0,40
Zygophyllum microcarpum	0,02	0,06	99,89	0,00	0,20

Key to column headings: Av. Dissim, Average dissimilarity; Contrib. %, Percentage contribution of each species to the average dissimilarity; Cumulative %, Cumulative contribution percentage; Mean abund., mean abundance per mapping unit.

Table B-37: Results for SIMPER, indicating the top fifteen plant species responsible for variations between mapping units F and H in the NMDS graphs.

Mapping unit F and H					
Taxon	**Av. dissim**	**Contrib. %**	**Cumulative %**	**Mean abund. F**	**Mean abund. H**
Stipagrostis obtuse	22,46	55,31	55,31	427,00	226,00
Stipagrostis ciliata var. ciliata	7,82	19,25	74,56	59,50	119,00
Aridaria noctiflora	7,22	17,77	92,33	68,50	7,40
Salsola tuberculate	1,25	3,08	95,40	13,00	2,00
Stipagrostis fastigiata	0,31	0,76	96,16	0,00	2,80
Aristida adscensionis	0,30	0,73	96,88	0,50	3,00
Eriocephalus ambiguus	0,19	0,46	97,34	0,50	1,60
Aptosimum spinescens	0,18	0,44	97,78	0,00	1,80
Aizoon schellenbergii	0,14	0,34	98,11	0,00	1,40
Salsola barbata	0,13	0,32	98,44	0,00	1,20
Hoodia gordonii	0,11	0,26	98,70	1,00	0,00
Zygophyllum microphyllum	0,11	0,26	98,97	1,00	0,40
Stipagrostis namaquensis	0,11	0,26	99,23	0,00	1,00
Calobota spinescens	0,09	0,21	99,44	0,00	0,80
Lycium oxycarpum	0,07	0,18	99,63	0,50	0,60

Key to column headings: Av. Dissim, Average dissimilarity; Contrib. %, Percentage contribution of each species to the average dissimilarity; Cumulative %, Cumulative contribution percentage; Mean abund., mean abundance per mapping unit.

Table B-38: Results for SIMPER, indicating the top fifteen plant species responsible for variations between mapping units F and I in the NMDS graphs.

Mapping unit F and I					
Taxon	**Av. dissim**	**Contrib. %**	**Cumulative %**	**Mean abund. F**	**Mean abund. I**
Stipagrostis obtuse	14,75	59,20	59,20	427,00	627,00
Aridaria noctiflora	5,25	21,07	80,27	68,50	0,00
Stipagrostis ciliata var. ciliata	3,67	14,72	94,99	59,50	105,00
Salsola tuberculate	0,93	3,75	98,74	13,00	1,00
Zygophyllum microphyllum	0,08	0,31	99,05	1,00	0,00
Hoodia gordonii	0,08	0,31	99,37	1,00	0,00
Aizoon schellenbergii	0,04	0,17	99,53	0,00	0,50
Aristida adscensionis	0,04	0,16	99,69	0,50	0,00
Lycium oxycarpum	0,04	0,16	99,85	0,50	0,50
Eriocephalus ambiguus	0,04	0,15	100,00	0,50	0,00
Eragrostis procumbens	0,00	0,00	100,00	0,00	0,00
Kleinia longiflora	0,00	0,00	100,00	0,00	0,00
Salsola barbata	0,00	0,00	100,00	0,00	0,00
Zygophyllum microcarpum	0,00	0,00	100,00	0,00	0,00
Eragrostis lehmanniana var. lehmanniana	0,00	0,00	100,00	0,00	0,00

Key to column headings: Av. Dissim, Average dissimilarity; Contrib. %, Percentage contribution of each species to the average dissimilarity; Cumulative %, Cumulative contribution percentage; Mean abund., mean abundance per mapping unit.

Table B-39: Results for SIMPER, indicating the top fifteen plant species responsible for variations between mapping units F and J in the NMDS graphs.

Mapping unit F and J					
Taxon	**Av. dissim**	**Contrib. %**	**Cumulative %**	**Mean abund. F**	**Mean abund. J**
Stipagrostis obtuse	29,02	58,10	58,10	427,00	233,00
Aridaria noctiflora	8,28	16,57	74,68	68,50	0,00
Stipagrostis ciliata var. ciliata	6,73	13,48	88,15	59,50	3,80
Stipagrostis fastigiata	1,85	3,70	91,85	0,00	17,20
Salsola tuberculate	1,55	3,11	94,96	13,00	0,40
Calobota spinescens	0,59	1,19	96,14	0,00	5,20
Salsola barbata	0,43	0,86	97,00	0,00	3,80
Eriocephalus ambiguus	0,34	0,68	97,68	0,50	3,00
Zygophyllum microphyllum	0,28	0,55	98,23	1,00	2,00
Acanthopsis disperma	0,22	0,44	98,68	0,00	1,60
Rhigozum trichotomum	0,16	0,32	99,00	0,00	1,40
Aptosimum spinescens	0,13	0,26	99,26	0,00	1,00
Hoodia gordonii	0,12	0,25	99,50	1,00	0,00
Aristida adscensionis	0,06	0,12	99,63	0,50	0,20
Lycium oxycarpum	0,06	0,12	99,75	0,50	0,40

Key to column headings: Av. Dissim, Average dissimilarity; Contrib. %, Percentage contribution of each species to the average dissimilarity; Cumulative %, Cumulative contribution percentage; Mean abund., mean abundance per mapping unit.

Table B-40: Results for SIMPER, indicating the top fifteen plant species responsible for variations between mapping units G and H in the NMDS graphs.

Mapping unit G and H					
Taxon	**Av. dissim**	**Contrib. %**	**Cumulative %**	**Mean abund. G**	**Mean abund. H**
Stipagrostis ciliata var. ciliata	12,87	41,35	41,35	44,60	119,00
Stipagrostis obtuse	10,53	33,84	75,19	220,00	226,00
Aridaria noctiflora	4,21	13,53	88,72	28,60	7,40
Stipagrostis fastigiata	0,67	2,14	90,86	3,80	2,80
Salsola tuberculate	0,52	1,67	92,52	3,80	2,00
Aristida adscensionis	0,47	1,50	94,03	0,00	3,00
Aptosimum spinescens	0,34	1,09	95,12	1,40	1,80
Eriocephalus ambiguus	0,26	0,84	95,96	0,40	1,60
Stipagrostis namaquensis	0,20	0,65	96,61	0,60	1,00
Salsola barbata	0,20	0,63	97,24	0,40	1,20
Aizoon schellenbergii	0,18	0,59	97,84	0,00	1,40
Calobota spinescens	0,17	0,56	98,40	0,60	0,80
Lycium oxycarpum	0,14	0,46	98,86	0,80	0,60
Lycium bosciifolium	0,06	0,20	99,06	0,00	0,40
Zygophyllum microphyllum	0,06	0,20	99,26	0,20	0,40

Key to column headings: Av. Dissim, Average dissimilarity; Contrib. %, Percentage contribution of each species to the average dissimilarity; Cumulative %, Cumulative contribution percentage; Mean abund., mean abundance per mapping unit.

Table B-41: Results for SIMPER, indicating the top fifteen plant species responsible for variations between mapping units G and I in the NMDS graphs.

Mapping unit G and I					
Taxon	**Av. dissim**	**Contrib. %**	**Cumulative %**	**Mean abund. G**	**Mean abund. I**
Stipagrostis obtuse	38,58	78,09	78,09	220,00	627,00
Stipagrostis ciliata var. ciliata	6,66	13,47	91,57	44,60	105,00
Aridaria noctiflora	2,90	5,87	97,43	28,60	0,00
Stipagrostis fastigiata	0,37	0,75	98,18	3,80	0,00
Salsola tuberculate	0,35	0,72	98,90	3,80	1,00
Aptosimum spinescens	0,13	0,26	99,16	1,40	0,00
Lycium oxycarpum	0,09	0,17	99,33	0,80	0,50
Stipagrostis namaquensis	0,06	0,12	99,45	0,60	0,00
Calobota spinescens	0,06	0,12	99,57	0,60	0,00
Aizoon schellenbergii	0,05	0,11	99,68	0,00	0,50
Eriocephalus ambiguus	0,04	0,08	99,76	0,40	0,00
Salsola barbata	0,04	0,08	99,84	0,40	0,00
Zygophyllum microcarpum	0,02	0,04	99,88	0,20	0,00
Acanthopsis disperma	0,02	0,04	99,92	0,20	0,00
Zygophyllum microphyllum	0,02	0,04	99,96	0,20	0,00

Key to column headings: Av. Dissim, Average dissimilarity; Contrib. %, Percentage contribution of each species to the average dissimilarity; Cumulative %, Cumulative contribution percentage; Mean abund., mean abundance per mapping unit.

Table B-42: Results for SIMPER, indicating the top fifteen plant species responsible for variations between mapping units G and J in the NMDS graphs.

Mapping unit G and J					
Taxon	**Av. dissim**	**Contrib. %**	**Cumulative %**	**Mean abund. G**	**Mean abund. J**
Stipagrostis obtuse	22,37	53,03	53,03	220,00	233,00
Stipagrostis ciliata var. ciliata	7,13	16,91	69,94	44,60	3,80
Aridaria noctiflora	5,78	13,71	83,65	28,60	0,00
Stipagrostis fastigiata	2,58	6,12	89,76	3,80	17,20
Calobota spinescens	0,83	1,96	91,73	0,60	5,20
Salsola tuberculate	0,70	1,67	93,40	3,80	0,40
Salsola barbata	0,58	1,37	94,77	0,40	3,80
Eriocephalus ambiguus	0,47	1,11	95,87	0,40	3,00
Acanthopsis disperma	0,36	0,85	96,72	0,20	1,60
Aptosimum spinescens	0,31	0,75	97,46	1,40	1,00
Zygophyllum microphyllum	0,28	0,67	98,14	0,20	2,00
Rhigozum trichotomum	0,23	0,56	98,70	0,00	1,40
Lycium oxycarpum	0,14	0,34	99,04	0,80	0,40
Stipagrostis namaquensis	0,11	0,26	99,30	0,60	0,00
Asparagus retrofractus	0,08	0,19	99,49	0,20	0,40

Key to column headings: Av. Dissim, Average dissimilarity; Contrib. %, Percentage contribution of each species to the average dissimilarity; Cumulative %, Cumulative contribution percentage; Mean abund., mean abundance per mapping unit.

Table B-43: Results for SIMPER, indicating the top fifteen plant species responsible for variations between mapping units H and I in the NMDS graphs.

Mapping unit H and I					
Taxon	**Av. dissim**	**Contrib. %**	**Cumulative %**	**Mean abund. H**	**Mean abund. I**
Stipagrostis obtuse	35,91	85,48	85,48	226,00	627,00
Stipagrostis ciliata var. ciliata	3,77	8,98	94,46	119,00	105,00
Aridaria noctiflora	0,69	1,63	96,09	7,40	0,00
Aristida adscensionis	0,28	0,67	96,77	3,00	0,00
Stipagrostisfastigiata	0,26	0,63	97,39	2,80	0,00
Aptosimum spinescens	0,15	0,37	97,76	1,80	0,00
Eriocephalus ambiguus	0,15	0,36	98,12	1,60	0,00
Aizoon schellenbergii	0,15	0,36	98,48	1,40	0,50
Salsola tuberculate	0,13	0,30	98,78	2,00	1,00
Salsola barbata	0,11	0,27	99,05	1,20	0,00
Stipagrostis namaquensis	0,09	0,22	99,27	1,00	0,00
Calobota spinescens	0,07	0,18	99,45	0,80	0,00
Lycium oxycarpum	0,07	0,16	99,60	0,60	0,50
Lycium bosciifolium	0,04	0,09	99,70	0,40	0,00
Zygophyllum microphyllum	0,04	0,08	99,78	0,40	0,00

Key to column headings: Av. Dissim, Average dissimilarity; Contrib. %, Percentage contribution of each species to the average dissimilarity; Cumulative %, Cumulative contribution percentage; Mean abund., mean abundance per mapping unit.

Table B-44: Results for SIMPER, indicating the top fifteen plant species responsible for variations between mapping units H and J in the NMDS graphs.

Mapping unit H and J					
Taxon	**Av. dissim**	**Contrib. %**	**Cumulative %**	**Mean abund. H**	**Mean abund. J**
Stipagrostis obtuse	20,87	43,25	43,25	226,00	233,00
Stipagrostis ciliata var. ciliata	19,52	40,46	83,71	119,00	3,80
Stipagrostis fastigiata	2,08	4,31	88,02	2,80	17,20
Aridaria noctiflora	1,25	2,59	90,61	7,40	0,00
Calobota spinescens	0,73	1,50	92,11	0,80	5,20
Eriocephalus ambiguus	0,57	1,18	93,29	1,60	3,00
Aristida adscensionis	0,49	1,02	94,32	3,00	0,20
Salsola barbata	0,49	1,01	95,32	1,20	3,80
Aptosimum spinescens	0,35	0,72	96,04	1,80	1,00
Acanthopsis disperma	0,31	0,64	96,69	0,20	1,60
Zygophyllum microphyllum	0,28	0,58	97,27	0,40	2,00
Salsola tuberculate	0,27	0,57	97,83	2,00	0,40
Rhigozum trichotomum	0,21	0,44	98,27	0,00	1,40
Aizoon schellenbergii	0,20	0,42	98,69	1,40	0,00
Stipagrostis namaquensis	0,17	0,34	99,03	1,00	0,00

Key to column headings: Av. Dissim, Average dissimilarity; Contrib. %, Percentage contribution of each species to the average dissimilarity; Cumulative %, Cumulative contribution percentage; Mean abund., mean abundance per mapping unit.

Table B-45: Results for SIMPER, indicating the top fifteen plant species responsible for variations between mapping units I and J in the NMDS graphs.

Mapping unit I and J					
Taxon	**Av. dissim**	**Contrib. %**	**Cumulative %**	**Mean abund. I**	**Mean abund. J**
Stipagrostis obtuse	41,42	74,76	74,76	627,00	233,00
Stipagrostis ciliata var. ciliata	10,36	18,71	93,47	105,00	3,80
Stipagrostis fastigiata	1,59	2,87	96,34	0,00	17,20
Calobota spinescens	0,51	0,91	97,25	0,00	5,20
Salsola barbata	0,37	0,66	97,91	0,00	3,80
Eriocephalus ambiguus	0,26	0,47	98,38	0,00	3,00
Acanthopsis disperma	0,18	0,33	98,71	0,00	1,60
Zygophyllum microphyllum	0,17	0,30	99,01	0,00	2,00
Rhigozum trichotomum	0,14	0,25	99,26	0,00	1,40
Aptosimum spinescens	0,11	0,20	99,45	0,00	1,00
Aizoon schellenbergii	0,06	0,11	99,56	0,50	0,00
Salsola tuberculate	0,06	0,10	99,66	1,00	0,40
Lycium oxycarpum	0,05	0,10	99,76	0,50	0,40
Lophiocarpus polystachyus	0,03	0,06	99,82	0,00	0,40
Asparagus retrofractus	0,03	0,06	99,88	0,00	0,40

Key to column headings: Av. Dissim, Average dissimilarity; Contrib. %, Percentage contribution of each species to the average dissimilarity; Cumulative %, Cumulative contribution percentage; Mean abund., mean abundance per mapping unit.

ANNEXURE C: SOIL DATA

LAND TYPE / *LANDTIPE* : **Ag3**

CLIMATE ZONE / *KLIMAATSONE* : 185S

Area / *Oppervlakte* : 529750 ha

Estimated area unavailable for agriculture

Beraamde oppervlakte onbeskikbaar vir landbou : 2520 ha

Occurrence (maps) and areas / *Voorkoms (kaarte) en oppervlakte* :

2818 Onseepkans (54250 ha) 2820 Upington (119200 ha)

2918 Pofadder (111920 ha) 2920 Kenhardt (244380 ha)

Inventory by / *Inventaris deur* :

R W Bruce, J P Coetzee & P R Swanepoel

Modal Profiles / *Modale profiele* :

P27 P437 P819

6393 11772 2151

Terrain unit / *Terreineenheid*	1	1(1)	2	3	3(1)	4	5
% of land type / *% van landtipe*	0.3	32	0.3	0.4	50	10	7
Area / *Oppervlakte (ha)*	1589	169520	1589	2119	264875	52975	37082
Slope / *Helling (%)*	0 - 8	0 - 2	>100	15 - 100	1 - 4	0 - 2	0 - 1
Slope length / *Hellingslengte (m)*	50 - 300	500 - 1500	10 - 100	50 - 400	1000 - 2500	300 - 1000	50 - 500
Slope shape / *Hellingsvorm*	Y	Y	Z	X	Z	Z-X	X-Z
MB0, MB1 (ha)	0	0	0	0	10595	26488	28924
MB2 - MB4 (ha)	1589	169520	1589	2119	254280	26487	8158

Soil series or land classes *Grondseries of landklasse*	**Depth** *Diepte* (mm)	MB	ha	%	ha	%	ha	%	ha	%	ha	%	ha	%	ha	%	**Total** *Totaal* ha	%	**Clay content %** *Klei-inhoud %* A	E	B21	Hor	**Texture** *Tekstuur* Class / *Klas*	**Depth limiting material** *Diepte-beperkende materiaal*
Rock / Rots		4	1065	67	25428	15	1589	100	1589	75	21190	8	2119	4			52980	10.0						
Mispah Ms10, Kalkbank Ms22, Muden Ms20	50-100	3	524	33	91541	54			530	25	66219	25	5298	10	1112	3	165224	31.2	5-12			A	me/coSa-LmSa	R,ka,db
Portsmouth Hu35, Vergenoeg Hu45, Zwartfontein Hu34, Malonga Hu44	100-400	3			32209	19					79462	30	8476	16	2225	6	122372	23.1	6-12		6-15	B	me/coSa-SaLm	R,so,ka,
Shorrocks Hu36, Shigalo Hu46	100-400	3			20342	12					87409	33	10595	20	2225	6	120571	22.8	9-20		15-25	B	me/coSaLm-SaClLm	R,ka,so,
Shorrocks Hu36, Shigalo Hu46	450-1200+	0									5298	2	13244	25	12979	35	31520	6.0	9-20		15-25	B	me/coSaLm-SaClLm	R,ka,so,
Portsmouth Hu35, Vergenoeg Hu45, Zwartfontein Hu34, Malonga Hu44	450-1200+	0									5298	2	13244	25	10754	29	29295	5.5	6-12		6-15	B	me/coSa-SaLm	R,ka,so,
Letaba Oa26, Leeufontein Oa16, Dundee Du10	450-1200+	0													5191	14	5192	1.0	10-25		15-30	B	me/coSaLm-SaClLm	R,ka,so
Stream beds/Stroombeddings		4													2596	7	2596	0.5						

Terrain type /*Terreintipe* : A2

Terrain form sketch / *Terreinvormskets*

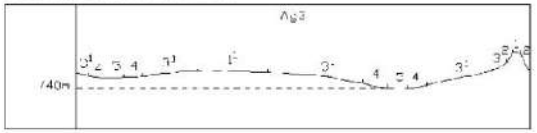

For an explanation of this table consult LAND TYPE INVENTORY (table of contents)

Ter verduideliking van hierdie tabel kyk LANDTIPE - INVENTARIS (inhoudsopgawe)

Geology: Migmatite, gneiss and granite predominantly; small outcrops of ultrametamorphic rocks in places (Namaqualand Metamorphic Complex). Lime nodules and calcrete abundant; dorbank in places; occasional very small pans.

Geologie: Migmatiet, gneis en graniet hoofsaaklik; klein dagsome van ultrametamorfe gesteentes op plekke (Namakwaland Metamorfe Kompleks). Volop kalknodules en kalkreet; dorbank op plekke; enkele baie klein panne.

14 November 2003 B16

Figure C-1: Land type data for land type Ag3 (Land Type Survey Staff, 2003).

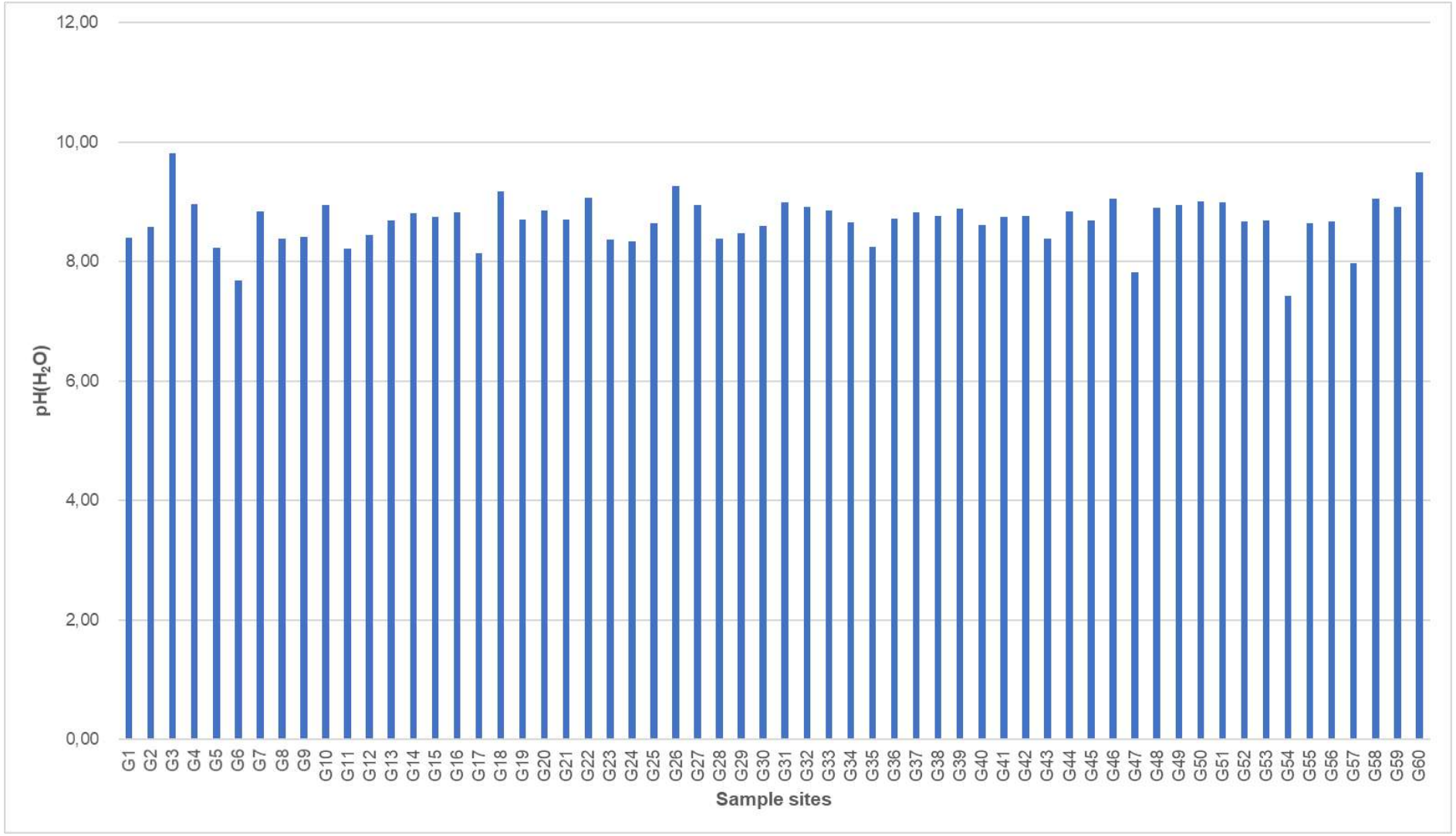

Figure C-2: The pH (H_2O) of all 60 samples taken during the soil survey.

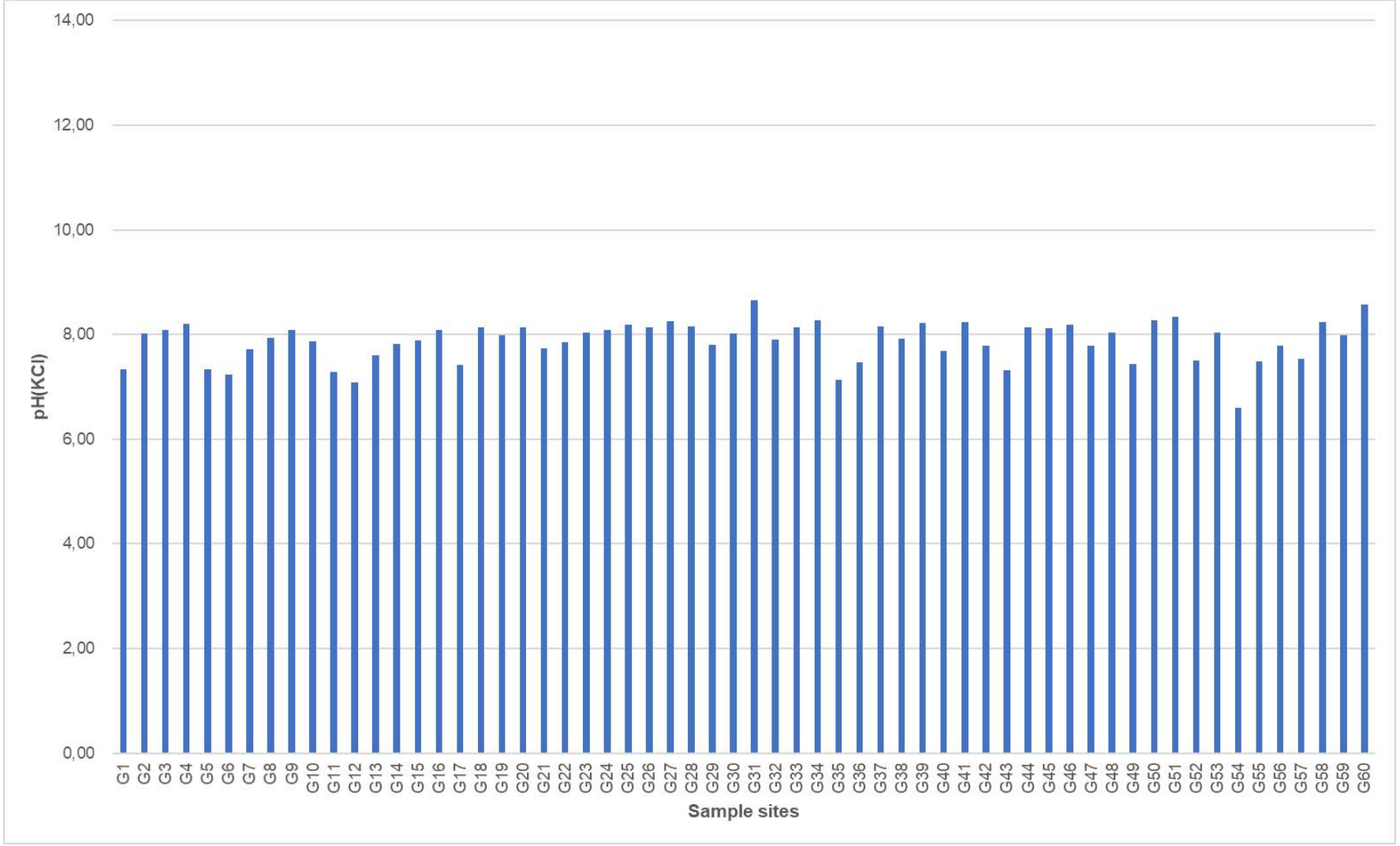

Figure C-3: The pH (KCl) of all 60 samples taken during the soil survey.

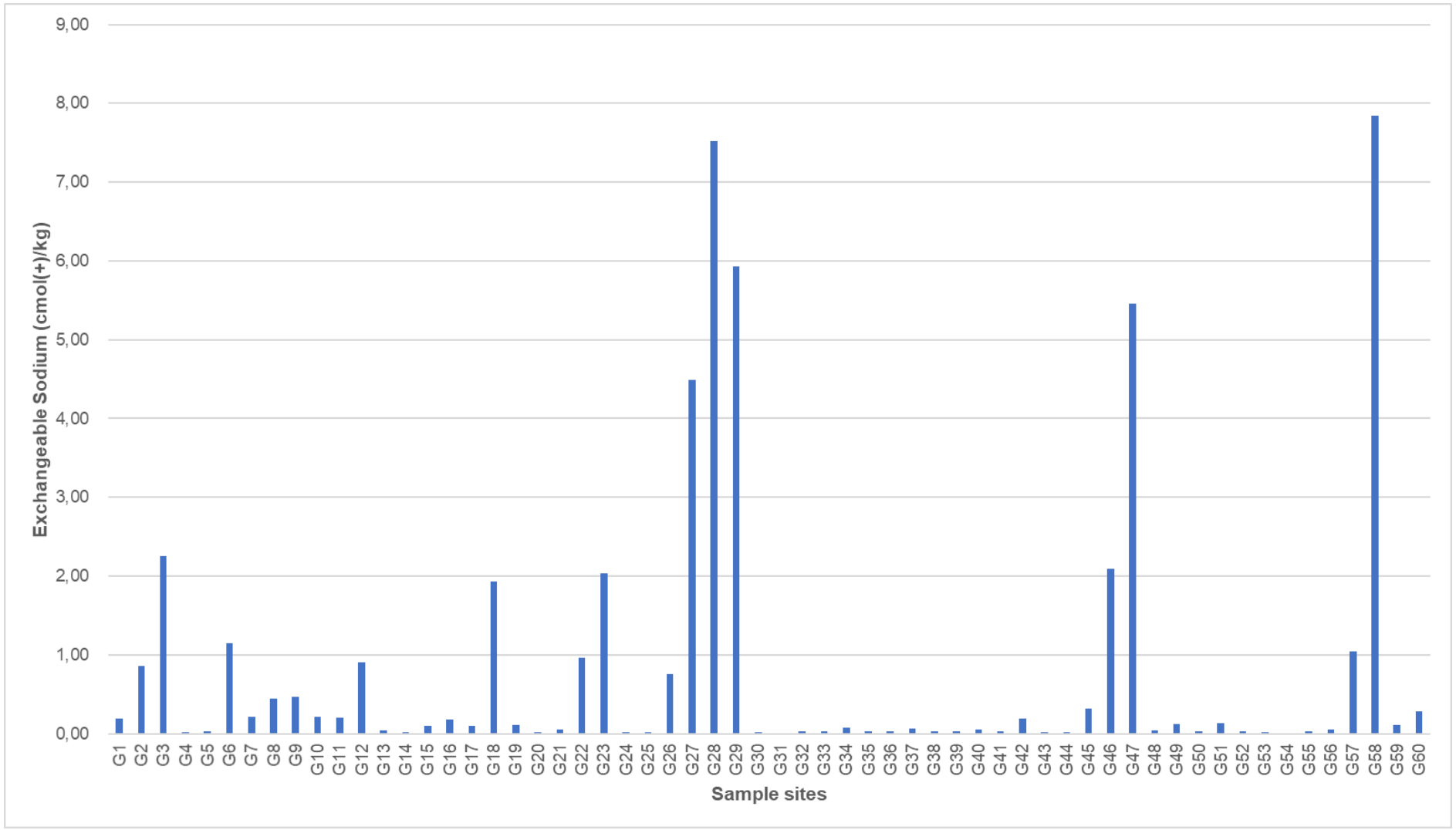

Figure C-4: Exchangeable sodium (cmol(+)/kg) of all 60 samples taken during the soil survey.

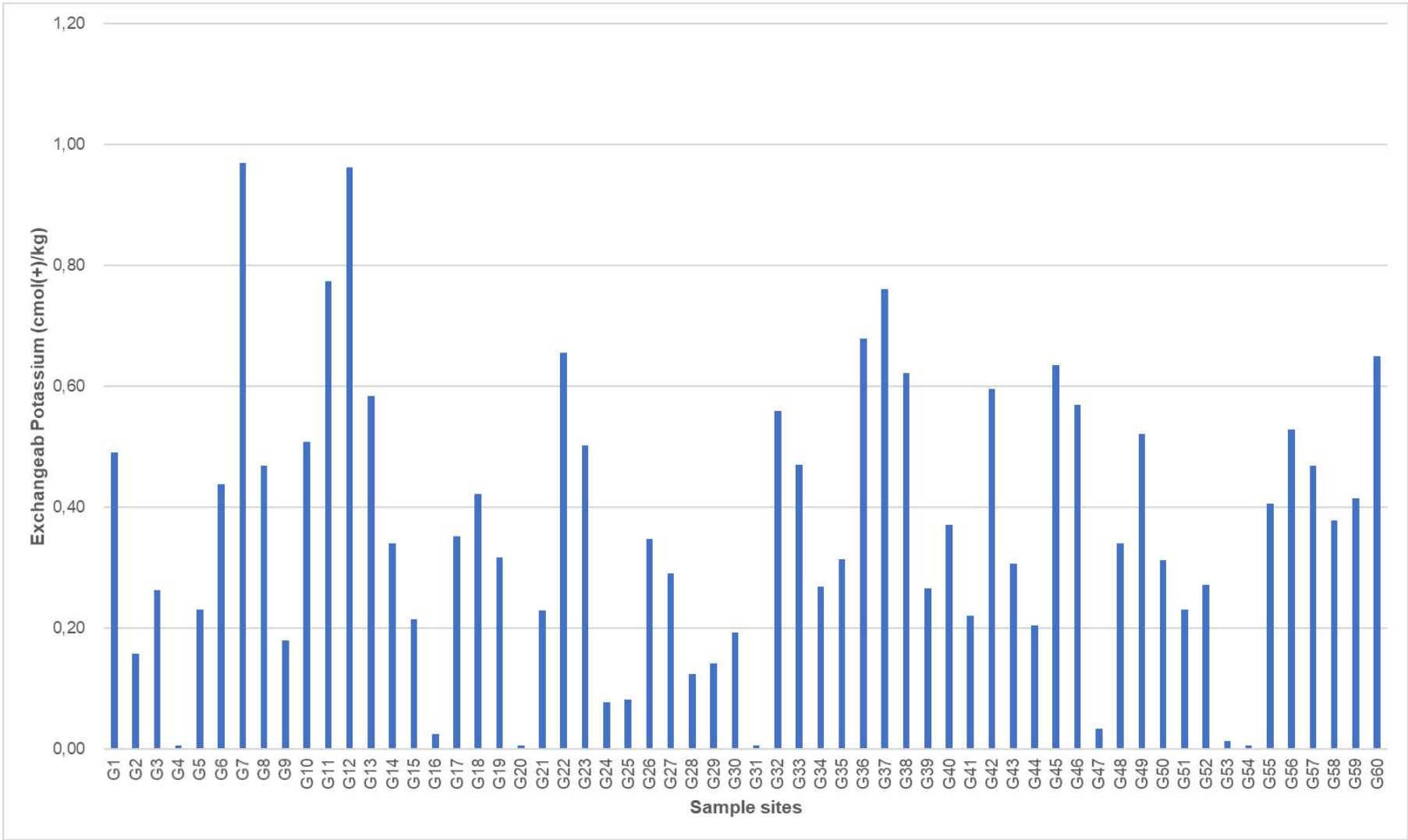

Figure C-5: Exchangeable potassium (cmol(+)/kg) of all 60 samples taken during the soil survey.

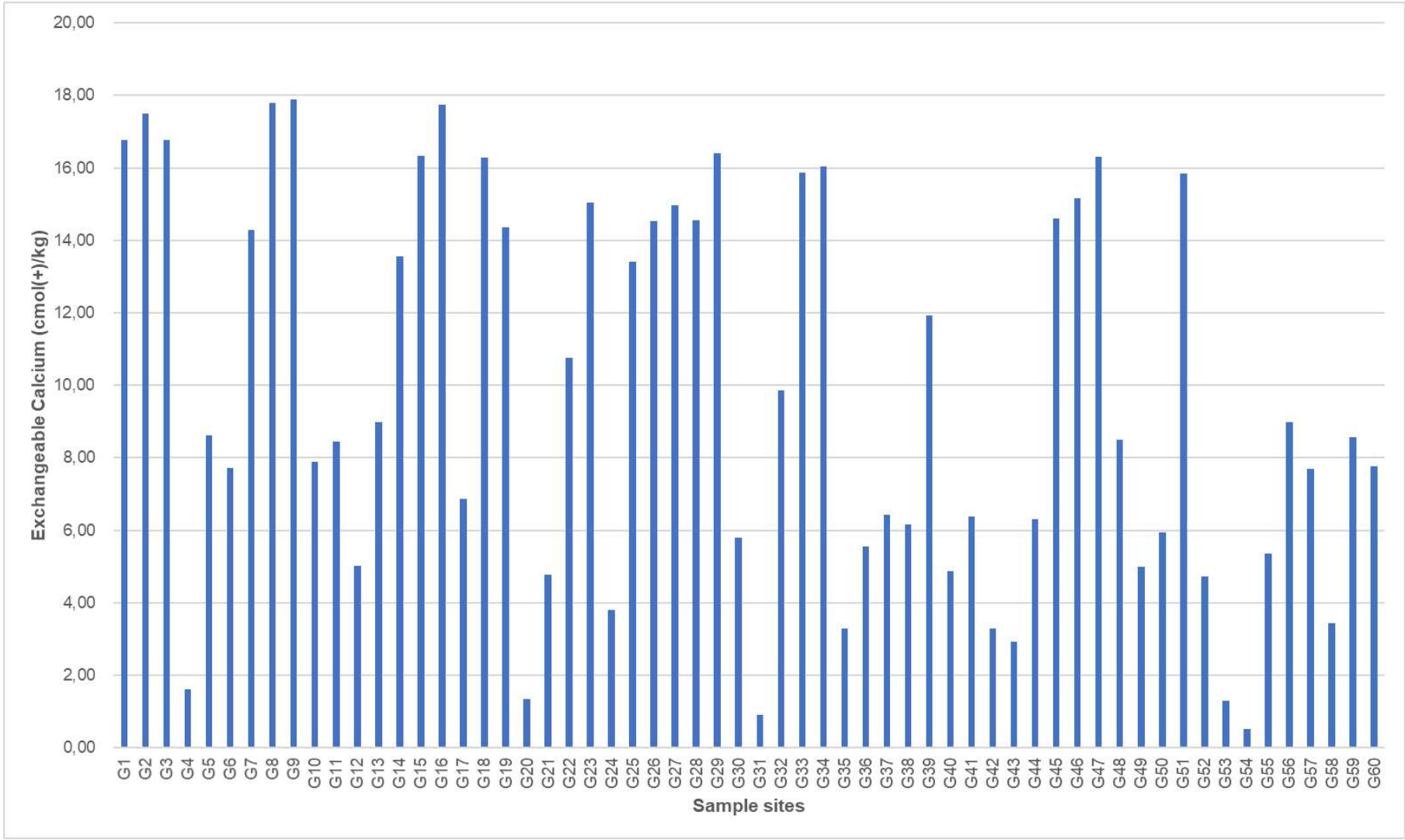

Figure C-6: Exchangeable calcium (cmol(+)/kg) of all 60 samples taken during the soil survey.

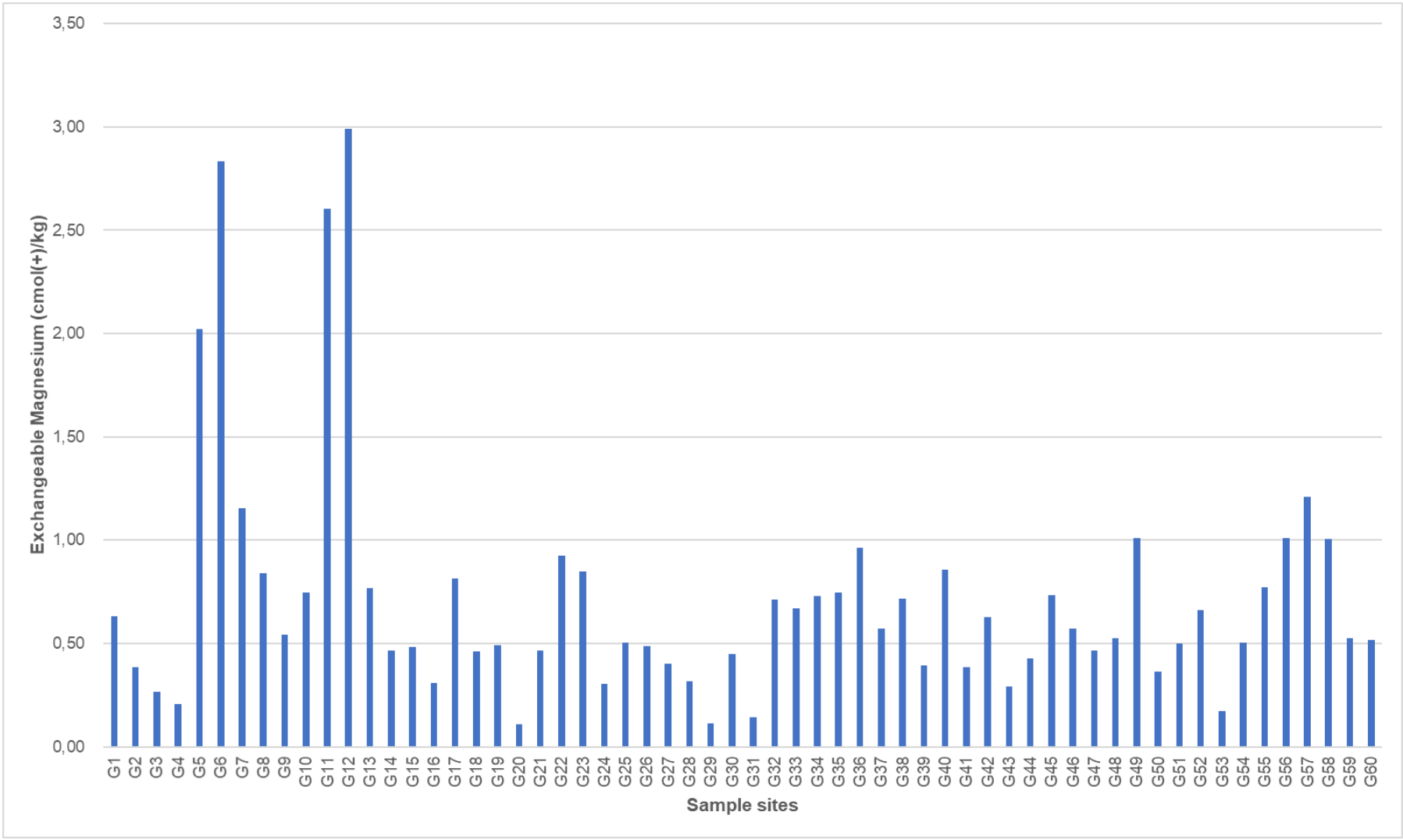

Figure C-7: Exchangeable magnesium (cmol(+)/kg) of all 60 samples taken during the soil survey.

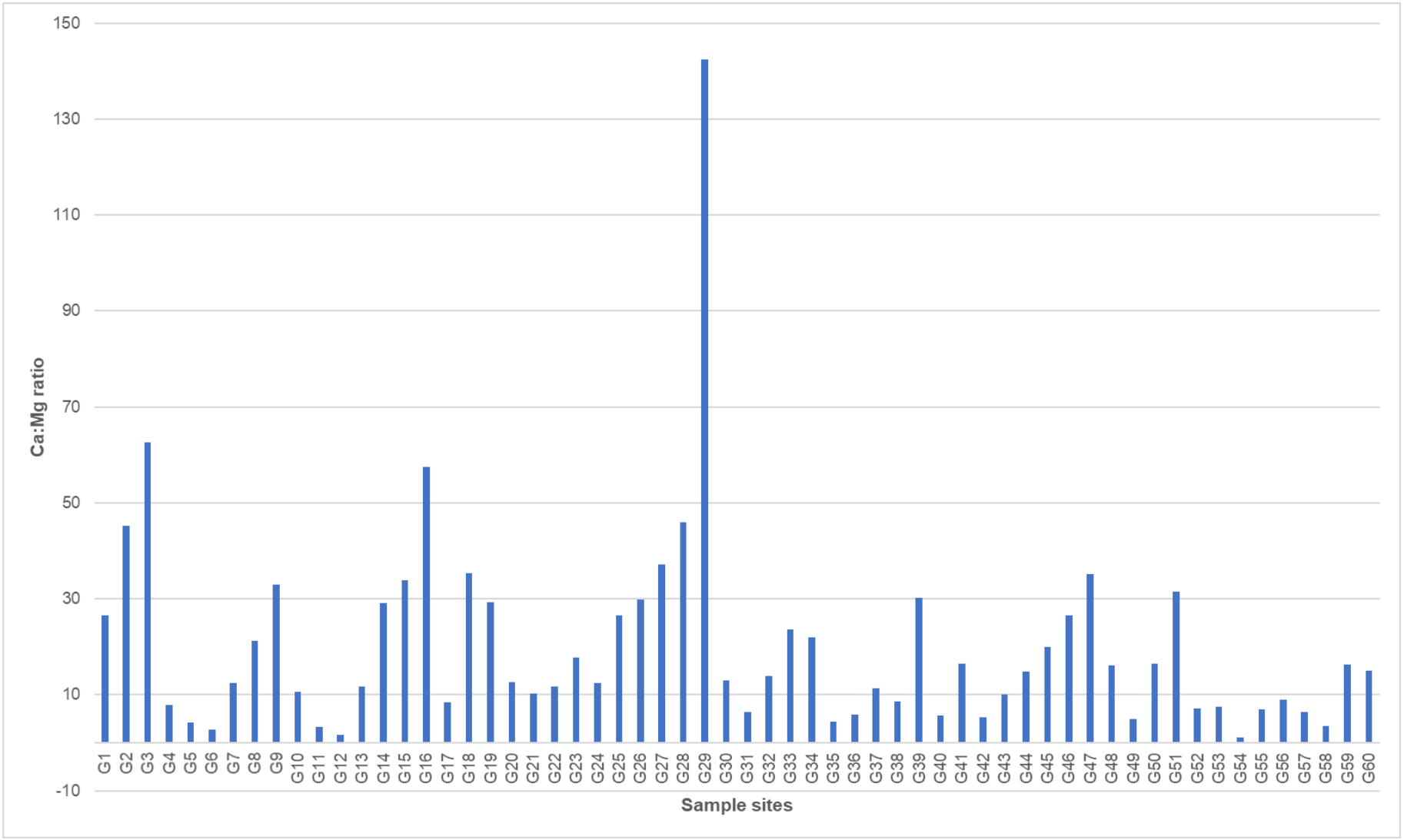

Figure C-8: Ca:Mg ratio of all 60 samples taken during the soil survey.

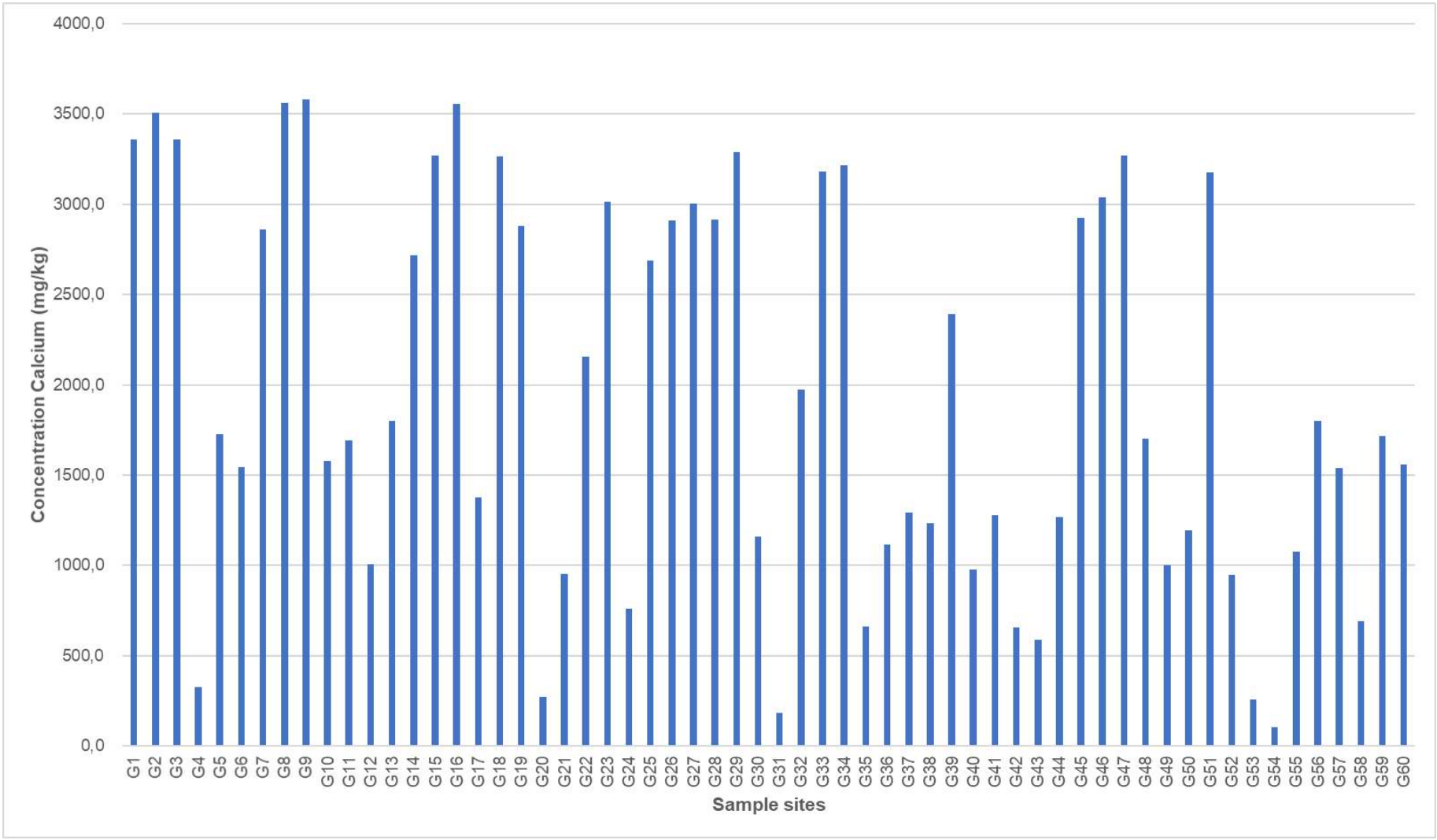

Figure C-9: Concentration calcium (mg/kg) of all 60 samples taken during the soil survey.

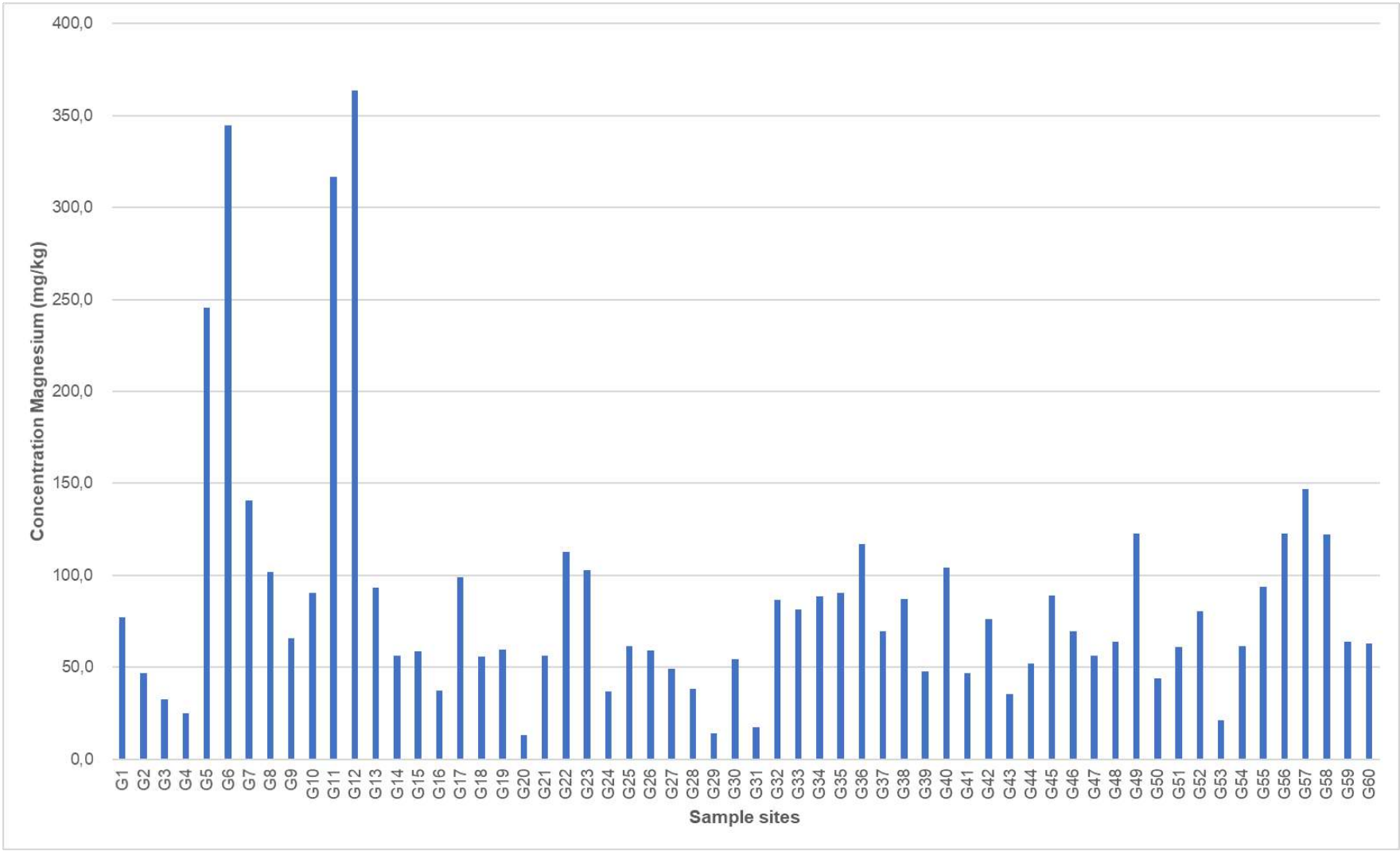

Figure C-10: Concentration magnesium (mg/kg) of all 60 samples taken during the soil survey.

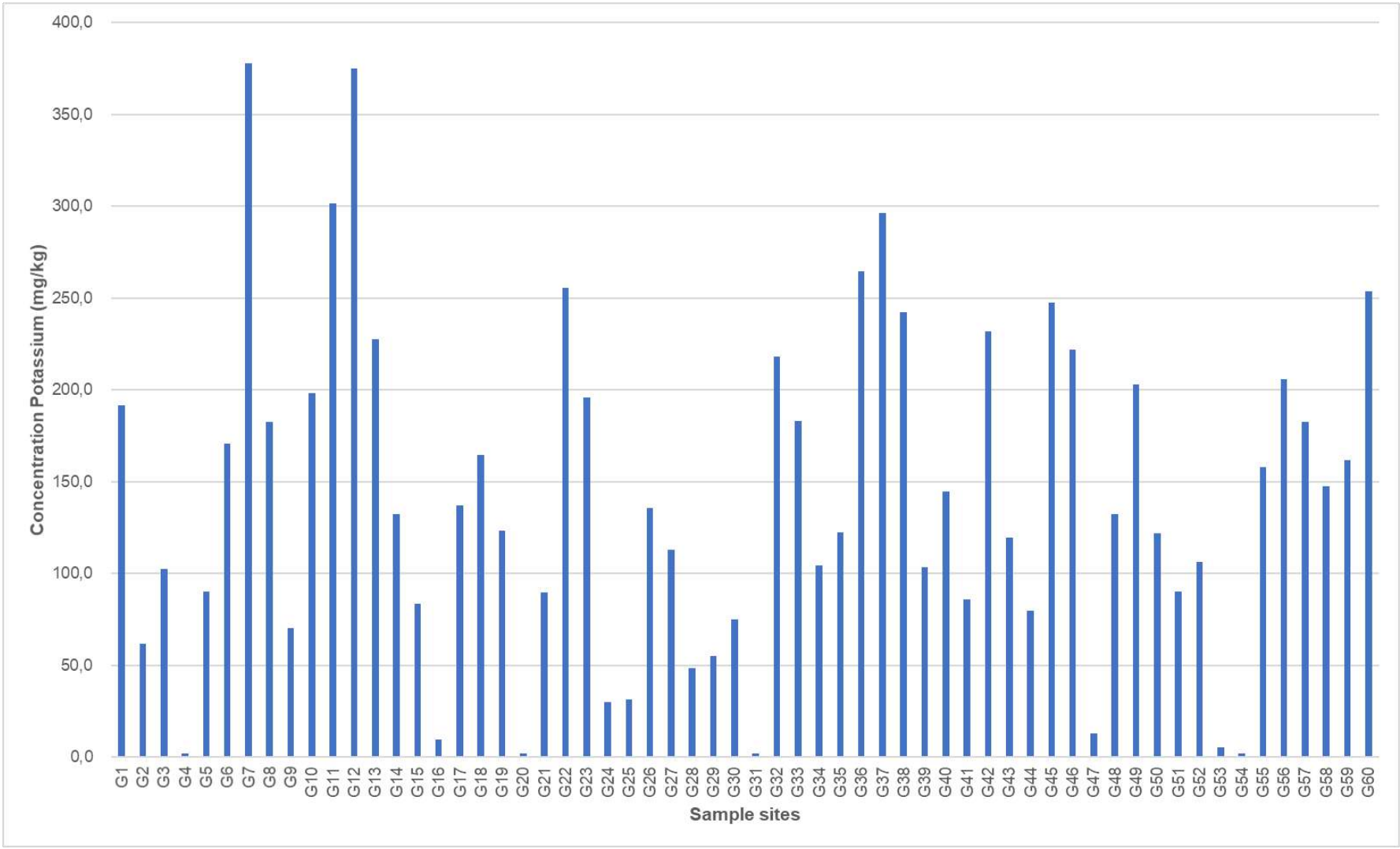

Figure C-11: Concentration potassium (mg/kg) of all 60 samples taken during the soil survey.

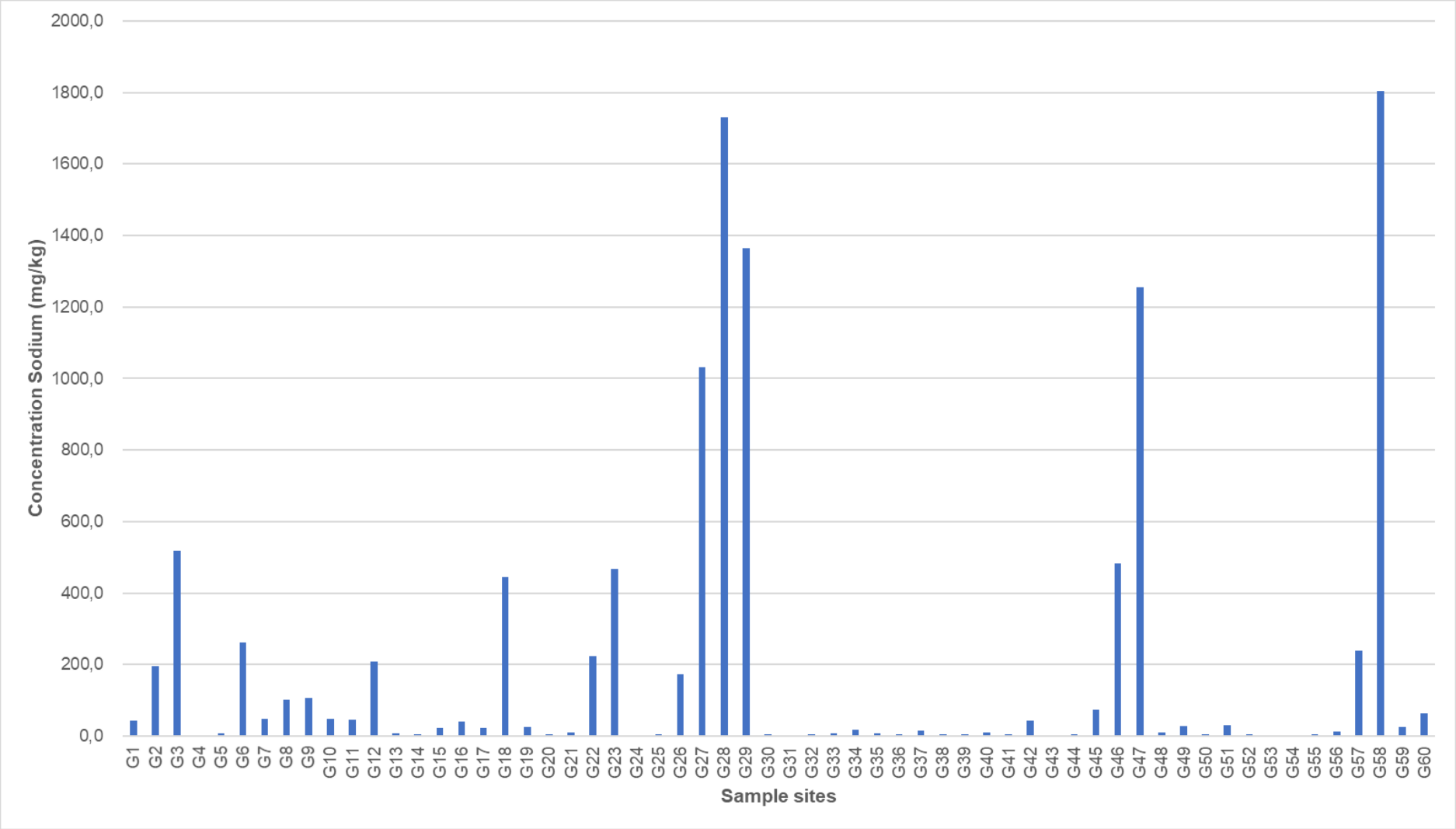

Figure C-12: Concentration sodium (mg/kg) of all 60 samples taken during the soil survey.

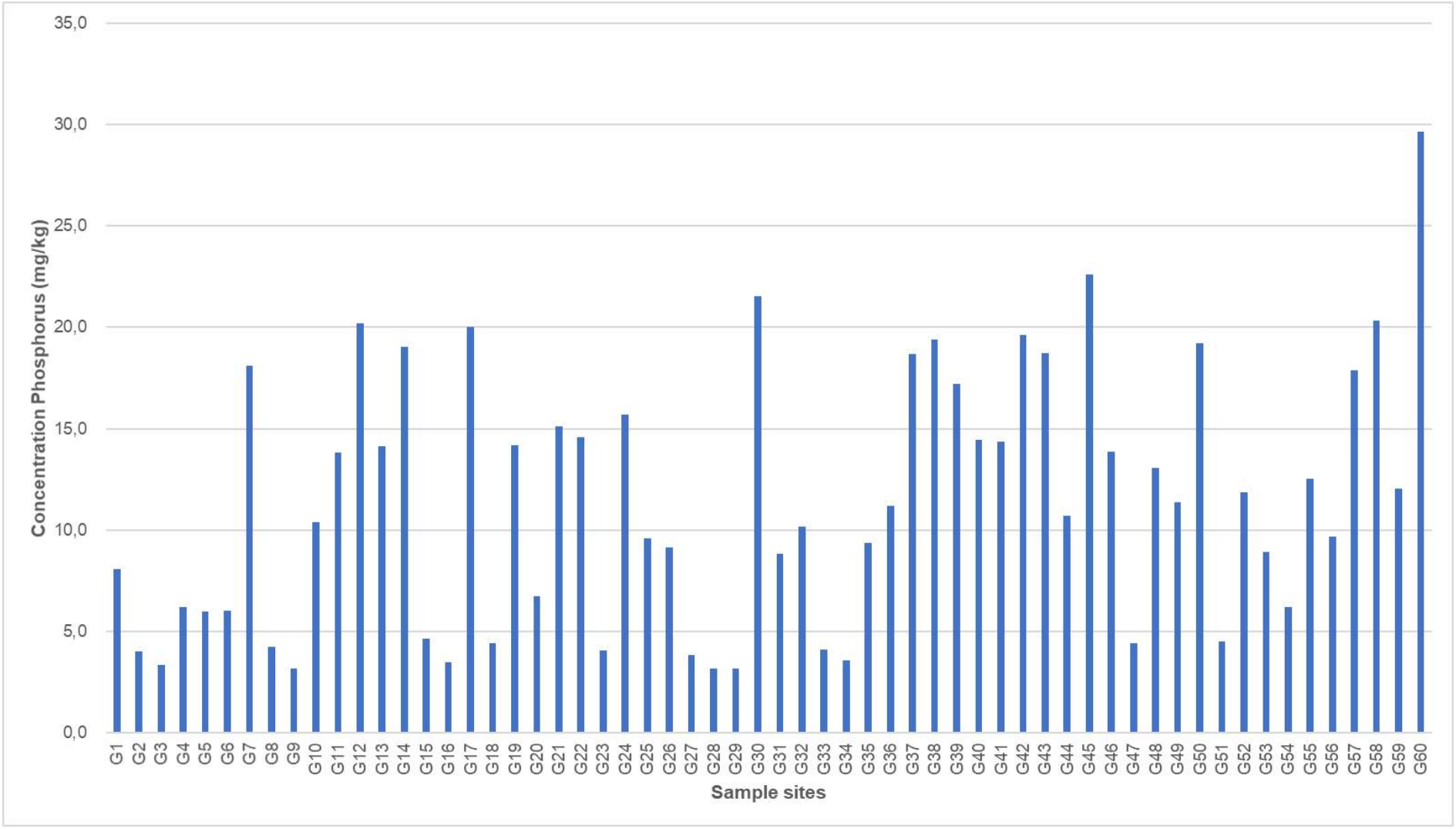

Figure C-13: Concentration phosphorus (mg/kg) of all 60 samples taken during the soil survey.

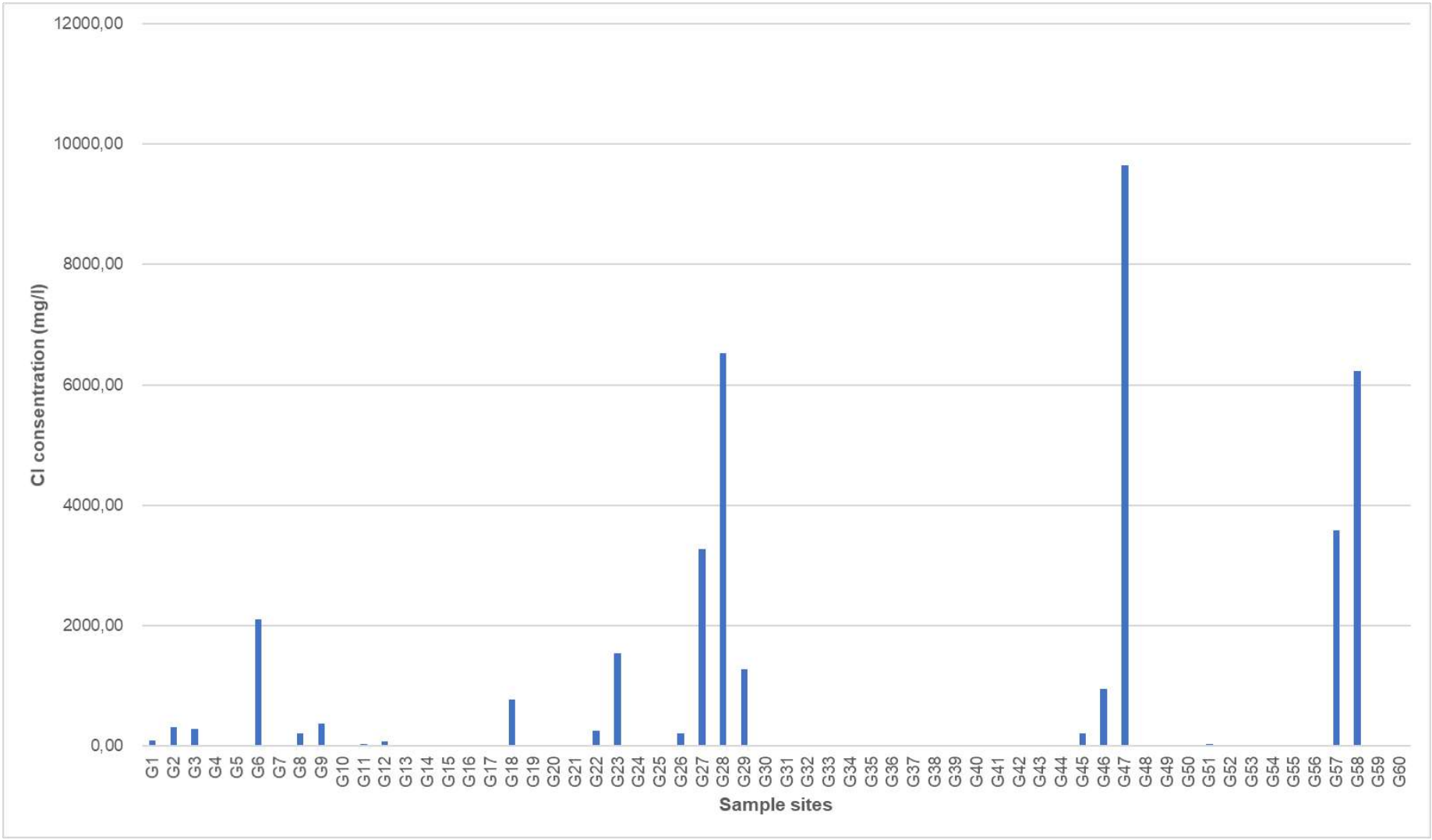

Figure C-14: Chloride concentration (mg/l) of all 60 samples taken during the soil survey.

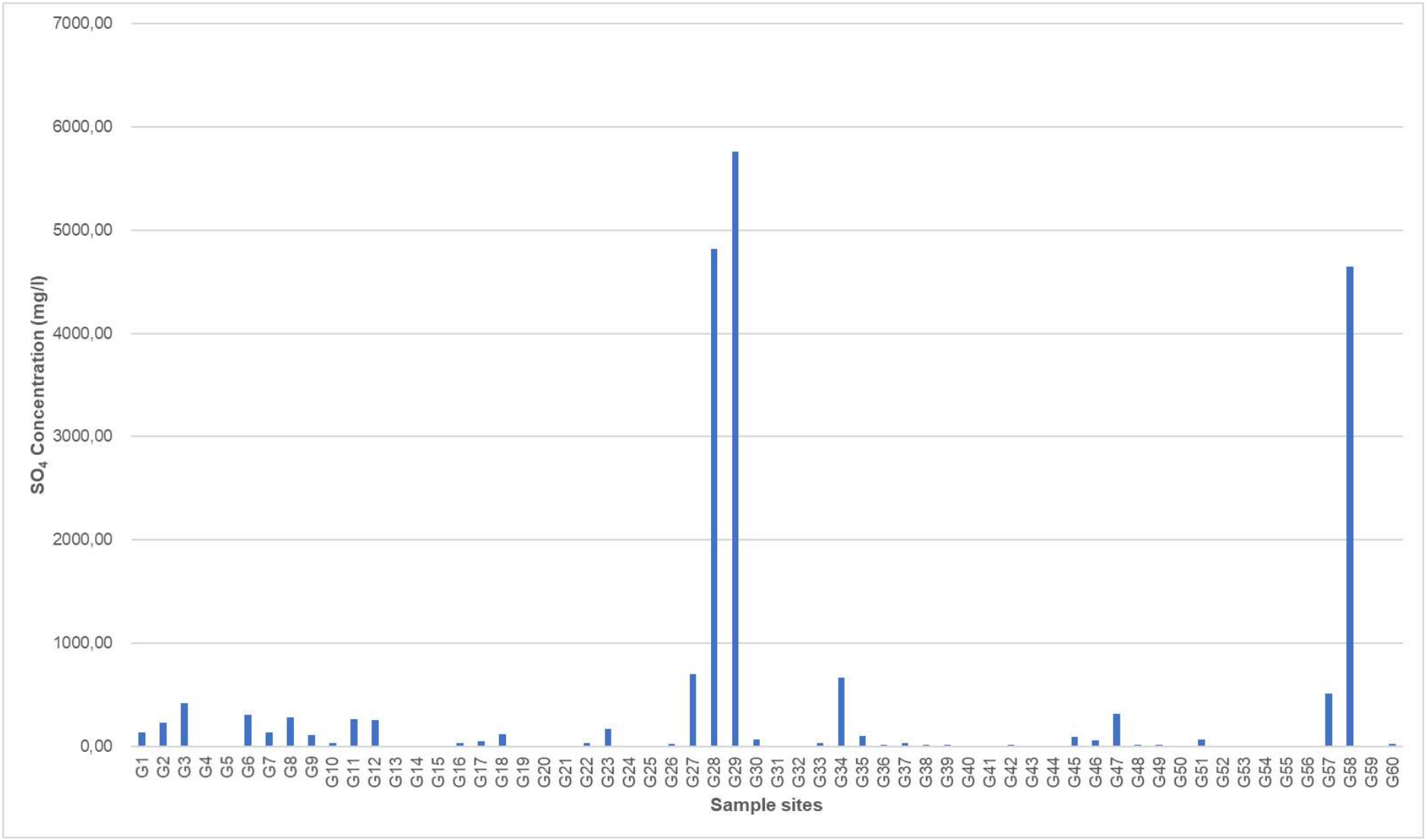

Figure C-15: Sulphate concentration (mg/l) of all 60 samples taken during the soil survey.

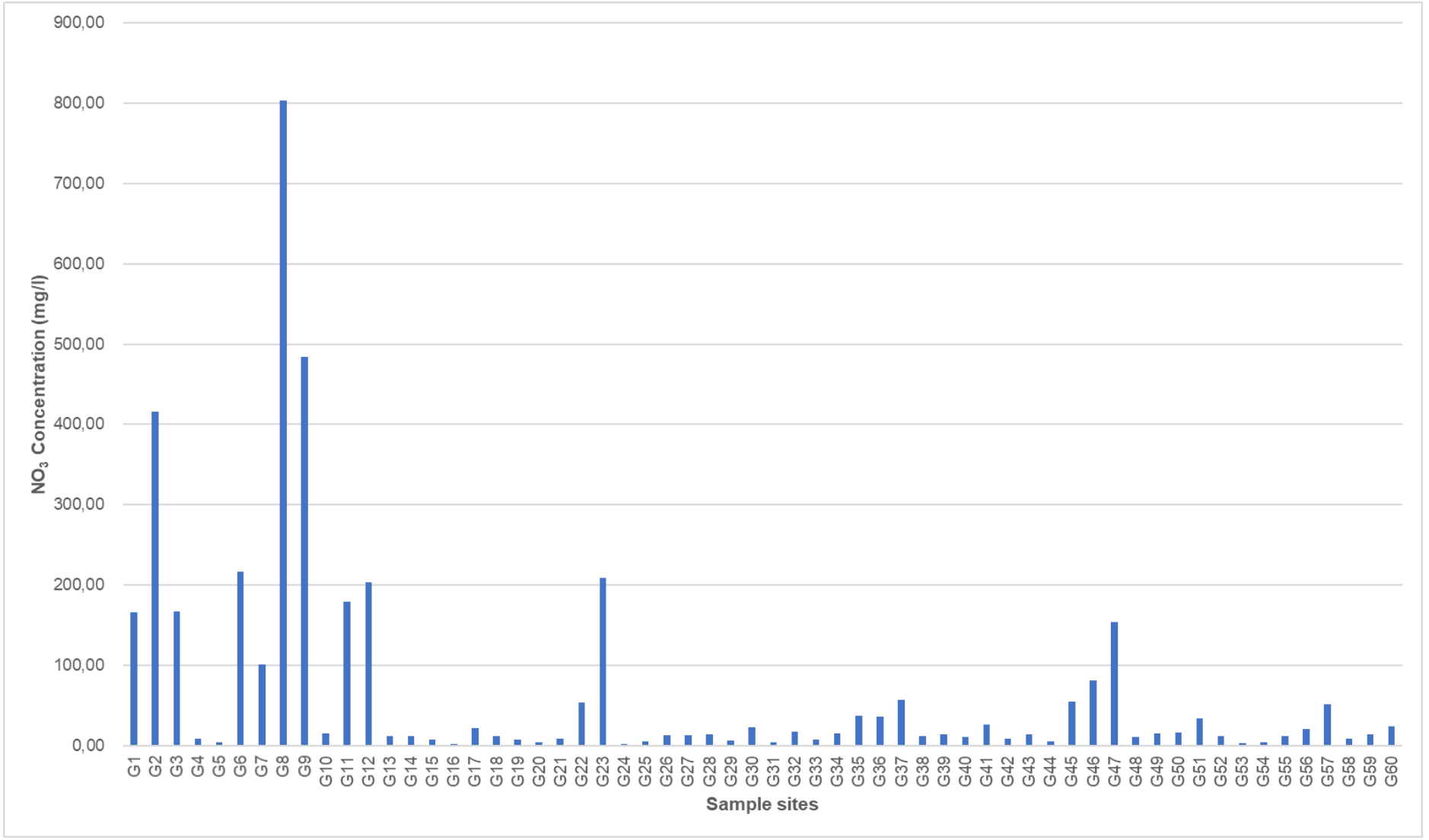

Figure C-16: Nitrate concentration (mg/l) of all 60 samples taken during the soil survey.

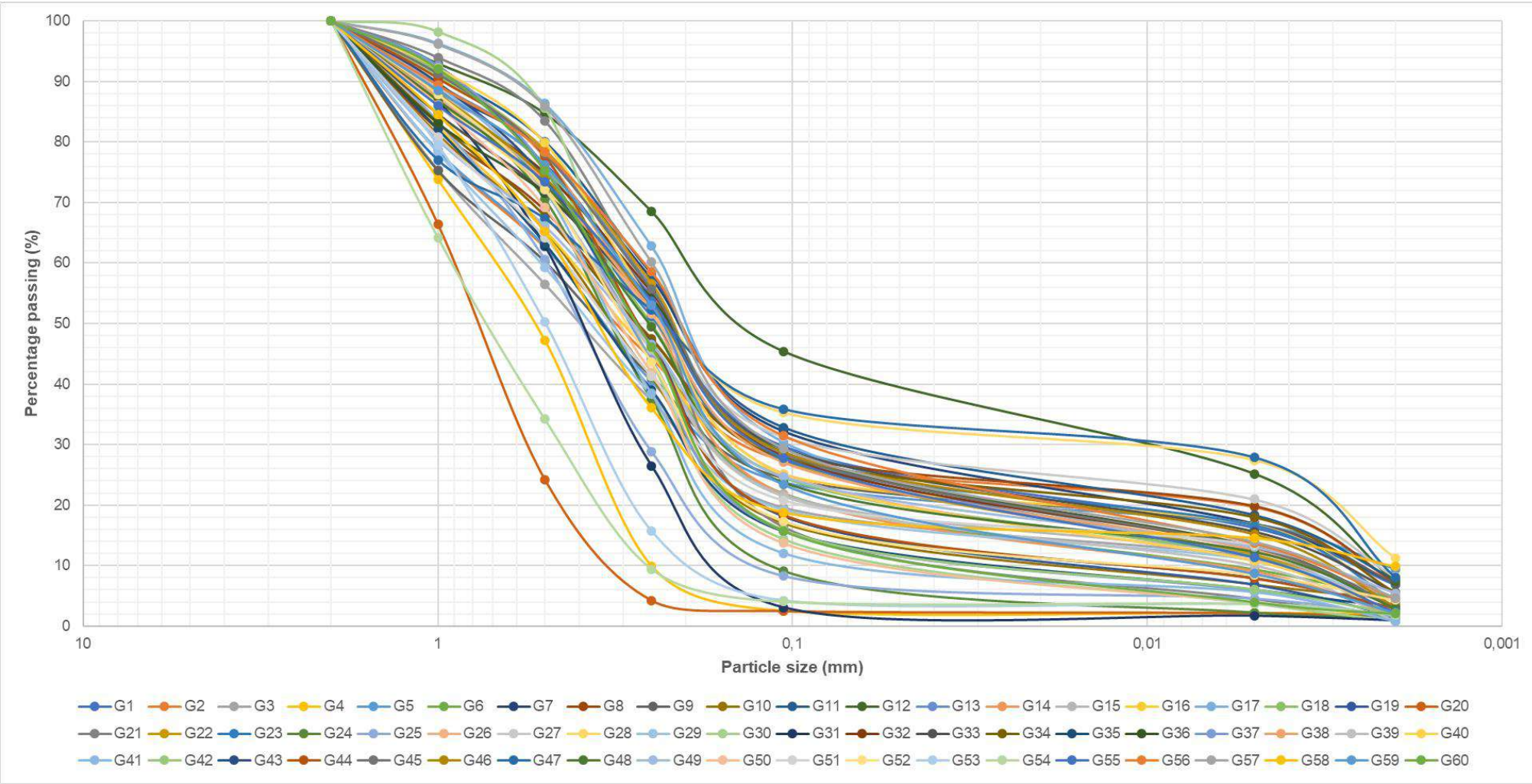

Figure C-17: Particle size distribution curves of all 60 samples taken during the soil survey.